Universitat Autònoma de Barcelona

Bioprocess engineering and characterization of HIV virus-like particle production in insect cells

Eduard Puente Massaguer

Universitat Autònoma de Barcelona

Escola d'Enginyeria

Departament d'Enginyeria Química, Biològica i Ambiental

Programa de Doctorat en Biotecnologia

Bioprocess engineering and characterization of HIV virus-like particle production in insect cells

Memòria per a optar al grau de Doctor

per la Universitat Autònoma de Barcelona,

per

Eduard Puente Massaguer

Bellaterra, setembre 2019

El Dr. Francesc Gòdia Casablancas, professor del Departament d'Enginyeria Química, Biològica i Ambiental de la Universitat Autònoma de Barcelona i el Dr. Martí Lecina Veciana, professor del Departament de Bioenginyeria de l'Institut Químic de Sarrià, Universitat Ramón Llull,

Certifiquem:

Que el graduat en Biotecnologia Eduard Puente Massaguer ha dut a terme al Departament d'Enginyeria Química, Biològica i Ambiental de la Universitat Autònoma de Barcelona i amb la nostra direcció, la tesi doctoral titulada **"Bioprocess engineering and characterization of HIV virus-like particle production in insect cells"**. La mateixa, es presenta en aquesta memòria i constitueix el manuscrit per optar al Grau de Doctor en Biotecnologia per la Universitat Autònoma de Barcelona.

I per tal que se'n prengui coneixement i consti als efectes oportuns, signem aquest certificat a Bellaterra, a 20 de setembre de 2019.

Eduard Puente Massaguer	Dr. Martí Lecina Veciana	Dr. Francesc Gòdia Casablancas
(autor)	(co-director)	(co-director)

Table of contents

Resum

Les *virus-like particles* (VLPs) han sorgit com a una alternativa a les vacunes convencionals basades en virus atenuats o inactivats. La seva capacitat d'autoacoblament en base a l'expressió d'una proteïna matriu i l'absència de material genòmic d'origen víric les fa candidats atractius per a una multitud d'aplicacions. Les VLPs de Gag del virus de la immunodeficiència humana (VIH) són un tipus de VLPs amb envolta que han atret especial interès degut a les seves propietats estructurals, amb aplicacions en teràpia gènica, nanotecnologia i el desenvolupament de vacunes multivalents. Les línies cel·lulars d'insecte són un sistema de referència per a produir aquest tipus de nanopartícules ja que proporcionen les condicions adients per la seva producció i assemblatge. En aquesta tesi s'ha avaluat la producció de VLPs del VIH-1 en les línies d'insecte Sf9 i High Five amb el sistema d'expressió baculovirus i transfecció transitòria. Per tal d'assolir aquest objectiu, s'ha emprat una aproximació basada en l'ús combinat de metodologies de disseny d'experiments i funcions de resposta combinada. Paral·lelament, s'han incorporat una sèrie de tècniques de mesura per tal de monitoritzar i quantificar el procés productiu i per a la caracterització final de les VLPs.

En el primer capítol s'analitzen les característiques d'ambdues línies cel·lulars d'insecte com a plataformes per a la producció de VLPs de GageGFP amb el sistema d'expressió baculovirus. Les cèl·lules High Five mostren un increment de 3.6 vegades en la producció de GageGFP respecte les cèl·lules Sf9 mentre que aquestes últimes permeten assolir un augment de 1.7 vegades en la producció de VLPs. En tots dos casos, l'observació de les VLPs per microscòpia electrònica de criogènia permet determinar que tenen una mida similar i també permet detectar la presència d'altres poblacions de nanopartícules. L'anàlisi dels nivells de producció de baculovirus resulta en un increment de 23 vegades de virus infectius en les cèl·lules Sf9 mentre que una proporció més gran de virus d'oclusió s'observa en les cèl·lules High Five. La presència d'aquest últim fenotip de baculovirus evidencia un canvi en la complexitat de la línia cel·lular High Five després de la infecció amb el baculovirus. Finalment, la combinació de les tècniques d'ultracentrifugació i virometria de flux mostra que les VLPs derivades de High Five tenen un major coeficient de sedimentació, la qual cosa indica que aquestes VLPs poden estar associades amb altres elements cel·lulars.

Al segon capítol es determinen les condicions òptimes per a la producció de VLPs en les cèl·lules Sf9 i High Five amb el sistema d'expressió baculovirus. En aquest sentit, s'apliquen metodologies de disseny d'experiments i funcions d'optimització amb tècniques de quantificació directa de nanopartícules per tal d'aprofundir en aquests sistemes. Inicialment s'aborden dues situacions objectiu, la primera cercant la maximització de la concentració de VLPs (Quantitat) i la segona buscant un balanç entre producció i percentatge de VLPs amb estructura completa (Qualitat). Les millors condicions de producció per a les cèl·lules High Five corresponen a multiplicitats d'infecció elevades i temps de recollida més curts; en canvi, les cèl·lules Sf9 requereixen multiplicitats d'infecció més baixes i temps de recollida més llargs. Els nivells de producció final de VLPs en la condició de qualitat són 4.5 vegades més elevats per a les cèl·lules Sf9 mentre que en la condició de quantitat s'obtenen concentracions similars de VLPs per a ambdues línies.

Al tercer capítol de la tesi es desenvolupa una estratègia de producció lliure de baculovirus i basada en la transfecció transitòria de ADN plasmídic amb polietilenimina (PEI). Anàlogament al capítol 2, s'implementa una aproximació sistemàtica de disseny d'experiments i funcions d'optimització. En ambdós casos, el recanvi de medi abans de la transfecció resulta ser beneficiós per tal d'assolir els nivells més alts d'expressió. La millor estratègia de transfecció per a les cèl·lules High Five s'obté amb la utilització de complexes d'ADN i PEI petits (< 300 – 400 nm), mentre que en el cas de les cèl·lules Sf9 s'obté amb una mida de complexes més heterogènia (200 – 1500 nm). Les condicions òptimes de concentració de cèl·lules viables, ADN i PEI es determinen en aquest estudi i la formació correcta de les VLPs produïdes es corrobora per microscòpia electrònica de criogènia. En aquest cas, les cèl·lules Sf9 assoleixen un increment de 8.4 vegades en la producció de VLPs respecte a la línia cel·lular High Five.

A l'últim capítol de la tesi es desenvolupen conjunts de cèl·lules Sf9 i High Five amb expressió estable i contínua de VLPs al llarg del temps. Aquests conjunts de cèl·lules d'expressió estable es generen a partir de la integració aleatòria d'ADN codificant al genoma de les cèl·lules, i les que són més productives se seleccionen per citometria en base a la seva fluorescència. Mitjançant aquesta metodologia, s'assoleix un enriquiment de 8.1 i 3.4 vegades en la intensitat de fluorescència de GageGFP en les cèl·lules Sf9 i High Five, respectivament, en comparació als

conjunts cel·lulars no enriquits. En relació a la producció de VLPs, s'aconsegueix un increment de 3.7 vegades en les cèl·lules High Five respecte les Sf9. Finalment, l'estabilitat d'aquests grups cel·lulars d'expressió estable es corrobora al llarg d'un mes en cultiu.

Resumen

Las *virus-like particles* (VLPs) han surgido como a una alternativa a las vacunes convencionales basadas en virus atenuados o inactivados. Su capacidad de autoensamblaje en base a la expresión de una proteína matriz y la ausencia de material genómico de origen vírico las hace candidatos atractivos para una multitud de aplicaciones. Las VLPs de Gag del virus de la inmunodeficiencia humana (VIH) son un tipo de VLPs con envuelta que ha suscitado especial interés debido a sus propiedades estructurales, con aplicaciones en terapia génica, nanotecnologia y el desarrollo de vacunas multivalentes. Las líneas celulares de insecto son un sistema de referencia para producir este tipo de nanopartículas puesto que proporcionan les condiciones adecuadas para su producción y ensamblaje. En esta tesis se ha evaluado la producción de VLPs del VIH-1 en las líneas de insecto Sf9 y High Five con el sistema de expresión baculovirus y transfección transitoria. Para conseguir este objetivo, se ha utilizado una aproximación basada en el uso combinado de metodologías de diseño de experimentos y funciones de respuesta combinada. Paralelamente, se han incorporado una serie de técnicas de medición para monitorizar y cuantificar el proceso productivo y para la caracterización final de las VLPs.

En el primer capítulo se analizan las características de ambas líneas celulares de insecto como plataformas para la producción de VLPs de GageGFP con el sistema de expresión baculovirus. Les células High Five muestran un incremento de 3.6 veces en la producción de GageGFP respecte a las células Sf9 mientras que estas últimas permiten conseguir un aumento de 1.7 veces en la producción de VLPs. En ambos casos, la observación de las VLPs mediante microscopia electrónica de criogenia permite determinar que tienen un tamaño similar y también permite detectar la presencia de otras poblaciones de nanopartículas. El análisis de los niveles de producción de baculovirus resulta en un incremento de 23 veces de virus infectivos en las células Sf9 mientras que una proporción más gran de virus de oclusión se observa en las células High Five. La presencia de este último fenotipo de baculovirus evidencia un cambio en la complejidad de la línea celular High Five después de la infección con el baculovirus. Finalmente, la combinación de les técnicas de ultracentrifugación y virometría de flujo muestran que las VLPs derivadas de High Five tienen un mayor coeficiente de sedimentación, lo que indica que éstas pueden estar asociadas con otros elementos celulares.

En el segundo capítulo se determinan las condiciones óptimas para la producción de VLPs en las células Sf9 y High Five con el sistema de expresión baculovirus. En este sentido, se aplican metodologías de diseño de experimentos y funciones de optimización con técnicas de cuantificación directa de nanopartículas para profundizar en estos sistemas. Inicialmente se consideran dos situaciones objetivo, la primera investiga la maximización de la concentración de VLPs (Cantidad) y la segunda busca un balance entre producción y porcentaje de VLPs ensambladas (Calidad). Las mejores condiciones de producción para las células High Five corresponden a multiplicidades de infección elevadas y tiempos de recogida más cortos; en cambio, las células Sf9 necesitan multiplicidades de infección más bajas y tiempos de recogida más largos. Los niveles de producción final de VLPs en la condición de calidad son 4.5 veces más elevados para las células Sf9 mientras que en la condición de cantidad se obtienen concentraciones de VLPs similares para ambas líneas.

En el tercer capítulo de la tesis se desarrolla una estrategia de producción libre de baculovirus y basada en la transfección transitoria de ADN plasmídico con polietilenimina (PEI). Análogamente al capítulo 2, se implementa una aproximación sistemática de diseño de experimentos y funciones de optimización. En ambos casos, el recambio de medio previo a la transfección resulta ser beneficioso para conseguir los niveles más altos de expresión. La mejor estrategia de transfección para las células High Five se obtiene con la utilización de complejos de ADN y PEI pequeños (< 300 – 400 nm), mientras que en el caso de las células Sf9 se obtiene con un tamaño de complejos más heterogenia (200 – 1500 nm). Las condiciones óptimas de concentración de células viables, ADN y PEI se determinan en este estudio y la formación correcta de las VLPs producidas se corrobora por microscopia electrónica de criogenia. En este caso, las células Sf9 consiguen un incremento de 8.4 veces en la producción de VLPs respecto a la línea celular High Five.

En el último capítulo de la tesis se desarrollan grupos de células Sf9 y High Five con expresión estable y continua de VLPs a lo largo del tiempo. Estos conjuntos celulares de expresión estable se generan a partir de la integración aleatoria de ADN codificante en el genoma de las células, y las que son más productivas se seleccionan por citometría en base a su fluorescencia. Mediante esta metodología, su intensidad de fluorescencia de GageGFP aumenta en 8.1 y 3.4 en las células

Sf9 y High Five, respectivamente, en comparación a los conjuntos celulares no enriquecidos. En cuanto a la producción de VLPs, se consigue un incremento de 3.7 veces en las células High Five respecto a las Sf9. Finalmente, la estabilidad de estos grupos celulares de expresión estable se corrobora a lo largo de un mes en cultivo.

Summary

Virus-like particles (VLPs) have emerged as an interesting alternative to conventional vaccines based on live-attenuated or inactivated viruses. Their capacity for self-assembling upon expression of the core protein and the lack of viral genomic material make them excellent candidates for a variety of purposes. Gag VLPs from the human immunodeficiency virus (HIV) are a type of enveloped VLPs that have drawn special attention due to their structural properties with applications in gene therapy, nanobiotechnology and multivalent vaccine development. Insect cell lines are a reference system to produce these types of nanoparticles since they provide the ideal conditions for their production and assembly. In this work, the production of HIV-1 GageGFP VLPs is assessed in Sf9 and High Five insect cells with the baculovirus expression vector system (BEVS) and transient gene expression (TGE). A rational approach based on the combination of Design of Experiments (DoE) and desirability functions is used to optimize the VLP production conditions. Advanced measurement techniques are implemented to monitor and quantify the production process and for final VLP characterization.

In the first chapter, the characteristics of both insect cell lines as platforms for GageGFP VLP production with the BEVS are analyzed. High Five cells achieve a 3.6-fold improvement in GageGFP production compared to Sf9 cells while a 1.7-fold increase in VLP titer is attained in the latter. In both cases, similar VLP sizes for both cells are measured by cryogenic electron microscopy (cryo-EM) and other nanoparticle populations are identified. The analysis of baculovirus production levels results in a 23-fold increase of budded virus in Sf9 cells while a larger amount of occlusion-derived virus is detected in High Five cells. The presence of this baculovirus phenotype evidences a shift in the cellular complexity of High Five cells upon baculovirus infection. Finally, the combination of analytical ultracentrifugation with flow virometry reveals a higher sedimentation coefficient for High Five-derived VLPs, indicating their possible association with other cellular compounds.

In the second chapter, the optimal conditions for VLP production in Sf9 and High Five cells with the BEVS are determined by means of DoE and desirability functions. Different methodologies based on direct nanoparticle quantification are used to gain insight into these systems. Two objective situations are defined, one targeting the maximization of the VLP titer (Quantity) and

the second one aiming to find a balance between production and assembled VLPs (Quality). A higher multiplicity of infection (MOI) and a shorter time of harvest (TOH) result in the best production conditions for High Five cells while a lower MOI and longer TOH work best for Sf9 cells. Final VLP production levels in the quality condition are 4.5-fold higher for Sf9 cells while similar VLP concentrations are found for both insect cells in the quantity condition.

In the third chapter of this thesis, a baculovirus-free VLP production strategy is optimized for both insect cells based on plasmid-mediated TGE with polyethylenimine (PEI). As in chapter 2, a systematic approach combining DoE and desirability functions is implemented. In both cases, medium exchange before transfection proves to be beneficial to achieve the highest transgene expression yields. Small DNA:PEI complexes (< 300 – 400 nm) are more adequate to transfect High Five cells while they are more size heterogeneous (200 – 1500 nm) for Sf9 cells. Then, the optimal conditions for viable cell concentration at transfection, DNA and PEI concentrations are determined and the correct formation of the VLPs produced is corroborated using cryo-EM. In this case, Sf9 cells achieve a 8.4-fold increase in VLP production compared to High Five cells.

In the last chapter, stable Sf9 and High Five cell pools to produce VLPs are developed by random integration and selection of the high producer cells using fluorescence-activated cell sorting. An 8.1 and 3.4-fold improvement in GageGFP fluorescence intensity is obtained for Sf9 and High Five stable cell pools over unsorted cell pools, respectively. In terms of VLP production, a 3.7-fold increase in VLP titer is achieved in High Five over Sf9 stable pools. Finally, cell pool stability is successfully corroborated during the course of a month.

Introduction

1. Vaccines

Infectious diseases have plagued humans throughout history. Nowadays, they continue to be among the principal causes of morbidity and mortality in humans. The development of efficient vaccines that specifically provide an active immunity to a specific disease caused by an infective pathogen has proven capital to protect individuals. However, this falls short if governments do not foster vaccination campaigns for combating these diseases. To this purpose, strategies such as the One Health approach have emerged with the aim to implement programs, legislation, policies and research to achieve better public health outcomes [1]. This is an initiative of the World Health Organization to fight infectious diseases by raising food safety levels, the control of zoonoses and the combat of antibiotic resistances. The application of these strategies as well as consciousness-raising of the benefits of vaccination are of upmost importance in the process to eradicate infectious diseases.

1.1. *Viral vaccines*

Since Edward Jenner's observation that cowpox virus administration to healthy individuals protected them from smallpox, the field of vaccinology has substantially advanced [2]. So far, most of the current preventive vaccines consist of live-attenuated or inactivated viruses. Live-attenuated vaccines are based on viruses that have lost their virulence but maintain their protective immunity. This is normally accomplished by the selection of reassorted mutants under several rounds in cell culture. This type of vaccine can elicit efficient humoral and cellular immune responses, but their use is limited in some cases since it is not always possible to identify a sufficiently attenuated strain and they have a risk of reversion to a virulent strain [3]. Inactivated vaccines require a chemical or heat inactivation process that render the virus unable to replicate, but viral antigens remain unaltered to trigger the immune system response. Their inability to replicate *in vivo* makes them less immunogenic than their live-attenuated counterparts and their activity is generally enhanced by combination with adjuvants [4]. Other strategies have been employed to circumvent the possible adverse effects of these vaccines. The production of soluble

antigens either by culture purification or recombinant expression has been used in some cases but it is frequently required the addition of an adjuvant to enhance the immunogenicity.

New vaccination strategies have focused on improving the potency and safety of vaccines. Nucleic acid vaccines, which are based on the delivery of a target DNA or RNA encoding a viral antigen, have shown a low efficiency in stimulating the immune system and also in the level of cellular uptake [5]. The development of viral vectored vaccines to target a specific cell type through virus engineering has allowed to improve the uptake efficiency of nucleic acids. Nevertheless, some of these viral vectors have a limited nucleic acid packaging capacity and others have reported a strong immunity against the viral vector itself that limits their effectiveness [6]. Virus-like particles (VLPs) emerged as system to retain the native virus conformation and thus increase the innate and adaptative immune responses [7]. Moreover, the great benefit of this type of vaccines is that the outer viral protein structure is maintained while keeping a high safety profile due to absence of viral genomic material. These characteristics have attracted the interest on VLPs as an efficient vaccine conformation in the last years.

1.2. *Virus-like particles*

VLPs are complex nanoparticles formed by a highly ordered repetitive assembly of viral proteins that mimic the natural virus configuration. As they are devoid of viral genetic material, they are unable to infect nor replicate. Considering their structure, VLPs can be classified as non-enveloped and enveloped (Figure 1).

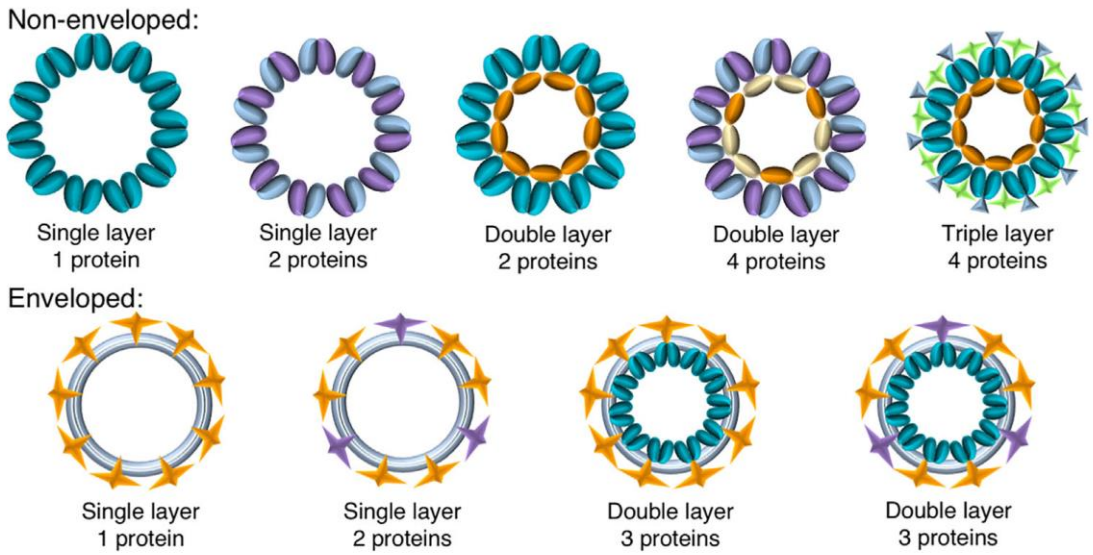

Figure 1. Single and multiple-layered configurations for non-enveloped and enveloped VLPs [8].

Non-enveloped VLPs consist of a single or multiple protein configuration. The more simple structures, single layer and reduced number of proteins, can be produced in prokaryotic systems and even assembled in a cell-free environment [9]. Multi-layered VLPs demand a higher processing complexity by the host cell and typically require from eukaryotic systems such as yeast, plants but preferentially animal cell lines. For instance, this is the case of multiple subunit VLPs from rotavirus [10] and poliovirus [11]. Some VLP types are surrounded by a lipid membrane acquired from the production host, the so-called enveloped VLPs [12]. This type of VLPs can contain different glycoproteins embedded in their surface which normally increase the immunogenicity. Influenza VLPs [13], human immunodeficiency virus (HIV) [14] and Ebola VLPs [15] are well-studied examples of enveloped VLPs.

Their use as vaccines has gone from promise to reality leading to a variety of licensed recombinant products for animal and human use (Figure 2), and many others are currently under investigation in clinical trials [16,17]. One VLP vaccine has been approved for veterinary use based on porcine circovirus type 2, commercially known as Porcilis® PCV [18]. Also, available vaccines for human diseases include: hepatitis B virus (Elovac®, Engerix®, Genevac®, Shanvac® and Recombivax®), human papillomavirus (Gardasil® and Cervarix®) and hepatitis E virus (Hecolin®) [19].

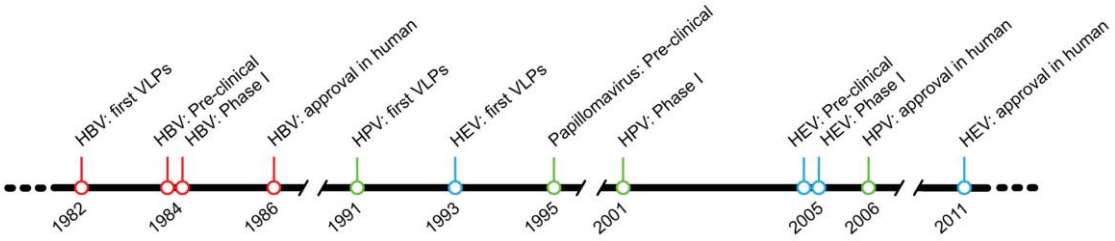

Figure 2. Timeline of approved VLP-based vaccines for human use [20].

1.3. *HIV-1 Gag VLPs*

There are basically two principal HIV serotypes, HIV-1 that accounts for approximately the 95% of all acquired immune deficiency syndrome (AIDS) infections worldwide, and HIV-2, which is less infectious and has a slower infection progression [21]. Most of the knowledge currently available is associated to serotype 1. In both cases, the group-specific antigen (Gag) polyprotein has been observed to travel to the vicinity of the plasma membrane of host cells upon expression, where it is able to self-assemble with other Gag monomers and bud from cells in the form of VLPs (Figure 3). VLP size generally fall in the range of 100 – 200 nm and their membrane composition is subjected to a certain extent of heterogeneity depending on the production host. The native Gag polyprotein is structured into four different smaller proteins (MA, CA, NP and LI) in the original infective virus but Gag remains unprocessed if not complementary viral proteins are expressed. The unprocessed Gag itself is able to interact with the plasma membrane through the myristic acid within the MA protein [22] and it is able to multimerize with other Gag polyproteins through the C-terminal part of the CA protein [23].

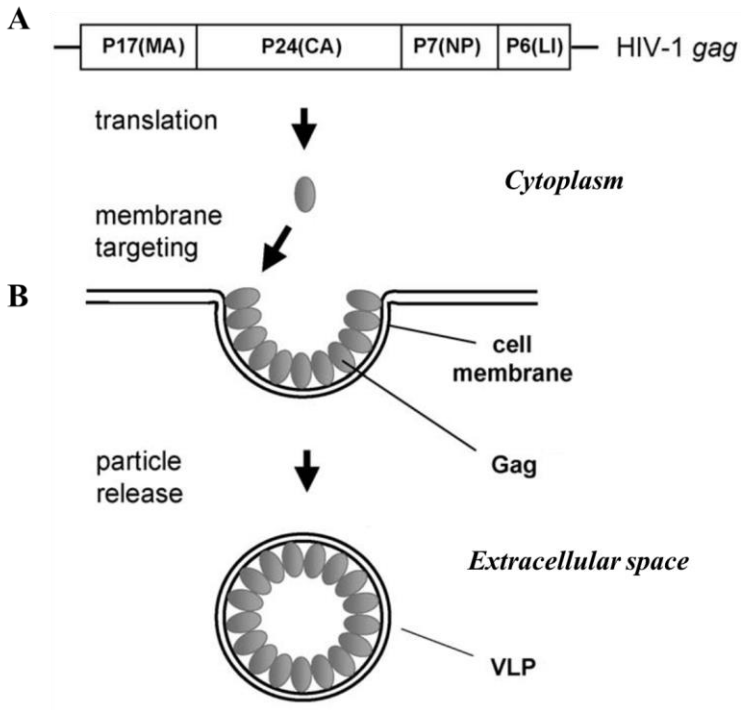

Figure 3. Gag structure and diagram representing the Gag VLP formation process. (A) Pr55Gag polyprotein integrating elements: p17 matrix protein (MA), p24 capsid protein (CA), p7 nucleocapsid protein (NP) and p6 linker protein (LI). (B) Schematic representation of the Gag VLP production process, from Gag polyprotein expression to release in the form of VLPs [24].

The properties of Gag VLPs makes them an interesting platform with multiple applications. These nanoparticles have the capacity to present envelope HIV proteins either by co-expression [25], as a fusion protein with the *gag* gene [26] or by chemical conjugation to specific peptides to boost their immunity [27]. Their robust structure has also shown an attractive means for the production of multivalent vaccines. In this sense, Gag can serve as a core scaffold for antigens targeting other diseases [28] or membrane receptors for drug discovery [29]. Moreover, cancer receptors have been incorporated on the surface of these VLPs to target specific tumors [30]. Advances have also been made in the use of Gag VLPs as nanocages, with successful results in the delivery of drugs [31], proteins [32] and nucleic acids [33]. All these possibilities have posited Gag VLPs on the edge of innovation in treatments and technologies for modern life.

2. Platforms and strategies for VLP production

VLPs have been produced in a variety of expression systems including bacteria, yeast, animal cells and plants. Bacteria and yeast are normally selected to produce non-enveloped VLPs requiring non or few post-translational modifications (PTMs) since they are the most productive platforms. However, bacteria and yeast to a lower extent are less adequate to produce more complex VLPs or enveloped nanoparticles. In this situation, more versatile production systems such as animal cell lines and plants are preferred. As for HIV-1 Gag VLPs, yeast spheroplasts have been successfully employed after removing the cell wall [34]. However, this platform may not be the most appropriate to provide an adequate PTM pattern. Owing to advancements in the field of plant biotechnology, transgenic plants have also been used to produce Gag VLPs [35]. Despite their low-cost and safety, low VLP yields and long production times are nowadays limiting their application. Currently, mammalian and insect animal cell lines are the preferred hosts to produce these complex nanoparticles since high VLP amounts can be obtained with adequate PTMs. Although the glycosylation profile is similar, mammalian cells provide more human-like PTMs since insect cells mostly produce N-glycans with terminal mannose residues. Still, some studies have successfully addressed the production of "mammalianized" PTMs in insect cells [36,37]. On the other hand, insect cells offer a higher safety profile due to the absence of known pathogens for humans [38]. Also, higher VLP yields are generally obtained in insect cells when used in combination with the baculovirus expression vector system (BEVS). Nevertheless, baculovirus separation from Gag VLPs is a major drawback of the insect cell/BEVS although some progress has been reported by means of anion exchange chromatography [39]. Interestingly, some authors have reported that the baculovirus itself possesses an adjuvant activity that might be beneficial to stimulate an efficient immune response [40], but more research is required to elucidate if the neutralization capacity is not masked by the baculovirus itself or baculovirus-derived proteins.

2.1. *Insect cell lines*

The first immortalized insect cell lines were established in 1960s [41]. Ever since, insect cells have been used to produce different recombinant products, from very simple ones to complex

multi-layered nanoparticles. Most common insect cell lines employed to this purpose are derived from *Diptera* (flies) or *Lepidoptera* orders.

Basal media such as Grace's medium, TNM-FH or TC-100 were initially used to culture insect cells and these formulations have been improved yielding to several currently available commercial media [42]. Serum supplementation was a common practice in early stages of insect culture development but problems such as lot-to-lot inconsistency, limited supply and the risk of animal pathogen contamination shifted the interest to serum-free media. Protein hydrolysates emerged as a good alternative to serum but lot-to-lot variability was also reported [43]. Media development companies have focused their efforts on developing chemically defined media, which has been recently achieved with the ExpiSf medium, or minimizing the amount of protein hydrolysates such as in Sf900III medium.

Lepidopteran insect cells are the most used platform to produce recombinant products due to their susceptibility to baculovirus infection. They include cell lines derived from *Spodoptera frugiperda* such as Sf21 and Sf9 cells and others that have been exclusively developed for serum-free culture (ExpresSF+®) or chemically-defined media (ExpiSf9™). *Trichoplusia ni*-derived BTI-Tn5B1-4 (High Five™) and TN-368, and Bm-N from *Bombyx mori* have also been used for recombinant protein production. Dipteran insect cells such as *Drosophila melanogaster* S2 cells are typically employed in baculovirus-free production systems although it has been demonstrated that it is possible to use the BEVS to transduce them [44]. Recently, both insect orders have shown to be adventitiously infected by viruses but none of them has shown pathogenicity in humans [38]. Specifically, Sf-rhabdovirus have been observed to infect cell lines derived from *Spodoptera frugiperda* while nodavirus and entomobirnavirus have been reported for some *Trichoplusia ni* and *Drosophila*-derived cells, respectively. In this regard, new virus-free insect cell lines such as the Sf-RVN *Spodoptera frugiperda*-rhabdovirus negative [45] or the *Trichoplusia ni*-derived Tnms42 [46] have been developed.

2.2. *The baculovirus expression vector system*

Baculoviridae is a family of viruses divided in four genera that infect invertebrates, mostly belonging to the orders *Lepidoptera* (moths and butterflies) and *Diptera* (flies and mosquitoes). The genus *Alphabaculovirus* is one the most commonly used for recombinant protein expression in insect cells, specifically the *Autographa californica* multiple nucleopolyhedrovirus (*Ac*MNPV). The *Ac*MNPV genome is made of 134 Kbp and 154 open reading frames and it has also demonstrated to accommodate large heterologous DNA sequences [47].

Briefly, the baculovirus infection cycle can be divided in four phases: immediate early, delayed early, late and very late (Figure 4).

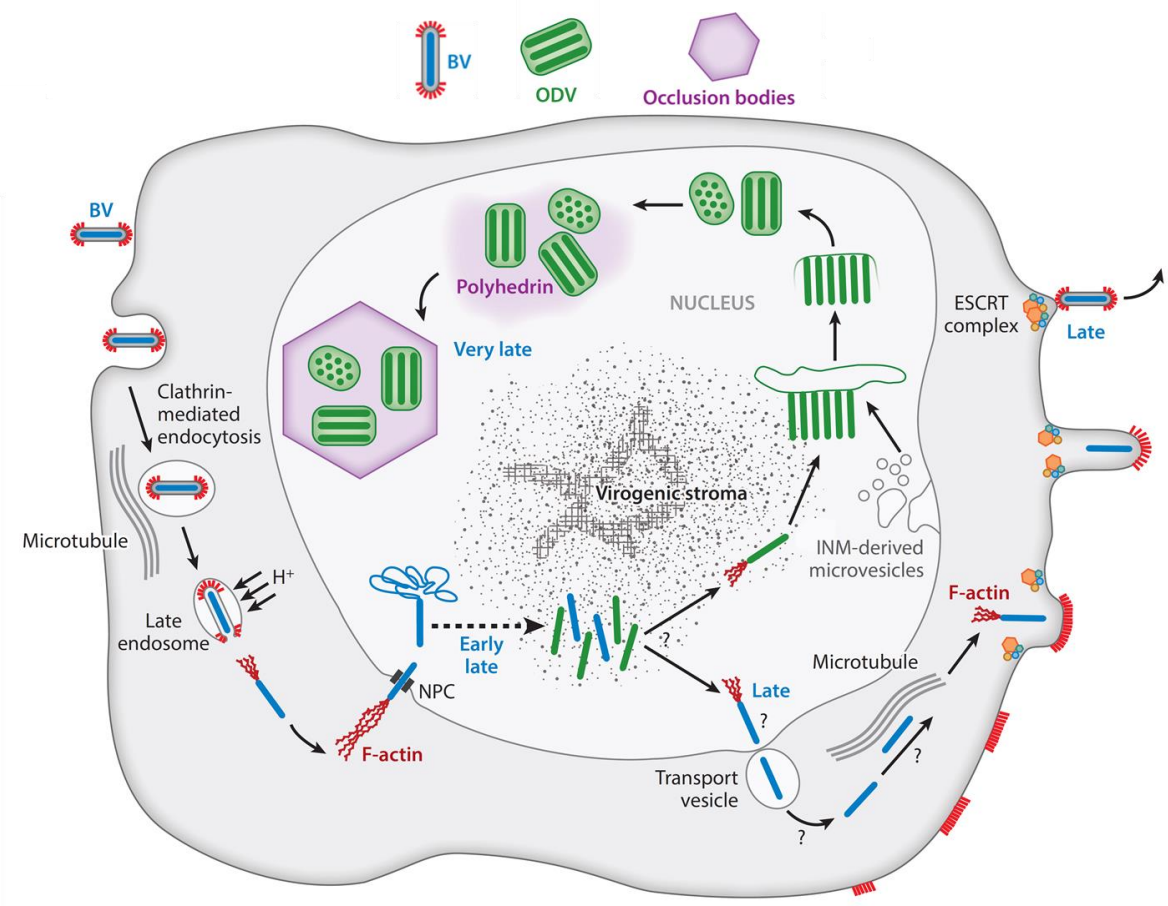

Figure 4. Representation of the *Ac*MNPV baculovirus infection life cycle in an insect cell. The different infection phases are represented: immediate early, early late (delayed early), late and very late, as well as the production process of the two baculovirus species including budded virus (BV or BudV) and the occlusion-derived virus (ODV). Briefly, following baculovirus binding and entry by clathrin-mediated endocytosis, the endosomes are transported to the nucleus and upon acidification of the endosome, the nucleocapsid is released. Nucleocapsid uncoating in the nucleus enables viral gene expression and formation of the progeny nucleocapsids. Some of these nucleocapsids egress from the nucleus and travel to the insect cell membrane where they bud in the form of BV via the ESCRT pathway. Nucleocapsids that remain inside the nucleus interact with the INM to eventually form ODVs. These ODVs are subsequently occluded to form OBs but OB formation only takes place if the gene/s encoding for the structural proteins such as polyhedrin have not been replaced to produce heterologous recombinant proteins. ESCRT: endosomal sorting complex required for transport; INM: inner nuclear membrane; OB: occlusion bodies; NPC: nuclear pore complex; [48].

The first phase involves the use of the host cell machinery for transactivation while delayed early genes are activated by viral products synthesized during the previous phase. The late and very late stages require from virus-encoded polymerases and gene transcription occurs between 6 and 24 hpi and 18 to 72 hpi, respectively [49]. In these phases, structural nucleocapsid and envelope proteins are synthesised including the membrane-associated GP64 protein, which is essential for baculovirus infection. Two enveloped virion phenotypes have been found in most baculovirus species, the budded virus (BudV) and the occlusion-derived virus (ODV). The former is

responsible of spreading cell-to-cell baculovirus infection whereas the ODV is a resisting form of the virus to cope with the harsh external environment conditions and is normally formed by more than one nucleocapsid. Of note, the ODV phenotype is much less infectious than the BudV since it is GP64-free and does not play a major role in cell culture conditions [50].

Typically, the gene of interest (GOI) is placed after a very late strong promoter such as the *polh* or *p10* promoters. Several technologies are available to clone the GOI in a baculovirus vector and basically differ in the strategy followed to obtain the final viral vector [51,52]. Additionally, the BEVS can be used to transduce mammalian cells for protein expression. In this case, the *polh*/*p10* promoter is replaced by a mammalian promoter that enables flexible and efficient expression of recombinant products [53].

To date, the BEVS has been used to manufacture several biologicals with applications in cancer, gene therapy and in vaccination (Table 1).

Table 1. Marketed pharmaceutical products for human or animal use produced with the BEVS. Adapted from [54].

Product	Type	Target	Year licensed	Cell line
Bayovac® CFS (Bayer AG)	Subunit vaccine	Classic swine fever virus	2002	Sf9
Porcilis® Pesti (Merck)	Subunit vaccine	Classic swine fever virus	2004	Sf9
Porcilis® PCV (Merck)	VLP-based vaccine	Porcine circovirus type 2	2004	Sf9
Cervarix® (GlaxoSmithKline)	VLP-based vaccine	Human papillomavirus	2007	High Five®
Ingelvac CircoFLEX® (Boehringer Ingelheim)	Subunit / VLP-based vaccine	Porcine circovirus type 2	2009	expreSF+®
Provenge® (Dendreon)	Immunotherapy	Prostate cancer	2010	Sf21
Best-H5® (Boehringer Ingelheim)	Subunit vaccine	Avian influenza virus A H5N1	2012	expreSF+®
Glybera® (UniQure)[a]	Gene therapy	Lipoprotein lipase enzyme	2012-17	expreSF+®
Flublok® (Sanofi Pasteur)	Subunit vaccine	Seasonal influenza	2013	expreSF+®

[a]This product was discontinued in 2017

The expression of more complex nanoparticles such as HIV-1 Gag has also been addressed with Sf9 [55] and High Five cells [56]. Some progress has been made in the production of a vaccine against HIV based on Gag VLPs with the BEVS [57], but such vaccine is still not available.

However, the ease of production and robustness of Gag have opened multiple possibilities for the production of this polyprotein in this system.

2.3. *Transient gene expression*

The transient gene expression (TGE) process is a non-viral method in which a DNA plasmid/s encoding for one or various GOI is introduced into a host cell. The DNA plasmid does not integrate in the genome of the host cell unless an external pressure is exerted but remains in the nucleus as an episome. This causes that the expression of the GOI is lost over time upon cell replication. This approach is frequently used in initial stages of biopharmaceutical development to rapidly produce some amount of a product in development and also enables to easily screen different products simultaneously. Besides their use in process development, TGE is gaining increasing interest since it is used for "in house" recombinant production for a variety of applications. Moreover, several efforts have been made to improve the efficiency of TGE and increase production volumes, to the point of reaching early clinical and even production stages, especially for products not requiring large quantities for their final use, such in the case of gene therapies [58].

Several strategies have been developed for cell culture transfection and can be classified as physical and chemical methods. Electroporation and more recently magnetofection are the most used physical methods for TGE. The former is based on the application of an electric field in order to increase the permeability of the cell membrane allowing the incorporation of the target DNA. On the other side, magnetofection requires a magnetic force, usually with magnetic nanoparticles, to deliver DNA into target cells [59]. Both methods have been basically used at small scale since difficulties in processing large culture volumes are encountered. Chemical reagents are more appropriate for large scale production using TGE and can be divided into three types: calcium phosphate, cationic lipids and cationic polymers. Calcium phosphate was one of the first chemical reagents employed for TGE. It is generally used with adherent cell lines but it has also been optimized for transfection in suspension [60]. A common limitation of this reagent

is its incompatibility with serum-free media and the need to add serum to the culture as a manner to alleviate its toxic side effects. Cationic lipids are amphiphilic molecules that have demonstrated to achieve high transfection yields, particularly in mammalian cell lines. Despite their efficiency, their use has been relegated to small scale and stable cell line generation due to their high cost [61]. Cationic polymers, specially polyethylenimine (PEI), have been a breakthrough in the field of TGE. They differ from cationic lipids in the fact they are completely soluble in water since they do not contain any hydrophobic moiety. Given their polymeric nature, their synthesis can be customized to obtain different molecular weights. Their capacity to achieve high transfection yields in a variety of cell lines and their low-cost in comparison to cationic polymers have brought PEI to be the gold-standard for TGE purposes [62,63].

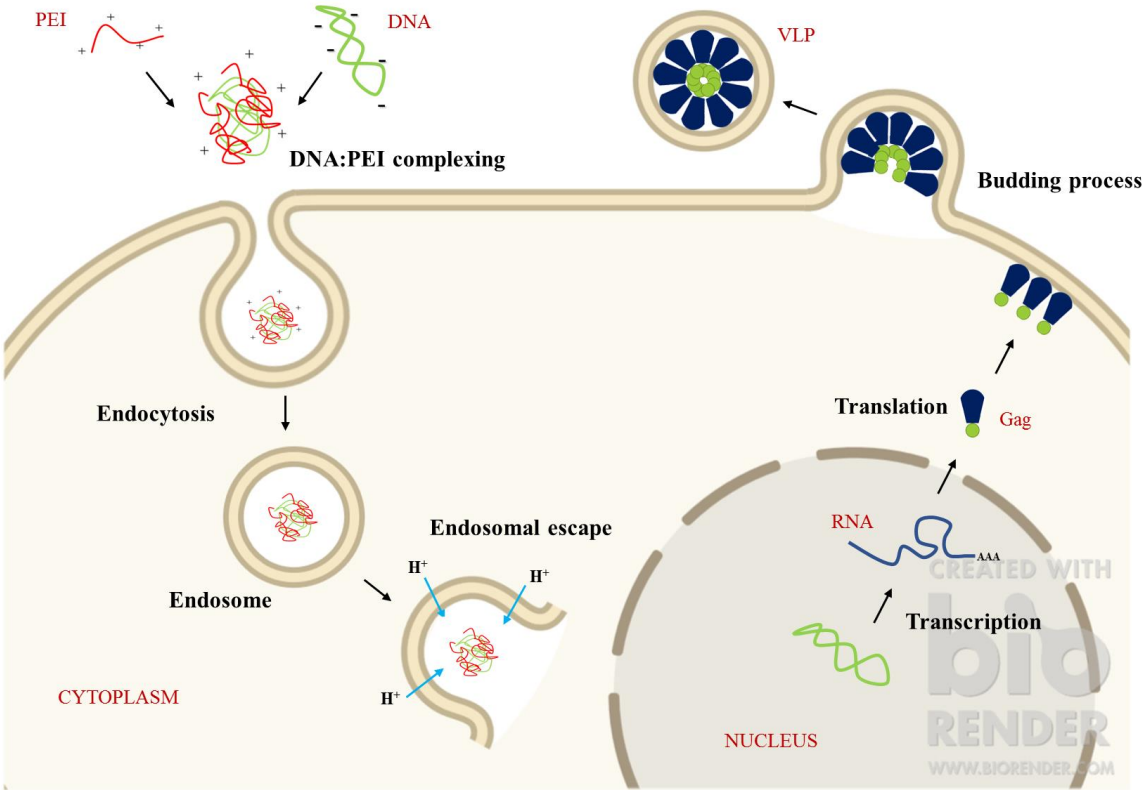

Figure 5. Schematic representation of the PEI-mediated transient gene expression process for Gag VLP production. Adapted from [64].

PEI-mediated TGE is based on the combination of the positively-charged PEI and the negatively-charged plasmid DNA harboring the GOI/s (Figure 5). The ability of PEI to condensate DNA through the amino-phosphate interactions is key to form a stable DNA:PEI complex with an

overall positive charge. The solution and time used for DNA and PEI complexing have also proven relevant since they determine the size, charge and stability of the complexes [65]. Several conditions including aqueous or hypertonic solutions have been previously used in animal cell transfection and the results have shown to be cell line dependent [66,67]. This indicates that the definition of the transfection conditions has to be independently assessed for each cell line [68].

Upon formation, the DNA:PEI complexes contact with the negatively-charged cell membrane and are incorporated by the cell via the clathrin or caveolae pathway [69,70]. DNA:PEI complexes are incorporated in endosome vesicles, and later complexes can escape through what is known as "proton sponge effect" by the buffer action of PEI [71]. Then, the DNA:PEI complexes can enter the nucleus where DNA is transcribed. The mechanism of entrance is not fully known yet and some evidences point in the direction of complexes entrance after nucleus membrane fragmentation during cell division [72] while other indicate that their incorporation is mediated via active transport [73]. Once transcribed, mRNA is transported to the cytoplasm where it is translated to the Gag polyprotein, which travels to the inner part of the plasma membrane where VLPs are formed and released through a budding process. Interestingly, it has been demonstrated that PEI-mediated delivery is very efficient to incorporate DNA:PEI complexes in almost all cells. However, not all cells are capable of expressing the delivered DNA possibly indicating a limiting step in the translocation of DNA:PEI complexes into the nucleus [64,74].

TGE has been widely tested and used in mammalian cell lines to produce different recombinant products [58], but few information is available about its performance in insect cell lines, especially in suspension culture conditions. The possibility to apply plasmid-mediated TGE in insect cells emerged from the discovery of baculovirus promoters that were immediately activated by host cell elements without requiring the presence of other baculovirus factors [75]. First studies were conducted with cationic lipids, but the elevated cost of these transfection reagents relegated their use to the small scale [76]. The boom of PEI in the field of mammalian cells made that some groups recently evaluated their performance in suspension culture of Sf9 [77] and High Five [78–81] cell lines. Hence, this baculovirus-free production strategy has opened up the possibility of

using insect cells and TGE as a system to produce VLPs, specially HIV-1 Gag VLPs, since problems related to the presence of baculovirus and baculovirus-derived proteins at the downstream stage will be avoided.

2.4. *Stable gene expression*

Stable gene expression (SGE) is based on the constitutive expression of a GOI/s. This production strategy is widely used in industry when a product of interest has been selected as the candidate for a bioprocess [82]. In contrast to TGE, stable expression allows for a constant production of the GOI and is also subjected to less process variability. However, it usually takes longer time lines to develop a platform for SGE. The process begins in the same way as TGE, by transiently transfecting the host cells with a DNA encoding for the GOI and afterwards a selection pressure is applied. The cell phenotype stably expressing the GOI is generally selected by means of adding an antibiotic or metabolic selectable marker [83].

Several strategies are available to integrate the GOI into the genome and can be divided in targeted and non-targeted gene integration. Targeted integration directs gene incorporation into a "hot-spot", a zone of the cell host genome with a high transcription rate. This approach enables that the GOI is specifically incorporated into these regions and normally only one copy is integrated. To this purpose, different methodologies are available including transcription activator-like effector nucleases (TALENs), zinc finger nucleases (ZFNs), meganucleases, recombinant-mediated cassette exchange (RMCE) [84] and clustered regularly interspaced short palindromic repeats associated to the Cas9 nuclease (CRISPR/Cas9) [85]. All these techniques rely on a double strand break at a certain sequence of the genome, allowing then the integration of the GOI by means of homologous recombination. Non-targeted integration is based on the incorporation of the GOI in an undefined region of the genome. Random integration and transposons are the two typical strategies for non-targeted integration. In both cases, the gene is randomly incorporated into the host cell genome, but transposons tend to incorporate to highly active transcription regions. The number of copies can greatly vary from cell-to-cell which is considered to add a higher degree of heterogeneity. The Piggy-Bac™ is the most widely used transposon for cell line

generation with successful results in insect [86] and mammalian cell lines [87]. However, this methodology is not always easily accessible due to intellectual property restrictions.

The development of stable cell lines is generally a laborious and long process that can take from two months to one year depending on the methodology used [83]. Specifically, this process involves that after transfection the selection pressure is maintained until a stable polyclonal expression is achieved. Then, the generation of a monoclonal cell line entails the separation of the cells one by one by limiting dilution, which is a very labor-intensive process. The appearance of automated technologies such as cell sorting have simplified this process. In parallel, the more the clones that are evaluated add better chances of selecting a high producer one. Then, the possibility to have access to high-throughput screening systems is especially relevant, but not always affordable, at this stage. After clonal selection, cells are grown and screened to select clones with high growth rates and production titers. From that, it is clear that one of the principal causes influencing most the process of cell line development is establishing a clonal cell line. In this sense, attention has focused on the use of stable polyclonal cell pools in recent years as a strategy to reduce the time line from gene transfer to recombinant product production [88,89]. Despite the higher heterogeneity of a stable cell pool in comparison to a stable cell line which is derived from a single cell clone, similar production titers can be achieved [90]. Furthermore, some authors have reported large genomic rearrangements of clonal cell lines that put into question their status as a genetically homogenic system [91,92]. In this regard, the development of stable cell pools by targeted and non-targeted gene integration methods is gaining increasing interest as a platform to produce recombinant products [93,94].

Insect cells lines have found their niche as stable producers for different recombinant products since they are easy to manipulate, can tolerate high levels of by-products and exhibit a fast cell growth [42]. Furthermore, some authors have reported better efficiencies in the production of secreted proteins using stable expression than with the BEVS [95]. Stable cell lines have also recently been developed for Gag VLP production in Sf9 [29,86] and Hi5 cell lines [96,97] as a strategy to improve the presentation of antigen and complex membrane proteins. Hence, the

development of stable insect cell pools can be an interesting approach for fast and stable production of different recombinant products including VLPs.

3. Methodologies to assess HIV-1 Gag VLP and nanoparticle production

The production of recombinant products in animal cell lines is associated to the concomitant expression of other undesired specimens. Although this might not be a problem for simple recombinant proteins, the characterization and quantification of complex nanoparticles such as Gag VLPs can be compromised to a certain extent. Extracellular vesicles (EVs) are heterogeneous membrane-enclosed structures that display similar biochemical properties and size to Gag VLPs. Besides their structural resemblance, there is evidence that Gag VLPs and EVs share several expression routes [98,99]. EVs are generally classified into shed microvesicles, exosomes and apoptotic vesicles, each of them differing in their biogenesis pathways [100]. Shedding microvesicles (150 – 1000 nm) are actively released from the cell plasma membrane through a budding process while apoptotic vesicles are generated by dying or apoptotic cells. On the other hand, exosomes are generally smaller (30 – 150 nm) and they are derived from multivesicular bodies (MVB) and secreted upon MVB fusion with the plasma membrane (Figure 6) [101].

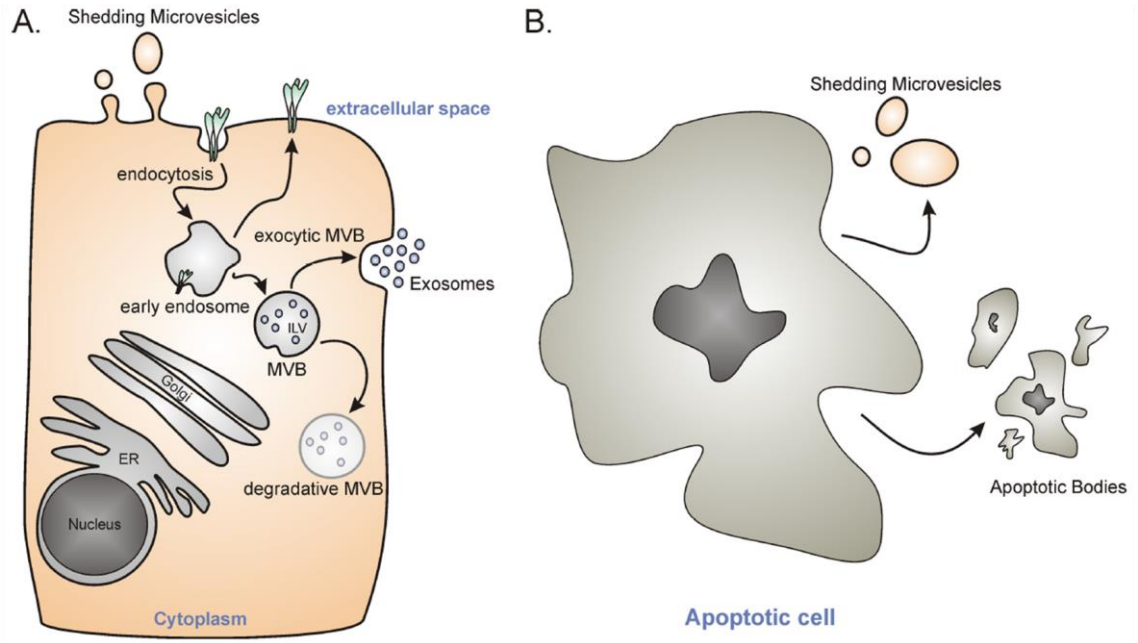

Figure 6. Extracellular vesicle biogenesis pathways. (A) Endocyted vesicles from the plasma membrane can be sorted back to the plasma membrane or become multivesicular bodies (MVB). These MVB contain intraluminal vesicles (ILV) that are generated from the MVB membrane and their fate can be a degradative lysosomal destruction or to release the ILVs to the milieu in the form of exosomes. Also, cells actively release microvesicles to the extracellular space through a budding process. (B) Dying cells can release shedding microvesicles in the early stages of apoptosis and larger vesicles (apoptotic bodies) at later times of cell degradation [99].

Over the past decade, EVs have attracted the attention of researches due to their capacity to mediate cell-to-cell communication via nucleic acids, lipids and proteins. However, most of the studies conducted so far are centred in the field of cancer research and little is known about their performance in cell culture-based processes, and sometimes are even ignored [102]. In addition to EVs, recent studies have also detected the presence of adventitious viruses persistently infecting some animal cell lines, which further increases the load of undesired nanoparticles. This varied mixture of nanoparticles, including the different baculovirus phenotypes if the BEVS is used as the production platform, has to be carefully considered to fully characterize the product purity and meet the requirements of regulatory agencies for its use.

Several analytical technologies are available for HIV-1 Gag VLP characterization and quantification. These can be classified into three main groups according to the properties under evaluation: biochemical, biophysical and biological (Table 2) [20].

Table 1. A summary of analytical technologies for Gag VLP-based vaccines. Adapted from [20,103,104].

Property	Technique	Type of method	Properties analyzed
Biochemical	Mass spectrometry	Indirect	Purity Composition Molecular weight Identification
	RP-HPLC	Direct	
	SDS-PAGE	Indirect	
	Immunoblotting	Indirect	
	BCA or Bradford	Indirect	
	Protein sequencing	Indirect	
Biophysical	TEM	Direct	Size Quantification Purity Morphology Polydispersity Density Aggregation
	Cryo-TEM		
	SEM		
	Confocal microscopy		
	AFM		
	DLS		
	NTA		
	MALS		
	Disc centrifugation		
	RPS		
	Density gradient		
	ES-DMA		
	Flow virometry		
	NAGE		
Biological	ELISA	Indirect	Quantification Antibody binding
	LSPR	Direct	
	Spectrofluorometry	Indirect	

RP-HPLC: reversed phase high-performance liquid chromatography. SDS-PAGE: sodium dodecyl sulphate polyacrylamide gel electrophoresis. BCA: bicinchoninic acid. TEM: transmission electron microscopy. Cryo-TEM: cryogenic transmission electron microscopy. SEM: scanning electron microscopy. AFM: atomic force microscopy. DLS: dynamic light scattering. NTA: nanoparticle tracking analysis. MALS: multiangle light scattering. RPS: resistive pulse sensing. ES-DMA: electrospray-differential mobility analysis. NAGE: native agarose gel electrophoresis. ELISA: enzyme-linked immunosorbent assay. LSPR: localized surface-plasmon resonance.

Methods relying on the measurement of virus infectivity (TCID50, plaque assay, end-point dilution assay) or viral genome quantification (qPCR, RT-qPCR) are not adequate for VLP quantification since these nanoparticles are non-infective and do not contain a viral genome [103]. The most traditional techniques are based on the identification of protein monomers, such as ELISA or Western blot. However, these methodologies do not consider Gag VLPs as a

nanoparticle but rely on the detection of their individual components. Therefore, it is difficult to differentiate between assembled and non-assembled monomers and the evaluation of VLP titers is hindered. In addition, the presence of nanoparticle populations other than VLPs is often not considered.

Transmission electron microscopy (TEM) has been frequently used to characterize VLP productions. TEM usually requires sample staining, usually uranyl acetate, for proper nanoparticle visualization but this can lead to the introduction of artifacts and an alteration of the native particle morphology. Over the last years, cryogenic electron microscopy (Cryo-EM) has emerged as a tool for sample visualization with unaltered properties [105]. The different particle structures can be resolved at higher level and a better differentiation between VLPs and EVs is possible. Nonetheless, some technical expertise is required, and it is not always possible to have these equipments at disposal.

Novel technologies have appeared that enable quantifying the size and concentration of nanoparticles in a short window of time. Among them, dynamic light scattering (DLS) [106], nanoparticle tracking analysis (NTA) [107], resistive pulse sensing (RPS) [108] and flow virometry [109] are becoming increasingly popular in the field nanobiotechnology. However, these techniques cannot distinguish between VLPs and other nanoparticles, for instance EVs, that fall in the same size range. This can lead to an overestimation of the real number of VLPs and a misinterpretation of the nanoparticle populations in the sample. VLP purification is one option to ensure a more reliable quantification but, although some progress has been made by chromatographic procedures [110,111], it is still difficult to achieve a complete separation from the other contaminating nanoparticles. Combining different techniques to analyze VLP production and the presence of other nanoparticle populations is probably the most reasonable approach to determine the real titers. Staining with antibodies targeting specific markers of the VLP membrane or the fusion of the Gag polyprotein with a fluorescent reporter protein can also help in this respect. Gag fusion to the enhanced green fluorescent protein (eGFP) has proved to be a useful strategy to generate fluorescent VLPs with a reduced impact in their structure [112].

This methodology has been applied as an indirect measurement of the VLP concentration (fluorescence) in a sample but, although it is significantly faster than conventional techniques, it also fails in the discrimination of assembled and non-assembled monomer [113]. Nonetheless, the fluorescent tag itself introduces the possibility of direct VLP evaluation with the aforementioned new technologies and their discrimination from non-fluorescent nanoparticle populations. In addition, the combined use with other analytical technologies can improve the characterization of other non-fluorescent populations, for example with analytical or density gradient ultracentrifugation [114] or asymmetric flow field-flow fractionation coupled to multiangle light scattering [115]. Confocal microscopy has also benefited from fluorescent tagging for a variety of applications [116]. The development of super-resolution confocal microscopy has enabled to surpass the Abbe's diffraction limit (~250 nm) [117,118] and it is now possible to apply this methodology to evaluate VLPs (González-Domínguez, I., in preparation).

The implementation of these new methodologies in combination with traditional ones represents an advancement to characterize and quantify VLPs. However, there is still a long way to go in order to universalize VLP quantification and fully distinguish the different nanoparticle populations arising from cell culture-based processes.

4. Rational optimization

4.1. *Design of Experiments*

Quite often, experimentation is conducted by monitoring the effect of one-factor-at-a-time (OFAT) on an objective response. This is normally achieved by changing one parameter while maintaining the others unaltered. Design of experiments (DoE) is an experimental approach dedicated to understanding and improving the performance of a given process or system [119]. The fundaments behind this methodology rely on the geometric distribution of the experiments integrating the DoE as a manner to capture the synergies between factors, otherwise not possible by means OFAT methods. Moreover, besides the possibility of detecting factor interactions, the number of experiments is significantly reduced with DoE compared to OFAT. The different

experiments of a DoE allow for a better precision and provide more information which, in practical terms, imply less work and offer higher quality data. Since Fisher's first proposal of DoE as an approach to rationally identify the drivers of a system, different areas have been developed, including factor screening, response surface methodology [120], quality control [121] and design optimality [122].

The principal goal of experimentation is to determine the effect of several input factors (independent variables) on a target response (dependent variable). In preliminary phases of process development with many factors to be analyzed, it is necessary to evaluate which of these variables are important and which are not. Factorial and fractional factorial designs are commonly used to this purpose because they are efficient and require a reduced number of experiments. This type of designs normally contains two levels for each variable under evaluation which simplifies their analysis. A special case of these designs that has been widely applied for compound screening is the Plackett-Burman design [123,124]. At a certain point, the determination of the optimal conditions for a number of factors of interest is required, and Response Surface Methodologies (RSM) are generally used to this end. A minimum of three levels for each variable is required, providing a higher degree of potency and sophistication to the models. The analysis of these type of designs is generally performed by means of second-order polynomial equations and three-dimensional plots are often constructed to facilitate model interpretation. Different types of designs are grouped into this category, including full three-level factorial designs, Box-Behnken designs (BBD), Uniform Shell designs (Doehlert designs) and Central Composite designs (CCD) [125]. Among them, BBD and CCD have acquired a remarkable acceptance as optimization techniques in the field of cell culture [108,126,127].

Although the use of DoE has been intensified in the last few years, their application as a method to improve the performance of cell culture-based process is still scarce. Several studies have been conducted in the search of optimal baculovirus infection, transfection and supplementation conditions in insect cells by means of OFAT experiments [55,128,129]. However, the analysis of the synergies between the different factors influencing the objective response cannot be fully

evaluated. In this sense, a window of opportunity appears for DoE as a tool to optimize these production systems and its potential has been intensively used in this thesis.

4.2. *Multiple response optimization*

An interesting approach to follow for a better comprehension of the system or process under evaluation is the inclusion of more than one objective response. In such case, it is possible that the optimal conditions for each of the responses fall in different regions of the design space and it is then required to find a compromise solution [130]. If the number of factors and responses in the study is kept at a low level, visual inspection of the overlapping areas for each model can be a good solution [131]. However, this method is not the best option if the numerical scales of the different models are distant since they might not intersect themselves. A solution to this problem was proposed by Derringer and Suich who developed the concept of "desirability function" [132]. The idea underlying this function is the definition of a global optimum response that depends on the different responses integrating the study and provides the best value of compromise in a joint response. To overcome the numerical scale problem, a minimum and maximum interval of each objective response is defined and then the responses are transformed to an equivalent dimensionless scale. The importance of the different responses in the global desirability function is assigned by an individual weight according to the priorities of the researcher. Low weight values indicate that it is not strictly required for the objective response to be near the target value. Conversely, higher weight values put more pressure on the response since unless it is very close to the target value, its value will be low. After weight assignation is accomplished, all the transformed responses are combined into a global desirability function to identify the best joint response. The higher the restrictions of the responses, the more difficult will be the determination of a subset of variable values that satisfy the global desirability function. The use of desirability functions has been mainly restricted to the field of chemistry [133,134], but it is gaining an increasing acceptation in the field of biology as a tool for multiple response optimization [135,136].

In this thesis, the production of Gag VLPs in Sf9 and High Five insect cells has been optimized and characterized with different expression approaches. To this purpose, a combination of DoE and desirability functions with direct nanoparticle quantification techniques is applied. The Gag polyprotein is fused in frame to eGFP to facilitate VLP detection, quantification and discrimination from other nanoparticle populations. Initially, an analysis of both insect cells as platforms to produce GageGFP VLPs with the BEVS is performed. Second, the optimal conditions for GageGFP VLP production are determined in each cell line and compared based on two criteria: quantity and quality. Third, a PEI-mediated TGE method is developed for each cell line to produce GageGFP VLPs as a strategy to avoid the production of baculoviruses and associated proteins. Finally, the development of stable cell pools is evaluated as a strategy to constitutively produce GageGFP VLPs.

References

[1] M. Rock, B.J. Buntain, J.M. Hatfield, B. Hallgrímsson, Animal-human connections, "one health," and the syndemic approach to prevention, Soc. Sci. Med. 68 (2009) 991–995.

[2] S. Plotkin, History of vaccination, Proc. Natl. Acad. Sci. U. S. A. 111 (2014) 12283–12287.

[3] J.B. Ulmer, U. Valley, R. Rappuoli, Vaccine manufacturing: challenges and solutions, Nat. Biotechnol. 24 (2006) 1377–1383.

[4] S.A. Plotkin, Vaccines: past, present and future, Nat. Med. 11 (2005) S5–S11.

[5] D. Hobernik, M. Bros, DNA Vaccines—How Far From Clinical Use?, Int. J. Mol. Sci. 19 (2018).

[6] H. Jeong, B.L. Seong, Exploiting virus-like particles as innovative vaccines against emerging viral infections, J. Microbiol. 55 (2017) 220–230.

[7] A. Roldao, M.C. Mellado, L.R. Castilho, M.J. Carrondo, P.M. Alves, Virus-like particles in vaccine development, Expert Rev. Vaccines. 9 (2010) 1149–1176.

[8] X. Ding, D. Liu, G. Booth, W. Gao, Y. Lu, Virus-Like Particle Engineering: From Rational Design to Versatile Applications, Biotechnol. J. 13 (2018) 1700324.

[9] B.C. Bundy, M.J. Franciszkowicz, J.R. Swartz, Escherichia coli-based cell-free synthesis of virus-like particles, Biotechnol. Bioeng. 100 (2008) 28–37.

[10] H.L.A.A. Vieira, C. Estêvão, A. Roldão, C.C. Peixoto, M.F.Q.Q. Sousa, P.E. Cruz, M.J.T.T. Carrondo, P.M. Alves, Triple layered rotavirus VLP production: Kinetics of vector replication, mRNA stability and recombinant protein production, J. Biotechnol. 120 (2005) 72–82.

[11] S. Bräutigam, E. Snezhkov, D.H.L. Bishop, Formation of Poliovirus-like Particles by Recombinant Baculoviruses Expressing the Individual VP0, VP3, and VP1 Proteins by Comparison to Particles Derived from the Expressed Poliovirus Polyprotein, Virology. 192 (1993) 512–524.

[12] F. Pitoiset, T. Vazquez, B. Bellier, Enveloped virus-like particle platforms: vaccines of the future?, Expert Rev. Vaccines. 14 (2015).

[13] M. Keshavarz, H. Mirzaei, M. Salemi, F. Momeni, M.J. Mousavi, M. Sadeghalvad, Y. Arjeini, F. Solaymani-Mohammadi, J. Sadri Nahand, H. Namdari, T. Mokhtari-Azad, F. Rezaei, Influenza vaccine: Where are we and where do we go?, Rev. Med. Virol. 29 (2019) e2014.

[14] L.X. Doan, M. Li, C. Chen, Q. Yao, Virus-like particles as HIV-1 vaccines, Rev. Med. Virol. 15 (2005) 75–88.

[15] K.L. Warfield, M.J. Aman, Advances in virus-like particle vaccines for filoviruses., J. Infect. Dis. 204 Suppl 3 (2011) S1053-9.

[16] E. Crisci, J. Bárcena, M. Montoya, Virus-like particles: The new frontier of vaccines for animal viral infections, Vet. Immunol. Immunopathol. 148 (2012) 211–225.

[17] N. Kushnir, S.J. Streatfield, V. Yusibov, Virus-like particles as a highly efficient vaccine platform: Diversity of targets and production systems and advances in clinical development, Vaccine. 31 (2012) 58–83.

[18] J.A. Mena, A.A. Kamen, Insect cell technology is a versatile and robust vaccine manufacturing platform, Expert Rev. Vaccines. 10 (2011) 1063–1081.

[19] B. Donaldson, Z. Lateef, G.F. Walker, S.L. Young, V.K. Ward, Virus-like particle vaccines: immunology and formulation for clinical translation, Expert Rev. Vaccines. 17 (2018) 833–849.

[20] L.H.L. Lua, N.K. Connors, F. Sainsbury, Y.P. Chuan, N. Wibowo, A.P.J. Middelberg, Bioengineering virus-like particles as vaccines, Biotechnol. Bioeng. 111 (2014) 425–440.

[21] J. Esbjörnsson, F. Månsson, A. Kvist, Z.J. da Silva, S. Andersson, E.M. Fenyö, P.-E. Isberg, A.J. Biague, J. Lindman, A.A. Palm, S.L. Rowland-Jones, M. Jansson, P. Medstrand, H. Norrgren, B. Sweden and Guinea-Bissau Cohort Research Group, A.J. Biague, A. Biai, C. Camara, J. Esbjörnsson, M. Jansson, S. Karlson, J. Lindman, P. Medstrand, F. Månsson, H. Norrgren, A.A. Palm, G.Ö. Sahin, Z.J. da Silva, S. Wilhelmson, Long-term follow-up of HIV-2-related AIDS and mortality in Guinea-Bissau: a prospective open cohort study., Lancet. HIV. 6 (2018) e25–e31.

[22] H.G. Göttlinger, J.G. Sodroski, W.A. Haseltine, Role of capsid precursor processing and

myristoylation in morphogenesis and infectivity of human immunodeficiency virus type 1., Proc. Natl. Acad. Sci. U. S. A. 86 (1989) 5781–5.

[23] J.B.M. Jowett, D.J. Hockley, M. V. Nermut, I.M. Jones, Distinct signals in human immunodeficiency virus type 1 Pr55 necessary for RNA binding and particle formation, J Gen Virol. 73 (Pt 12 (1992) 3079–3086.

[24] L. Deml, C. Speth, M.P. Dierich, H. Wolf, R. Wagner, Recombinant HIV-1 Pr55 gag virus-like particles: Potent stimulators of innate and acquired immune responses, Mol. Immunol. 42 (2005) 259–277.

[25] J. Hammonds, X. Chen, T. Fouts, A. DeVico, D. Montefiori, P. Spearman, Journal of Virology, J. Virol. 69 (2005) 4628–4632.

[26] J.C. Griffiths, S.J. Harris, G.T. Layton, E.L. Berrie, T.J. French, N.R. Burns, S.E. Adams, A.J. Kingsman, Hybrid human immunodeficiency virus Gag particles as an antigen carrier system: induction of cytotoxic T-cell and humoral responses by a Gag:V3 fusion., J. Virol. 67 (1993) 3191–8.

[27] H. Rostami, M. Ebtekar, M.S. Ardestani, M.H. Yazdi, M. Mahdavi, Co-utilization of a TLR5 agonist and nano-formulation of HIV-1 vaccine candidate leads to increased vaccine immunogenicity and decreased immunogenic dose: A preliminary study, Immunol. Lett. 187 (2017) 19–26.

[28] A. Venereo-Sanchez, R. Gilbert, M. Simoneau, A. Caron, P. Chahal, W. Chen, S. Ansorge, X. Li, O. Henry, A. Kamen, Hemagglutinin and neuraminidase containing virus-like particles produced in HEK-293 suspension culture: An effective influenza vaccine candidate, Vaccine. 34 (2016) 3371–3380.

[29] J. Vidigal, B. Fernandes, M.M. Dias, M. Patrone, A. Roldão, M.J.T. Carrondo, P.M. Alves, A.P. Teixeira, RMCE-based insect cell platform to produce membrane proteins captured on HIV-1 Gag virus-like particles, Appl. Microbiol. Biotechnol. 102 (2018) 655–666.

[30] R. Cubas, S. Zhang, M. Li, C. Chen, Q. Yao, Chimeric Trop2 virus-like particles: A potential immunotherapeutic approach against pancreatic cancer, J. Immunother. 34 (2011) 251–263.

[31] V.K. Deo, T. Kato, E.Y. Park, Chimeric Virus-Like Particles Made Using GAG and M1 Capsid Proteins Providing Dual Drug Delivery and Vaccination Platform, Mol. Pharm. 12 (2015) 839–845.

[32] S.J. Kaczmarczyk, K. Sitaraman, H. a Young, S.H. Hughes, D.K. Chatterjee, Protein delivery using engineered virus-like particles, October. 108 (2011) 16998–17003.

[33] I. Voráčková, P. Ulbrich, W.E. Diehl, T. Ruml, Engineered retroviral virus-like particles for receptor targeting, Arch. Virol. 159 (2014) 677–688.

[34] S. Sakuragi, T. Goto, K. Sano, Y. Morikawa, HIV type 1 Gag virus-like particle budding from spheroplasts of Saccharomyces cerevisiae., Proc. Natl. Acad. Sci. U. S. A. 99 (2002) 7956–61.

[35] S.A. Kessans, M.D. Linhart, N. Matoba, T. Mor, Biological and biochemical characterization of HIV-1 Gag/dgp41 virus-like particles expressed in Nicotiana benthamiana., Plant Biotechnol. J. 11 (2013) 681–90.

[36] D. Palmberger, I.B.H. Wilson, I. Berger, R. Grabherr, D. Rendic, Sweetbac: A new approach for the production of mammalianised glycoproteins in insect cells, PLoS One. 7 (2012) 1–8.

[37] R.L. Harrison, D.L. Jarvis, Protein N-Glycosylation in the Baculovirus-Insect Cell Expression System and Engineering of Insect Cells to Produce "Mammalianized" Recombinant Glycoproteins, in: Adv. Virus Res., 2006: pp. 159–191.

[38] C. Geisler, D.L. Jarvis, Adventitious viruses in insect cell lines used for recombinant protein expression, Protein Expr. Purif. 144 (2018) 25–32.

[39] P. Gerster, E. Kopecky, N. Hammerschmidt, M. Klausberger, F. Krammer, R. Grabherr, C. Mersich, L. Urbas, P. Kramberger, T. Paril, M. Schreiner, K. Nöbauer, E. Razzazi-fazeli, A. Jungbauer, Purification of infective baculoviruses by monoliths, J. Chromatogr. A. 1290 (2013) 36–45.

[40] S. Heinimäki, K. Tamminen, M. Malm, T. Vesikari, V. Blazevic, Live baculovirus acts as a strong B and T cell adjuvant for monomeric and oligomeric protein antigens, Virology. 511 (2017) 114–122.

[41] M.A. Brooks, T.J. Kurtti, Insect Cell and Tissue Culture, Annu. Rev. Entomol. 16 (1971) 27–52.

[42] L. Ikonomou, Y.-J. Schneider, S.N. Agathos, Insect cell culture for industrial production of recombinant proteins, Appl. Microbiol. Biotechnol. 62 (2003) 1–20.

[43] M.S.M.S. Donaldson, M.L.M.L. Shuler, Low-cost serum-free medium for the BTI-Tn5b1-4 insect cell line, Biotechnol. Prog. 14 (1998) 573–579.

[44] D.-F. Lee, C.-C. Chen, T.-A. Hsu, J.-L. Juang, A Baculovirus Superinfection System: Efficient Vehicle for Gene Transfer into Drosophila S2 Cells, J. Virol. 74 (2000) 11873–11880.

[45] A.B. Maghodia, C. Geisler, D.L. Jarvis, Characterization of an Sf-rhabdovirus-negative Spodoptera frugiperda cell line as an alternative host for recombinant protein production in the baculovirus-insect cell system, Protein Expr. Purif. 122 (2016) 45–55.

[46] K. Koczka, P. Peters, W. Ernst, H. Himmelbauer, L. Nika, R. Grabherr, Comparative transcriptome analysis of a Trichoplusia ni cell line reveals distinct host responses to intracellular and secreted protein products expressed by recombinant baculoviruses, J. Biotechnol. 270 (2018) 61–69.

[47] A. Contreras-Gómez, A. Sánchez-Mirón, F. García-Camacho, E. Molina-Grima, Y. Chisti, Protein production using the baculovirus-insect cell expression system, Biotechnol. Prog. 30 (2014) 1–18.

[48] G.W. Blissard, D.A. Theilmann, Baculovirus Entry and Egress from Insect Cells, Annu. Rev. Virol. 5 (2018) 113–139.

[49] A. Lu, P.J. Krell, J.M. Vlak, G.F. Rohrmann, Baculovirus DNA Replication, in: The Baculoviruses, Springer US, Boston, MA, 1997: pp. 171–191.

[50] D.E. Lynn, Comparative susceptibilities of twelve insect cell lines to infection by three baculoviruses, J. Invertebr. Pathol. 82 (2003) 129–131.

[51] F. Liu, X. Wu, L. Li, Z. Liu, Z. Wang, Use of baculovirus expression system for generation of virus-like particles: Successes and challenges, Protein Expr. Purif. 90 (2013) 104–116.

[52] P. Stolt-Bergner, C. Benda, T. Bergbrede, H. Besir, P.H.N. Celie, C. Chang, D. Drechsel,

A. Fischer, A. Geerlof, B. Giabbai, J. van den Heuvel, G. Huber, W. Knecht, A. Lehner, R. Lemaitre, K. Nordén, G. Pardee, I. Racke, K. Remans, A. Sander, J. Scholz, M. Stadnik, P. Storici, D. Weinbruch, I. Zaror, L.H.L. Lua, S. Suppmann, Baculovirus-driven protein expression in insect cells: A benchmarking study, J. Struct. Biol. 203 (2018) 71–80.

[53] A. Dukkipati, H.H. Park, D. Waghray, S. Fischer, K.C. Garcia, BacMam system for high-level expression of recombinant soluble and membrane glycoproteins for structural studies, Protein Expr. Purif. 62 (2008) 160–170.

[54] L.A. Palomares, M. Realpe, O.T. Ramírez, An Overview of Cell Culture Engineering for the Insect Cell-Baculovirus Expression Vector System (BEVS), in: Anim. Cell Cult., Springer, Cham, 2015: pp. 501–519.

[55] S. Pillay, A. Meyers, A.L. Williamson, E.P. Rybicki, Optimization of chimeric HIV-1 virus-like particle production in a baculovirus-insect cell expression system, Biotechnol. Prog. 25 (2009) 1153–1160.

[56] L. Buonaguro, F.M. Buonaguro, M.L. Tornesello, D. Mantas, E. Beth-Giraldo, R. Wagner, S. Michelson, M.C. Prevost, H. Wolf, G. Giraldo, High efficient production of Pr55gag virus-like particles expressing multiple HIV-1 epitopes, including a gp120 protein derived from an Ugandan HIV-1 isolate of subtype A, Antiviral Res. 49 (2001) 35–47.

[57] M.L. Visciano, L. Diomede, M. Tagliamonte, M.L. Tornesello, V. Asti, M. Bomsel, F.M. Buonaguro, L. Lopalco, L. Buonaguro, Generation of HIV-1 Virus-Like Particles expressing different HIV-1 glycoproteins, Vaccine. 29 (2011) 4903–4912.

[58] S. Gutierrez-Granados, L. Cervera, A.A. Kamen, F. Godia, Advancements in mammalian cell transient gene expression (TGE) technology for accelerated production of biologics., Crit. Rev. Biotechnol. 0 (2018) 1–23.

[59] U. Schillinger, T. Brill, C. Rudolph, S. Huth, S. Gersting, F. Krötz, J. Hirschberger, C. Bergemann, C. Plank, Advances in magnetofection—magnetically guided nucleic acid delivery, J. Magn. Magn. Mater. 293 (2005) 501–508.

[60] V. Jäger, K. Büssow, T. Schirrmann, Transient Recombinant Protein Expression in Mammalian Cells, in: Anim. Cell Cult., Springer, Cham, 2015: pp. 27–64.

[61] C. Liu, B. Dalby, W. Chen, J.M. Kilzer, H.C. Chiou, Transient Transfection Factors for High-Level Recombinant Protein Production in Suspension Cultured Mammalian Cells, Mol. Biotechnol. 39 (2008) 141–153.

[62] Z. Zhong, J. Feijen, M.C. Lok, W.E. Hennink, L. V. Christensen, J.W. Yockman, Y.H. Kim, S.W. Kim, Low molecular weight linear polyethylenimine-b-poly(ethylene glycol)-b-polyethylenimine triblock copolymers: Synthesis, characterization, and in vitro gene transfer properties, Biomacromolecules. 6 (2005) 3440–3448.

[63] A. V Ulasov, Y. V Khramtsov, G. a Trusov, A. a Rosenkranz, E.D. Sverdlov, A.S. Sobolev, Properties of PEI-based polyplex nanoparticles that correlate with their transfection efficacy., Mol. Ther. 19 (2011) 103–112.

[64] L. Cervera, I. González-Domínguez, M.M. Segura, F. Gòdia, Intracellular characterization of Gag VLP production by transient transfection of HEK 293 cells, Biotechnol. Bioeng. 114 (2017) 2507–2517.

[65] I. González-Domínguez, N. Grimaldi, L. Cervera, N. Ventosa, F. Gòdia, Impact of physicochemical properties of DNA/PEI complexes on transient transfection of mammalian cells, N. Biotechnol. 49 (2019) 88–97.

[66] Y. Sang, K. Xie, Y. Mu, Y. Lei, B. Zhang, S. Xiong, Y. Chen, N. Qi, Salt ions and related parameters affect PEI-DNA particle size and transfection efficiency in Chinese hamster ovary cells., Cytotechnology. 67 (2015) 67–74.

[67] F. Bollin, V. Dechavanne, L. Chevalet, Design of experiment in CHO and HEK transient transfection condition optimization, Protein Expr. Purif. 78 (2011) 61–68.

[68] E.V.B. Van Gaal, R. Van Eijk, R.S. Oosting, R.J. Kok, W.E. Hennink, D.J.A. Crommelin, E. Mastrobattista, How to screen non-viral gene delivery systems in vitro?, J. Control. Release. 154 (2011) 218–232.

[69] M.E. Hwang, R.K. Keswani, D.W. Pack, Dependence of PEI and PAMAM Gene Delivery on Clathrin- and Caveolin-Dependent Trafficking Pathways, Pharm. Res. 32 (2015) 2051–2059.

[70] M. Gillard, Z. Jia, J.J.C. Hou, M. Song, P.P. Gray, T.P. Munro, M.J. Monteiro,

Intracellular trafficking pathways for nuclear delivery of plasmid DNA complexed with highly efficient endosome escape polymers, Biomacromolecules. 15 (2014) 3569–3576.

[71] A. Akinc, M. Thomas, A.M. Klibanov, R. Langer, Exploring polyethylenimine-mediated DNA transfection and the proton sponge hypothesis, J. Gene Med. 7 (2005) 657–663.

[72] A.S. Tait, C.J. Brown, D.J. Galbraith, M.J. Hines, M. Hoare, J.R. Birch, D.C. James, Transient production of recombinant proteins by Chinese hamster ovary cells using polyethyleneimine/DNA complexes in combination with microtubule disrupting anti-mitotic agents, Biotechnol. Bioeng. 88 (2004) 707–721.

[73] X. Han, Q. Fang, F. Yao, X. Wang, J. Wang, S. Yang, B.Q. Shen, The heterogeneous nature of polyethylenimine-DNA complex formation affects transient gene expression, Cytotechnology. 60 (2009) 63–75.

[74] T. Bieber, W. Meissner, S. Kostin, A. Niemann, H.-P. Elsasser, Intracellular route and transcriptional competence of polyethylenimine-DNA complexes., J. Control. Release. 82 (2002) 441–54.

[75] M. Lu, R.R. Johnson, K. Iatrou, Trans-activation of a cell housekeeping gene promoter by the IE1 gene product of baculoviruses, Virology. 218 (1996) 103–113.

[76] F. Fernandes, J. Vidigal, M.M. Dias, K.L.J. Prather, A.S. Coroadinha, A.P. Teixeira, P.M. Alves, Flipase-mediated cassette exchange in Sf9 insect cells for stable gene expression, Biotechnol. Bioeng. 109 (2012) 2836–2844.

[77] X. Shen, D.L. Hacker, L. Baldi, F.M. Wurm, Virus-free transient protein production in Sf9 cells, J. Biotechnol. 171 (2013) 61–70.

[78] K. Mori, H. Hamada, T. Ogawa, Y. Ohmuro-matsuyama, T. Katsuda, H. Yamaji, Efficient production of antibody Fab fragment by transient gene expression in insect cells, J. Biosci. Bioeng. 124 (2017) 221–226.

[79] X. Shen, A.K. Pitol, V. Bachmann, D.L. Hacker, L. Baldi, F.M. Wurm, A simple plasmid-based transient gene expression method using High Five cells, J. Biotechnol. 216 (2015) 67–75.

[80] E. Puente-Massaguer, M. Lecina, F. Gòdia, Nanoscale characterization coupled to multi-

parametric optimization of Hi5 cell transient gene expression, Appl. Microbiol. Biotechnol. 102 (2018) 10495–10510.

[81] M. Bleckmann, M. Schürig, M. Endres, A. Samuels, D. Gebauer, N. Konisch, J. van den Heuvel, Identifying parameters to improve the reproducibility of transient gene expression in High Five cells, PLoS One. 14 (2019) e0217878.

[82] J. Zhu, Mammalian cell protein expression for biopharmaceutical production, Biotechnol. Adv. 30 (2012) 1158–1170.

[83] A.D. Bandaranayake, S.C. Almo, Recent advances in mammalian protein production, FEBS Lett. 588 (2014) 253–260.

[84] S. Turan, C. Zehe, J. Kuehle, J. Qiao, J. Bode, Recombinase-mediated cassette exchange (RMCE) - A rapidly-expanding toolbox for targeted genomic modifications, Gene. 515 (2013) 1–27.

[85] T. Gaj, C.A. Gersbach, C.F. Barbas, ZFN, TALEN, and CRISPR/Cas-based methods for genome engineering, Trends Biotechnol. 31 (2013) 397–405.

[86] A.G. Lynch, F. Tanzer, M.J. Fraser, E.G. Shephard, A.L. Williamson, E.P. Rybicki, Use of the piggyBac transposon to create HIV-1 gag transgenic insect cell lines for continuous VLP production, BMC Biotechnol. 10 (2010) 30.

[87] Y. Rajendra, R.B. Peery, G.C. Barnard, Generation of stable Chinese hamster ovary pools yielding antibody titers of up to 7.6 g/L using the piggyBac transposon system, Biotechnol. Prog. 32 (2016) 1301–1307.

[88] D.L. Hacker, S. Balasubramanian, Recombinant protein production from stable mammalian cell lines and pools, Curr. Opin. Struct. Biol. 38 (2016) 129–136.

[89] A. Poulain, S. Perret, F. Malenfant, A. Mullick, B. Massie, Y. Durocher, Rapid protein production from stable CHO cell pools using plasmid vector and the cumate gene-switch, J. Biotechnol. 255 (2017) 16–27.

[90] J. Ye, K. Alvin, H. Latif, A. Hsu, V. Parikh, T. Whitmer, M. Tellers, M.C. de la Cruz Edmonds, J. Ly, P. Salmon, J.F. Markusen, Rapid protein production using CHO stable transfection pools, Biotechnol. Prog. 26 (2010) 1431–1437.

[91] S. Vcelar, M. Melcher, N. Auer, A. Hrdina, A. Puklowski, F. Leisch, V. Jadhav, T. Wenger, M. Baumann, N. Borth, Changes in Chromosome Counts and Patterns in CHO Cell Lines upon Generation of Recombinant Cell Lines and Subcloning, Biotechnol. J. 13 (2018) 1700495.

[92] S. Vcelar, V. Jadhav, M. Melcher, N. Auer, A. Hrdina, R. Sagmeister, K. Heffner, A. Puklowski, M. Betenbaugh, T. Wenger, F. Leisch, M. Baumann, N. Borth, Karyotype variation of CHO host cell lines over time in culture characterized by chromosome counting and chromosome painting, Biotechnol. Bioeng. 115 (2018) 165–173.

[93] Y. Yang, M. You, F. Chen, T. Jia, Y. Chen, B. Zhou, Q. Mi, Z. An, W. Luo, N. Xia, Efficient development of a stable cell pool for antibody production using a single plasmid, J. Biochem. 163 (2018) 391–398.

[94] T. Okumura, K. Masuda, K. Watanabe, K. Miyadai, K. Nonaka, M. Yabuta, T. Omasa, Efficient enrichment of high-producing recombinant Chinese hamster ovary cells for monoclonal antibody by flow cytometry, J. Biosci. Bioeng. 120 (2015) 340–346.

[95] D.L. Jarvis, J.-A.G.W. Fleming, G.R. Kovacs, M.D. Summers, L.A. Guarino, Use of Early Baculovirus Promoters for Continuous Expression and Efficient Processing of Foreign Gene Products in Stably Transformed Lepidopteran Cells, Nat. Biotechnol. 8 (1990) 950–955.

[96] M. Tagliamonte, M.L. Visciano, M.L. Tornesello, A. De Stradis, F.M. Buonaguro, L. Buonaguro, HIV-Gag VLPs presenting trimeric HIV-1 gp140 spikes constitutively expressed in stable double transfected insect cell line, Vaccine. 29 (2011) 4913–4922.

[97] M. Tagliamonte, M.L. Visciano, M.L. Tornesello, A. De Stradis, F.M. Buonaguro, L. Buonaguro, Constitutive expression of HIV-VLPs in stably transfected insect cell line for efficient delivery system, Vaccine. 28 (2010) 6417–6424.

[98] E.N.-'t Hoen, T. Cremer, R.C. Gallo, L.B. Margolis, Extracellular vesicles and viruses: Are they close relatives?, Proc. Natl. Acad. Sci. U. S. A. 113 (2016) 9155.

[99] D.G. Meckes, N. Raab-Traub, N. Raab-Traub, Microvesicles and viral infection., J. Virol. 85 (2011) 12844–54.

[100] T. Wurdinger, N.N. Gatson, L. Balaj, B. Kaur, X.O. Breakefield, D.M. Pegtel, Extracellular Vesicles and Their Convergence with Viral Pathways, Adv. Virol. 2012 (2012) 1–12.

[101] M.V.S. Dias, C.S. Costa, L.L.P. daSilva, The Ambiguous Roles of Extracellular Vesicles in HIV Replication and Pathogenesis, Front. Microbiol. 9 (2018) 2411.

[102] M. Colombo, G. Raposo, C. Théry, Biogenesis, Secretion, and Intercellular Interactions of Exosomes and Other Extracellular Vesicles, Annu. Rev. Cell Dev. Biol. 30 (2014) 255–289.

[103] S. Heider, C. Metzner, Quantitative real-time single particle analysis of virions, Virology. 462–463 (2014) 199–206.

[104] T. Vicente, A. Roldão, C. Peixoto, M.J.T.T. Carrondo, P.M. Alves, Large-scale production and purification of VLP-based vaccines, J. Invertebr. Pathol. 107 (2011) S42–S48.

[105] R.M. Glaeser, How good can cryo-EM become?, Nat. Methods. 13 (2016) 28–32.

[106] L. Lambricht, K. Vanvarenberg, A. De Beuckelaer, L. Van Hoecke, J. Grooten, B. Ucakar, P. Lipnik, N.N. Sanders, S. Lienenklaus, V. Préat, G. Vandermeulen, Coadministration of a Plasmid Encoding HIV-1 Gag Enhances the Efficacy of Cancer DNA Vaccines, Mol. Ther. 24 (2016) 1686–1696.

[107] P. Steppert, D. Burgstaller, M. Klausberger, A. Tover, E. Berger, A. Jungbauer, Quantification and characterization of virus-like particles by size-exclusion chromatography and nanoparticle tracking analysis, J. Chromatogr. A. 1487 (2017) 89–99.

[108] S. Gutierrez-Granados, L. Cervera, M. de las M.M. de L.M.M. de las M. Segura, J. Wolfel, F. Godia, S. Gutiérrez-Granados, L. Cervera, M. de las M.M. de L.M.M. de las M. Segura, J. Wölfel, F. Gòdia, S. Gutierrez-Granados, L. Cervera, M. de las M.M. de L.M.M. de las M. Segura, J. Wolfel, F. Godia, S. Gutiérrez-Granados, L. Cervera, M. de las M.M. de L.M.M. de las M. Segura, J. Wölfel, F. Gòdia, Optimized production of HIV-1 virus-like particles by transient transfection in CAP-T cells, Appl. Microbiol. Biotechnol. 100 (2016) 3935–3947.

[109] A. Arakelyan, W. Fitzgerald, L. Margolis, J.C. Grivel, Nanoparticle-based flow virometry for the analysis of individual virions, J. Clin. Invest. 123 (2013) 3716–3727.

[110] K. Reiter, P.P. Aguilar, V. Wetter, P. Steppert, A. Tover, A. Jungbauer, Separation of virus-like particles and extracellular vesicles by flow-through and heparin affinity chromatography, J. Chromatogr. A. 1588 (2019) 77–84.

[111] P. Steppert, D. Burgstaller, M. Klausberger, E. Berger, P. Pereira, T.A. Schneider, P. Kramberger, A. Tover, K. Nöbauer, E. Razzazi-fazeli, A. Jungbauer, Purification of HIV-1 gag virus-like particles and separation of other extracellular particles, J. Chromatogr. A. 1455 (2016) 93–101.

[112] L. Hermida-Matsumoto, M.D. Resh, Localization of human immunodeficiency virus type 1 Gag and Env at the plasma membrane by confocal imaging., J. Virol. 74 (2000) 8670–8679.

[113] S. Gutiérrez-Granados, L. Cervera, F. Gòdia, J. Carrillo, M.M. Segura, Development and validation of a quantitation assay for fluorescently tagged HIV-1 virus-like particles, J. Virol. Methods. 193 (2013) 85–95.

[114] S. Gutiérrez-Granados, L. Cervera, F. Gòdia, M. Segura, Characterization and quantitation of fluorescent Gag virus-like particles, BMC Proc. 7 (2013) P62.

[115] K. Agarwal, M. Saji, S.M. Lazaroff, A.F. Palmer, M.D. Ringel, M.E. Paulaitis, Analysis of Exosome Release as a Cellular Response to MAPK Pathway Inhibition, Langmuir. 31 (2015) 5440–5448.

[116] K. Inamdar, C. Floderer, C. Favard, D. Muriaux, K. Inamdar, C. Floderer, C. Favard, D. Muriaux, Monitoring HIV-1 Assembly in Living Cells: Insights from Dynamic and Single Molecule Microscopy, Viruses. 11 (2019) 72.

[117] B. Huang, H. Babcock, X. Zhuang, Breaking the diffraction barrier: super-resolution imaging of cells., Cell. 143 (2010) 1047–58.

[118] L. Schermelleh, R. Heintzmann, H. Leonhardt, A guide to super-resolution fluorescence microscopy, J. Cell Biol. 190 (2010) 165–175.

[119] R.P. Niedz, T.J. Evens, Design of experiments (DOE)—history, concepts, and relevance

to in vitro culture, Vitr. Cell. Dev. Biol. - Plant. 52 (2016) 547–562.

[120] G.E.P. Box, K.B. Wilson, On the Experimental Attainment of Optimum Conditions, J. R. Stat. Soc. Ser. B. 13 (1951) 1–45.

[121] S. Maghsoodloo, G. Ozdemir, V. Jordan, C.H. Huang, Strengths and limitations of taguchi's contributions to quality, manufacturing, and process engineering, J. Manuf. Syst. 23 (2004) 73–126.

[122] H. Chernoff, Gustav Elfving's impact on experimental design, Stat. Sci. 14 (1999) 201–205.

[123] L. Cervera, S. Gutiérrez-Granados, M. Martínez, J. Blanco, F. Gòdia, M.M. Segura, Generation of HIV-1 Gag VLPs by transient transfection of HEK 293 suspension cell cultures using an optimized animal-derived component free medium, J. Biotechnol. 166 (2013) 152–165.

[124] E. Puente-Massaguer, L. Badiella, S. Gutiérrez-Granados, L. Cervera, F. Gòdia, A statistical approach to improve compound screening in cell culture media, Eng. Life Sci. 19 (2019) 1–13.

[125] T. Lundstedt, E. Seifert, L. Abramo, B. Thelin, Å. Nyström, J. Pettersen, R. Bergman, Experimental design and optimization, Chemom. Intell. Lab. Syst. 42 (1998) 3–40.

[126] L. Cervera, J. Fuenmayor, I. Gonzalez-Dominguez, S. Gutierrez-Granados, M.M. Segura, F. Godia, I. González-Domínguez, S. Gutiérrez-Granados, M.M. Segura, F. Gòdia, I. González-Domínguez, S. Gutiérrez-Granados, M.M. Segura, F. Gòdia, I. González-Domínguez, S. Gutiérrez-Granados, M.M. Segura, F. Gòdia, I. Gonzalez-Dominguez, S. Gutierrez-Granados, M.M. Segura, F. Godia, Selection and optimization of transfection enhancer additives for increased virus-like particle production in HEK293 suspension cell cultures, Appl. Microbiol. Biotechnol. 99 (2015) 9935–9949.

[127] J. Fuenmayor, L. Cervera, S. Gutiérrez-Granados, F. Gòdia, Transient gene expression optimization and expression vector comparison to improve HIV-1 VLP production in HEK293 cell lines, Appl. Microbiol. Biotechnol. 102 (2018) 165–174.

[128] P.E. Cruz, a Cunha, C.C. Peixoto, J. Clemente, J.L. Moreira, M.J. Carrondo, Optimization

of the production of virus-like particles in insect cells., Biotechnol. Bioeng. 60 (1998) 408–18.

[129] F. Monteiro, V. Bernal, M. Chaillet, I. Berger, P.M. Alves, Targeted supplementation design for improved production and quality of enveloped viral particles in insect cell-baculovirus expression system, J. Biotechnol. 233 (2016) 34–41.

[130] L. Vera Candioti, M.M. De Zan, M.S. Cámara, H.C. Goicoechea, Experimental design and multiple response optimization. Using the desirability function in analytical methods development, Talanta. 124 (2014) 123–138.

[131] M.A. Bezerra, R.E. Santelli, E.P. Oliveira, L.S. Villar, L.A. Escaleira, Response surface methodology (RSM) as a tool for optimization in analytical chemistry, Talanta. 76 (2008) 965–977.

[132] G. Derringer, R. Suich, Simultaneous optimization of several response variables, J. Qual. Technol. 12 (1980) 214–219.

[133] A.L. Bukzem, R. Signini, D.M. dos Santos, L.M. Lião, D.P.R. Ascheri, Optimization of carboxymethyl chitosan synthesis using response surface methodology and desirability function, Int. J. Biol. Macromol. 85 (2016) 615–624.

[134] G. Martinez Delfa, A. Olivieri, C.E. Boschetti, Multiple response optimization of styrene-butadiene rubber emulsion polymerization, Comput. Chem. Eng. 33 (2009) 850–856.

[135] Y. Perez-Castillo, A. Sánchez-Rodríguez, E. Tejera, M. Cruz-Monteagudo, F. Borges, M.N.D.S. Cordeiro, H. Le-Thi-Thu, H. Pham-The, A desirability-based multi objective approach for the virtual screening discovery of broad-spectrum anti-gastric cancer agents., PLoS One. 13 (2018) e0192176.

[136] C. Paillet, G. Forno, N. Soldano, R. Kratje, M. Etcheverrigaray, Statistical optimization of influenza H1N1 production from batch cultures of suspension Vero cells (sVero), Vaccine. 29 (2011) 7212–7217.

Objectives

The main objective of this thesis is the optimization and characterization of different production strategies for HIV-1 Gag VLP production in insect cell lines. Hi5 and Sf9 cells are the selected cell lines due to their relevance as production platforms for a diversity of recombinant products. Consequently, the complete study will be performed using these two cell lines in parallel and comparing their performance. More specific objectives are defined as follows:

1- Evaluation of different quantification and characterization techniques to assess the production of nanoparticles in insect cells.
2- Optimization of baculovirus-based Gag VLP production in Hi5 and Sf9 cell lines and assessment of the different nanoparticle populations produced.
3- Determination and characterization of the conditions for an optimal production of different recombinant products, including VLPs, by means of polyethylenimine-mediated transient gene expression in both insect cells.
4- Generation of Gag VLP stable cell pools by random integration and fluorescence-activated cell sorting.

Results

Chapter 1

Coupling microscopy and flow cytometry for a comprehensive characterization of nanoparticle production in insect cells

---

Eduard Puente Massaguer, Paolo Saccardo, Neus Ferrer-Miralles, Martí Lecina and Francesc Gòdia

Abstract

Advancements in the field of characterization techniques have broadened the opportunities to deepen into nanoparticle production processes. Gag-based virus-like particles (VLPs) have shown their potential as candidates for recombinant vaccine development. However, comprehensive characterization of the production process is still a requirement to meet the desired critical quality attributes. In this work, the production process of Gag VLPs in the reference Hi5 and Sf9 insect cell lines with baculovirus (BV) infection is characterized in detail. To this end, the Gag polyprotein was fused in frame to eGFP to favor process evaluation with multiple analytical tools. Tracking of the infection process using super-resolution confocal microscopy and flow cytometry revealed a pronounced increase in the complexity of Hi5 over Sf9 cells. Cryo-electron microscopy characterization determined that changes in complexity were attributed to the presence of occlusion-derived virus (ODV) in Hi5 cells, whereas Sf9 cells evidenced a larger proportion of budded virus (23-fold). Initial evaluation of the VLP production process using spectrofluorometry showed that higher levels of the GageGFP polyprotein were obtained in Hi5 cells (3.6-fold). However, comparative analysis based on nanoparticle quantification by flow virometry proved that Sf9 cells were more productive in terms of assembled VLPs (1.7-fold). Finally, analytical ultracentrifugation coupled to flow virometry evidenced a larger sedimentation coefficient of Hi5-derived VLPs, indicating the interaction with other cellular compounds. Taken together, these results highlight the combined use of microscopy and flow cytometry techniques to improve vaccine development processes using the insect cell/BEVS platform.

Keywords: Baculovirus, Cryo-electron microscopy, Flow cytometry, Flow virometry, Occlusion-derived virus, Virus-like particle

Abbreviations: *Ac*MNPV, *Autographa californica* multiple nucleopolyhedrovirus; BEVS, Baculovirus expression vector system; BV, Baculovirus; BudV, Budded virus; Cryo-EM, cryo electron microscopy; eGFP, enhanced green fluorescent protein; EV, Extracellular vesicle; HIV, human immunodeficiency virus; hpi, hours post infection; MOI, Multiplicity of infection; NC, Nucleocapsid; NTA, Nanoparticle tracking analysis; ODV, occlusion-derived virus; pfu, plaque forming unit; TEM, Transmission electron microscopy; VLP, Virus-like particle.

Introduction

Virus-like particles (VLPs) are a promising means for vaccination, nanotechnology, gene therapy and diagnostics [1,2]. These nanoparticles are composed of virus-derived proteins that have the ability to self-assemble, emulating the natural virus structure [3]. VLPs themselves are non-infective since they are devoid of genome and thus replication incompetent. Nowadays, human-based VLP vaccines are commercially available for hepatitis B, E and human papillomavirus, and several clinical trials are under investigation [4]. Enveloped VLPs have shown great promise as stimulators of the immune system. The capacity to accommodate a diversity of membrane antigens has underlined their potential as multivalent vaccines. In particular, the Gag polyprotein from the HIV is conventionally the preferred scaffold for protein display in the lipid envelope [5,6].

Up to date, Gag-based VLPs have been successfully produced in animal cell lines [7] and plants [8]. Among them, the insect cell/BEVS has become a reference system to achieve high protein yields with adequate post-translational modifications [9]. Initially, Gag VLP production studies with BEVS were reported in Sf9 cells (*Spodoptera frugiperda*) [10,11] and later on with the Hi5 cell line (*Trichoplusia ni*) [12,13]. Typically, Sf9 cells have been described to achieve higher baculovirus yields while Hi5 are more efficient for protein production [14,15]. In these cell lines, the baculovirus (BV) life cycle involves the production of two different virion phenotypes: the budded virus (BudV) which is responsible for cell-to-cell infection spreading, and the occlusion-derived virus (ODV), a resistance form to protect the baculovirus nucleocapsids from the interaction with the environment [16]. Both specimens are enveloped but BudVs acquire their envelope in the plasma membrane whereas ODVs take it from the nucleus. In turn, ODVs have a limited infection capacity since they do not incorporate the cell membrane-associated GP64 protein that accounts for viral infectivity [17].

The evolution of vaccine production platforms over the last years has raised the need to deepen into cell-based processes. Tools to monitor and control the critical quality attributes are then of

upmost importance [18]. Advancements in imaging and quantification methodologies have increased the opportunities to expand cell line characterization. In this regard, recent improvements in confocal microscopy have enabled to study the assembly process of different viruses [19]. Live cell characterization up to single molecule level has been accomplished by the combination of high-speed acquisition and advanced super-resolution microscopy techniques [20,21]. In parallel, cryo-electron microscopy (Cryo-EM) has emerged as a powerful tool to evaluate the structure and morphology of nanoparticles [22,23]. The advantage of cryo-EM over other related techniques is that it enables sample visualization in native conditions without staining [24,25]. Also, the progress achieved in the field of nanoparticle quantification has allowed to complement the standard measurement procedures of viruses and virus-like particles. Among them flow virometry and nanoparticle tracking analysis (NTA) are becoming more and more popular. Both methods can directly measure particle concentration in suspension while keeping a high level of sensitivity.

Here, we aim to complement the current knowledge of HIV-based nanoparticle production in insect cell lines by integrating different characterization and quantification methodologies. To do so, the HIV-1 *gag* gene was fused in frame to *eGFP* towards facilitating the follow-up of the infection process as well as VLP quantification. Super-resolution confocal microscopy in combination with flow cytometry were applied to evaluate the susceptibility to *Ac*MNPV BV infection, variations in cell morphology, and VLP production in both infected cell lines. The kinetics of VLP production could be tracked using the cutting-edge flow virometry and NTA techniques and compared to spectrofluorometry-based quantification. Cryo-EM analysis allowed to gain insight of different specimens being co-produced with VLPs and describe their structure. Moreover, VLPs were purified using analytical ultracentrifugation to assess the quality of GageGFP assembly into these nanoparticles and evaluate the co-distribution with the rest of particles. In this study, we demonstrate the synergistic combination of microscopy and flow cytometric techniques to gain insight into cell-based vaccine development processes.

Materials and methods

Cell lines

The *Spodoptera frugiperda* (Sf9, cat. num. 71104, Merck, Darmstadt, Germany) and *Trichoplusia ni* BTI-TN-5B1-4 cells (Hi5, cat. num. B85502, Thermo Fisher Scientific, Grand Island, NY, USA) were adapted to grow in the Sf900III medium (Thermo Fisher Scientific) in suspension conditions. Both insect cell lines were subcultured three times a week at a density of 4 - 6 x 10^5 cells/mL (Sf9) and 2 - 4 x 10^5 cells/mL (Hi5) in 125 mL disposable polycarbonate Erlenmeyer flasks (Corning, Steuben, NY, USA). All cultures were grown at 27 °C under 130 rpm agitation in an orbital shaker (Stuart, Stone, UK). Cell count and viability were measured with the Nucleocounter NC-3000 (Chemometec, Allerød, Denmark).

Construction of the BV-GageGFP recombinant baculovirus

The recombinant baculovirus encoding the HIV-1 Gag matrix protein fused in frame to eGFP (BV-GageGFP) was constructed as follows. The pGageGFP (NIH AIDS Reagent Program, cat. num. 11468) [26] and the pVL1393 plasmids (BD Biosciences, San Jose, CA, USA) were digested with *Eco*RI and *Not*I. Fragments containing the sequences of interest were ligated, obtaining the pVL1393-GageGFP transfer plasmid.

The recombinant BV-GageGFP was generated upon Sf9 cell co-transfection with the transfer plasmid and the BaculoGold *Ac*MNPV genome (BD Biosciences) with calcium phosphate, according to manufacturer's instructions. Five days post-transfection, the baculovirus-containing supernatant was harvested at 1000 x*g* for 10 min. The baculovirus seed stock (P0) was then selected through the plaque assay technique to discard non-recombinant viruses. The baculovirus working stock was then generated with three rounds of amplification at MOI = 0.1 for 4 days in Sf9 cells. The viral titers of the harvested supernatants were measured by plaque assay. The master stock (P2) and the working stock (P3) were both kept at -80 °C and 4 °C, respectively.

Insect cell infection conditions

To produce HIV-1 GageGFP VLPs, exponentially growing Sf9 and Hi5 cells at 2 x 10^6 cell/mL were infected with BV-GageGFP at MOI = 1. Infected cultures were sampled twice a day for extra and intracellular GageGFP analysis, until 40 hours post infection (hpi). The experimental conditions were then selected to achieve suitable VLP yields while keeping cell integrity and minimizing the release of intracellular content. Supernatants were harvested by centrifugation at 3000 x*g* for 5 min and maintained at 4 °C until analysis. Cell pellets were stored at -20 °C.

Flow cytometry

The percentage of GageGFP expressing cells was assessed twice a day based on the number of GFP-fluorescent cells using a BD FACS Canto II flow cytometer equipped with a 488 nm laser configuration (BD Biosciences). Briefly, 0.3 mL of the infected insect cell cultures were harvested by centrifugation at 300 x*g* for 5 min and fixed using 4 % *p*-formaldehyde for 10 min. Fixed cells were then centrifuged at 500 x*g* for 5 min to remove *p*-formaldehyde, resuspended in 0.3 mL ice-cold DPBS (Thermo Fisher Scientific) and maintained at 4 °C until analysis. The number of GageGFP positive cells was determined in the FITC PMT detector and analyzed using BD FACSDIVA software (BD Biosciences).

Confocal microscopy

GageGFP infected Sf9 and Hi5 cells were observed using a TCS SP5 confocal microscope (Leica, Wetzlar, Germany). Of note, videos of the GageGFP VLP budding process in each cell line were captured for 5 min using a TCS SP8 confocal microscope (Leica) equipped with a white light laser. To achieve this, a combination of super-resolution (Lightning) and high-speed acquisition (Resonant) was employed. Cell staining was performed with 0.05 % (Hi5) or 0.1 % v/v (Sf9) of CellMask™ and 0.1 % v/v of Hoechst (Thermo Fisher Scientific) for lipid membrane and cell

nucleus visualization, respectively. A washing step was performed to remove dye excess by centrifuging the cells at 300 x*g* for 5 min and resuspending them in fresh DPBS. Samples were then placed in 35 mm glass bottom Petri dishes with 14 mm microwell (MatTek Corporation, Ashland, MA, USA) for visualization.

Spectrofluorometry

The infected cultures were sampled twice a day by centrifugation at 3000 x*g* for 5 min. For intracellular GageGFP measurement, pelleted cells were disrupted through three freeze-thaw cycles (2.5 h at -20 °C and 0.5 h at 37 °C) and vortexed 5s 3 times between each cycle. Lysed pellets were then resuspended in TMS buffer (50 mM Tris-HCl, 150 mM NaCl, 2 mM $MgCl_2$, pH 8.0) and centrifuged at 13700 x*g* for 20 min. Supernatants were stored at 4 °C until analysis. GageGFP fluorescence was measured with a Cary Eclipse spectrophotometer (Agilent Technologies, Santa Clara, CA, USA) at RT as follows: λex = 488 nm (slit = 5), λem= 500 – 530 nm (slit = 10). Relative fluorescence units (R.F.U) were calculated by measuring the difference between infected cultures and negative controls.

Sucrose cushion ultracentrifugation

The supernatant of Sf9 and Hi5 infected cells with the BV-GageGFP at 40 hpi was sublayered with 5 mL of 25 % and 8 mL of 45 % (w/v) sucrose (Sigma Aldrich, Sant Louis, MO, USA) solution prepared in DPBS and DMEM (Thermo Fisher Scientific), respectively. 10 mL of the harvested supernatant from triplicate experiments were loaded in ultracentrifuge tubes (Beckman Coulter, Brea, CA, USA) and filled to the top with sterile DPBS. The ultracentrifugation conditions were set at 31000 rpm for 2.5 h at 4 °C using a Beckman Optima L100XP centrifuge equipped with a SW-32Ti rotor. Samples were taken from each sucrose fraction and the pellets were resuspended in 100 µL of sterile DPBS and maintained at 4 °C O/N. All samples were stored at -80 °C until fluorescence measurement and kept at 4 °C for nanoparticle analysis.

SDS-PAGE and Western Blot analysis

Infected insect cell supernatants and sucrose cushion ultracentrifugation fractions were examined by SDS-PAGE analysis and Western Blotting for HIV-1 p24 (A2-851-100, Icosagen, Tartu, Estonia) and GP64 (A2980, Abcam, Cambridge, United Kingdom), according to the method described by Steppert et al. [27]. Before antibody staining of the different ultracentrifugation fractions for Western Blot analysis, each fraction was diluted according to the sample volume added to the ultracentrifuge to normalize sample fraction concentration.

Flow virometry

Fluorescent and non-fluorescent particles from infected insect cell lines were measured in a CytoFlex LX (Beckman Coulter) equipped with a 488 nm blue laser for fluorescent particle detection and a 405 nm laser/violet side scatter configuration for improved nanoparticle size resolution. Samples were diluted in 0.22 µm-filtered DPBS and analyzed with the CytExpert 2.3 software.

Nanoparticle tracking analysis

A NanoSight NS300 (Malvern Panalytical, Malvern, United Kingdom) was used to measure fluorescent and non-fluorescent particles from harvested supernatants. Samples were diluted in 0.22 µm-filtered DPBS and continuously injected into the device chamber through a pump at an average concentration of 10^8 particles/mL (20 – 60 particles/frame). Videos of 60 s from independent triplicate measurements at room temperature were analyzed with the NanoSight NTA 3.2 software.

Cryo-electron microscopy

GageGFP VLP supernatants from infected Sf9 and Hi5 cells at 40 hpi were visualized with a cryo-transmission electron microscope. Briefly, 4 μL of sample were blotted onto EMR Holey carbon films on 400 mesh copper grids (Micro to Nano, Wateringweg, Netherlands) for 3 s at 77 % relative air humidity. The grids were previously subjected to a glow discharge treatment in a PELCO easiGlow™ Discharge Cleaning System (PELCO, Fresno, CA, USA). The samples were subsequently plunged into liquid ethane at −180 °C using a Leica EM GP workstation (Leica, Wetzlar, Germany) and observed with a JEM-2011 TEM operating at 200 kV (Jeol Ltd., Akishima, Tokyo, Japan). Samples were kept at −180 °C during visualization and images were taken using a CCD 895 USC 4000 multiscan camera (Gatan, Pleasanton, CA, USA). Image analysis was performed with the ImageJ software (NIH, Madison, WI, USA).

Transmission electron microscopy

The different fractions obtained after the ultracentrifugation of the infected supernatants at 40 hpi were examined with TEM. Samples were prepared by the air-dried negative staining method as previously reported by González-Domínguez et. al [24] before the examination in a JEM-1400 (Jeol) transmission electron microscope equipped with an ES1000W Erlangshen charge-coupled device camera (Gatan).

Statistical analyses

Statistical analyses of the different equations were performed using the unpaired Student *t*-test in Microsoft Excel 2016 (Microsoft, Redmond, WA, USA). A p-value < 0.05 was considered as statistically significant.

Results

Cell growth and study of infection

The Sf9 and Hi5 insect cell lines were selected since they are commonly used for recombinant protein production with the BEVS, typically with the *Autographa californica multiple nucleopolyhedrovirus* (*Ac*MNPV) species. Upon BV-GageGFP infection, Sf9 cell growth was completely arrested [28] whereas Hi5 cells kept growing until 24 hpi (Figure 1A). BV infection progressed more rapidly in Sf9 cells and both lines were completely infected after 40 hpi (Figure 1B). Flow cytometry analysis of infected cells showed that Hi5 were 1.6-fold more fluorescent than Sf9 cells when the infection was at its maximum (Figure 1C).

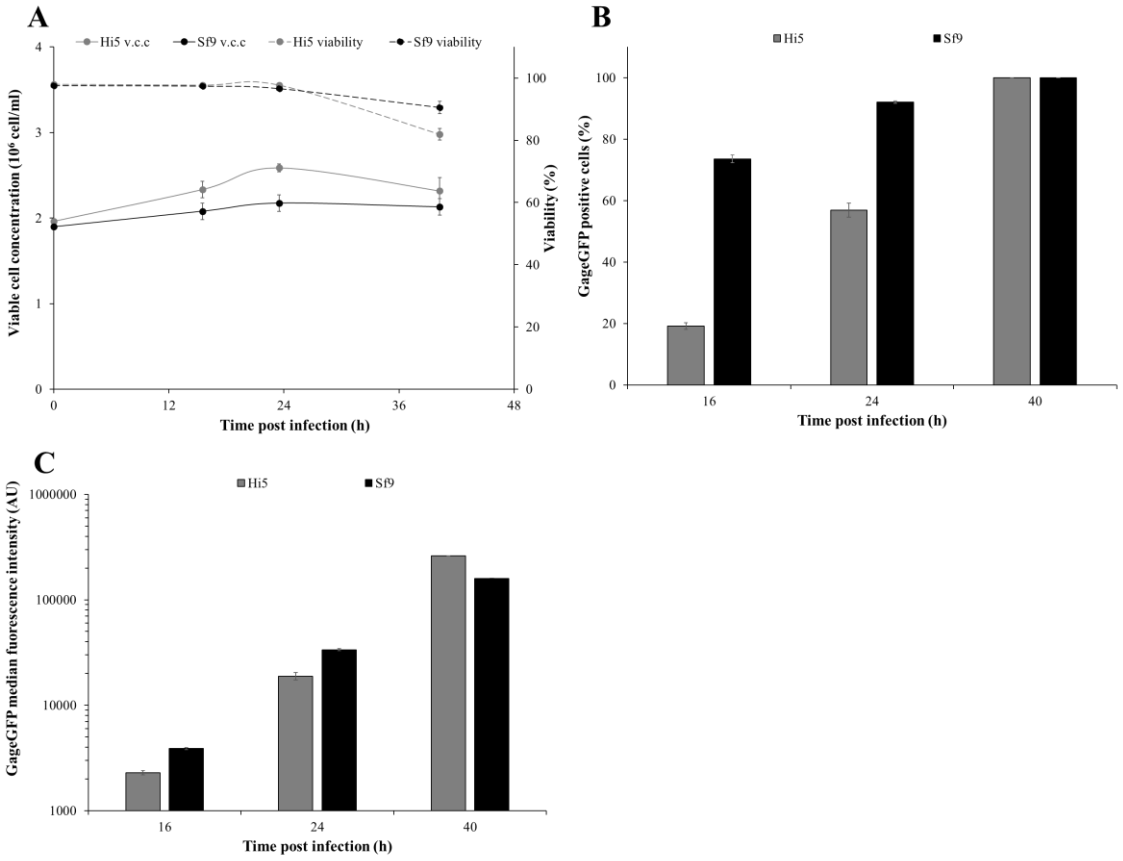

Figure 1. Cell growth and BV-GageGFP infection of Sf9 and Hi5 cells. (A) Viable cell concentration and viability profiles. (B – C) Infection kinetics and median fluorescence intensity of infected cells. (D) Cell complexity progression in infected cell lines. (E – F) Confocal fluorescence microscopy images of infected Hi5 and Sf9 cells, respectively. Cell nucleus was stained with Hoechst (blue) and membrane was stained with CellMask^{TM} (red). Mean values ± standard deviation of triplicate experiments are represented.

Interestingly, the analysis of the infection kinetics revealed a distinctive morphology in both cell lines. A marked increase in internal Hi5 cell complexity (i. e. granularity) was observed in the side scatter detector of the flow cytometer (Figure 2A – B). Though Sf9 cells were infected at a higher pace, the increase in cell complexity did not progress as fast as in Hi5 cells. Indeed, roughly the 90 % of the Hi5 cell culture exhibited this behavior at 40 hpi.

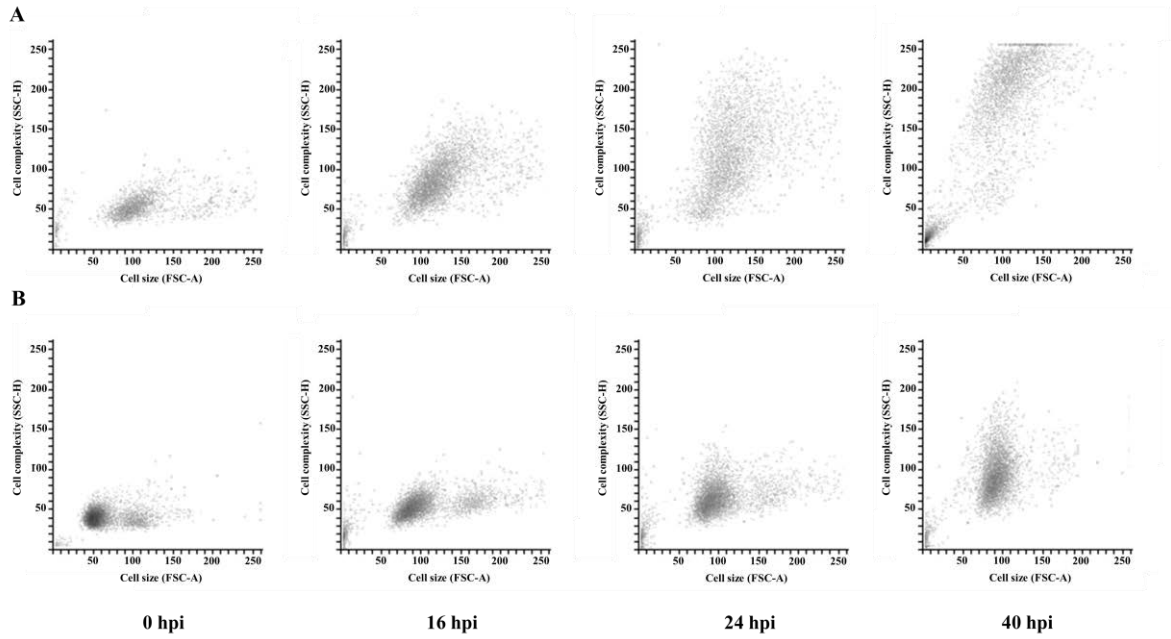

Figure 2. Infection kinetics of BV-GageGFP infected insect cell lines. (A – B) Progression of changes in cell complexity (0 – 40 hpi) in Hi5 and Sf9 cells, respectively.

Confocal microscopy visualization of infected cultures confirmed that the whole cell population was infected at 40 hpi (Figure 3A – B). Cell diameter analysis of 50 infected cells of each type determined that Hi5 cells (23.4 ± 4.2 µm) were bigger than Sf9 cells (18.9 ± 3.9 µm) with a *p*-value = $2 \cdot 10^{-5}$ (Table 1). Therefore, considering the cell as a spherical body, a 1.9-fold increase in cell biovolume was calculated for an infected Hi5 cell in average (6575 μm^3) compared to a Sf9 cell (3515 μm^3). Some of the Hi5 cells analyzed showed the presence of fluorescent vesicle-like structures with sizes ranging 0.5 – 5 µm (Figure 3A). On the other hand, several Sf9 cells evidenced a grained-like structure of their nuclei (blue, Hoechst) likely associated to the baculovirus infection process (Figure 3B). In these cells, co-localization of the GageGFP (green) polyprotein with the nuclear membrane was also observed. Cell membrane (red, CellMask™) co-localization with GageGFP was visualized as yellow regions in the cell membrane of both cell

lines, hence indicating that VLP budding was taking place. The latter was confirmed using a cutting-edge strategy based on the combination of super-resolution (Lightning) and high-speed acquisition (Resonant, Leica). Using this approach, the live VLP formation process and budding to the extracellular space could be recorded in both infected cell lines (Figure S1).

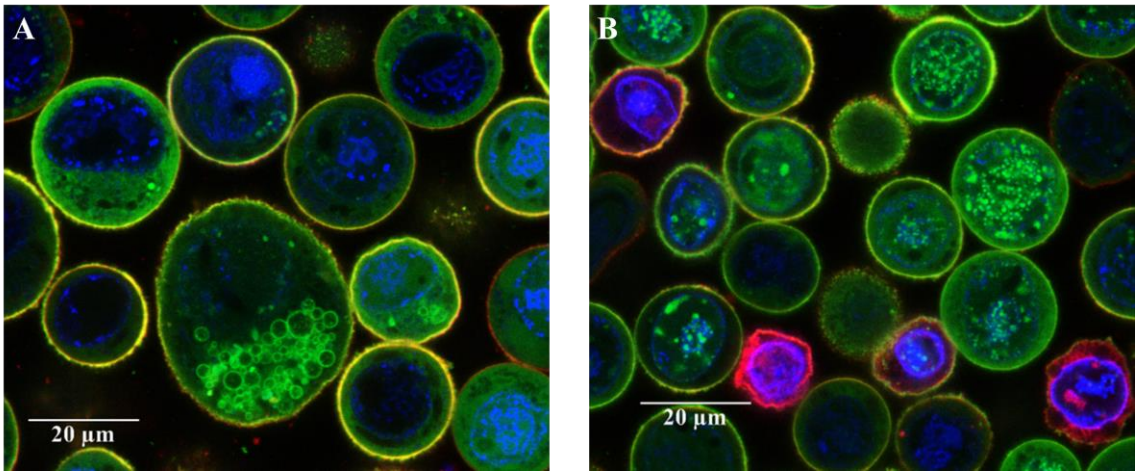

Figure 3. Confocal fluorescence microscopy images of infected insect cell lines. (A – B) Hi5 (A) and Sf9 (B) cell nucleus was stained with Hoechst (blue) and membrane was stained with CellMask^{TM} (red).

HIV-1 Gag VLP production kinetics

The assessment of GageGFP production showed that Hi5 cells achieved higher GageGFP fluorescence yields both in the supernatant and intracellularly over the studied time (Figure 4A – B). A 3.6-fold increase in total GageGFP fluorescence was reached in Hi5 (2202 ± 148 R.F.U.) in comparison to Sf9 cells (620 ± 25 R.F.U.) at 40 hpi. Considering the differences in size between cell lines, total GageGFP fluorescence was estimated per cell biovolume corresponding to a million cells. A specific production of 0.13 was calculated for Hi5 cells compared to 0.08 R.F.U./10^6 biovolume of infected cell measured in Sf9 cells. However, nanoparticle quantification using flow virometry revealed that Sf9 cells were more efficient regarding VLP production (Figure 4C). A similar trend was observed using NTA, with Sf9 cells achieving 1.7-fold more VLP production in comparison to infected Hi5 cells. In parallel, a 23-fold difference in terms of infectious baculovirus particles was also quantified in Sf9 over Hi5 cells (Table 1).

Table 1. Significant parameters measured in BV-GageGFP infected insect cell lines.

Parameter	Methodology	Hi5	Sf9
VLP concentration (10^9 fluorescent particle/mL)	NTA	10.7 ± 0.7	18.5 ± 1.2
	Flow virometry	2.9 ± 0.6	4.3 ± 0.3
Concentration of total nanoparticles (10^9 particle/mL)	NTA	85.2 ± 6.7	62.6 ± 1.4
	Flow virometry	1.3 ± 0.3	1.8 ± 0.1
Baculovirus concentration (10^7 pfu/mL)	Plaque assay	1.9 ± 0.1	43.8 ± 7.5
Median cell diameter (µm)	Confocal microscopy	23.4 ± 4.2	18.9 ± 3.9

Qualitative analysis of total protein expression with SDS-PAGE showed a larger amount of proteins in Hi5 cell supernatants (Figure 4D). Specific detection of the GageGFP polyprotein and the baculovirus-derived GP64 was confirmed in both systems using Western Blot. GageGFP was identified as a polyprotein of 88 kDa whereas a band corresponding to 64 kDa was found for GP64 (Figure 4D).

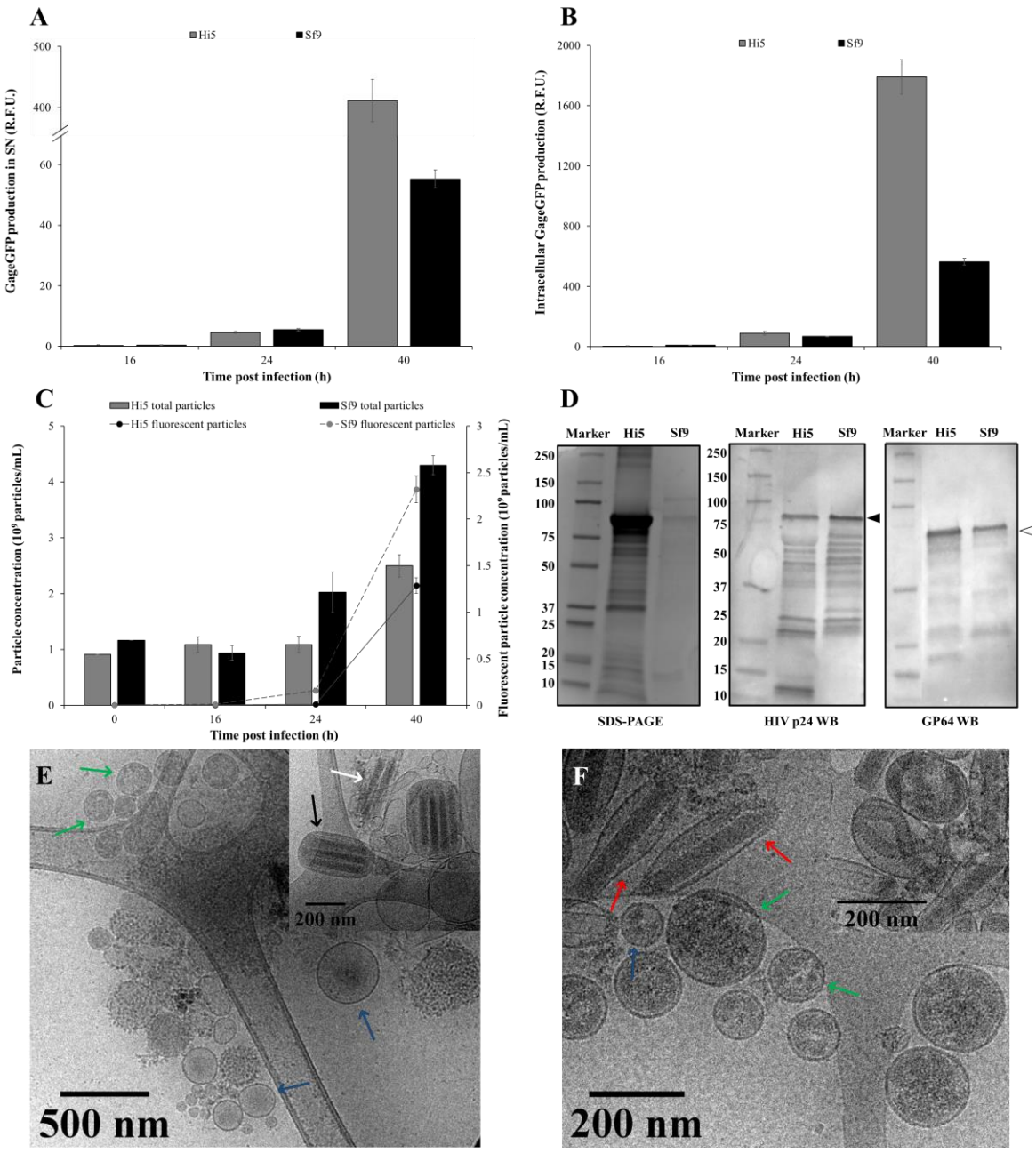

Figure 4. GageGFP VLP production and supernatant characterization. (A – B) Supernatant and intracellular GageGFP production measured in relative fluorescence units (R.F.U.). (C) GageGFP VLP and total nanoparticle production kinetics assessed with flow virometry. (D) SDS-PAGE and Western Blot analysis of BV-GageGFP infected supernatants at 40 hpi. Band detection of the GageGFP polyprotein (black arrow) and the GP64 protein (white) are indicated in kilodaltons. (E – F) Cryo-electron microscopy images of infected Hi5 and Sf9 cells at 40 hpi, respectively. The arrows indicate the different specimens: VLP (green), EV (blue), NC (white), BudV (red) and ODV (black). Mean values ± standard deviation of triplicate experiments are represented.

Cryo-EM characterization

A mixture of different specimens was found in each of the supernatants. VLPs were identified as electron-dense spherical structures with a defined lipid bilayer (Figure 4E-F). Sf9-derived VLPs had an average diameter of 161 ± 44 nm whereas Hi5 VLPs were 184 ± 16 nm, all of them in 100 – 200 nm diameter range. Extracellular vesicles (< 400 nm) were also detected as less electrodense structures and proved to be more size heterogeneous in contrast to VLPs (50 - 400 nm). Comparison of membrane thickness of VLPs and EVs derived from infected Hi5 cells (VLP, 6.4 ± 1.1 nm; EV, 7.3 ± 0.9 nm) did not exhibit any significant difference (*p*-value = 0.10). The same trend was observed for infected Sf9 cells (VLP, 6.0 ± 1.2 nm; EV, 6.0 ± 1.1 nm) (*p*-value = 0.95).

Different structures were specifically present in Hi5 cell supernatants. Multiple rod-shaped nucleocapsids were observed inside vesicular bodies (ODV) (Figure 4E, upper right). All the NCs inside the ODV were non-enveloped and arranged in parallel disposition. The whole ODV structure was 384 ± 28 nm in length and 206 ± 37 nm in diameter. Also, small structures with a mean diameter of 55 ± 6 nm were detected in these supernatants (Figure 4E, bottom). A remarkable characteristic of these samples was the detection of enveloped particles containing multiple spikes (Figure 4E, center left to right). These nanoparticles were rather different in size (251 ± 68 nm) and bigger compared to VLPs (*p*-value = 0.004). Conversely, Sf9 cell supernatants were less heterogeneous in terms of the nanoparticles observed. In comparison, a higher presence of ovoid-like structures containing one NC, which could be identified as the typical budded baculovirus structure (BudV), was detected. This form of the BV had an average length of 334 ± 13 nm and 107 ± 7 nm membrane-to-membrane diameter (Figure 4F). No differences were observed when comparing the size of the NCs in each system (Hi5, 41.7 ± 1.3 nm; Sf9, 41.3 ± 2.8 nm) as well as in the membrane thickness of the different baculovirus phenotypes: ODV (5.8 ± 1.2 nm) and BudV (5.2 ± 0.3 nm) (*p*-value = 0.22).

Study of nanoparticle distribution using analytical ultracentrifugation

The infected cell supernatants were fractionated on a double sucrose cushion ultracentrifugation. Roughly the 90 % of the GageGFP fluorescence from Hi5 cell supernatants was measured in the SN, SN-25 % and 25 % sucrose fractions. For Sf9 cells, the majority of the GageGFP fluorescence was found in the 25-45 % and 45 % fractions (Figure 5A). Flow virometry analysis of the different fractions revealed that fluorescent and non-fluorescent nanoparticles were mainly detected in the 25-45 %, 45 % and pellet fractions (Figure 5B). However, fluorescent particles derived from Hi5 cells were located in the 45 % and pellet fractions, while they were in the 25-45 % and 45 % in Sf9 cell samples.

Baculovirus distribution in each of the ultracentrifugation fractions was also measured by plaque assay (Figure 5C). Of note, co-purification with the rest of the nanoparticles was evidenced in the bottom fractions of the ultracentrifugation. Baculovirus were equally distributed in the 25-45 %, 45 % sucrose and pellet fractions in Hi5 cell supernatants whereas they were predominantly concentrated in the 45 % fraction for Sf9 cells.

The presence of p24 (GageGFP) and GP64 (BV) in these fractions was confirmed by Western Blot, with a similar distribution as observed with flow virometry and plaque assay, respectively (Figure 5D).

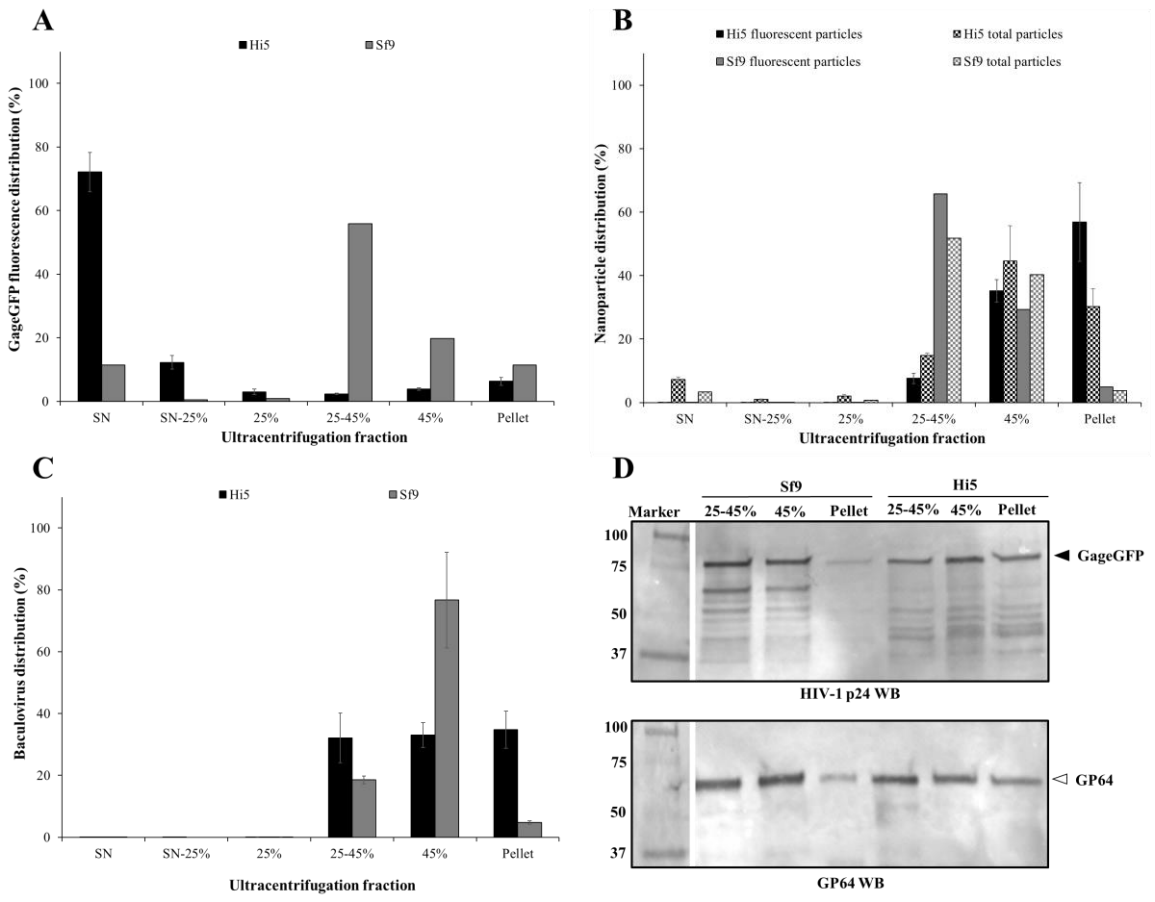

Figure 5. GageGFP VLP and BV distribution in sucrose cushion ultracentrifugation of Hi5 and Sf9 infected cell lines. (A) GageGFP protein distribution measured with spectrofluorometry (R.F.U.). (B) GageGFP VLP and total nanoparticle in each fraction assessed using flow virometry. (C) Quantification of BV infectious particles with plaque assay. (D) GP64 and p24 Western Blot analysis of the nanoparticle-containing ultracentrifugation fractions (25-45%, 45% and pellet). Band detection of the GageGFP polyprotein (black arrow) and the GP64 protein (white) are indicated in kilodaltons. Mean values ± standard deviation of triplicate experiments are represented.

Assessment of samples from the ultracentrifugation fractions using TEM showed that most of the nanoparticles were in the 25-45 %, 45 % and pellet fractions (Figure 6B-C). A similar pattern between Hi5 and Sf9 supernatants was seen in the upper fractions of the ultracentrifuge tube. Salt precipitates were observed in the SN and SN-25 % fractions and only few EVs could be detected in the 25 %. Interestingly, small particles of 26 ± 6 nm were detected in this fraction in Hi5 cell supernatants (Figure 6B, 25 %, upper left). These particles were also present in the 25-45 % interphase along with EVs and VLPs. Measurement of VLPs using TEM showed no significant differences in VLP size for Hi5 (186 ± 60 nm) and Sf9 (144 ± 21 nm) samples (p-value = 0.15). A higher amount of BudVs were seen in the Sf9 25-45 % fraction, with an average length of 330

± 30 nm and 60 ± 11 nm in diameter. Pellet analysis revealed the presence of different populations in both systems. ODVs were identified in Hi5 pellets (328 ± 13 x 205 ± 39 nm) along with VLPs, EVs, NCs and BudVs (Figure 6B, pellet) while only NCs could be identified in Sf9 pellets.

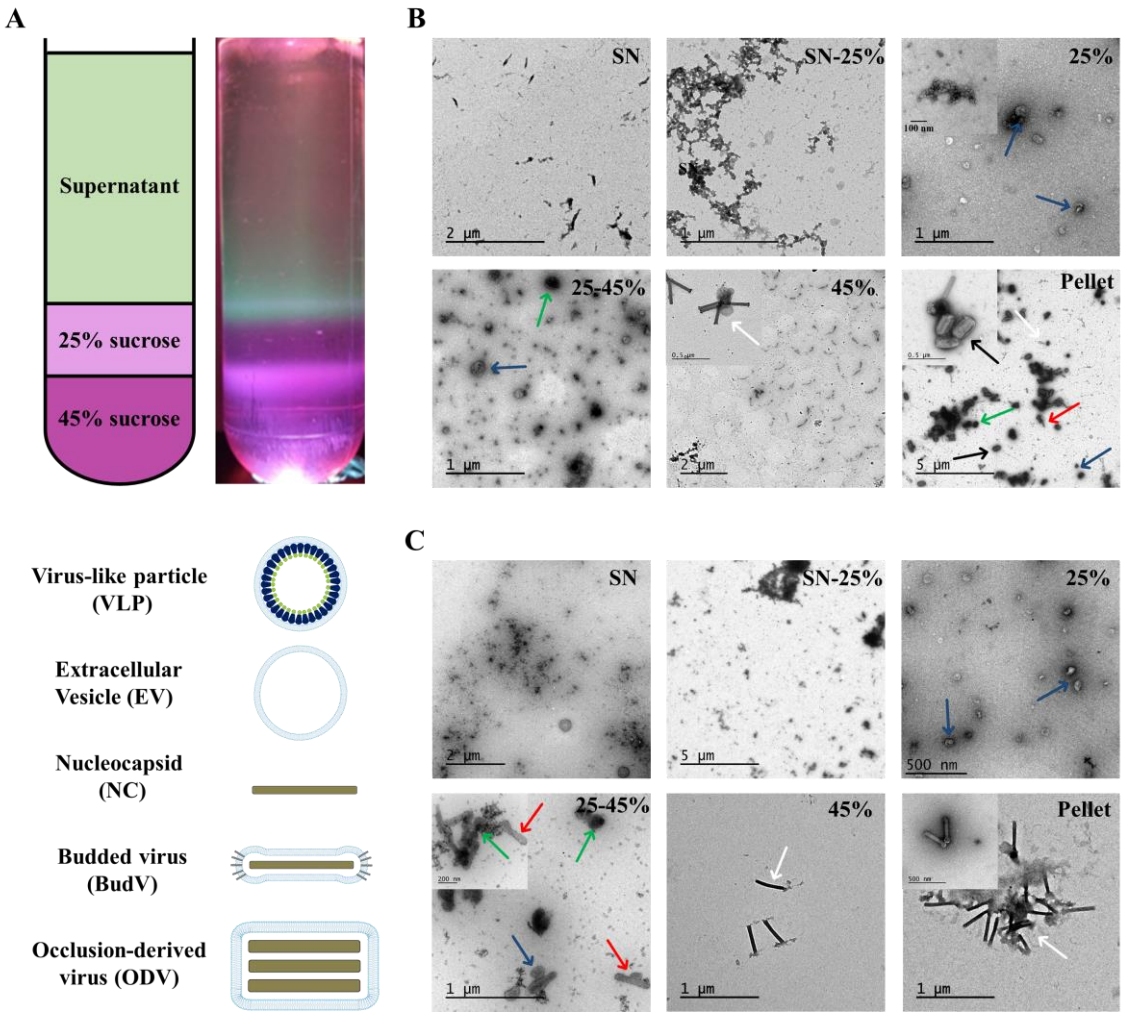

Figure 6. Transmission electron microscopy characterization. (A) Representation of the different ultracentrifugation fractions and illustration of the specimens encountered. (B – C) Different ultracentrifugation fractions of Hi5 and Sf9 infected cells, respectively. The arrows indicate the different specimens: VLP (green), EV (blue), NC (white), BudV (red) and ODV (black).

Discussion

The BEVS has demonstrated to be one of the most efficient and productive systems of recombinant proteins [29]. Complex protein structures such as VLPs have been successfully produced using this platform, typically with the Sf9 and Hi5 insect cell lines [30–32]. Advancements in the field of characterization techniques have broadened the opportunities to

deepen into these systems, in matters of the infection process, product yield and quality. This is paramount since proper evaluation of the production process in the cell line of interest is a key to meet the desired critical quality attributes [18].

Comparison of the baculovirus infection process in both cell lines using flow cytometry showed that infection progressed more rapidly in Sf9 cells. This accelerated kinetics is probably connected to the higher BV replication rate in the form of BudV achieved in Sf9 cells [14,33]. However, we observed that the complexity of Hi5 cells substantially increased upon baculovirus infection. Confocal microscopy analysis of infected Hi5 cells evidenced the presence of cytoplasmatic vesicles formed of GageGFP. However, this behavior was not homogeneous throughout the whole cell population and did not correlate with the marked increase in cell complexity. Cryo-EM assessment of infected Hi5 cell supernatants disclosed the existence of a remarkable amount of ODVs. This virion phenotype was not observed in Sf9 cells, although it is known that these cells can produce this type of particles [34]. In any case, Hi5 cells demonstrated a higher level of nucleocapsid production as ODVs, which are known to be poorly infectious in cultured cells [17]. In fact, they are normally associated to the BV resistance form in the natural environment as polyhedrin occlusion bodies. The improved capacity of Hi5 cells to produce this virion phenotype could explain the increase in cell complexity and the slower progression of the infection compared to Sf9 cells. Further studies of the mechanisms directing the formation of nucleocapsids to ODVs or BudVs could help to understand the differences between the two cell lines [16].

The Sf9 cell proved to be the most productive system for GageGFP VLPs. Moreover, flow virometry assessment of the VLP production kinetics demonstrated that this process was faster in this cell line, probably due to the higher BudV replication rate achieved. Initial comparison based on spectrofluorometry indicated that Hi5 cells achieved higher levels of the GageGFP polyprotein. Nevertheless, sample analysis using cutting-edge techniques based on flow virometry and NTA revealed that a higher yield of assembled GageGFP nanoparticles was obtained in Sf9 cells. These results indicate that Hi5 cells probably surpass their own capacity to process such amount of GageGFP protein to form nanoparticles. In turn, this could indicate that

there is an impaired production of the GageGFP polyprotein and VLPs in the Hi5 cell line. Analysis of fluorescence in the different ultracentrifugation fractions evidenced that only the 9 % corresponded to VLPs, whereas a 77 % was measured in Sf9 cells.

Visualization of infected supernatants using Cryo-EM and TEM indicated that a higher load of contaminating particles was present in Hi5 cells. Apart from ODVs, a larger amount of EVs was detected. Also, the existence of small nanoparticles with a size of 55 ± 6 nm measured with Cryo-EM and 26 ± 6 nm with TEM was identified. These particles could be related to *Alphanodavirus*, which have been described to latently infect this cell line [35–37].

Regarding VLPs, no significant differences in size and structure were observed between both platforms. Distinction of VLPs from EVs was highly improved with the Cryo-EM. Uranyl acetate sample staining in TEM made both specimens to look similar, while native observation with Cryo-EM enabled to identify VLPs as more electrodense structures. The study of the VLP distribution pattern using ultracentrifugation evidenced that these particles were highly concentrated in the 25-45 % fraction in Sf9 while they pelleted in Hi5 cells. Typically, VLPs should principally appear in the 25-45 % and 45 % fractions [38,39]. This indicates that Hi5-derived VLPs have a higher sedimentation coefficient, raising the possibility that these nanoparticles associate with cellular elements in this cell line [12]. Accordingly, a larger amount of total proteins was detected in Hi5 cell supernatants using SDS-PAGE.

The Hi5 cell line is conventionally accepted as a higher protein producer host compared to Sf9 cells [14,40]. In this regard, several works have focused on using this cell line for VLP production [15,41–43]. However, quality assessment of the VLPs and the associated contaminants has not been addressed in detail. Here, we performed a comparative analysis of the Gag VLP production process in both cell lines using the same culture medium and infection conditions. To do so, a combination of advanced characterization and quantification techniques were implemented. Our results suggest that Sf9 cells are more susceptible to *Ac*MNPV BV infection and that a higher replication of the BudV phenotype is accomplished. Hi5 cells demonstrated a higher

heterogeneity of contaminating particles besides the expected BudVs. In this regard, the ODV virion phenotype appeared as a remarkable contaminant. EVs were present in both samples and could be efficiently distinguished from VLPs using the Cryo-EM. In terms of VLP production, the Sf9 cell line was the most efficient and productive platform. Higher GageGFP fluorescence yields were obtained in Hi5 cells but the use of flow virometry and NTA techniques unveiled that most of the GageGFP was not assembled as VLPs.

Overall, these results provide valuable information on the use of both insect cell lines for recombinant vaccine development, highlighting the combined use of microscopy and flow cytometry in process evaluation. Although we specifically focused on HIV-1 VLP production, the integration of these methodologies is applicable to other systems targeting the production of nanoparticles.

Acknowledgement

The authors would like to thank Marta Martínez-Calle for developing the BV-GageGFP. We would also like to thank Dr. Nick Berrow (Institute for Research in Biomedicine, Barcelona, Spain), Dr. Paula Alves (Instituto de Biologia Experimental e Tecnológica, Oeiras, Portugal) and Dr. Julià Blanco (Irsi Caixa, Badalona, Spain) for providing the Sf9 cells, the Hi5 cell line and the pGageGFP plasmid, respectively. We also appreciate the collaboration of Jorge Fomaro and Ángel Calvache (Beckman Coulter) in ceding the CytoFlex LX flow cytometer. The technical support of Mónica Roldán from Servei de Microscòpia (UAB) and Servei d'Anatomia Patològica (Hospital Sant Joan de Déu, Barcelona, Spain) with TCS SP5 and SP8 confocal microscopes, respectively, is acknowledged. Martí de Cabo from Servei de Microscòpia (UAB) provided support with the Cryo-EM analyses and Katrin Reiter (University of Natural Resources and Life Sciences, Vienna, Austria) with SDS-PAGE and Western Blot. The advice of Manuela Costa (Servei de Cultius Cel·lulars, Producció d'Anticossos i Citometria, UAB) with cytometry and José Amable Bernabé (Institut de Ciència de Materials de Barcelona, CSIC) with NTA is

recognized. The support from the ICTS "NANBIOSIS", more specifically by the Protein Production Platform of CIBER in Bioengineering, Biomaterials & Nanomedicne (CIBER-BBN)/ IBB, at the UAB SePBioEs scientific-technical service (www.nanbiosis.es) is also acknowledged. Eduard Puente-Massaguer is a recipient of an FPU grant from Ministerio de Educación, Cultura y Deporte of Spain (FPU15/03577). The research group is recognized as 2017 SGR 898 by Generalitat de Catalunya.

Compliance with Ethical Standards

Conflict of interest

The authors declare that they have no competing interests.

Ethical approval

This article does not contain any studies with human participants performed by any of the authors.

References

[1] Z. Shirbaghaee, A. Bolhassani, Different applications of virus like particles in biology and medicine: Vaccination and delivery systems, Biopolymers. 105 (2015) 113–32.

[2] A.M.C. Andersson, M. Schwerdtfeger, P.J. Holst, Virus-like-vaccines against HIV, Vaccines. 6 (2018) 1–17.

[3] Y. Gao, C. Wijewardhana, J.F.S. Mann, Virus-Like Particle, Liposome, and Polymeric Particle-Based Vaccines against HIV-1, Front. Immunol. 9 (2018) 345.

[4] B. Donaldson, Z. Lateef, G.F. Walker, S.L. Young, V.K. Ward, Virus-like particle vaccines: immunology and formulation for clinical translation, Expert Rev. Vaccines. 17 (2018) 833–849.

[5] J. Vidigal, B. Fernandes, M.M. Dias, M. Patrone, A. Roldão, M.J.T. Carrondo, P.M. Alves, A.P. Teixeira, RMCE-based insect cell platform to produce membrane proteins captured on HIV-1 Gag virus-like particles, Appl. Microbiol. Biotechnol. 102 (2018) 655–666.

[6] L. Nika, J. Wallner, D. Palmberger, K. Koczka, K. Vorauer-Uhl, R. Grabherr, Expression of full-length HER2 protein in Sf 9 insect cells and its presentation on the surface of budded virus-like particles, Protein Expr. Purif. 136 (2017) 27–38.

[7] L. Cervera, S. Gutiérrez-Granados, M. Martínez, J. Blanco, F. Gòdia, M.M. Segura, Generation of HIV-1 Gag VLPs by transient transfection of HEK 293 suspension cell cultures using an optimized animal-derived component free medium, J. Biotechnol. 166 (2013) 152–165.

[8] S.A. Kessans, M.D. Linhart, N. Matoba, T. Mor, Biological and biochemical characterization of HIV-1 Gag/dgp41 virus-like particles expressed in Nicotiana benthamiana., Plant Biotechnol. J. 11 (2013) 681–90.

[9] G. Walsh, R. Jefferis, Post-translational modifications in the context of therapeutic

proteins, Nat. Biotechnol. 24 (2006) 1241–1252.

[10] D. Gheysen, E. Jacobs, F. de Foresta, C. Thiriart, M. Francotte, D. Thines, M. De Wilde, Assembly and release of HIV-1 precursor Pr55gag virus-like particles from recombinant baculovirus-infected insect cells, Cell. 59 (1989) 103–112.

[11] R. Wagner, H. Fließbach, G. Wanner, M. Motz, M. Niedrig, G. Deby, A. von Brunn, H. Wolf, Studies on processing, particle formation, and immunogenicity of the HIV-1 gag gene product: a possible component of a HIV vaccine, Arch. Virol. 127 (1992) 117–137.

[12] S.D. Parker, E. Hunter, A cell-line-specific defect in the intracellular transport and release of assembled retroviral capsids., J. Virol. 74 (2000) 784–795.

[13] S. Pillay, A. Meyers, A.L. Williamson, E.P. Rybicki, Optimization of chimeric HIV-1 virus-like particle production in a baculovirus-insect cell expression system, Biotechnol. Prog. 25 (2009) 1153–1160.

[14] M. Wilde, M. Klausberger, D. Palmberger, W. Ernst, R. Grabherr, Tnao38, high five and Sf9-evaluation of host-virus interactions in three different insect cell lines: Baculovirus production and recombinant protein expression, Biotechnol. Lett. 36 (2014) 743–749.

[15] F. Krammer, T. Schinko, D. Palmberger, C. Tauer, P. Messner, R. Grabherr, Trichoplusia ni cells (High Five™) are highly efficient for the production of influenza A virus-like particles: A comparison of two insect cell lines as production platforms for influenza vaccines, Mol. Biotechnol. 45 (2010) 226–234.

[16] G.W. Blissard, D.A. Theilmann, Baculovirus Entry and Egress from Insect Cells, Annu. Rev. Virol. 5 (2018) 113–139.

[17] D.E. Lynn, Comparative susceptibilities of twelve insect cell lines to infection by three baculoviruses, J. Invertebr. Pathol. 82 (2003) 129–131.

[18] L.H.L. Lua, N.K. Connors, F. Sainsbury, Y.P. Chuan, N. Wibowo, A.P.J. Middelberg,

Bioengineering virus-like particles as vaccines, Biotechnol. Bioeng. 111 (2014) 425–440.

[19] R. Witte, V. Andriasyan, F. Georgi, A. Yakimovich, U. Greber, R. Witte, V. Andriasyan, F. Georgi, A. Yakimovich, U.F. Greber, Concepts in Light Microscopy of Viruses, Viruses. 10 (2018) 202.

[20] A.C. Francis, G.B. Melikyan, Live-cell imaging of early steps of single HIV-1 infection, Viruses. 10 (2018) 275.

[21] K. Inamdar, C. Floderer, C. Favard, D. Muriaux, K. Inamdar, C. Floderer, C. Favard, D. Muriaux, Monitoring HIV-1 Assembly in Living Cells: Insights from Dynamic and Single Molecule Microscopy, Viruses. 11 (2019) 72.

[22] R. Danev, H. Yanagisawa, M. Kikkawa, Cryo-Electron Microscopy Methodology: Current Aspects and Future Directions, Trends Biochem. Sci. (2019).

[23] J.G. Heddle, S. Chakraborti, K. Iwasaki, Natural and artificial protein cages: design, structure and therapeutic applications, Curr. Opin. Struct. Biol. 43 (2017) 148–155.

[24] I. González-Domínguez, N. Grimaldi, L. Cervera, N. Ventosa, F. Gòdia, Impact of physicochemical properties of DNA/PEI complexes on transient transfection of mammalian cells, N. Biotechnol. 49 (2019) 88–97.

[25] E. Puente-Massaguer, M. Lecina, F. Gòdia, Nanoscale characterization coupled to multi-parametric optimization of Hi5 cell transient gene expression, Appl. Microbiol. Biotechnol. 102 (2018) 10495–10510.

[26] L. Hermida-Matsumoto, M.D. Resh, Localization of human immunodeficiency virus type 1 Gag and Env at the plasma membrane by confocal imaging., J. Virol. 74 (2000) 8670–8679.

[27] P. Steppert, D. Burgstaller, M. Klausberger, P. Kramberger, A. Tover, E. Berger, K. Nöbauer, E. Razzazi-Fazeli, A. Jungbauer, Separation of HIV-1 gag virus-like particles

from vesicular particles impurities by hydroxyl-functionalized monoliths, J. Sep. Sci. 40 (2017) 979–990.

[28] M. Lecina, A. Soley, J. Gràcia, E. Espunya, B. Lázaro, J.J. Cairó, F. Gòdia, Application of on-line OUR measurements to detect actions points to improve baculovirus-insect cell cultures in bioreactors, J. Biotechnol. 125 (2006) 385–394.

[29] L.A. Palomares, J.A. Mena, O.T. Ramírez, Simultaneous expression of recombinant proteins in the insect cell-baculovirus system: Production of virus-like particles, Methods. 56 (2012) 389–395.

[30] H. Yamaji, M. Nakamura, M. Kuwahara, Y. Takahashi, T. Katsuda, E. Konishi, Efficient production of Japanese encephalitis virus-like particles by recombinant lepidopteran insect cells, Appl. Microbiol. Biotechnol. 97 (2013) 1071–1079.

[31] K.L. Warfield, N.A. Posten, D.L. Swenson, G.G. Olinger, D. Esposito, W.K. Gillette, R.F. Hopkins, J. Costantino, R.G. Panchal, J.L. Hartley, M.J. Aman, S. Bavari, Filovirus-Like Particles Produced in Insect Cells: Immunogenicity and Protection in Rodents, J. Infect. Dis. 196 (2007) S421–S429.

[32] J.M. Wagner, J.D. Pajerowski, C.L. Daniels, P.M. McHugh, J.A. Flynn, J.W. Balliet, D.R. Casimiro, S. Subramanian, Enhanced production of Chikungunya virus-like particles using a high-pH adapted Spodoptera frugiperda insect cell line, PLoS One. 9 (2014) 1–14.

[33] L. Matindoost, H. Hu, L.C.L. Chan, L.K. Nielsen, S. Reid, The effect of cell line, phylogenetics and medium on baculovirus budded virus yield and quality, Arch. Virol. 159 (2014) 91–102.

[34] I.L. Yu, D. Bray, Y.C. Lin, O. Lung, Autographa californica multiple nucleopolyhedrovirus ORF 23 null mutant produces occlusion-derived virions with fewernucleocapsids, J. Gen. Virol. 90 (2009) 1499–1504.

[35] T.-C. Li, P.D. Scotti, T. Miyamura, N. Takeda, Latent Infection of a New Alphanodavirus in an Insect Cell Line, J. Virol. 81 (2007) 10890–10896.

[36] H. Bai, Y. Wang, X. Li, H. Mao, Y. Li, S. Han, Z. Shi, X. Chen, Isolation and characterization of a novel alphanodavirus, Virol. J. 8 (2011) 311.

[37] C. Geisler, D.L. Jarvis, Adventitious viruses in insect cell lines used for recombinant protein expression, Protein Expr. Purif. 144 (2018) 25–32.

[38] P. Steppert, D. Burgstaller, M. Klausberger, E. Berger, P. Pereira, T.A. Schneider, P. Kramberger, A. Tover, K. Nöbauer, E. Razzazi-fazeli, A. Jungbauer, Purification of HIV-1 gag virus-like particles and separation of other extracellular particles, J. Chromatogr. A. 1455 (2016) 93–101.

[39] F. Liu, X. Wu, L. Li, Z. Liu, Z. Wang, Use of baculovirus expression system for generation of virus-like particles: Successes and challenges, Protein Expr. Purif. 90 (2013) 104–116.

[40] R.R. Granados, G. Li, G.W. Blissard, Insect cell culture and biotechnology, Virol. Sin. 22 (2007) 83–93.

[41] Z. Shoja, M. Tagliamonte, S. Jalilvand, Y. Mollaei-Kandelous, A. De stradis, M.L. Tornesello, F. M. Buonaguro, L. Buonaguro, Formation of Self-Assembled Triple-Layered Rotavirus-Like Particles (tlRLPs) by Constitutive Co-Expression of VP2, VP6, and VP7 in Stably Transfected High-Five Insect Cell Lines, J. Med. Virol. 87 (2015) 102–111.

[42] G.P. Hong, J.H. Park, H.H. Lee, K.O. Jang, D.K. Chung, W. Kim, I.S. Chung, Production of influenza virus-like particles from stably transfected Trichoplusia ni BT1 TN-5B1-4 cells, Biotechnol. Bioprocess Eng. 20 (2015) 506–514.

[43] M. Tagliamonte, M.L. Visciano, M.L. Tornesello, A. De Stradis, F.M. Buonaguro, L. Buonaguro, HIV-Gag VLPs presenting trimeric HIV-1 gp140 spikes constitutively expressed in stable double transfected insect cell line, Vaccine. 29 (2011) 4913–4922.

Supplementary material

Figure S1. VLP production time lapse (5 min) of High Five (left) and Sf9 cells (right) infected with BV-GageGFP. Cell membrane was stained with CellMask™ (red) and cell nucleus with Hoechst (blue).

Chapter 2

Virus-like particle production in High Five and Sf9 insect cell lines by recombinant baculovirus infection

Eduard Puente Massaguer, Martí Lecina and Francesc Gòdia

Chapter 2 – Part I

Integrating nanoparticle quantification and orthogonal designs for efficient HIV-1 virus-like particle production in High Five cells

Eduard Puente Massaguer, Martí Lecina and Francesc Gòdia

Abstract

The nature of enveloped virus-like particles (VLPs) has triggered high interest in its application to different research fields, including vaccine development. The baculovirus expression vector system (BEVS) has been used as an efficient platform for obtaining large amounts of these complex nanoparticles. To date, most of the studies dealing with VLP production by recombinant baculovirus infection utilize indirect detection or quantification techniques that hinder the appropriate characterization of the process and product. Here, we propose the application of cutting-edge quantification methodologies in combination to advanced statistical designs to exploit the full potential of the Hi5/BEVS as a platform to produce HIV-1 Gag VLPs. The synergies between CCI, MOI and TOH were studied using a response surface methodology approach on four different responses: infection, VLP production, VLP assembly and VLP productivity. TOH and MOI proved to be the major influencing factors in contrast to previous reported data. Interestingly, a remarkable competition between Gag VLP production and non-assembled Gag was detected. Also, the use of nanoparticle tracking analysis and flow virometry revealed the existence of remarkable quantities of extracellular vesicles. The different responses of the study were combined to determine two global optimum conditions, one aiming to maximize the VLP titer (Quantity) and the second aiming to find a compromise between VLP titer and the ratio of assembled VLPs (Quality). This study provides a valuable approach to optimize VLP production and demonstrates that the Hi5/BEVS can support mass production of Gag VLPs and potentially other complex nanoparticles.

Keywords: High five cells, Virus-like particle, Response surface methodology, Multiple criteria decision analysis, Nanoparticle

Abbreviations: *Ac*MNPV, *Autographa californica* multiple nucleopolyhedrovirus; BEVS, baculovirus expression vector system; BV, baculovirus; CCI, cell concentration at infection; cryo-TEM, cryogenic transmission electron microscopy; DoE, design of experiments; eGFP, enhanced green fluorescent protein; EV, extracellular vesicle; HIV, human immunodeficiency virus; hpi, hours post infection; MCDA, multiple-criteria decision analysis; MOI, multiplicity of infection; NTA, nanoparticle tracking analysis; NS, non-significant term; PAT, process analytical technologies; pfu, plaque forming unit; RSM, response surface methodology; TOH, time of harvest; VLP, virus-like particle.

Introduction

Virus-like particles (VLPs) have emerged as promising nanoparticles, particularly in the field of new recombinant vaccines [1]. Compared to other conventional vaccines such as live-attenuated or inactivated viruses, VLPs can elicit potent antibody and T cell responses in a safe manner, since they do not contain genetic material from the virus itself [2]. Among the different proteins able to self-assemble as VLPs, the group-specific antigen (Gag) polyprotein has demonstrated a wide applicability in different research areas. These include their use as immunogens [3], drug delivery vehicles [4], scaffolds for surface antigen presentation [5] and research surrogates [6]. A common need in all these applications is the understanding of the production system itself, which is paramount to define most adequate conditions for VLP production.

The baculovirus species *Autographa californica* multiple nucleopolyhedrovirus (*Ac*MNPV) has been successfully used for the production of a variety of VLP types. The ease of handling, the high productivities associated and the capacity to accommodate large quantities of DNA have made the baculovirus expression vector system (BEVS) a very attractive platform [7,8]. From the different available insect cell lines, Hi5 cells have been reported to produce high VLP titers with a reduced level of contaminant baculovirus [9]. In fact, Cervarix®, the first VLP-based human papillomavirus vaccine approved, is produced using the Hi5/BEVS.

Recent advances in the field of nanoparticle quantification and characterization have brought the opportunity to deepen into the BEVS. In the frame of initiatives such as Process Analytical Technologies (PAT), the application of new and more sophisticated characterization technologies will be a powerful tool to increase the understanding of how the process conditions influence the quality of the final product. Nanoparticle tracking analysis (NTA) and flow virometry are gaining interest as tools to monitor the production of different particles, including VLPs [10,11]. To date, most of the studies dealing with VLPs are performed with indirect quantification methods based on monomer detection, which hinder the appropriate assessment of the final product and the yields obtained [12–14]. In addition, the simultaneous production of extracellular vesicles (EV), which frequently fall in the size range of VLPs, is not often considered and may lead to an erroneous estimation of VLP production. With the aim to deepen in the characterization of the different

existing populations, the *eGFP* was fused in frame to the *gag* gene from the human immunodeficiency virus serotype 1 (HIV-1).

Considering the information from previous reports, we decided to apply these novel techniques for optimizing the Gag VLP production process using the Hi5/BEVS platform. Different methods are available for process improvement, from the classical one-variable-at-a-time approach to more sophisticated statistical design of experiments (DoE) [15]. So far, studies dealing with the production of VLPs have focused either on the former approach [16,17] or on simple factorial designs [12,18], limiting the analysis of higher order effects between the variables influencing VLP production. This is of special relevance since the use of lower or higher MOI than strictly required might reduce the maximum VLP yield obtained or be detrimental to the system, respectively. Here, we applied a response surface methodology (RSM) to evaluate the impact of cell concentration at infection (CCI), multiplicity of infection (MOI) and time of harvest (TOH) on VLP production. To go a step further in process understanding, the inclusion of several responses during process optimization has shown successful results and applicability in different research areas [19–21]. Particularly, the three responses considered in addition to VLP production were: VLP assembly, baculovirus infection and VLP productivity. These are of special relevance in processes with recombinant baculovirus since it is desirable to define production conditions encompassing high production yields with an acceptable ratio of correctly assembled Gag in the form of VLPs, but at the same time maintaining high productivities. A multiple criteria decision analysis (MCDA) was implemented to combine the RSM optimized responses into a global optimal set of conditions based on two criteria: quantity and quality. The two optimal production conditions were successfully validated, and the quantity optimum was compared to other Gag VLP production strategies using the Hi5/BEVS. Finally, correct formation of the VLPs with the typical size and morphology from immature HIV-1 VLPs was characterized using cryogenic transmission electron microscopy (cryo-TEM). The results presented in this work represent an advance with respect to current literature related to Gag VLP production in the Hi5/BEVS and provide useful insights into nanoparticle-based process characterization.

Materials and Methods

Cell line and culture maintenance

Hi5 cells (High Five, cat. num. B85502, Thermo Fisher Scientific, Grand Island, NY, USA) were cultured in suspension in low-hydrolysate content and animal origin-free Sf900III medium (Thermo Fisher Scientific). Cells were routinely maintained at exponential growth phase in 125-mL disposable polycarbonate Erlenmeyer flasks (Corning, Steuben, NY, USA) in 15 mL of medium and subcultured three times a week at a density of 2 - 4 x 10^5 cells/mL [22]. All cultures were shaken at 130 rpm using an orbital shaker (Stuart, Stone, UK) and maintained at 27°C in an incubator. Cell count and viability were performed using the Nucleocounter NC-3000 (Chemometec, Allerod, Denmark) according to manufacturer's instructions.

Baculovirus stock preparation and titration

The recombinant *Autographa californica* multicapsid nucleopolyhedrovirus (*Ac*MNPV), containing the HIV-1 Gag matrix protein fused in frame to eGFP (BV-GageGFP) [23] and under the control of the polyhedrin promoter, was constructed using the BaculoGold system (BD Biosciences, San Jose, CA, USA). Baculovirus amplification was performed in the Sf9 cell line (cat. num. 71104, Merck, Darmstadt, Germany) by infection at 3 x 10^6 cells/mL, a multiplicity of infection (MOI) of 0.1 and harvest at 96 hours post infection (hpi) in Sf900III medium.

Titration of baculovirus infectious particles was conducted using the plaque assay method. Briefly, 1 x 10^6 Sf9 cell/well were infected with serial dilutions of BV-GageGFP samples in 6-well plates (Nunc, Roskilde, Denmark) at 27 °C without agitation. The number of plaque forming units (pfu) was measured by visual inspection and counting after 6 days.

Cell growth and infection conditions

Growth and infection studies were performed in Hi5 cell cultures seeded at 3 x 10^5 cell/mL in 15 mL and maintained at mid-exponential phase by cell passaging every 48h. Several MOI, cell concentrations at infection (CCI) and times of harvest (TOH) were evaluated and the different parameter combinations were defined according to a DoE-based approach. Samples were taken

every 12 – 24 h to monitor viable cell concentration, cell viability, baculovirus infection, intra- and extracellular GageGFP expression and nanoparticle production. Samples were harvested by centrifugation at 3000 x*g* for 5 min and supernatants were maintained at 4 °C until analysis. Cell pellets were stored at -20 °C.

Flow cytometry

The percentage of GageGFP expressing cells was assessed using a BD FACS Canto II flow cytometer equipped with a 488 nm laser configuration (BD Biosciences). Briefly, 0.3 mL of infected cell cultures were harvested by centrifugation at 300 x*g* for 5 min and fixed using 4 % *p*-formaldehyde for 10 min. Cells were then centrifuged at 500 x*g* for 5 min to remove *p*-formaldehyde, resuspended in 0.3 mL ice-cold DPBS (Thermo Fisher Scientific) and maintained at 4 °C until further analysis.

Fluorescence confocal microscopy

BV-GageGFP infected Hi5 cells were observed using a TCS SP5 confocal microscope (Leica, Wetzlar, Germany). Cells were stained with 0.05% v/v of CellMask™ and 0.1% v/v of Hoechst (Thermo Fisher Scientific, Eugene, OR, USA) to visualize the lipid membrane and cell nucleus, respectively. A washing step prior to observation was performed by centrifugation at 300 x*g* during 5 min and then cells were resuspended in fresh Sf900III medium. Samples were placed in 35 mm glass bottom Petri dishes with 14 mm microwell (MatTek Corporation, Ashland, MA, USA) for visualization. The VLP production process was monitored during 6.5 minutes at 48 hpi using the Resonant scanner mode of the confocal microscope (Leica).

GageGFP quantification

The amount of GageGFP produced by Hi5 infected cells was measured intra- and extracellularly. Supernatant of GageGFP producing cells was harvested by centrifugation at 3000 x*g* for 5 min and maintained at 4 °C until analysis. Intracellular GageGFP content was evaluated by disruption of pelleted cells by means of three freeze-thaw cycles (2h frozen at -20ªC and thawed at 37ºC for

0.5 h). Samples were vortexed for 5 seconds between cycles. Lysed pellets were resuspended in 0.5 mL of TMS buffer (50 mM Tris-HCl, 150 mM NaCl, 2 mM $MgCl_2$, pH 8.0), centrifuged at 13700 x*g* for 20 min and kept at 4 °C. GageGFP fluorescence was measured with a Cary Eclipse fluorescence spectrophotometer (Agilent Technologies, Santa Clara, CA, USA) at RT as follows: λ_{ex} = 488 nm (5 nm slit), λ_{em} = 500 - 530 nm (10 nm slit). Relative fluorescence unit values (R.F.U.) were calculated by subtracting fluorescence unit values of BV-GageGFP infected and non-infected samples. R.F.U. values were converted into GageGFP VLPs as described by Gutiérrez-Granados et al. [24] and detailed in the following equation:

$$\text{GageGFP VLP (particles/mL)} = 1.53 \cdot 10^8 \text{ x R.F.U.} \quad (1)$$

The Sf900III medium and a 0.1 mg/mL quinine sulphate solution were used as control patterns to normalize R.F.U. values in samples between different experiments.

VLP quantification using nanoparticle tracking analysis

A NanoSight NS300 (Malvern Panalytical, Malvern, United Kingdom) was used to measure fluorescent and non-fluorescent particles by nanoparticle tracking analysis (NTA). Samples were diluted in 0.22 µm-filtered DPBS and continuously injected into the device chamber through a pump at an average concentration of 10^8 particles/mL (20 – 60 particles/frame). Videos of 60 s from independent triplicate measurements were analyzed with the NTA 3.2 software at RT. The nanoparticle number was evaluated in the 100 – 250 nm range.

Nanoparticle quantification using flow virometry

Fluorescent and non-fluorescent nanoparticles were also analyzed using a CytoFlex LX (Beckman Coulter, Brea, CA, USA) equipped with a 488 nm blue laser for fluorescent particle detection. Samples were diluted in 0.22 µm-filtered DPBS and triplicate measurements from independent samples were analyzed with the CytExpert 2.3 software at RT.

Analytical ultracentrifugation

Supernatants of infected Hi5 cells with BV-GageGFP were harvested at the different conditions of the DoE were ultracentrifuged in a double cushion of 5 mL of 25 % and 8 mL of 45 % (w/v) sucrose (Sigma Aldrich, Sant Louis, MO, USA) solution prepared in DPBS and DMEM (Thermo Fisher Scientific), respectively. 5 mL of supernatants from triplicate experiments were loaded in ultracentrifuge tubes (Beckman Coulter) and filled to the top with sterile DPBS. Sample ultracentrifugation and analyses were performed as previously reported in chapter 1. The same procedure was applied to characterize the optimal conditions of the DoE and MCDA approach.

Cryogenic transmission electron microscopy

VLP morphology was assessed using a transmission electron microscope equipped for sample cryogenics (cryo-TEM). Briefly, 4 µL of sample were blotted onto EMR Holey carbon films on 400 mesh copper grids (Micro to Nano, Wateringweg, Netherlands) previously subjected to a glow discharge treatment in a PELCO easiGlow^{TM} Discharge Cleaning System (PELCO, Fresno, CA, USA). Deposited samples were then plunged into liquid ethane at −180 °C using a Leica EM GP workstation (Leica) and observed in a JEM-2011 TEM operating at 200 kV (Jeol Ltd., Akishima, Tokyo, Japan).

Multiple optimization of VLP production conditions

Response surface methodology (RSM) was applied to assess the effect of the main factors influencing the BEVS: CCI (cell/mL), MOI (pfu/cell) and TOH (h) on different responses. The selected DoE responses were infection (% of infected cells), VLP production (fluorescent particle/mL), GageGFP polyprotein assembled in the form of VLPs (% of GageGFP assembled as VLPs) and VLP productivity (fluorescent particle/mL·h). VLP production and VLP productivity responses were transformed to *log* values using the logarithmic regression to reduce the funnel shape effect of the residuals. This transformation compensated softened the increasing differences in standard deviation associated to higher figures, a common feature when simultaneously considering values with more than 1000-fold difference [25]. In parallel, infection

and VLP assembly responses were converted using the logistic regression to limit the possible values of the functions to the 0 – 100 % range:

$$Y_n = \log\left(\frac{y_n}{100 - y_n}\right) \quad (2)$$

where Y_n is the converted response and y_n is the experimental response in natural values.

A Box-Behnken design was used to determine the influence of CCI, MOI and TOH on each evaluated response. These variables were screened at a low (-1), medium (0) and high level (+1) as indicated in Table 1. The different levels were linearly related for CCI and TOH and exponentially for MOI, always in an equidistant manner. The results obtained for each response were fitted to a second-order polynomial by the least squares method (Eq. 3):

$$Y = \beta_0 + \beta_1 \cdot CCI + \beta_2 \cdot MOI + \beta_3 \cdot TOH + \beta_4 \cdot CCI \cdot MOI + \beta_5 \cdot CCI \cdot TOH + \beta_6 \cdot MOI \cdot TOH + \beta_7 \cdot CCI^2 + \beta_8 \cdot MOI^2 + \beta_9 \cdot TOH^2 + \varepsilon \quad (3)$$

where Y is the response variable, β_0 is the model intercept term, $\beta_1 - \beta_9$ are the model coefficients and ε is the experimental error. Fitting of the different equations based on Eq. 3 was performed with R software (R Foundation for Statistical Computing, Vienna, Austria). Three-dimensional plots were constructed to facilitate model interpretation.

The most common DoE approach involves the optimization of a single response. However, such analysis may not be enough for the BEVS, since the definition of a production condition cannot be accurately predicted from an individual property. Then, the objective of including more than one response in the study was to determine global conditions integrating different key aspects of BEVS. To this purpose, a multiple criteria decision analysis (MCDA) based on desirability functions was implemented. The different responses were transformed to a dimensionless desirability value (d_n) ranging between 0 and 1:

$$d_n = 0 \quad \text{if } y_n < min_n \quad (4)$$

$$d_n = \left(\frac{y_n - min_n}{max_n - min_n}\right)^w \quad \text{if } min_n \leq y_n \leq max_n$$

$$d_n = 1 \quad \text{if } y_n > max_n$$

where y_n is the predicted response of the fitted equation, d_n is the desirability response function, w accounts for the weight value and min_n and max_n are the minimum and maximum acceptable values of y_n, respectively. The weight (w value) depended on the relative importance assigned to each individual response. Then, all the different desirability response functions under study were combined in a single equation, denoted as overall desirability (OD):

$$OD = \sqrt[N]{\prod_{1}^{N} d_n} \quad (5)$$

where OD is the overall desirability function to be maximized and N is the number of responses studied in the optimization process.

Statistical analyses

The experimental design and statistical analyses of the different equations were performed using R software. The quality of the regression of the fitted equations was evaluated with the R^2 and R^2_{adj} coefficients in percentage units. An analysis of variance (ANOVA) F-test was used to determine the significance of the equations and the individual coefficients were assessed with a t-test. The lack-of-fit (LOF) test was used to evaluate differences between experimental and pure error of the fitted equations. In all analyses, p-values of 0.05 and 0.1 were considered statistically significant with 95 % and 90 % confidence, respectively.

Results

Definition of the space boundaries

Initially, the growth of Hi5 cells was characterized to determine an adequate range of viable cell concentration at infection (CCI) for the DoE. Cells maintained a high viability (> 90 %) until 96 h of culture, coinciding with the peak of viable cell concentration. In these conditions, cells reached a maximum of 7.3 ± 0.2 x 10^6 cells/mL and a doubling time (T_d) of 18.7 ± 0.5 h (Fig. 1).

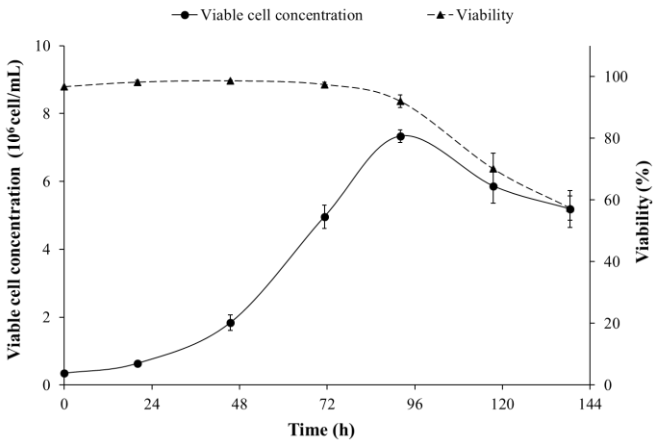

Figure 1. Cell growth and viability profiles of Hi5 cells in batch culture in Sf900III medium. Exponentially growing cells were seeded at 0.3 x 10^6 cells/mL in 125-mL flasks. Mean values ± standard deviation of triplicate experiments are represented.

Considering the extent of the exponential phase and the T_d, the range for cell concentration at infection was restricted to 0.5 – 2.5 x 10^6 cells/mL. Some difficulties were encountered when defining the different levels of multiplicity of infection (MOI) and time of harvest (TOH) since very little information of the BEVS with Hi5 in Sf900III medium was available. The ranges for both variables were eventually fixed according to previous experience with this system (data not shown), as well as based on studies of the Hi5/BEVS in other cell culture media [12,26]. MOI experimental range was fixed between 0.01 and 5 with the aim to screen low and high MOI conditions therein the same DoE. In the case of TOH, the boundaries were defined as 24 – 84 hpi. DoE space boundaries did not involve high CCI out of the exponential phase or medium exchange in order to simplify their industrial application, but these conditions were evaluated as a contrast to the optimal conditions obtained in this work.

Combining RSM and MCDA to define the optimal VLP production conditions

A three-variable (CCI, MOI and TOH) Box-Behnken RSM was constructed and the following objective responses were analyzed: baculovirus infection efficiency, VLP production, VLP assembly and VLP productivity. This experimental design was selected among different candidates due to its variance distribution and spatial properties [22,27,28]. The resulting matrix consisted in 15 experiments including a triplicated center point to account for the inherent

variability of the system (Table 1). The different datasets were adjusted to second order polynomial functions by the least squares method according to Eq. 3.

Table 1. Matrix design, independent variable levels and regression coefficients for the Box-Behnken design. VLP concentration values were quantified using nanoparticle tracking analysis.

Box-Behnken design

Experimental run	Variables			Responses			
	CCI (10^6 cell/mL)	MOI (pfu/cell)	TOH (h)	Infection (%)	VLP production (10^8 fluorescent particle/mL)	VLP assembly (%)	VLP productivity (10^6 fluorescent particle/mL·h)
1	1.5	0.01	84	98.5	345.5	14.4	411.3
2	0.5	0.22	84	99.5	118.1	31.5	140.6
3	1.5	0.22	54	99.2	230.0	17.1	420.0
4	1.5	0.22	54	99.6	214.8	15.2	410.0
5	2.5	5	54	99.3	320.2	13.4	593.0
6	1.5	5	84	99.4	265.3	17.5	315.8
7	1.5	0.01	24	3.3	0.2	98.2	0.9
8	1.5	5	24	95.5	11.6	57.2	48.3
9	2.5	0.01	54	21.7	8.7	14.6	16.1
10	0.5	0.01	54	97.8	34.3	37.7	63.4
11	0.5	0.22	24	56.4	1.9	94.6	7.7
12	2.5	0.22	84	99.5	465.4	13.2	554.1
13	0.5	5	54	99.7	101.8	34.3	188.5
14	1.5	0.22	54	99.4	200.0	13.1	370.0
15	2.5	0.22	24	30.7	1.1	93.9	4.4

Analysis

Function	*F* test, *p*-value	LOF test, *p*-value	R^2	Adjusted R^2	Predicted R^2
Infection	<0.01	0.1	95.0	90.0	68.7
VLP production	<0.01	0.05	99.7	99.1	95.0
VLP assembly	<0.01	0.06	94.9	92.1	79.9
VLP productivity	<0.01	0.05	99.5	98.7	92.9

Model	Infection		VLP production		VLP assembly		VLP productivity	
Parameters	Coefficient	*p*-value	Coefficient	*p*-value	Coefficient	*p*-value	Coefficient	*p*-value
Constant	4.7	<0.01	5.4	<0.01	-1.4	<0.01	6.0	<0.01
CCI	-0.9	0.03	0.1	>0.1	-0.5	0.04	0.1	>0.1
CCI^2	NS	>0.1	-0.8	<0.01	NS	>0.1	-0.8	<0.01
MOI	2.0	<0.01	1.1	<0.01	-0.5	0.04	1.1	<0.01
MOI^2	-1.0	0.08	-0.6	<0.01	NS	>0.1	-0.6	<0.01
TOH	2.6	<0.01	2.3	<0.01	-2.0	<0.01	2.0	<0.01
TOH^2	-1.8	<0.01	-1.7	<0.01	-1.9	<0.01	-1.5	<0.01
CCI · MOI	1.1	0.06	0.6	<0.01	NS	>0.1	0.6	<0.01
CCI · TOH	NS	>0.1	0.6	<0.01	NS	>0.1	0.5	<0.01
MOI · TOH	-1.4	0.02	-1.1	<0.01	1.0	<0.01	-1.1	<0.01

NS: Non-statistically significant

The statistical significance of the different functions and their associated coefficients was confirmed by ANOVA (Table 1). Each function was used to construct three-dimensional plots for a better comprehension of the synergies between CCI, MOI and TOH (Fig. 2). As expected, baculovirus infection progressed more rapidly with increasing MOI (Fig. 2a – c). However, the pace of infection decreased when using the same MOI at higher CCI. A similar behavior was observed between VLP production and VLP productivity (Fig. 2d – i). Low MOI required longer TOH to achieve higher VLP yields whereas higher MOI shortened this period. In both cases, the best production and productivity titers were obtained in the 1.5 – 2.5 x 10^6 cell/mL CCI range. Extracellular vesicles (EV) were also present in all conditions and their concentration increased with longer TOH (data not shown). TOH also proved to be the most significant regarding the amount of GageGFP monomer assembled in the form of VLPs (Fig. 2j – l). Increasing TOH and MOI substantially decreased the ratio of VLPs to non-assembled monomers, regardless the value of CCI.

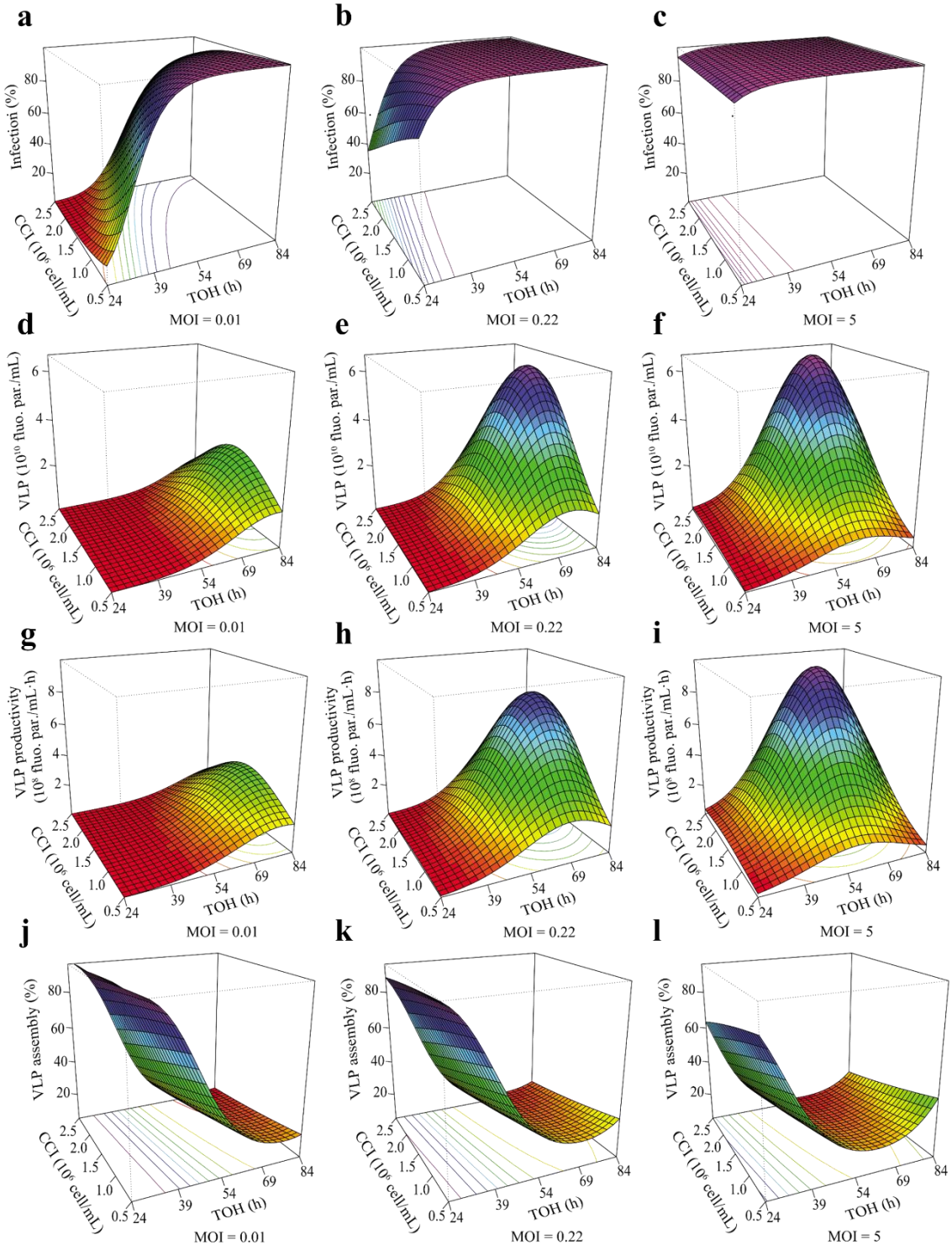

Figure 2. Three-dimensional plots of the different functions based on the Box-Behnken experimental results. (a – c) Infection (d – f) VLP production (g – i) VLP productivity (j – l) VLP assembly as a function of CCI, MOI and TOH. All the graphs were constructed by representing the effect of two independent variables on a response while maintaining the third one at a fixed level.

The models were used to predict an optimal combination of CCI, MOI and TOH to maximize each specific response. In this case, different independent variable combinations resulted in the

optimum condition for each function (Table 2), thus making difficult to define a global optimum condition combining all the different models at once.

Table 2. Optimal CCI, MOI and TOH conditions maximizing each response function.

Response function	CCI (10^6 cell/mL)	MOI (pfu/cell)	TOH (h)
Infection efficiency	0.5	0.2	76.4
VLP production	2.0	1.3	73.5
VLP assembly	0.5	0.01	24.0
VLP productivity	2.0	2.3	67.8

Therefore, a multiple-criteria decision analysis (MCDA) based on desirability functions was applied in order to determine a global optimum combining the different functions. Every model function was transformed to a dimensionless scale (Eq. 4) and given a weight according to the importance of each response. A higher priority was assigned to VLP production, VLP assembly and VLP productivity (w = 2) whilst a lower restriction was assigned to infection (w = 1). Two possible response combinations were considered in the MCDA, the first focused on maximizing product quantity and the second one maximizing product quality. To do this, the VLP assembly function was excluded from the MCDA in the definition of a global optimal condition targeting product quantity. The application of the MCDA for the product quality optimal resulted in a CCI, MOI and TOH of 1.1 x 10^6 cell/mL, 1 pfu/cell and 33.6 hpi, respectively. The optimum maximizing product quantity was determined as 2.0 x 10^6 cell/mL for CCI, a MOI of 2.5 pfu/cell and a TOH of 69.3 hpi.

Validating the quantity and quality global optima

The two global optimal conditions obtained by the combination of RSM and MCDA were successfully corroborated in a validation experiment. Hi5 cell growth was arrested after BV-GageGFP infection with > 80 % of the culture infected at 24 hpi (Fig. 3a – b). As expected, a higher cell viability was observed for the quality optima (33.6 hpi) compared to the quantity condition at TOH (69.3 hpi). Confocal microscopy analysis of infected cells showed successful

colocalization (yellow) of the GageGFP polyprotein (green) with the cell membrane (red), thus indicating that VLP formation and production was taking place (Fig. 3c). This process could be tracked in real time using a confocal fluorescence microscope with the high-speed acquisition mode (Fig. S1).

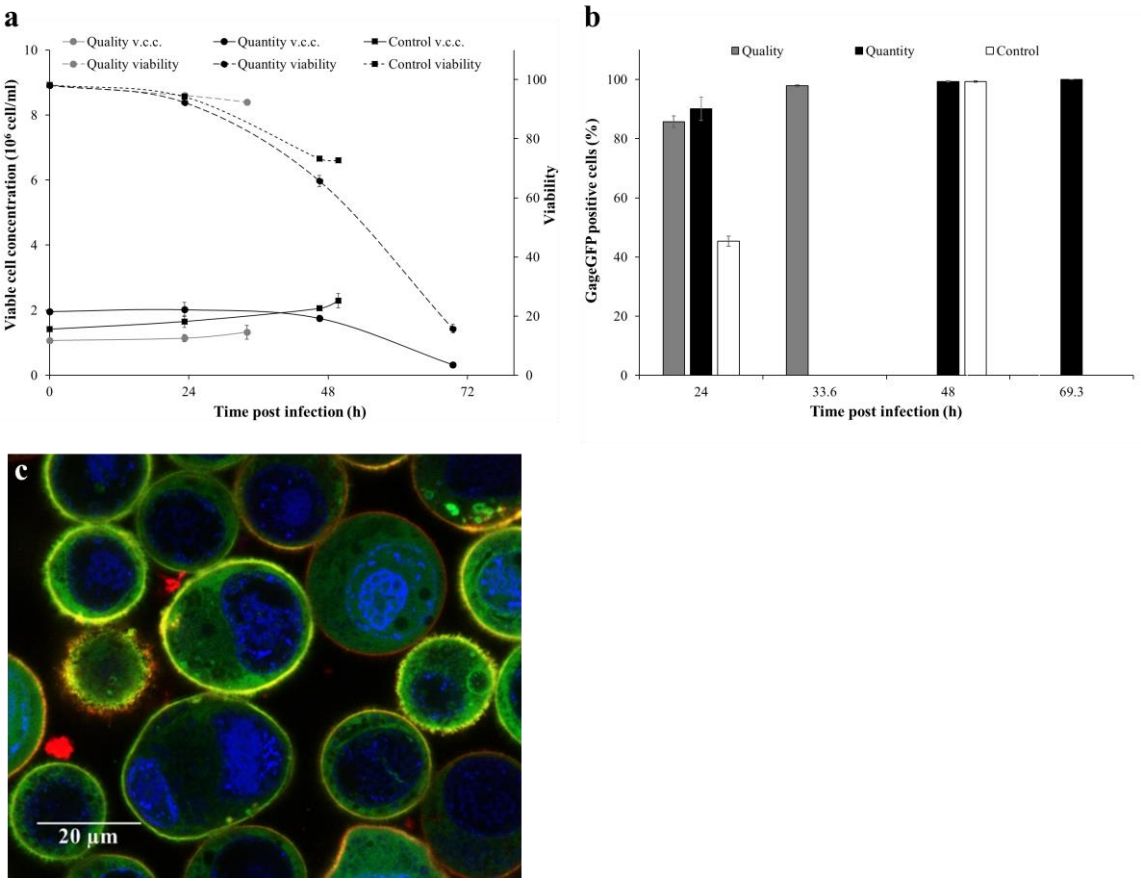

Figure 3. Validation experiment of the quality and quantity optima. (a) Viable cell concentration and viability progression after infection with the BV-GageGFP. The center point (infection control) of the Box-Behnken DoE was also included to account for the robustness of the infection process, with cells infected with a MOI of 0.22 at 1.5 x 10^6 cell/mL and harvested at 54 hpi. (b) BV-GageGFP infection kinetics in the different conditions tested. Infected cells were measured every 24 h until their optimal TOH. (c) Hi5 cells infected with the BV-GageGFP at 2.0 x 10^6 cell/mL and a MOI of 2.5 and observed at 48 hpi. Cell nucleus was stained with Hoechst (blue) and cell membrane with CellMask^{TM} (red). The mean and standard deviation of triplicate experiments are represented.

Measurement of fluorescence indicated that the highest pace of GageGFP production was achieved with higher MOI. Also, the highest fluorescence yield in the supernatant was achieved with the quantity optimum (2448.6 ± 23.8 R.F.U.) at 69.3 hpi (Fig. 4a). The TOH for the quality optimum condition coincided with the peak of intracellular GageGFP production, but not for the quantity optimum. In all cases, GageGFP production in the supernatant progressively increased

with longer TOH although the intracellular GageGFP levels reached a maximum concentration that subsequently decreased (Fig. 4b). Analysis of the VLP production kinetics of the quantity optimum by flow virometry evidenced that there was a continuous increase in VLP concentration (Fig. 4c). Comparison of VLP production in both optima by means of NTA yielded a 10-fold and 4.8-fold increase in production and productivity in the quantity over the quality optimum, respectively. In all cases, the experimental outcome was within the predicted limits (Table 3).

Table 3. Experimental validation of the global optimal conditions and comparison to model predictions. VLP concentrations measurements were carried out with NTA. Prediction interval represent the lower limit and the upper limits according to the logarithmic or logistic response transformation.

	Product quality		Product quantity	
Response	Experimental	Model prediction	Experimental	Model prediction
Infection (%)	97.8 ± 2.0	[71.6 – 99.7]	100	[96.6 – 100]
VLP production (10^8 fluorescent particle/mL)	39.0 ± 4.5	[15.6 – 60.2]	391.0 ± 13.9	[337.2 – 1333.4]
VLP assembly (%)	64.6 ± 5.1	[46.4 – 72.9]	13.2 ± 1.0	[5.7 – 18.2]
VLP productivity (10^6 fluorescent particle/mL·h)	118.1 ± 27.8	[48.3 – 186.2]	564.2 ± 20.2	[477.6 – 1884.8]

Similar ratios of VLPs to total nanoparticles were observed, representing the 9.7 ± 3.1 % for the quality and a 9.3 ± 1.1 % for the quantity condition. In contrast, analysis of the optima by sucrose cushion ultracentrifugation showed a higher degree of GageGFP monomer assembled in the form of VLPs in the quality optimum (64.6 ± 5.1 %). The SN and SN-25 % fractions, corresponding to non-assembled GageGFP, showed significantly larger levels of fluorescence in the quantity optimum (Fig. 4d). However, VLP containing fractions (25 – 45 % and 45 %) were more enriched in the quality condition. BV-GageGFP titration of both optima by plaque assay resulted in a 2.7-fold increase of infectious particles in the quantity (13.2 ± 5.1 x 10^7 pfu/mL) compared to quality condition (4.8 ± 1.5 x 10^7 pfu/mL).

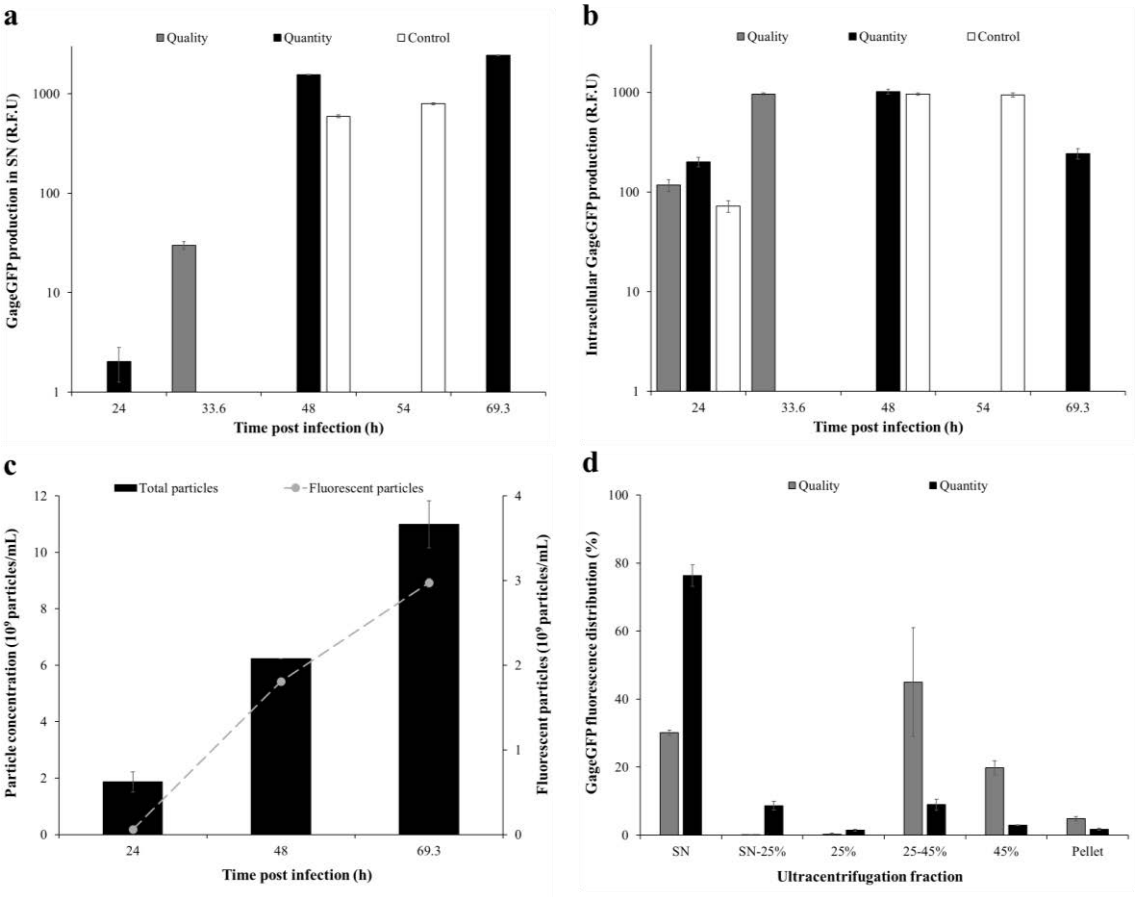

Figure 4. GageGFP and VLP production in the validation experiment. (a – b) GageGFP production kinetics in the supernatant and intracellularly. Samples were taken every 24 h until their respective TOH. (c) Fluorescent and total nanoparticle production time profile measured by flow virometry in the quantity optimal condition. (d) Fluorescence distribution after double sucrose cushion ultracentrifugation of the quality and quantity optima. These experiments were performed in triplicate.

An acceptable correlation between indirect VLP quantification with spectrofluorometry and direct measurement with NTA was only achieved for the quality optimum condition (Eq. 1). Contrariwise, the GageGFP fluorescence levels of the quantity optimum by spectrofluorometry (2448.6 ± 23.8 R.F.U.) and conversion to VLP concentration resulted in a 9.6-fold increase compared to NTA quantification. Introducing the assembly factor measured by ultracentrifugation (Table 3) allowed to determine the GageGFP fluorescence exclusively attributed VLPs (323.2 ± 3.1 R.F.U.) and discard that of unassembled GageGFP monomer. Hence, a close prediction to the NTA quantification was achieved ($4.9 \pm 0.5 \times 10^{10}$ VLP/mL).

Supernatant characterization of the quality and quantity optima by cryogenic transmission electron microscopy (cryo-TEM) indicated that VLPs were correctly formed in both conditions

(Fig. 5). Interestingly, the median VLP size was higher in the quality (181.4 ± 4.4 nm) compared to the quantity optimum (164.7 ± 0.3 nm). The presence of EV and baculovirus was also detected, in agreement with the existence of a non-fluorescent particle population observed with the NTA.

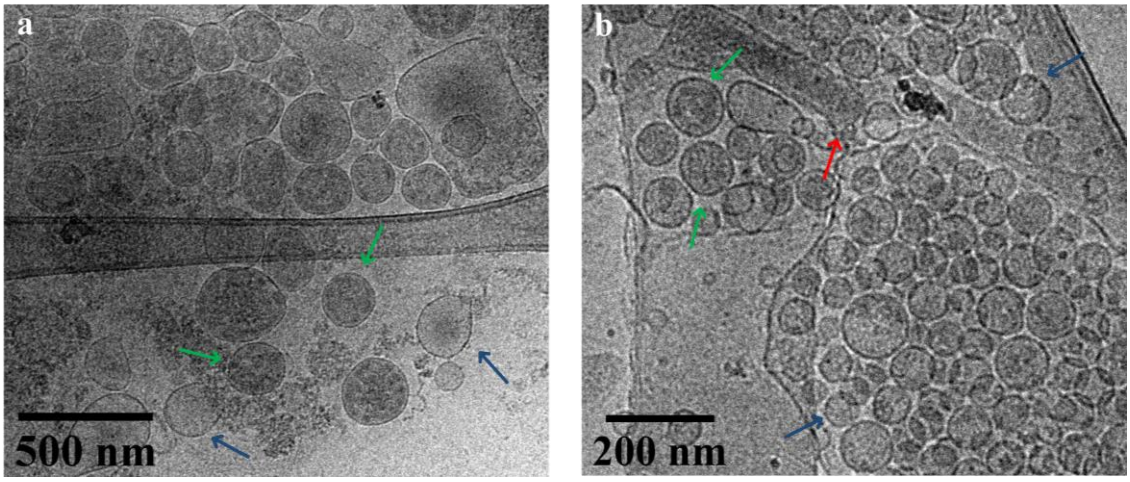

Figure 5. GageGFP VLP characterization by cryo-TEM. (a – b) Supernatant visualization of the quality (33.6 hpi) and quantity (69.3 hpi) optimal conditions, respectively. The arrows indicate the different specimens: VLP (green), EV (blue) and baculovirus (red).

Comparison to other VLP production conditions

From both optimal conditions, the quantity optimum, which achieved the highest VLP titer, was compared to other baculovirus infection strategies not considered in the DoE. The first approach consisted in infecting the Hi5 cell line at a high cell concentration and MOI. To this purpose, Hi5 cells were infected at the concentration 6 x 10^6 cell/mL with a MOI of 5. The second strategy consisted in performing a medium replacement before infection using the quantity optimum. This option was considered as a means to value if the added effort of performing a medium replacement would provide a substantial advantage in VLP concentration. Baculovirus infection progressed more rapidly after medium exchange that in the original condition but the drop in cell viability was not significantly affected (Fig. 6a – b). On the other hand, baculovirus infection advanced more slowly in the high CCI condition, to the point that cell culture was not fully infected after 72 hpi. Medium exchange before infection increased GageGFP production by 1.3-fold at 69.3 hpi, corresponding to 3168.6 ± 100.2 R.F.U. in comparison to the 2528.0 ± 76.3 R.F.U. achieved in the quantity condition (Fig. 6c – d). The same improvement was observed in VLP quantification

by NTA, with 4.3 ± 0.2 x 10^{10} VLP/mL for medium exchange while 3.4 ± 0.3 x 10^{10} VLP/mL were measured for the quantity optimum condition. However, baculovirus infection at the high CCI condition reached a significantly lower GageGFP production (66.6 ± 3.3 R.F.U.) as well as in terms of VLP production (2.3 ± 0.6 x 10^{8} VLP/mL).

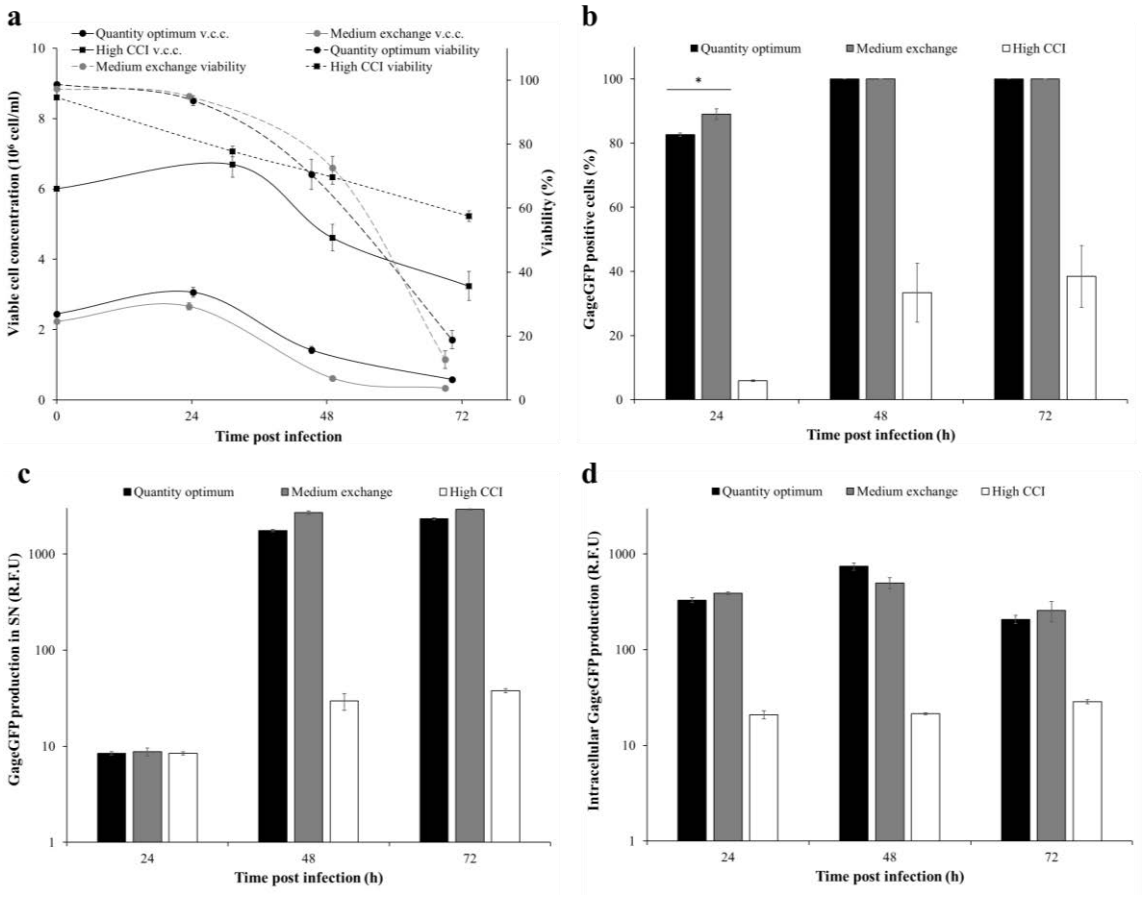

Figure 6. VLP production using medium exchange (Ex) and baculovirus infection at high CCI (High). (a – b) Viable cell concentration, cell viability and BV-GageGFP infection kinetics in the different conditions tested. (c – d) Supernatant and intracellular GageGFP production. The average of triplicate experiments is represented.

The median size of VLPs in these conditions did not substantially vary from the quantity optimum (168.2 ± 3.3 nm), being 169.6 ± 3.3 nm for the medium exchange and 160.5 ± 3.7 nm for the high CCI. Similar levels of total nanoparticles were obtained in the three different conditions, thus representing a big difference in the ratio of VLP to total nanoparticles (Table 4). Remarkable differences were also observed in terms of infectious baculovirus particles. Medium replacement before infection increased the levels by 2.1-fold (47.0 ± 9.9 x 10^{7} pfu/mL) compared to the 22.7 ± 2.5 x 10^{7} pfu/mL achieved in the quantity optimum condition. However, a much lower baculovirus titer of 0.9 ± 0.3 x 10^{7} pfu/mL was obtained for the high CCI condition.

Table 4. Comparison of GageGFP VLP production levels of the quantity optimum, medium exchange and high CCI conditions measured by NTA.

Condition	VLP production (10^8 fluorescent particle/mL)	Total particle production (10^8 particle/mL)	Ratio fluor. particles/total particles (%)	VLP size (nm)
Quantity optimum	335.0 ± 29.0	4260.0 ± 609.0	8 ± 1.7	168.2 ± 3.3
Medium Exchange	432.0 ± 22.0	5510.0 ± 232.0	7.8 ± 0.2	169.6 ± 3.3
High CCI	2.3 ± 0.6	523.0 ± 767	0.1	160.5 ± 3.7

Discussion

The Hi5/BEVS has demonstrated a high versatility to produce a wide variety of recombinant proteins. However, the capabilities of the Hi5 cell line as a production platform of complex multimeric structures, such as enveloped VLPs, have not been explored into detail. To date, the quantification of VLP production has been performed based on indirect quantification methods [12]. Moreover, most of the research have been conducted either in low performing or animal compound containing culture media [16,29]. Although these studies have brought advances in the production of nanoparticles using the Hi5/BEVS, a deeper study would contribute to exploit the full potential of such platform.

CCI, MOI and TOH were selected as the critical parameters affecting the production of HIV-1 Gag VLP in the BEVS. For a comprehensive analysis, four different responses were considered and simultaneously evaluated by means of RSM and MCDA. TOH and MOI were shown to be particularly relevant to achieve a high VLP concentration but also in maintaining an adequate ratio of GageGFP assembly in the form of VLPs. Pillay and co-workers used a factorial experiment to assess the effect of different MOI comprised in the range of 0.1 – 5 in Hi5 cells [12]. They did not identify any significant different in Gag yield but here we observed that MOI plays a significant role in VLP production. Interestingly, including a function for VLP assembly based on GageGFP fluorescence distribution in the different fractions of an ultracentrifugation proved to be highly relevant. These results in combination with direct nanoparticle quantification by NTA and flow virometry permitted to obtain a much accurate perspective of the process.

A pronounced decrease in VLP assembly was shown with increasing TOH, limiting a favorable combination with the other three responses. To this purpose, two different global optimization strategies were examined by MCDA, one considering the VLP assembly function (therefore with priority on product quality) and the other not (therefore with priority on product quantity). Remarkable differences were encountered between the two optima, achieving a 10-fold higher VLP production in the quantity condition whereas a 4.9-fold increase in the assembly of GageGFP as VLPs was obtained in the quality optimum. Then, it is evident that Hi5 cells possess a high capacity to produce GageGFP but there is a remarkable competition between the formation of VLPs and the release of unassembled GageGFP monomer. The large amount of GageGFP produced, potentially overcoming the capacity of the cell line itself to process all the GageGFP in the form of VLPs, combined to cell membrane disruption could be the reason explaining these results. This could be appreciated even in the quality optimum itself, in which a high cell viability of 92.4 ± 0.6 % was measured at 33.6 hpi (Fig. 3a) and a 64.6 ± 5.1 % of the fluorescence in the supernatant was associated to VLPs, meaning that around the 35 % remaining was due to unassembled GageGFP monomer. These results emphasize the need to complement the methods most currently used for VLP identification or quantification based on monomer detection with direct nanoparticle assessment techniques, specially using the Hi5 cell line [12,30–34].

The application of cryo-TEM helped to gain insight into the identification of the morphological features of the VLPs produced (Fig. 5). Cryo-TEM has recently been highlighted as powerful methodology for nanoparticle characterization as the different specimens can be observed in native conditions [35–37]. GageGFP VLPs presented the expected size of 100 – 200 nm and morphology consistent with immature HIV-1 VLPs, comparable to VLPs produced in Sf9 [38] and HEK 293 cells [39]. The rod-shaped structure corresponding to the infective form of the baculovirus was also detected. The presence of EVs was observed alongside VLPs, which are known to be produced as way of communication in eukaryotic cells [40]. EVs were more heterogeneous in size and shape (50 – 500 nm) compared to VLPs as well as less electron-dense. These results coincide with the measurements performed by the NTA and flow virometry where

a remarkable population of non-fluorescent nanoparticles was detected. Future efforts are needed to understand their role in insect cell lines since little information is available.

A maximum HIV-1 GageGFP VLP concentration of 3.9 ± 0.1 x 10^{10} VLP/mL was achieved in the supernatant using the product quantity optimum. Thus, these conditions would be selected in case of designing a VLP manufacturing process. However, if the presence of baculoviruses posed a risk for the final VLP application, the quality optimum provides a 2.7-fold reduction in infectious particles, which would facilitate the downstream process. Difficulties were encountered in the comparison of the VLP yield obtained since most of the studies producing Gag VLPs with the insect cell/BEVS used indirect quantification methods based on monomer detection [12,13,41]. Nevertheless, when the comparison of nanoparticle production was possible, this optimum condition proved to be superior to Gag VLP production in HEK 293 cells without [42] and with [27] additive supplementation by 14.4 and 1.7-fold, respectively. Moreover, these conditions proved to be superior to influenza VLP production using the Sf9 [43] and Hi5/BEVS [44] by 6.7 and 25-fold, respectively. The potential of the quantity optimum was also evaluated against other baculovirus infection strategies in this work. Infection at high CCI using a high MOI resulted in a much lower yield of VLP production probably owing to the scarcity of some nutrients in the medium (Table 4). BV production was also significantly reduced in such conditions. These differences in production could be related to the cell density effect previously described in insect cells with the BEVS [45–47]. On the other side, medium replacement before BV infection moderately increased VLP production but duplicated baculovirus production. This strategy has proven to be an efficient manner to increase both the yield of recombinant proteins [48] and baculoviruses [49] with the Sf9/BEVS cells and also in mammalian cells [50,51]. In this case, no substantial benefit was obtained, thus indicating that the added efforts required to perform medium replacement might not be advantageous.

In conclusion, a detailed study of Gag VLP production using the Hi5/BEVS was conducted. The application of RSM and MCDA allowed to go a step further and capture the synergies between the influential factors affecting the VLP production process. The combination of advanced statistical methods with a variety of nanoparticle quantification and characterization techniques

allowed to obtain a full picture of the process as well as to determine a high-yielding and reproducible condition for VLP production. The approach here proposed is valuable for studies dealing with the production of other complex nanoparticles. Future efforts in transferring this process into bioreactor scale should allow to define a robust platform for VLP production.

Acknowledgments

The authors would like to thank Dr. Paula Alves (Instituto de Biologia Experimental e Tecnológica, Oeiras, Portugal) for providing the BTI-TN-5B1-4 cell line. Marta Martínez-Calle developed the BV-GageGFP. Ángel Calvache (Beckman Coulter) facilitated the access to CytoFlex LX flow cytometer. The support of Martí de Cabo and Mónica Roldán from Servei de Microscòpia of UAB with the cryo-TEM and confocal microscopy, respectively, are appreciated. Eduard Puente-Massaguer is a recipient of an FPU grant from Ministerio de Educación, Cultura y Deporte of Spain (FPU15/03577). The research group is recognized as 2017 SGR 898 by Generalitat de Catalunya.

Compliance with Ethical Standards

Conflict of interest

The authors declare that they have no competing interests.

Ethical approval

This article does not contain any studies with human participants performed by any of the authors.

References

[1] M.O. Mohsen, L. Zha, G. Cabral-Miranda, M.F. Bachmann, Major findings and recent advances in virus–like particle (VLP)-based vaccines, Semin. Immunol. 34 (2017) 123–132.

[2] A.M.C. Andersson, M. Schwerdtfeger, P.J. Holst, Virus-like-vaccines against HIV, Vaccines. 6 (2018) 1–17.

[3] K.R. Young, T.M. Ross, Elicitation of immunity to HIV type 1 Gag is determined by Gag structure, AIDS Res. Hum. Retroviruses. 22 (2006) 99–108.

[4] V.K. Deo, T. Kato, E.Y. Park, Chimeric Virus-Like Particles Made Using GAG and M1 Capsid Proteins Providing Dual Drug Delivery and Vaccination Platform, Mol. Pharm. 12 (2015) 839–845.

[5] J. Vidigal, B. Fernandes, M.M. Dias, M. Patrone, A. Roldão, M.J.T. Carrondo, P.M. Alves, A.P. Teixeira, RMCE-based insect cell platform to produce membrane proteins captured on HIV-1 Gag virus-like particles, Appl. Microbiol. Biotechnol. 102 (2018) 655–666.

[6] L. Buonaguro, M. Tagliamonte, M.L. Visciano, Chemokine receptor interactions with virus-like particles, in: Methods Mol. Biol., Humana Press, Totowa, NJ, 2013: pp. 57–66.

[7] S. Gómez-Sebastián, J. López-Vidal, J.M. Escribano, Significant productivity improvement of the baculovirus expression vector system by engineering a novel expression cassette, PLoS One. 9 (2014) 1–10.

[8] F. Fernandes, A.P. Teixeira, N. Carinhas, M.J.T. Carrondo, P.M. Alves, Insect cells as a production platform of complex virus-like particles., Expert Rev. Vaccines. 12 (2013) 225–36.

[9] T. Senger, L. Schädlich, L. Gissmann, M. Müller, Enhanced papillomavirus-like particle production in insect cells, Virology. 388 (2009) 344–353.

[10] P. Pereira Aguilar, T.A. Schneider, V. Wetter, D. Maresch, W.L. Ling, A. Tover, P. Steppert, A. Jungbauer, Polymer-grafted chromatography media for the purification of enveloped virus-like particles, exemplified with HIV-1 gag VLP, Vaccine. (2019).

[11] L. Nika, S. Cuadrado-Castano, G. Asthagiri Arunkumar, C. Grünwald-Gruber, M.

McMahon, K. Koczka, A. García-Sastre, F. Krammer, R. Grabherr, L. Nika, S. Cuadrado-Castano, G. Asthagiri Arunkumar, C. Grünwald-Gruber, M. McMahon, K. Koczka, A. García-Sastre, F. Krammer, R. Grabherr, A HER2-Displaying Virus-Like Particle Vaccine Protects from Challenge with Mammary Carcinoma Cells in a Mouse Model, Vaccines. 7 (2019) 1–19.

[12] S. Pillay, A. Meyers, A.L. Williamson, E.P. Rybicki, Optimization of chimeric HIV-1 virus-like particle production in a baculovirus-insect cell expression system, Biotechnol. Prog. 25 (2009) 1153–1160.

[13] M.L. Visciano, L. Diomede, M. Tagliamonte, M.L. Tornesello, V. Asti, M. Bomsel, F.M. Buonaguro, L. Lopalco, L. Buonaguro, Generation of HIV-1 Virus-Like Particles expressing different HIV-1 glycoproteins, Vaccine. 29 (2011) 4903–4912.

[14] J.R. Haynes, L. Dokken, J.A. Wiley, A.G. Cawthon, J. Bigger, A.G. Harmsen, C. Richardson, Influenza-pseudotyped Gag virus-like particle vaccines provide broad protection against highly pathogenic avian influenza challenge, Vaccine. 27 (2009) 530–541.

[15] E. Puente-Massaguer, L. Badiella, S. Gutiérrez-Granados, L. Cervera, F. Gòdia, A statistical approach to improve compound screening in cell culture media, Eng. Life Sci. 19 (2019) 1–13.

[16] F. Krammer, T. Schinko, D. Palmberger, C. Tauer, P. Messner, R. Grabherr, Trichoplusia ni cells (High Five™) are highly efficient for the production of influenza A virus-like particles: A comparison of two insect cell lines as production platforms for influenza vaccines, Mol. Biotechnol. 45 (2010) 226–234.

[17] P. Pushko, I. Tretyakova, R. Hidajat, A. Zsak, K. Chrzastek, T.M. Tumpey, D.R. Kapczynski, Virus-like particles displaying H5, H7, H9 hemagglutinins and N1 neuraminidase elicit protective immunity to heterologous avian influenza viruses in chickens, Virology. 501 (2017) 176–182.

[18] A.R. Pastor, G. González-Domínguez, M.A. Díaz-Salinas, O.T. Ramírez, L.A. Palomares, Defining the multiplicity and time of infection for the production of Zaire Ebola virus-like

particles in the insect cell-baculovirus expression system, Vaccine. (2019).

[19] S. Pinzi, D. Leiva, G. Arzamendi, L.M. Gandia, M.P. Dorado, Multiple response optimization of vegetable oils fatty acid composition to improve biodiesel physical properties, Bioresour. Technol. 102 (2011) 7280–7288.

[20] S. Honary, P. Ebrahimi, R. Hadianamrei, Optimization of particle size and encapsulation efficiency of vancomycin nanoparticles by response surface methodology, Pharm. Dev. Technol. 19 (2014) 987–998.

[21] A.L. Bukzem, R. Signini, D.M. dos Santos, L.M. Lião, D.P.R. Ascheri, Optimization of carboxymethyl chitosan synthesis using response surface methodology and desirability function, Int. J. Biol. Macromol. 85 (2016) 615–624.

[22] E. Puente-Massaguer, M. Lecina, F. Gòdia, Nanoscale characterization coupled to multi-parametric optimization of Hi5 cell transient gene expression, Appl. Microbiol. Biotechnol. 102 (2018) 10495–10510.

[23] L. Hermida-Matsumoto, M.D. Resh, Localization of human immunodeficiency virus type 1 Gag and Env at the plasma membrane by confocal imaging., J. Virol. 74 (2000) 8670–8679.

[24] S. Gutiérrez-Granados, L. Cervera, F. Gòdia, J. Carrillo, M.M. Segura, Development and validation of a quantitation assay for fluorescently tagged HIV-1 virus-like particles, J. Virol. Methods. 193 (2013) 85–95.

[25] V.A. Barbur, D.C. Montgomery, E.A. Peck, Introduction to Linear Regression Analysis., Wiley, 1994.

[26] L. Sander, A. Harrysson, Using cell size kinetics to determine optimal harvest time for Spodoptera frugiperda and Trichoplusia ni BTI-TN-5B1-4 cells infected with a baculovirus expression vector system expressing enhanced green fluorescent protein, Cytotechnology. 54 (2007) 35–48.

[27] L. Cervera, J. Fuenmayor, I. Gonzalez-Dominguez, S. Gutierrez-Granados, M.M. Segura, F. Godia, I. González-Domínguez, S. Gutiérrez-Granados, M.M. Segura, F. Gòdia, I. González-Domínguez, S. Gutiérrez-Granados, M.M. Segura, F. Gòdia, I. González-

Domínguez, S. Gutiérrez-Granados, M.M. Segura, F. Gòdia, I. Gonzalez-Dominguez, S. Gutierrez-Granados, M.M. Segura, F. Godia, Selection and optimization of transfection enhancer additives for increased virus-like particle production in HEK293 suspension cell cultures, Appl. Microbiol. Biotechnol. 99 (2015) 9935–9949.

[28] S. Gutierrez-Granados, L. Cervera, M. de las M.M. de L.M.M. de las M. Segura, J. Wolfel, F. Godia, S. Gutiérrez-Granados, L. Cervera, M. de las M.M. de L.M.M. de las M. Segura, J. Wölfel, F. Gòdia, S. Gutierrez-Granados, L. Cervera, M. de las M.M. de L.M.M. de las M. Segura, J. Wolfel, F. Godia, S. Gutiérrez-Granados, L. Cervera, M. de las M.M. de L.M.M. de las M. Segura, J. Wölfel, F. Gòdia, Optimized production of HIV-1 virus-like particles by transient transfection in CAP-T cells, Appl. Microbiol. Biotechnol. 100 (2016) 3935–3947.

[29] M. Wilde, M. Klausberger, D. Palmberger, W. Ernst, R. Grabherr, Tnao38, high five and Sf9-evaluation of host-virus interactions in three different insect cell lines: Baculovirus production and recombinant protein expression, Biotechnol. Lett. 36 (2014) 743–749.

[30] M. Tagliamonte, M.L. Visciano, M.L. Tornesello, A. De Stradis, F.M. Buonaguro, L. Buonaguro, Constitutive expression of HIV-VLPs in stably transfected insect cell line for efficient delivery system, Vaccine. 28 (2010) 6417–6424.

[31] Z. Shoja, M. Tagliamonte, S. Jalilvand, T. Mokhtari-Azad, R. Hamkar, S. Shahmahmoodi, F. Rezaei, M. Tornesello, F.M. Buonaguro, L. Buonaguro, R. Nategh, Development of a stable insect cell line constitutively expressing rotavirus VP2, Virus Res. 172 (2013) 66–74.

[32] F. Monteiro, V. Bernal, M. Chaillet, I. Berger, P.M. Alves, Targeted supplementation design for improved production and quality of enveloped viral particles in insect cell-baculovirus expression system, J. Biotechnol. 233 (2016) 34–41.

[33] L. Maranga, T.F. Brazao, M.J.T. Carrondo, Virus-like particle production at low multiplicities of infection with the baculovirus insect cell system, Biotechnol. Bioeng. 84 (2003) 245–253.

[34] J. Fuenmayor, L. Cervera, F. Gòdia, A. Kamen, Extended gene expression for Gag VLP

production achieved at bioreactor scale, J. Chem. Technol. Biotechnol. 94 (2019) 302–308.

[35] J. Maldonado, S. Cao, W. Zhang, L. Mansky, Distinct Morphology of Human T-Cell Leukemia Virus Type 1-Like Particles, Viruses. 8 (2016) 1–11.

[36] J.L. Martin, S. Cao, J.O. Maldonado, W. Zhang, L.M. Mansky, Distinct Particle Morphologies Revealed through Comparative Parallel Analyses of Retrovirus-Like Particles, J. Virol. 90 (2016) 8074–8084.

[37] J. Gallagher, D. McCraw, U. Torian, N. Gulati, M. Myers, M. Conlon, A. Harris, Characterization of Hemagglutinin Antigens on Influenza Virus and within Vaccines Using Electron Microscopy, Vaccines. 6 (2018) 1–21.

[38] L. Nika, J. Wallner, D. Palmberger, K. Koczka, K. Vorauer-Uhl, R. Grabherr, Expression of full-length HER2 protein in Sf 9 insect cells and its presentation on the surface of budded virus-like particles, Protein Expr. Purif. 136 (2017) 27–38.

[39] A. Venereo-Sanchez, R. Gilbert, M. Simoneau, A. Caron, P. Chahal, W. Chen, S. Ansorge, X. Li, O. Henry, A. Kamen, Hemagglutinin and neuraminidase containing virus-like particles produced in HEK-293 suspension culture: An effective influenza vaccine candidate, Vaccine. 34 (2016) 3371–3380.

[40] J. Ratajczak, M. Wysoczynski, F. Hayek, A. Janowska-Wieczorek, M.Z. Ratajczak, Membrane-derived microvesicles: important and underappreciated mediators of cell-to-cell communication, Leukemia. 20 (2006) 1487–1495.

[41] L. Buonaguro, F.M. Buonaguro, M.L. Tornesello, D. Mantas, E. Beth-Giraldo, R. Wagner, S. Michelson, M.C. Prevost, H. Wolf, G. Giraldo, High efficient production of Pr55gag virus-like particles expressing multiple HIV-1 epitopes, including a gp120 protein derived from an Ugandan HIV-1 isolate of subtype A, Antiviral Res. 49 (2001) 35–47.

[42] L. Cervera, S. Gutiérrez-Granados, M. Martínez, J. Blanco, F. Gòdia, M.M. Segura, Generation of HIV-1 Gag VLPs by transient transfection of HEK 293 suspension cell cultures using an optimized animal-derived component free medium, J. Biotechnol. 166 (2013) 152–165.

[43] C.M. Thompson, E. Petiot, A. Mullick, M.G. Aucoin, O. Henry, A.A. Kamen, Critical assessment of influenza VLP production in Sf9 and HEK293 expression systems., BMC Biotechnol. 15 (2015) 31.

[44] S.B. Carvalho, J.M. Freire, M.G. Moleirinho, F. Monteiro, D. Gaspar, M.A.R.B. Castanho, M.J.T. Carrondo, P.M. Alves, G.J.L. Bernardes, C. Peixoto, Bioorthogonal Strategy for Bioprocessing of Specific-Site-Functionalized Enveloped Influenza-Virus-Like Particles., Bioconjug. Chem. 27 (2016) 2386–2399.

[45] H.T. Huynh, T.T.B. Tran, L.C.L. Chan, L.K. Nielsen, S. Reid, Effect of the peak cell density of recombinant AcMNPV-infected Hi5 cells on baculovirus yields, Appl. Microbiol. Biotechnol. 99 (2014) 1687–1700.

[46] V. Bernal, N. Carinhas, A.Y. Yokomizo, M.J.T. Carrondo, P.M. Alves, Cell density effect in the baculovirus-insect cells system: A quantitative analysis of energetic metabolism, Biotechnol. Bioeng. 104 (2009) 162–180.

[47] H.T. Huynh, T.T.B. Tran, L.C.L. Chan, L.K. Nielsen, S. Reid, Decline in baculovirus-expressed recombinant protein production with increasing cell density is strongly correlated to impairment of virus replication and mRNA expression, Appl. Microbiol. Biotechnol. 97 (2013) 5245–5257.

[48] A.W. Caron, J. Archambault, B. Massie, High-level recombinant protein production in bioreactors using the baculovirus-insect cell expression system, Biotechnol. Bioeng. 36 (1990) 1133–1140.

[49] N. Carinhas, V. Bernal, A.Y. Yokomizo, M.J.T. Carrondo, R. Oliveira, P.M. Alves, Baculovirus production for gene therapy: The role of cell density, multiplicity of infection and medium exchange, Appl. Microbiol. Biotechnol. 81 (2009) 1041–1049.

[50] L. Cervera, S. Gutiérrez-Granados, N.S. Berrow, M.M. Segura, F. Gòdia, Extended gene expression by medium exchange and repeated transient transfection for recombinant protein production enhancement, Biotechnol. Bioeng. 112 (2015) 934–946.

[51] F. Bollin, V. Dechavanne, L. Chevalet, Design of experiment in CHO and HEK transient transfection condition optimization, Protein Expr. Purif. 78 (2011) 61–68.

Supplementary information

Figure S1. Time lapse of High Five cells infected with BV-GageGFP recorded during 6.5 min. Cell membrane was stained with CellMask™ (red) and cell nucleus with Hoechst (blue). Green dots in the cell membrane and in the supernatant correspond to GageGFP VLPs.

Chapter 2 – Part II

Application of advanced quantification techniques in nanoparticle-based vaccine development with the baculovirus-insect cell system

Eduard Puente Massaguer, Martí Lecina and Francesc Gòdia

Abstract

Nanoparticles generated by recombinant technologies are receiving increased interest in several applications, particularly the use of virus like particles (VLPs) for the generation of safer vaccines. The characterization and quantification of these nanoparticles with complex structures is very relevant for a better comprehension of the production systems and should circumvent the limitations of the most conventional quantification techniques often used. Here, we applied confocal microscopy, flow virometry and nanoparticle tracking analysis (NTA) to assess the production process of Gag virus-like particles (VLPs) in the Sf9 cell/ baculovirus expression vector system (BEVS). These novel techniques were implemented in an optimization workflow based on Design of Experiments (DoE) and desirability functions to determine the best production conditions. A higher level of sensitivity was observed for NTA and confocal microscopy but flow virometry proved to be more accurate. Interestingly, extracellular vesicles were detected as an important source of contamination of this system. The synergistic interplay of viable cell concentration at infection (CCI), MOI and TOH was assessed on five objective responses: VLP assembly, infection, VLP production, viability and VLP productivity. Two global optimal conditions were defined, one targeting the maximal amount of VLPs and the other providing a balance between production and assembled VLPs. In both cases, a low MOI proved to be the best condition to achieve the highest VLP production and productivity yields. Cryo-EM analysis of nanoparticles produced in these conditions showed the typical size and morphology of HIV-1 VLPs. This study presents an integrative approach based on the combination of DoE and direct nanoparticle quantification techniques to comprehensively optimize the production of VLPs and other viral-based biotherapeutics.

Keywords: flow virometry, nanoparticle tracking analysis, confocal microscopy, baculovirus expression vector system, virus-like particle, statistical design, Sf9 cells.

Abbreviations: *Ac*MNPV, *Autographa californica* multiple nucleopolyhedrovirus; BBD, Box-Behnken design; BEVS, baculovirus expression vector system; BV, baculovirus; CCI, cell concentration at infection; cryo-EM, cryogenic electron microscopy; DoE, Design of Experiments; eGFP, enhanced green fluorescent protein; EV, extracellular vesicle; HIV, human immunodeficiency virus; hpi, hours post infection; MOI, multiplicity of infection; NTA, nanoparticle tracking analysis; pfu, plaque forming unit; TOH, time of harvest; VLP, virus-like particle.

Introduction

The development of vaccines based on virus-like particles (VLPs) has gained interest in the last few years. These complex nanoparticles emerged as an alternative to inactivated and live-attenuated viruses since they resemble the native viral structure but do not contain genomic material of the virus [1]. This feature makes VLPs an attractive vaccine platform since they are unable to replicate nor infect thus improving their safety profile [2]. Also, the repetitive structure acquired from the assembly of multiple subunits has proven to stimulate humoral and cellular immune responses to a higher level than that of their soluble counterparts [3]. Enveloped VLPs are class of these nanoparticles that are composed of a lipid membrane that obtain from the host producing cells. These type of VLPs provide a very flexible means to introduce different antigen epitopes and form chimeric VLPs [4,5]. The HIV-1 Gag polyprotein is able to generate these nanoparticles through a self-assembly process when expressed in a heterologous system. Gag VLPs are produced via a budding process after the pressure exerted by the Gag monomers accumulated in the vicinity of the cell membrane is enough to completely bend it [6].

Several studies have been conducted to appraise the production of Gag VLPs in a range of eukaryotic systems, including animal cell lines [7], yeast [8] and plants [9]. Among them, the insect cell/baculovirus expression vector system (BEVS) offers a good compromise between production yield and capacity of efficiently processing these complex nanoparticles [10]. The Sf9 cell line, a clonal isolate of *Spodoptera frugiperda* Sf21 cells, has been successfully used to produce Gag VLPs over the last 30 years [11]. However, most often the actual presence of VLPs is not followed directly but rely on the use of disruptive methods for quantification. Therefore, the implementation of novel techniques enabling to quantify VLPs as well as other nanoparticle populations in native conditions, would provide substantial information to better characterize the process. Nanoparticle tracking analysis (NTA) has shown an increasing acceptance as a tool to quantify and characterize nanoparticles in the last years. Its use has been validated in the characterization of different VLP types [12,13] as well as in the assessment of extracellular vesicle (EV) populations [14,15]. Recent progress made in the field of flow cytometry has increased its possibilities as an analytical technique at nanoscale level [16]. These upgrades have enabled to

apply flow virometry for the detection of small nanoparticles, especially in the field of EVs [17]. Confocal microscopy has also been underlined as a tool with great potential to characterize nanoparticles [18,19]. Advancements in this technique have allowed the detection of structures beyond the Abbe diffraction limit (~250 nm), which make VLPs and EVs ideal candidates for microscopy studies. A breadth of applications in the field of nanoparticles is possible for these emerging technologies, with special relevance in the characterization of biological production platforms.

So far, current literature dealing with production optimization of Gag VLPs is very scarce, and few information on the synergies between the main variables influencing baculovirus-based production is available [20,21]. Here, we analyzed the effect of cell concentration at infection (CCI), multiplicity of infection (MOI) and time of harvest (TOH) as the critical parameters involved in the BEVS by means of Design of Experiments (DoE). This rational statistical approach depends on the combination of a defined number of experiments that enable to determine the individual and combined effects of different independent variables on one objective response [22,23]. To go a step further, different objective responses were simultaneously considered for a better comprehension of the process, including baculovirus infection, VLP production, VLP assembly, cell viability and VLP productivity. The different responses were combined by means of desirability functions [24,25] into a global optimal condition based on two criteria: quality and quantity. Both conditions were successfully corroborated in comparison to other VLP production approaches with the Sf9/BEVS. A final characterization of the morphology of Gag VLPs was performed using cryogenic electron microscopy.

In summary, an exhaustive evaluation of the Gag VLP production process was performed by means of combining advanced statistical designs and cutting-edge VLP quantification techniques. To facilitate process characterization and nanoparticle quantification, the *eGFP* fluorescent reporter was fused to HIV-1 *gag* gene. This study provides an interesting workflow to design production strategies for VLPs and potentially other complex nanoparticles using the Sf9/BEVS.

Materials and Methods

Cell line, media and culture conditions

The Sf9 insect cell line (cat. num. 71104, Merck, Darmstadt, Germany) was adapted to grow in the animal origin-free and low-hydrolysate Sf900III medium (Thermo Fisher Scientific, Grand Island, NY, USA). Cells were routinely maintained at the exponential growth phase in 125-mL disposable polycarbonate Erlenmeyer flasks (Corning, Steuben, NY, USA) and subcultured three times a week at a density of 4 - 6 x 10^5 cells/mL. The flasks were shaken at 130 rpm using an orbital shaker (Stuart, Stone, UK) placed in an incubator maintained at 27°C. Cell count and viability assessment were performed using the Nucleocounter NC-3000 (Chemometec, Allerod, Denmark).

Recombinant baculovirus and infection conditions

The recombinant *Autographa californica* multicapsid nucleopolyhedrovirus (*Ac*MNPV) was constructed with the BaculoGold baculovirus expression system (BD Biosciences, San Jose, CA, USA). The baculovirus contained a gene encoding for a Rev-independent full-length *gag* gene [26] fused in frame to eGFP and under the control of the polyhedrin promoter.

Baculovirus amplification was performed by infection at 3 x 10^6 cells/mL at a multiplicity of infection (MOI) of 0.1 and harvest at 96 hours post infection (hpi). Baculovirus titration was performed by the plaque assay method. Shortly, 2 mL of Sf9 cells at 5 x 10^5 cell/mL were infected with serial dilutions of baculovirus-containing samples in 6-well plates (Nunc, Roskilde, Denmark). The number of recombinant baculovirus was measured at 6 days and the titers were expressed as plaque forming units (pfu).

Sf9 cell growth characterization was performed with cells seeded at 4 x 10^5 cell/mL in 15 mL of medium from a 48-h expanded culture maintained in high viability conditions. Infections were conducted at different variable combinations according to the Box-Behnken design (Table 1). Samples were taken at several hpi to monitor viable cell concentration, cell viability, baculovirus infection, nanoparticle production and GageGFP expression in the supernatant and intracellularly.

The number of GageGFP expressing cells was measured at 488 nm in a BD FACS Canto II flow cytometer (BD Biosciences).

Fluorescence confocal microscopy

Sf9 cells infected with the baculovirus encoding for GageGFP were visualized in a TCS SP5 confocal microscope (Leica, Wetzlar, Germany). First, cells were stained with 0.1% v/v of CellMask^{TM} and 0.1% v/v of Hoechst (Thermo Fisher Scientific, Eugene, OR, USA), which stain the cell membrane in a deep red color and the cell nucleus in cyan blue, respectively. Stained cell samples were washed by centrifugation at 300 x*g* during 5 min to remove dye excess and resuspended in fresh Sf900III. 200 µL of sample were placed in 35 mm bottom Petri dishes (MatTek Corporation, Ashland, MA, USA) for visualization. The VLP production process was monitored during 6 min at 48 hpi in baculovirus-infected cells using the SP5 Resonant scanner mode (Leica).

GageGFP quantification by spectrofluorometry

The intra- and extracellular concentration of GageGFP was measured by spectrofluorometry. Supernatant of GageGFP producing cells was harvested by centrifugation at 3000 x*g* for 5 min whereas the intracellular content was evaluated after three freeze-thaw disruption cycles of pelleted cells. Lysed pellets were resuspended in 0.5 mL of TMS buffer and centrifuged at 13700 x*g* for 20 min. GageGFP fluorescence was measured with a Cary Eclipse fluorescence spectrophotometer (Agilent Technologies, Santa Clara, CA, USA) at RT as follows: λ_{ex} = 488 nm (5 nm slit), λ_{em} = 510 nm (10 nm slit). Relative fluorescence unit values (R.F.U.) were calculated by subtracting the fluorescence of non-infected cultures. The Sf900III medium and a 0.1 mg/mL quinine sulphate solution were used to normalize R.F.U. values between experiments.

VLP quantification

VLPs and extracellular vesicles in the size range of 100 – 250 nm were quantified using nanoparticle tracking analysis (NTA) in a NanoSight NS300 (Malvern Panalytical, Malvern,

United Kingdom). Samples were diluted in 0.22 µm-filtered DPBS and injected into the device chamber through a pump at an average concentration of 10^8 particles/mL (20 – 60 particles/frame) at RT. Videos of 60 s from triplicate experiments were recorded and analyzed with the NTA 3.2 software. VLP quantification was also performed using a TCS SP8 confocal microscope (Leica). 50 µL of harvested supernatant were placed in a glass slide (Linealab, Barcelona, Spain) and left 30 min at RT for nanoparticles to settle before visualization (González-Domínguez, in preparation).

Flow virometry was also used for VLP quantification as well as to track the production kinetics of different nanoparticle populations. A CytoFlex LX (Beckman Coulter, Brea, CA, USA) equipped with a 488 nm blue laser for fluorescent particle detection (laser gain = 106) and a 405 nm laser/violet side scatter configuration for improved nanoparticle size resolution (laser gain = 9) was used. Samples were diluted in 0.22 µm-filtered DPBS and analyzed with the CytExpert 2.3 software at room temperature.

Analysis of VLP assembly by analytical ultracentrifugation

VLPs from Sf9 baculovirus infected cells were ultracentrifuged in a double sucrose cushion. Briefly, a volume of 5 mL of clarified supernatant was sublayered in 5 mL of 25 % and 8 mL of 45 % (w/v) sucrose (Sigma Aldrich, Sant Louis, MO, USA) solution prepared in DPBS and DMEM (Thermo Fisher Scientific), respectively. Samples were ultracentrifuged at 31000 rpm and 4ºC for 2.5 h using a SW-32Ti in an Optima L100XP centrifuge (Beckman Coulter). Then, the different fractions were collected and maintained at 4ºC until further analysis.

VLP characterization by cryo-EM

VLP structure and morphology were assessed using cryogenic transmission electron microscopy (cryo-EM). To do this, 4 µL of sample were blotted onto EMR Holey carbon films on 400 mesh copper grids (Micro to Nano, Wateringweg, Netherlands) previously subjected to a glow discharge treatment in a PELCO easiGlow™ Discharge Cleaning System (PELCO, Fresno, CA, USA). Samples were then plunged into liquid ethane at −180 °C using a Leica EM GP workstation

(Leica) and visualized in a JEM-2011 TEM operating at 200 kV (Jeol Ltd., Akishima, Tokyo, Japan).

Design of experiments and desirability functions

A three-variable Box-Behnken design (BBD) was employed to determine the optimal conditions for VLP production using as independent variables viable cell concentration at infection (CCI), multiplicity of infection (MOI) and time of harvest (TOH). Five different responses were analyzed: baculovirus infection efficiency, VLP production, cell viability, VLP productivity and VLP assembly (Table 1). Responses expressed in percentage (infection, viability and VLP assembly) were transformed using logistic regression to limit their values in the 0 – 100 % range. VLP production and VLP productivity responses were converted to the logarithmic scale to normalize the variability of the residuals. The different levels of the BBD were equidistantly related in a linear manner for CCI and TOH and exponentially for MOI. The data obtained for each response was fitted to a second-order polynomial equation by the least squares method as described below:

$$Y = \beta_0 + \sum \beta_i \cdot X_i + \sum \beta_{ij} \cdot X_i \cdot X_j + \sum \beta_{ii} \cdot X_i^2 + \varepsilon \qquad (1)$$

where Y is the response variable under consideration, β_0 is the offset term and β_i, β_{ij} β_{ii} are the linear, interaction and quadratic coefficients, respectively, whereas ε accounts for the experimental error. The functions obtained based on Eq. 1 were used to predict the optimal values of the independent variables with the L-BFGS-B quasi-Newton method of the R Studio software (R foundation for statistical computing, Vienna, Austria).

A multiple response optimization strategy based on desirability functions was applied to find a unique optimal condition including the different functions of the study. These functions were transformed into a dimensionless scale *d* with values comprised between 0 and 1, and combined to maximize the overall desirability (OD) of the multiple response system:

$$d_i = \begin{cases} 0 & if\ f_i < L \\ \left(\frac{f_i - L}{U - L}\right)^w & if\ L \leq f_i \leq U \\ 1 & if\ f_i > U \end{cases} \qquad (2)$$

where d_i is the individual desirability of the response under consideration, f_i is the original response function, w accounts for the weight value assigned to the response and L and U are the lower and upper acceptable values of f_i, respectively. When $w > 1$ indicates that a higher importance is given to values around the maximum whereas $w = 1$ and $w < 1$ mean that the desirability function is linear or is of lower importance, respectively.

Statistical analysis

Statistical analysis of the different functions was conducted using R software (R foundation for statistical computing). The quality of fit of the different equations was evaluated with the R^2 and R^2_{adj} coefficients. The overall significance of each function was determined with the analysis of variance (ANOVA) *F*-test and the relevance of the individual coefficients was assessed with the corresponding *t*-test. The lack-of-fit (LOF) test was used to evaluate differences between experimental and pure error of the fitted equations. In addition, the predicted-R^2 was calculated to compare the experimental error to the prediction error. *p*-values of 0.05 and 0.1 were considered as statistically significant with 95 % and 90 % confidence, respectively.

Results

Optimization of the VLP production process

The different parameters influencing the VLP production process, from baculovirus infection to Gag production and release in the form of assembled VLPs, should be considered as continuous variables. To this purpose, an advanced optimization strategy based on Design of Experiments (DoE) was selected to screen a broad spectrum of possible values of the different variables considered in the study: viable cell concentration at infection (CCI), multiplicity of infection (MOI) and time of harvest (TOH). The Sf9 cell growth was initially evaluated to define the appropriate range for CCI in the Box-Behnken design (Fig. 1). Cells maintained the exponential phase up to 5 - 6 x 10^6 cells/mL, reaching a maximum viable cell concentration of 11.6 ± 0.3 x 10^6 cells/mL at 8 days after seeding. The design space for CCI was defined as 0.5 – 5 x 10^6 cells/mL since higher CCI have been reported to decrease the productivity of the system [27,28]. However, this condition was evaluated as a comparison to the conditions determined after optimization since very few information is available about the performance of Sf9 cells in Sf900III medium at high CCI.

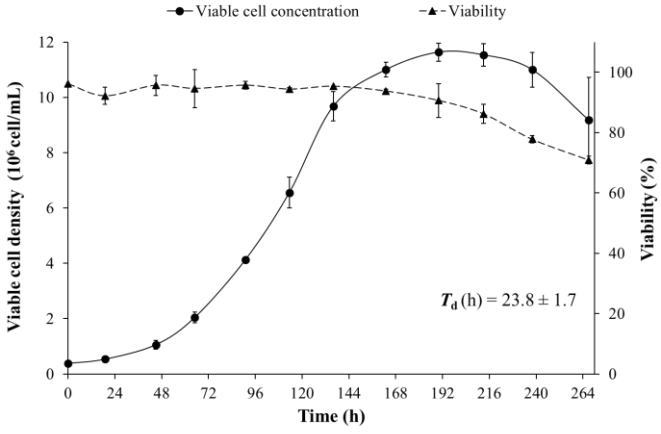

Figure 1. Cell growth and viability of Sf9 cells in Sf900III medium. Cells were seeded at 0.4 x 10^6 cells/mL in 125-mL flasks. The mean and standard deviation of triplicated experiments is represented.

The MOI range was considered as 0.01 – 5 to include experimental conditions allowing cell replication after baculovirus infection and others representing an immediate arrest of cell growth. For TOH, the design space was defined as 24 – 84 hpi to cover a large subset of harvest times depending on the CCI and MOI used. Medium replacement prior to infection was not included in

the DoE in order to simplify the industrial application of the optimal conditions. However, this strategy was analyzed in contrast to the optimal conditions since it has been reported to increase the product titers with the BEVS [29,30].

The synergies between CCI, MOI and TOH were assessed by five different responses relevant to the baculovirus-based Gag VLP production process. These include baculovirus infection efficiency, VLP production, viability, VLP productivity and VLP assembly. The Box-Behnken design matrix with the different independent variables and the observed responses is presented in Table 1. The data were fitted to a second-order polynomial (Eq. 1) for each one of the responses and the statistical significance of the function and the model coefficients were confirmed by ANOVA. The predictability of the different functions was also validated, thus confirming their suitability to navigate the design space.

Table 1. Box-Behnken design, experimental results for each response and ANOVA analysis. VLP concentration values were measured by NTA.

Box-Behnken design

Coded levels	-1	0	1
CCI (10^6 cell/mL)	0.5	2.75	5
MOI (pfu/cell)	0.01	0.22	5
TOH (H)	24	54	84

Experimental run	Variables			Responses				
	CCI (10^6 cell/mL)	MOI (pfu/cell)	TOH (h)	Infection (%)	VLP production (10^8 fluorescent particle/mL)	Viability (%)	VLP productivity (10^6 fluorescent particle/mL·h)	VLP assembly (%)
1	0	-1	1	99.1	225.8	70.3	268.8	33.1
2	-1	0	1	99.5	47.3	64.3	56.3	23.0
3	0	0	0	99.2	120.2	76.4	222.7	45.2
4	0	0	0	99.1	136.1	81.3	252.0	46.4
5	1	1	0	98.8	167.6	71.3	310.4	37.3
6	0	1	1	99.7	146.3	53.9	174.1	22.2
7	0	-1	-1	3.7	1.3	96.4	5.4	98.8
8	0	1	-1	93.6	26.7	94.4	111.1	64.6
9	1	-1	0	95	73.5	93.8	136.1	81.1
10	-1	-1	0	98.3	28.5	93.1	52.8	91.1
11	-1	0	-1	59.6	1.7	94.2	7.1	99.5
12	1	0	1	99.6	168.0	60.8	200.0	17.7
13	-1	1	0	99.5	16.3	61.9	30.2	20.8

14	0	0	0	99	86.7	74.1	160.6	51.4
15	1	0	-1	48.8	11.8	96.8	49.2	97.7

Analysis

Function	*F* test, *p*-value	LOF test, *p*-value	R^2	Adjusted R^2	Predicted R^2
Infection	<0.01	0.07	95.4	93.6	84.2
VLP production	<0.01	0.19	95.7	92.5	78.7
Viability	<0.01	0.05	88.9	87.0	82.4
VLP productivity	<0.01	0.19	93.0	87.8	65.3
VLP assembly	<0.01	0.07	89.9	86.8	64.9

Model	Infection		VLP production		Viability		VLP productivity		VLP assembly	
Parameter	Coefficient	*p*-value	Coefficient	*p*-value	Coefficient	*p*-value	Coefficient	*p*-value	Coefficient	*p*-value
Constant	4.4	<0.01	4.6	<0.01	1.65	<0.01	5.2	<0.01	0.2	>0.1
CCI	n.s	>0.1	0.8	<0.01	n.s	>0.1	0.8	<0.01	n.s	>0.1
CCI^2	n.s	>0.1	-0.7	0.02	n.s	>0.1	-0.7	0.02	n.s	>0.1
MOI	1.2	<0.01	0.4	0.05	-0.6	<0.01	0.4	0.05	-1.2	<0.01
MOI^2	n.s	>0.1	n.s	>0.1	n.s	>0.1	n.s	>0.1	n.s	>0.1
TOH	2.7	<0.01	1.6	<0.01	-1.3	<0.01	1.0	<0.01	-2.3	<0.01
TOH^2	-1.8	<0.01	-1.1	<0.01	n.s	>0.1	-0.9	<0.01	0.9	0.06
CCI · MOI	n.s	>0.1	n.s	>0.1	n.s	>0.1	n.s	>0.1	n.s	>0.1
CCI · TOH	n.s	>0.1	n.s	>0.1	n.s	>0.1	n.s	>0.1	n.s	>0.1
MOI · TOH	-1.2	<0.01	-0.9	<0.01	n.s	>0.1	-0.9	<0.01	0.8	0.08

n.s: non-statistically significant

The interactive effects of the independent variables on the different responses were further investigated by constructing three-dimensional surface plots (Fig. 2). TOH and MOI proved to be the most relevant parameters governing the baculovirus infection efficiency, cell viability and VLP assembly, with no significant contribution of CCI. Higher MOI and TOH increased the infection rate but also decreased cell viability more rapidly (Fig. 2a – b). Analytical ultracentrifugation and fluorescence measurements from the different fractions of each experimental run of the DoE allowed to detect a principal role of longer TOH in decreasing VLP assembly, with a less intense detrimental effect of MOI (Fig. 2c). On the contrary, the three independent variables showed a significant effect in VLP production and productivity (Fig. 2d – i). Higher CCI were the most productive conditions for VLPs in all cases. Larger MOI exhibited the best VLP production and productivity levels at shorter TOH (~54 hpi) but the highest overall production conditions were obtained at low MOI and long TOH for both responses (~84 hpi).

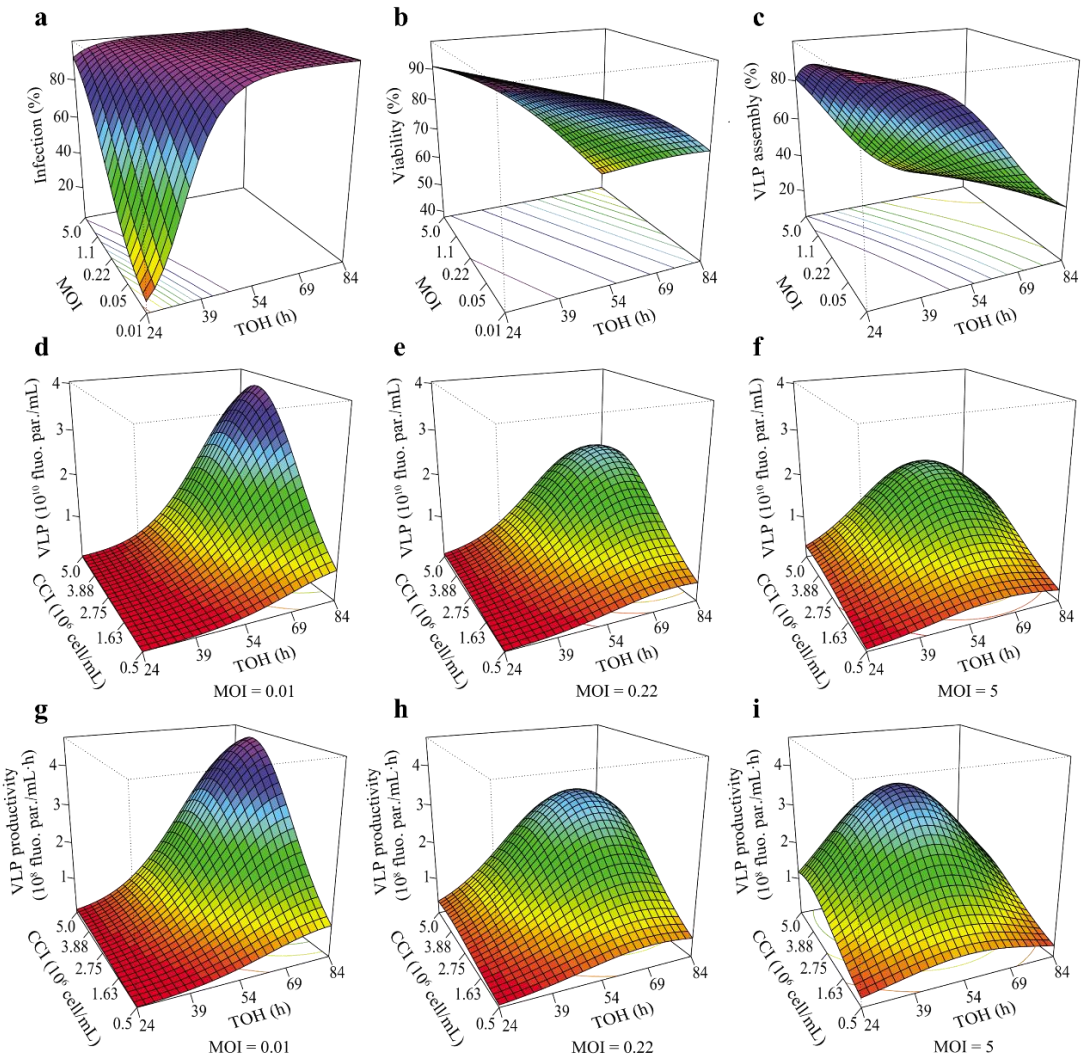

Figure 2. Surface plots based on the experimental results of the Box-Behnken design. (a) Infection (b) Viability (c)VLP assembly (d – f) VLP production (g – i) VLP productivity as a function of CCI, MOI and TOH. The different graphs were constructed by depicting two variables at a time and keeping the third one at a fixed level.

The optimization of the different functions resulted in distinct optimal conditions (Table 2). Therefore, a multiple response optimization approach based on the desirability optimization criteria [31] was adopted to determine a global VLP production condition integrating the information of the responses of the study (Eq. 2).

Table 2. Independent variable optimal values maximizing each response function.

Response function	CCI (10^6 cell/mL)	MOI (pfu/cell)	TOH (h)
VLP production	4.2	0.01	84
Infection	n.s	5.0	66.6
Viability	n.s	0.01	24
VLP productivity	4.2	0.01	84
VLP assembly	n.s	0.01	24

n.s: non-statistically significant

A weight value *w* was attributed to each function based on their relative importance. A higher priority was given to VLP production, VLP assembly and VLP productivity ($w = 2$), whereas a lower limitation was assigned to infection and viability ($w = 1$). Two possible optimal combinations were considered in the desirability function optimization, one pursuing the maximum quantity of VLPs (Quantity) and the other providing a balance between the amount of Gag VLPs produced and Gag assembled into VLPs (Quality). To this purpose, the VLP assembly function was excluded from the desirability function targeting a maximum VLP concentration (Quantity) but maintained in the quantity condition. The optimal conditions for the two global optimization approaches resulted in the same CCI (3.7×10^6 cell/mL) and MOI (0.01) but differed in the TOH, being 60 hpi for the quality and 80 hpi for the quantity condition.

Characterization of the quantity and quality optima

Baculovirus infection at a MOI of 0.01 enabled Sf9 cells to grow until 48 hpi with a progressive decrease in the growth rate. Sf9 cells were completely infected around 60 hpi, time in which cell viability started dropping significantly (Fig. 3a – b). GageGFP expression (green) and trafficking to the cell membrane could be observed in Sf9 baculovirus infected cells (Fig. 3c). The cell nucleus (blue) showed a pronounced enlargement and a granulated-like structure probably associated to baculovirus infection. A time-lapse of VLP formation and release from the cell membrane could be recorded with the high-speed acquisition mode of the confocal microscope. Using this methodology, VLPs were observed as green dots budding from the cell membrane of Sf9 infected cells (Fig. S1).

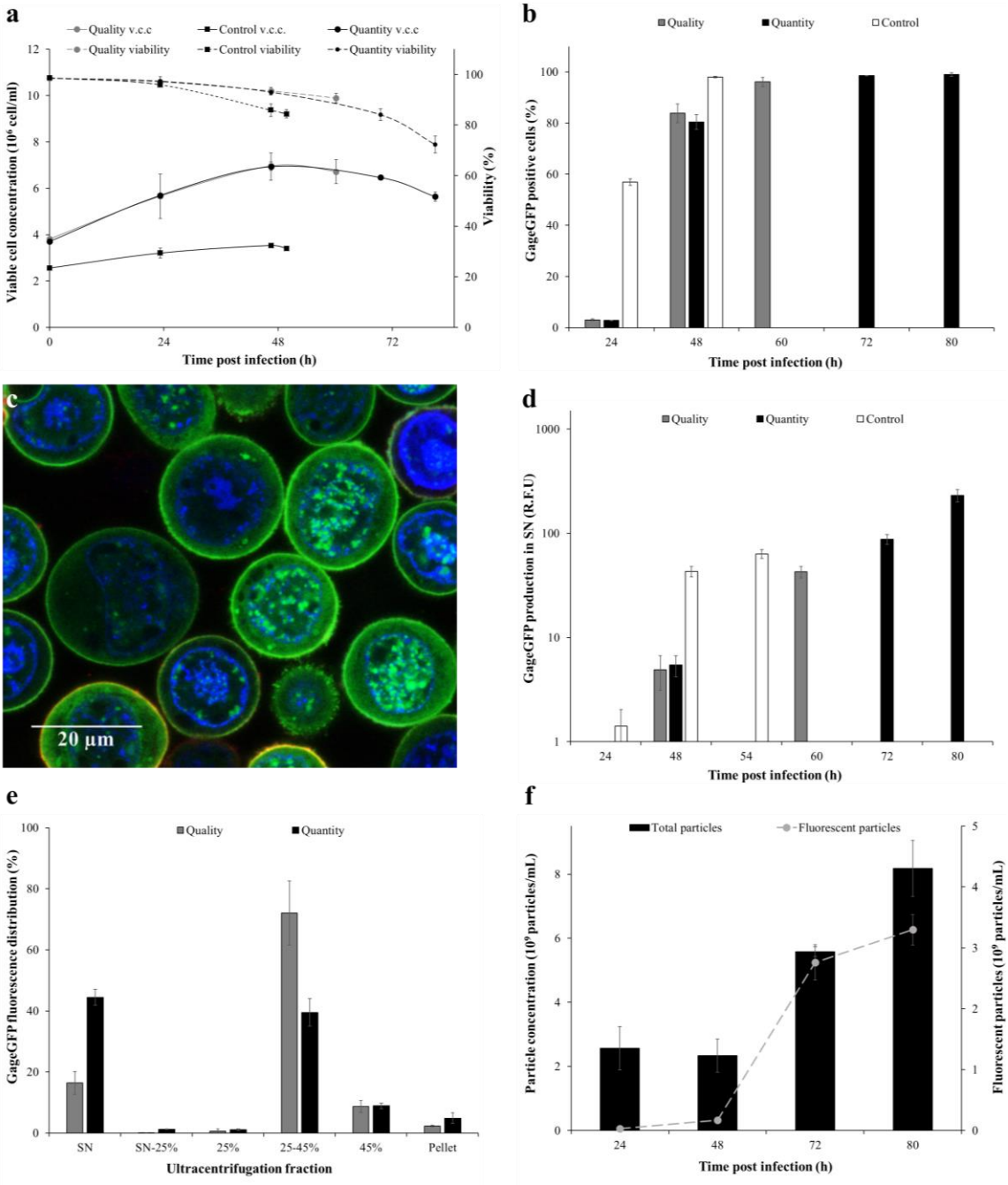

Figure 3. Validation experiment of the quantity and quality optima. (a) Viable cell concentration and viability profiles upon baculovirus infection. A control condition corresponding to the center point of the Box-Behnken design was included to account for the robustness of the infection process. The infection conditions of the center point consisted in a MOI of 0.22 at 2.75 x 10^6 cell/mL and harvest at 54 hpi. (b) Baculovirus infection kinetics. Infected cells were measured every 24 h until their optimal TOH. (c) Baculovirus infected Sf9 cells at 2.0 x 10^6 cell/mL and a MOI of 1 and visualised at 48 hpi. Cell membrane was stained in red with CellMask^{TM} and in blue with Hoechst. (d) Fluorescence measurement of GageGFP production in the supernatant. (e) GageGFP fluorescence distribution after double cushion ultracentrifugation. (f) Nanoparticle production kinetics assessed by flow virometry. The averages of triplicate experiments are represented.

A continuous increase in GageGFP production in the supernatant (Fig. 3d) and intracellularly (Fig. S2) was observed in both conditions by spectrofluorometry. A 2.7-fold increase in total

GageGFP fluorescence was achieved in the quantity optimum (1499.6 ± 85.8 R.F.U.) compared to the quality condition (560.0 ± 74.0 R.F.U.). However, a higher proportion of the GageGFP fluorescence was detected in the 25, 25 – 45 and 45 % fractions in the latter (81.3 ± 13.1 %), indicating a larger amount of GageGFP assembled in the form of VLPs (Fig. 3e). A profound analysis of the nanoparticle production kinetics was performed in the quantity optimum by means of flow virometry (Fig. 3f). Different nanoparticle populations were observed, including VLPs (fluorescent particles) and non-fluorescent particles that could be associated with extracellular vesicles (EV) and baculoviruses. A similar production kinetics could be observed for both nanoparticle populations, achieving the maximum peak of expression at 80 hpi. In these conditions, VLPs accounted for the 40 % of the total nanoparticles produced. VLP quantification using nanoparticle tracking analysis (NTA) revealed a 2-fold increase in the final concentration of the quantity optimum with respect to the quality condition. VLP productivity was also maintained at a higher level in the former, thus proving that extending the TOH from 60 to 80 hpi was valuable (Table 3). Interestingly, this time extension did not significantly increase the titer of baculovirus infectious particles probably because the majority of the cells were already infected at 60 hpi (data not shown). In all cases, the both optimal conditions were within the predicted limits (Table 3).

Table 3. Experimental validation of the quantity and quality global optimal conditions and comparison to model predictions. VLP concentration values were calculated by NTA. Model prediction intervals indicate the lower and upper boundaries for each function according to the logistic or logarithmic response transformation.

	Quality		Quantity	
Response	Experimental	Model prediction	Experimental	Model prediction
VLP production (10^8 fluorescent particle/mL)	176.7 ± 24.2	[44.2 – 466.1]	361.7 ± 39.3	[99.7 – 1279.7]
Infection (%)	96.1 ± 1.8	[91.0 – 99.6]	99.0 ± 0.7	[97.0 – 99.9]
Viability (%)	90.7 ± 1.9	[74.0 – 95.3]	72.3 ± 3.3	[53.0 – 89.7]
VLP assembly (%)	81.3 ± 1.3	[48.0 – 86.5]	49.5 ± 2.3	[13.0 – 67.7]
VLP productivity (10^6 fluorescent particle/mL·h)	295.0 ± 30.3	[131.4 – 424.4]	452.5 ± 49.1	[204.1 – 941.4]

Evaluation of nanoparticle size and morphology by cryogenic electron microscopy (cryo-EM) in both optimal conditions confirmed the presence of different nanoparticle populations (Fig. 4). VLPs were visualized as electron-dense spherical bodies surrounded by a lipid bilayer. Their size ranged in the 100 – 200 nm and not significant differences were found in the median VLP size of the production (153.9 ± 3.6 nm) and assembly condition (149.6 ± 5.8 nm). Besides VLPs, EVs and the budded form of the baculovirus could be detected. EVs were observed as empty particles probably due to the absence of the Gag polyprotein integrating the nanoparticle core. The baculovirus displayed their typical rod-shaped structure consisting of the nucleocapsid surrounded by a lipidic membrane.

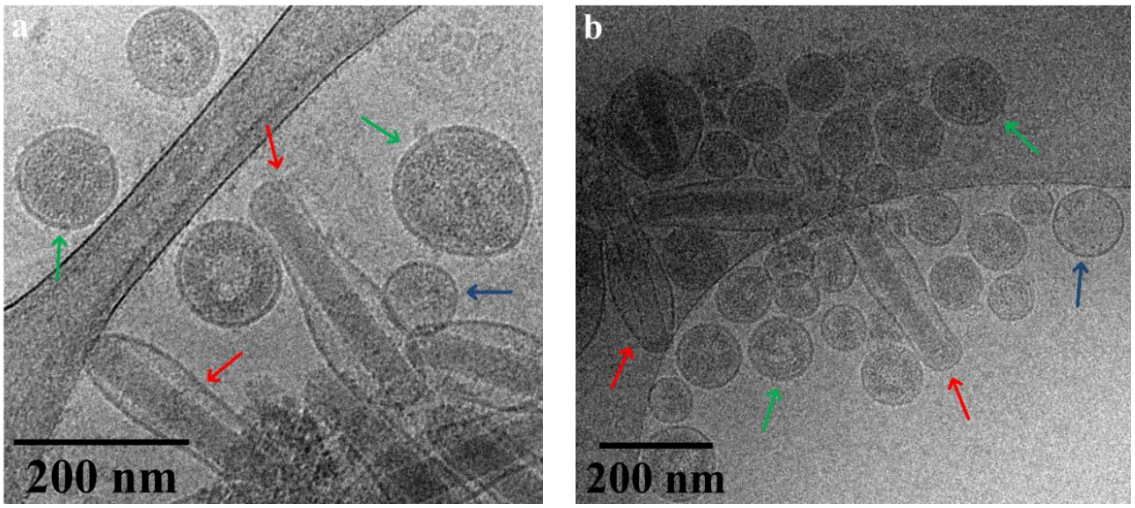

Figure 4. Nanoparticle visualization in the optimal conditions by cryo-EM. (a – b) Supernatant of the quality (60 hpi) and quantity (80 hpi) optimal conditions, respectively. The arrows indicate the different specimens: VLP (green), EV (blue) and baculovirus (red).

Comparison to alternative VLP production conditions using the Sf9/BEVS

The quantity optimum, which achieved the highest VLP titer, was tested against other VLP production strategies not considered in the DoE. These approaches include medium exchange before infection and infection at a high CCI using a high MOI. Medium exchange caused baculovirus infection to progress slightly faster than the quantity optimum, as well as advancing the death phase (Fig. 5a – b). Baculovirus infection at a high CCI was performed at 9 x 10^6 cell/mL and a MOI of 3 to ensure a synchronous infection. The infection progressed more rapidly in the high cell density experiment during the first 24 hpi but decelerated to the levels of the quantity optimum afterwards. GageGFP quantification by spectrofluorometry yielded similar fluorescence levels for the quantity optimum and high CCI condition at harvest, while a 1.3-fold improvement was attained by means of medium exchange (Fig. S3).

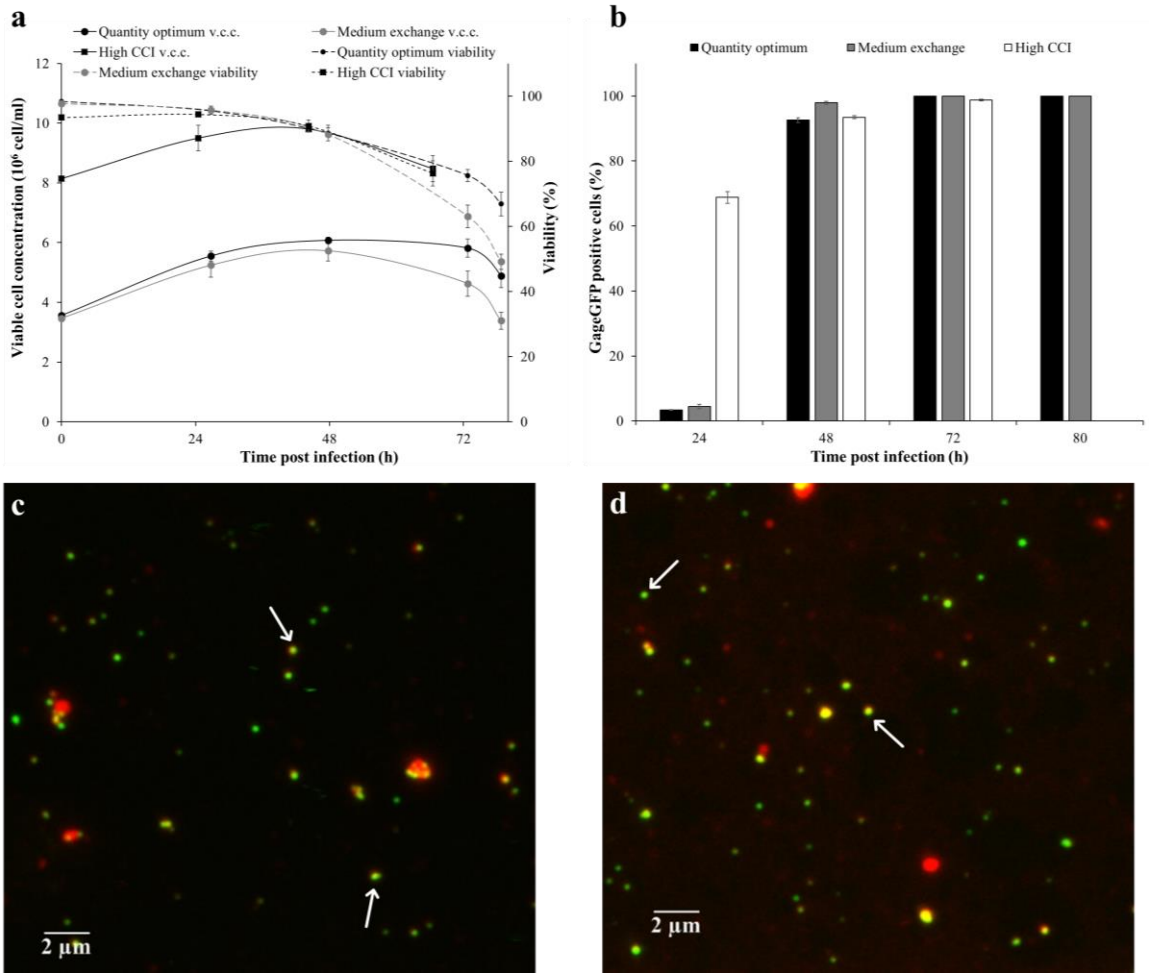

Figure 5. Comparison of the quantity condition to medium exchange and infection at high CCI. (a – b) Cell growth and baculovirus infection kinetics. (c – d) VLP quantification of the quantity optimum and medium exchange, respectively, by confocal microscopy. Nanoparticle lipid membrane was stained with CellMask™ (red).

Likewise, VLP quantification by NTA resulted in comparable levels between the quantity optimum and the high CCI condition, whereas medium exchange yielded a 1.5-fold improvement (Table 4). Similar results to those obtained with the NTA were also measured by confocal microscopy (Fig. 5c – d). However, VLP quantification using flow virometry showed approximately 10-fold lower VLP concentrations in the different conditions tested. The ratio of VLPs over total nanoparticles was also considered and evaluated by means of these three orthogonal techniques. Higher ratios were measured by confocal microscopy and flow virometry in all the conditions tested due to the larger total nanoparticle concentration measured by NTA in comparison to these techniques (Table 4). In terms baculovirus infectious particles, comparable levels were quantified in the quantity optimum ($4.3 \pm 1.9 \times 10^8$ pfu/mL) and medium exchange

condition ($6.3 \pm 2.5 \times 10^8$ pfu/mL), with the high CCI infection achieving the largest concentration ($12.7 \pm 3.8 \times 10^8$ pfu/mL).

Table 4. Nanoparticle quantification of the different conditions using NTA, flow virometry and confocal microscopy.

Quantification method	Condition	VLP production (10^8 fluorescent particle/mL)	Total particle production (10^8 particle/mL)	Ratio fluor. particles/total particles (%)	VLP size (nm)
NTA	Quantity optimum	393.0 ± 72.4	1806.7 ± 185.0	21.6 ± 1.8	153.7 ± 2.7
	Medium Exchange	587.3 ± 19.3	1850.0 ± 501.2	33.4 ± 9.1	157.3 ± 9.5
	High CCI	321.3 ± 22.3	2336.7 ± 265.0	13.9 ± 2.2	157.4 ± 4.8
Flow virometry	Quantity optimum	27.9 ± 0.8	74.6 ± 3.9	37.4 ± 1.4	n.m
	Medium Exchange	52.3 ± 7.0	102.0 ± 8.3	51.2 ± 4.0	
	High CCI	36.8 ± 0.9	86.5 ± 10.5	43.0 ± 5.8	
Confocal microscopy	Quantity optimum	235.2 ± 39.1	221.8 ± 34.0	n.m	n.m
	Medium Exchange	563.5 ± 276.9	476.8 ± 405.8		

n.m: not measured

Discussion

The production of VLPs in Sf9 cells using the BEVS has been quite extensively used, however, most of the studies conducted do not address VLP characterization taking into account the integrity of the nanoparticles themselves but usually rely on monomer detection as a tool for VLP quantification [20,21]. Moreover, the presence of additional nanoparticle populations in the production process is frequently not considered, thus complicating an adequate selection of the critical variables influencing VLP production using the BEVS. EVs are also relevant in the downstream phase since they generally represent a high fraction of the nanoparticles produced. Consequently, a complete characterization of the process should not be based on an indirect measurement of the amount of VLP protein but in a direct measurement of the number of VLPs and the total concentration of nanoparticles, as proposed in this work. To this purpose, a rational experimentation approach and the application of a series of novel orthogonal techniques based on direct nanoparticle quantification were implemented.

The synergies between CCI, MOI and TOH on five objective responses were assessed by means of a Box-Behnken experimental design. Typically, the use of these advanced statistical designs

aims to optimize one individual response [7,32]. However, including more than one critical property in the study has enabled a better comprehension and control of the system [33,34]. TOH and MOI proved to be the most relevant factors governing baculovirus infection, cell viability and VLP assembly whereas CCI also showed an important role on VLP production and productivity. These results differ from other Gag VLP optimization studies in Sf9 cells in which the assessment of different MOI was not found to be significant for VLP production [21]. A global optimization approach based on desirability functions was implemented to find an overall production condition [31]. Two optimal conditions were determined, one maximizing the amount of VLPs produced and the other aiming to find a balance between VLP production and the ratio of GageGFP assembled as VLPs. In both cases, a very low MOI combined with a CCI close to the upper limit of the exponential growth phase resulted in highest VLP yields. Different infection optima are available in the literature depending on the VLP type, the infection strategy and the cell culture medium used [35]. The use of a low MOI is generally preferred for process scale-up since the volume of baculovirus is greatly reduced and the life span of the master stock is extended. However, infection in these conditions requires several rounds of baculovirus re-infection for the culture to be completely infected, which lengthens the TOH, and enables the cell culture to grow during this period of time. The use of low MOI has shown to decrease VLP productivity [36], but the application of a rational experimental design can be used to identify a combination of variables that maintain this property using a low MOI and a CCI at the upper range of the exponential growth phase. This is one of the main advantages of process development based on a holistic approximation, since it is possible to combine the synergic effects of the principal variables to find the optimal production conditions.

The highest GageGFP VLP yield was achieved with the quantity optimum and thus would be the selected option for process scale-up. Comparison to other Gag VLP production studies with the BEVS was not possible since no direct Gag VLP quantification is available. However, comparison to GageGFP VLP production with the widely used HEK 293 cell line resulted in a 4.2 [37] and 1.7-fold [22] improvement. The quantity optimum was also tested in comparison to other VLP production that were not considered in the DoE in order to simplify their industrial application.

These include medium replacement prior to baculovirus infection with quantity optimum and infection at a high CCI. Ikonomou et al. [29] and Huynh et al. [30] reported an increase in β-Gal production using medium replacement, however, a modest increase in VLP production was observed in these conditions, indicating that the quantity optimum was adequate to sustain the production of a high VLP yield. Therefore, the added efforts to perform a medium replacement would not provide a substantial advantage, especially considering process scale-up. Regarding the high CCI condition, similar VLP production levels to the quantity optimum were obtained, but a 3-fold increase in baculovirus titer was measured in the latter. VLP productivity could not be maintained at high CCI owing to the 1.6-fold difference in maximum viable cell concentration. This decrease in VLP productivity could be associated to the cell density effect observed in different insect cell lines with increasing CCI [27,30]. In this sense, there is no advantage in using a high CCI with a high MOI since larger baculovirus stocks are required and the downstream processing is also hindered.

The application of direct methods for nanoparticle quantification is under the spotlight to overcome the limitations of measurement techniques based on monomer quantification [38]. A comparison between NTA, flow virometry and confocal microscopy was performed, with similar VLP quantification results for NTA and confocal microscopy and around a 10-fold decrease for flow virometry. Flow virometry yielded the best accuracy levels while confocal microscopy and NTA displayed a larger variability. Besides VLPs, the presence of EVs could also be appreciated and efficiently discriminated by the three methodologies. Interestingly, these nanoparticles were generally more abundant in comparison to VLPs when measured by NTA and flow virometry but not with confocal microscopy. This could be explained from the perspective of an incomplete staining of the nanoparticle lipidic membrane since it is expected that all Gag VLPs are enveloped [39]. Efforts to improve the detection of these nanoparticles by confocal microscopy are ongoing by the authors to address this issue. NTA proved to be more sensitive than flow virometry in the quantification of EVs, thus explaining the higher ratio of VLPs to total nanoparticles observed in the latter. The underestimation in overall nanoparticle quantification observed in flow virometry could be a consequence of swarm detection, which means that multiple small particles are

detected as a single event, as observed by van der Pol and co-workers in the characterization of exosomes by this technique [40]. This phenomenon is believed to occur in nanoparticles with a refractive index lower than detection limit of the flow cytometer [41]. Future improvements in the sensitivity of this technique should help to widen its applicability for VLP and other nanoparticle quantification.

In conclusion, an optimized production of HIV-1 Gag VLPs was achieved by the combination of DoE statistical designs and direct nanoparticle quantification with different orthogonal techniques. We believe this data will provide new insights and a better comprehension of the Sf9/BEVS for VLP production.

Acknowledgments

The authors thank Dr. Nick Berrow (Institute for Research in Biomedicine, Barcelona, Spain) for providing the Sf9 cell line. Marta Martínez-Calle developed the BV-GageGFP. Ángel Calvache (Beckman Coulter) facilitated the access to CytoFlex LX flow cytometer. The technical support of Mónica Roldán and Martí de Cabo from Servei de Microscòpia (Universitat Autònoma de Barcelona) with the confocal fluorescence microscope and the cryo-EM is also appreciated. Eduard Puente-Massaguer is a recipient of an FPU grant from Ministerio de Educación, Cultura y Deporte of Spain (FPU15/03577). The research group is recognized as 2017 SGR 898 by Generalitat de Catalunya.

Compliance with Ethical Standards

Conflict of interest

The authors declare that they have no competing interests.

Ethical approval

This article does not contain any studies with human participants performed by any of the authors.

References

[1] N. Kushnir, S.J. Streatfield, V. Yusibov, Virus-like particles as a highly efficient vaccine platform: Diversity of targets and production systems and advances in clinical development, Vaccine. 31 (2012) 58–83.

[2] B. Donaldson, Z. Lateef, G.F. Walker, S.L. Young, V.K. Ward, Virus-like particle vaccines: immunology and formulation for clinical translation, Expert Rev. Vaccines. 17 (2018) 833–849.

[3] R.W. Sanders, J.P. Moore, Native-like Env trimers as a platform for HIV-1 vaccine design, Immunol. Rev. 275 (2017) 161.

[4] V.K. Deo, T. Kato, E.Y. Park, Chimeric Virus-Like Particles Made Using GAG and M1 Capsid Proteins Providing Dual Drug Delivery and Vaccination Platform, Mol. Pharm. 12 (2015) 839–845.

[5] J.R. Haynes, L. Dokken, J.A. Wiley, A.G. Cawthon, J. Bigger, A.G. Harmsen, C. Richardson, Influenza-pseudotyped Gag virus-like particle vaccines provide broad protection against highly pathogenic avian influenza challenge, Vaccine. 27 (2009) 530–541.

[6] L. Cervera, I. González-Domínguez, M.M. Segura, F. Gòdia, Intracellular characterization of Gag VLP production by transient transfection of HEK 293 cells, Biotechnol. Bioeng. 114 (2017) 2507–2517.

[7] L. Cervera, S. Gutiérrez-Granados, M. Martínez, J. Blanco, F. Gòdia, M.M. Segura, Generation of HIV-1 Gag VLPs by transient transfection of HEK 293 suspension cell cultures using an optimized animal-derived component free medium, J. Biotechnol. 166 (2013) 152–165.

[8] S. Sakuragi, T. Goto, K. Sano, Y. Morikawa, HIV type 1 Gag virus-like particle budding from spheroplasts of Saccharomyces cerevisiae., Proc. Natl. Acad. Sci. U. S. A. 99 (2002) 7956–61.

[9] S.A. Kessans, M.D. Linhart, N. Matoba, T. Mor, Biological and biochemical characterization of HIV-1 Gag/dgp41 virus-like particles expressed in Nicotiana

benthamiana., Plant Biotechnol. J. 11 (2013) 681–90.

[10] J.A. Mena, A.A. Kamen, Insect cell technology is a versatile and robust vaccine manufacturing platform, Expert Rev. Vaccines. 10 (2011) 1063–1081.

[11] D. Gheysen, E. Jacobs, F. de Foresta, C. Thiriart, M. Francotte, D. Thines, M. De Wilde, Assembly and release of HIV-1 precursor Pr55gag virus-like particles from recombinant baculovirus-infected insect cells, Cell. 59 (1989) 103–112.

[12] C.-M.J. Hu, C.-Y. Chien, M.-T. Liu, Z.-S. Fang, S.-Y. Chang, R.-H. Juang, S.-C. Chang, H.-W. Chen, Multi-antigen avian influenza a (H7N9) virus-like particles: particulate characterizations and immunogenicity evaluation in murine and avian models, BMC Biotechnol. 17 (2017) 2.

[13] P. Steppert, D. Burgstaller, M. Klausberger, A. Tover, E. Berger, A. Jungbauer, Quantification and characterization of virus-like particles by size-exclusion chromatography and nanoparticle tracking analysis, J. Chromatogr. A. 1487 (2017) 89–99.

[14] C. Gardiner, M. Shaw, P. Hole, J. Smith, D. Tannetta, C.W. Redman, I.L. Sargent, Measurement of refractive index by nanoparticle tracking analysis reveals heterogeneity in extracellular vesicles, J. Extracell. Vesicles. 3 (2014) 25361.

[15] B. Vestad, A. Llorente, A. Neurauter, S. Phuyal, B. Kierulf, P. Kierulf, T. Skotland, K. Sandvig, K.B.F. Haug, R. Øvstebø, Size and concentration analyses of extracellular vesicles by nanoparticle tracking analysis: a variation study, J. Extracell. Vesicles. 6 (2017) 1344087.

[16] M.J. McVey, C.M. Spring, W.M. Kuebler, Improved resolution in extracellular vesicle populations using 405 instead of 488 nm side scatter., J. Extracell. Vesicles. 7 (2018) 1454776.

[17] R. Lippé, Flow Virometry: a Powerful Tool To Functionally Characterize Viruses, J. Virol. 92 (2017).

[18] J. Chojnacki, C. Eggeling, Super-resolution fluorescence microscopy studies of human immunodeficiency virus., Retrovirology. 15 (2018) 41.

[19] K. Inamdar, C. Floderer, C. Favard, D. Muriaux, K. Inamdar, C. Floderer, C. Favard, D. Muriaux, Monitoring HIV-1 Assembly in Living Cells: Insights from Dynamic and Single Molecule Microscopy, Viruses. 11 (2019) 72.

[20] P.E. Cruz, a Cunha, C.C. Peixoto, J. Clemente, J.L. Moreira, M.J. Carrondo, Optimization of the production of virus-like particles in insect cells., Biotechnol. Bioeng. 60 (1998) 408–18.

[21] S. Pillay, A. Meyers, A.L. Williamson, E.P. Rybicki, Optimization of chimeric HIV-1 virus-like particle production in a baculovirus-insect cell expression system, Biotechnol. Prog. 25 (2009) 1153–1160.

[22] L. Cervera, J. Fuenmayor, I. Gonzalez-Dominguez, S. Gutierrez-Granados, M.M. Segura, F. Godia, I. González-Domínguez, S. Gutiérrez-Granados, M.M. Segura, F. Gòdia, I. González-Domínguez, S. Gutiérrez-Granados, M.M. Segura, F. Gòdia, I. González-Domínguez, S. Gutiérrez-Granados, M.M. Segura, F. Gòdia, I. Gonzalez-Dominguez, S. Gutierrez-Granados, M.M. Segura, F. Godia, Selection and optimization of transfection enhancer additives for increased virus-like particle production in HEK293 suspension cell cultures, Appl. Microbiol. Biotechnol. 99 (2015) 9935–9949.

[23] E. Puente-Massaguer, L. Badiella, S. Gutiérrez-Granados, L. Cervera, F. Gòdia, A statistical approach to improve compound screening in cell culture media, Eng. Life Sci. 19 (2019) 1–13.

[24] S. Honary, P. Ebrahimi, R. Hadianamrei, Optimization of particle size and encapsulation efficiency of vancomycin nanoparticles by response surface methodology, Pharm. Dev. Technol. 19 (2014) 987–998.

[25] M.A. Bezerra, R.E. Santelli, E.P. Oliveira, L.S. Villar, L.A. Escaleira, Response surface methodology (RSM) as a tool for optimization in analytical chemistry, Talanta. 76 (2008) 965–977.

[26] L. Hermida-Matsumoto, M.D. Resh, Localization of human immunodeficiency virus type 1 Gag and Env at the plasma membrane by confocal imaging., J. Virol. 74 (2000) 8670–8679.

[27] V. Bernal, N. Carinhas, A.Y. Yokomizo, M.J.T. Carrondo, P.M. Alves, Cell density effect in the baculovirus-insect cells system: A quantitative analysis of energetic metabolism, Biotechnol. Bioeng. 104 (2009) 162–180.

[28] N. Carinhas, V. Bernal, A.Y. Yokomizo, M.J.T. Carrondo, R. Oliveira, P.M. Alves, Baculovirus production for gene therapy: The role of cell density, multiplicity of infection and medium exchange, Appl. Microbiol. Biotechnol. 81 (2009) 1041–1049.

[29] L. Ikonomou, G. Bastin, Y.J. Schneider, S.N. Agathos, Effect of partial medium replacement on cell growth and protein production for the high-five™ insect cell line, Cytotechnology. 44 (2004) 67–76.

[30] H.T. Huynh, T.T.B. Tran, L.C.L. Chan, L.K. Nielsen, S. Reid, Effect of the peak cell density of recombinant AcMNPV-infected Hi5 cells on baculovirus yields, Appl. Microbiol. Biotechnol. 99 (2014) 1687–1700.

[31] G. Derringer, R. Suich, Simultaneous optimization of several response variables, J. Qual. Technol. 12 (1980) 214–219.

[32] J. Fuenmayor, L. Cervera, S. Gutiérrez-Granados, F. Gòdia, Transient gene expression optimization and expression vector comparison to improve HIV-1 VLP production in HEK293 cell lines, Appl. Microbiol. Biotechnol. 102 (2018) 165–174.

[33] A.L. Bukzem, R. Signini, D.M. dos Santos, L.M. Lião, D.P.R. Ascheri, Optimization of carboxymethyl chitosan synthesis using response surface methodology and desirability function, Int. J. Biol. Macromol. 85 (2016) 615–624.

[34] E. Puente-Massaguer, M. Lecina, F. Gòdia, Nanoscale characterization coupled to multi-parametric optimization of Hi5 cell transient gene expression, Appl. Microbiol. Biotechnol. 102 (2018) 10495–10510.

[35] T. Vicente, A. Roldão, C. Peixoto, M.J.T.T. Carrondo, P.M. Alves, Large-scale production and purification of VLP-based vaccines, J. Invertebr. Pathol. 107 (2011) S42–S48.

[36] L. Maranga, T.F. Brazao, M.J.T. Carrondo, Virus-like particle production at low multiplicities of infection with the baculovirus insect cell system, Biotechnol. Bioeng. 84 (2003) 245–253.

[37] J. Fuenmayor, L. Cervera, C. Rigau, F. Gòdia, Enhancement of HIV-1 VLP production using gene inhibition strategies, Appl. Microbiol. Biotechnol. 102 (2018) 4477–4487.

[38] L.H.L. Lua, N.K. Connors, F. Sainsbury, Y.P. Chuan, N. Wibowo, A.P.J. Middelberg, Bioengineering virus-like particles as vaccines, Biotechnol. Bioeng. 111 (2014) 425–440.

[39] L. Deml, C. Speth, M.P. Dierich, H. Wolf, R. Wagner, Recombinant HIV-1 Pr55 gag virus-like particles: Potent stimulators of innate and acquired immune responses, Mol. Immunol. 42 (2005) 259–277.

[40] E. Van der Pol, M.J.C. Van Gemert, A. Sturk, R. Nieuwland, T.G. Van Leeuwen, Single vs. swarm detection of microparticles and exosomes by flow cytometry, J. Thromb. Haemost. 10 (2012) 919–930.

[41] E. van der Pol, F.A.W. Coumans, a. E. Grootemaat, C. Gardiner, I.L. Sargent, P. Harrison, A. Sturk, T.G. van Leeuwen, R. Nieuwland, Particle size distribution of exosomes and microvesicles determined by transmission electron microscopy, flow cytometry, nanoparticle tracking analysis, and resistive pulse sensing, J. Thromb. Haemost. 12 (2014) 1182–1192.

Supplementary material

Figure S1. Time lapse of Sf9 cells infected with BV-GageGFP recorded during 6 min. Cell membrane was stained with CellMask™ (red) and cell nucleus with Hoechst (blue). Green dots in the cell membrane and in the supernatant correspond to GageGFP VLPs.

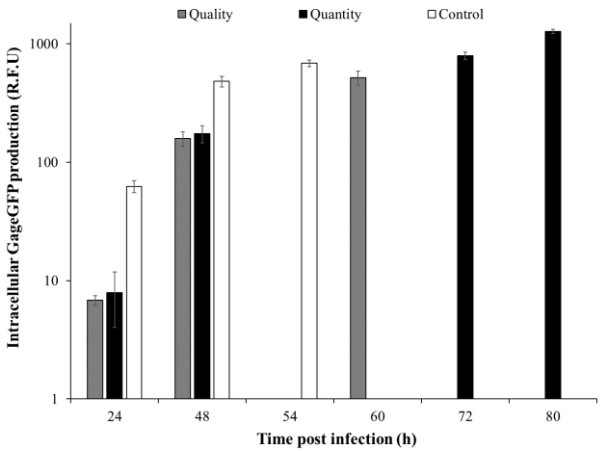

Figure S2. Intracellular GageGFP production kinetics measured by spectrofluorometry. The means and standard deviation of triplicate experiments are represented.

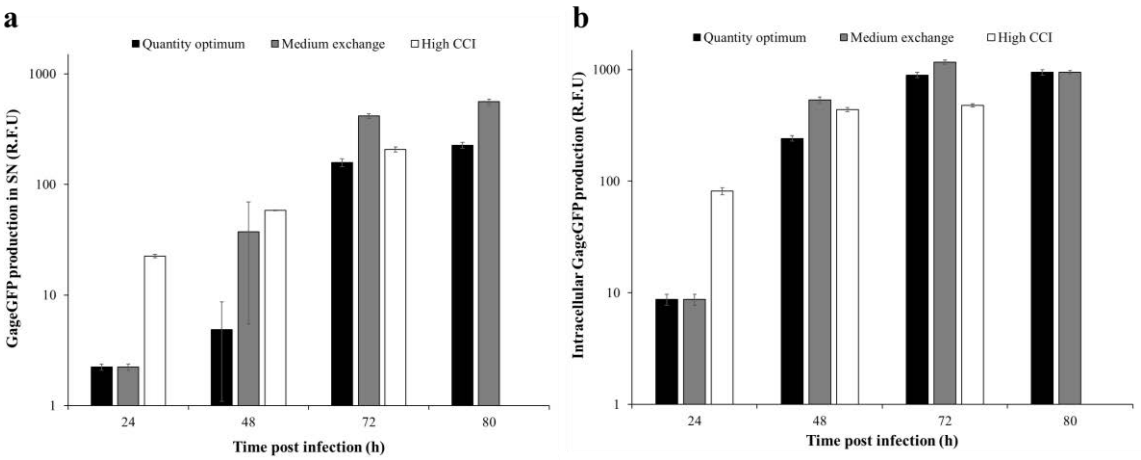

Figure S3. GageGFP production kinetics of the global production optimum, medium exchange and high CCI infection with large MOI. (a – b) GageGFP production in the supernatant and intracellularly quantified using spectrofluorometry, respectively. The results from triplicate experiments are represented.

Chapter 3

Polyethylenimine-based transient gene expression in Sf9 and High Five cell lines

Eduard Puente Massaguer, Martí Lecina and Francesc Gòdia

Chapter 3 – Part I

Development of a non-viral platform for rapid virus-like particle production in Sf9 cells

Eduard Puente Massaguer, Francesc Gòdia and Martí Lecina

Abstract

Insect cells have shown a high versatility to produce multiple recombinant products. The ease of culture, low risk of contamination with human pathogens and high expression capacity render an attractive platform to generate virus-like particles (VLPs). The baculovirus expression vector system (BEVS) has been frequently used to produce these complex nanoparticles. However, the BEVS entails several difficulties in the downstream phase as well as undesirable side-effects due to the expression of baculovirus-derived proteins. In this work, we developed a baculovirus-free system on Sf9 cells based on the transient gene expression (TGE) of plasmids using polyethylenimine. An exhaustive study of the DNA:PEI polyplex formation was performed and the optimal TGE conditions were determined by the combination of Design of Experiments and desirability functions. The TGE approach was successfully applied to produce HIV-1 Gag VLPs, with the *gag* gene fused to eGFP to facilitate process characterization. Cell membrane co-localization with the Gag polyprotein was detected by fluorescence microscopy, and nanoparticle tracking analysis and flow virometry enabled to monitor the VLP production process. Analysis of VLP production revealed that 48 h were optimal for VLP harvest since the ratio of VLPs to extracellular vesicles was the highest. In these conditions, a maximum of $1.9 \pm 0.8 \cdot 10^9$ VLP/mL was achieved with ~80 % of the fluorescence assembled as VLPs. Cryo-electron microscopy confirmed the presence of immature Gag VLPs (100 – 200 nm). Thus, the TGE approach here proposed provides a baculovirus-free platform to rapidly produce VLPs and potentially other recombinant products in insect cells.

Keywords: Virus-like particle, Sf9 cells, Transient gene expression, Cryo-electron microscopy, Flow virometry, Polyethylenimine

Abbreviations: ANOVA, analysis of variance; BEVS, baculovirus expression vector system; Cryo-EM, cryo-electron microscopy; DoE, Design of Experiments; eGFP, enhanced green fluorescent protein; HIV, human immunodeficiency virus; hpt, hours post transfection; hSEAP, human placental alkaline phosphatase; LOF, lack-of-Fit; NTA, nanoparticle tracking analysis; PEI, polyethylenimine; SN, supernatant; TGE, transient gene expression; VLP, virus-like particle.

Introduction

The development of rapid and efficient systems for recombinant protein production is pivotal to meet the increasing demand in biotechnological products. Animal cell lines are frequently used to this purpose since many of the recombinant proteins require from complex post-translational modifications [1]. The insect cell/baculovirus expression vector system (BEVS) is used extensively since high production yields can be achieved in short time-frames. Moreover, insect cells are easy to culture and can tolerate higher levels of osmolarity and by-product concentrations compared to mammalian cells [2]. Common insect cell lines used with the BEVS belong to the order of the lepidoptera, mainly Sf9 (a clonal isolate from Sf21) from *Spodoptera frugiperda* and Hi5 from *Trichoplusia ni*. Several recombinant products have been produced using this strategy, from simple [3] to more complex ones such as G-protein-coupled receptors [4] and virus-like particles (VLP) [5]. However, the baculovirus infection cycle jeopardises cell integrity, product quality due to protease release as well as hindering the separation of complex nanoparticles from the baculovirus itself [6]. Also, the BEVS is time-consuming for high-throughput screening applications mainly due to the effort in developing the baculovirus working stock [7].

In this context, the use of new production methodologies free of baculoviruses is of general interest. Transient gene expression (TGE) of several recombinant products has proved to achieve high concentrations in mammalian cell lines [8]. Nevertheless, little information is available regarding their performance in insect cell lines. Initial transfection experiments of insect cells were performed in adherent cultures using liposome-based reagents in most cases [9,10]. Despite the initial efforts with these transfection carriers at small scale, difficulties are encountered in process scale-up due to their high cost. Polyethylenimine (PEI) has demonstrated to work adequately as transfection reagent for a handful of animal cell lines [11]. Recently, the successful production of several simple recombinant proteins using PEI-mediated TGE in suspension-adapted insect cells has been reported [12–14]. However, the benefit of using this system as a platform to produce complex nanoparticles such as VLPs has not yet been investigated. Albeit some progress has been achieved in the insect cell/TGE system, there is still a requirement to reduce the experimental variability due to the presence of hydrolysates in the media composition.

This is of special relevance in the production of VLPs to ensure the reliability of the process and eliminate the risk of contamination with infectious agents.

In the current study, we have developed a TGE approach for the Sf9 cell line with PEI using a low-hydrolysate culture medium. The plasmid vector used for TGE was pIZTV5, which harbours the immediate-early OpIE2 promoter, with positive results recently reported for transient protein production in Hi5 insect cells [15,16]. The first part of the study is focused on the investigation of the DNA:PEI polyplex formation conditions mediating transfection. Then, a rational approach is used to detect the synergies between the main variables influencing the production process and determine an optimal condition for TGE. To this end, an approach based on the combination of Design of Experiments (DoE) and multiple response evaluation using desirability functions is applied. The reproducibility of the TGE condition is successfully validated with three different recombinant products: intracellular enhanced green fluorescent protein (eGFP), human placental alkaline phosphatase (hSEAP) and the human immunodeficiency virus (HIV-1) Gag polyprotein responsible for VLP formation. The *gag* gene is fused in frame to eGFP with the aim to facilitate the detection of GageGFP in the cell membrane and release in the form of assembled VLPs. This process is thoroughly monitored and characterized by multiple analytical tools, including confocal microscopy, nanoparticle tracking analysis (NTA) and flow virometry. Also, correct formation of these nanoparticles is confirmed with cryo-electron microscopy (cryo-EM). The methodology here proposed represents an advancement for VLP production in insect cells devoid of the BEVS. This strategy should facilitate the production and downstream processing of these complex nanoparticles and other recombinant products.

Methods

Cell culture conditions

The suspension-adapted lepidopteran insect cell line used in this work was the *Spodoptera frugiperda* (Sf9, cat. num. 71104, Merck, Darmstadt, Germany) kindly provided by Dr. Nick Berrow (Institute for Research in Biomedicine, Barcelona, Spain). Cells were adapted to grow in Sf900III medium (Thermo Fisher Scientific, Grand Island, NY, USA) and subcultured three times

a week at a density of 4 - 6 x 10^5 cells/mL in 125/250-mL disposable polycarbonate Erlenmeyer flasks (Corning, Steuben, NY, USA). All cultures were shaken at 130 rpm using an orbital shaker (Stuart, Stone, UK) and were maintained at 27°C as previously described [17]. Cell count and viability were measured with the Nucleocounter NC-3000 (Chemometec, Allerød, Denmark) for five days.

Plasmid vectors

The plasmid vector used in this work was the pIZTV5 (cat. num. V801001, Thermo Fisher Scientific) which contains the immediate-early OPIE2 promoter. The genes encoding for the intracellular enhanced green fluorescent protein (eGFP), the truncated form of human placental alkaline phosphatase (hSEAP) and the human immunodeficiency virus (HIV-1) Gag fused in frame to the eGFP were cloned into this vector using standard cloning procedures. Briefly, the hSEAP gene was PCR amplified from the pUNO1-hSEAP plasmid (InvivoGen, San Diego, CA, USA) using the following primer pair: fwd 5'-CGTAGGTACCTCATGATTCTGGGGCCCTGC-3', rev 5'-CGTAGCGGCCGCGTCCAAACTCATCAATGTATC-3'. The amplified fragment was digested with *Kpn*I and *Not*I and ligated resulting in the pIZTV5-hSEAP. The GageGFP gene was obtained by digesting the pGageGFP plasmid (NIH AIDS Reagent Program, cat. num. 11468) [18] with *Kpn*I and *Not*I obtaining the pIZTV5-GageGFP plasmid after ligation. The pIZTV5-eGFP plasmid was developed as previously reported in [15].

Transient gene expression

Sf9 cells were transiently transfected with the different DNA plasmids using the 25 kDa linear polyethylenimine (PEI, PolySciences, Warrington, PA, USA). The linear PEI 25 kDa stock solution was prepared in ultrapure water at a concentration of 1 mg/mL with a final pH of 7 and sterilized by filtration. The initial transfection protocol was defined according to initial transfection experiments. Exponentially growing cells were centrifuged at 300 x*g* for 5 min and concentrated to 20 x 10^6 cell/mL in 8 mL of pre-warmed Sf900III medium. DNA and PEI

polyplex formation was performed in 0.8 mL of incubation solution with DNA at 1 pg/cell added first and vortexed for 10 s. Then PEI at 2 pg/cell was added to DNA and vortexed 3 s 3 times. After 10 min of incubation at room temperature, the mixture was added to the concentrated culture for 1h and then diluted to 4 x 10^6 cell/mL with Sf900III medium. Different incubation solutions were tested for DNA:PEI polyplex formation. These solutions include 150 mM NaCl (Sigma-Aldrich, Saint Louis, MO, USA), ultrapure water (Merck Millipore, Burlington, MA, USA) and the Sf900III medium.

Flow cytometry

The percentage of eGFP and GageGFP expressing cells was assessed using a BD FACS Canto II flow cytometer equipped with a 488 nm laser configuration (BD Biosciences, San Jose, CA, USA). The number of eGFP and GageGFP positive cells was determined in the FITC PMT detector.

Fluorescence confocal Microscopy

eGFP and GageGFP transfected cells were visualized using a TCS SP5 confocal microscope (Leica, Wetzlar, Germany). To do this, cells were dyed with 0.1 % v/v of CellMask™ and 0.1 % v/v of Hoechst (Thermo Fisher Scientific) for lipid membrane and cell nucleus staining, respectively. A washing step was performed to remove dye excess by centrifuging the cells at 300 x*g* during 5 min and resuspending them in fresh Sf900III medium (Thermo Fisher Scientific). Samples were placed in 35 mm glass bottom Petri dishes with 14 mm microwell (MatTek Corporation, Ashland, MA, USA) for visualization.

Fluorescence quantification by spectrofluorometry

The supernatant of eGFP and GageGFP producing cells was harvested by centrifugation at 3000 x*g* for 5 min. Pelleted cells were then subjected to three freeze-thaw cycles for intracellular eGFP and GageGFP measurement. Green fluorescence was measured with a Cary Eclipse fluorescence spectrophotometer (Agilent Technologies, Santa Clara, CA, USA) at room temperature set as

follows: λ_{ex} = 488 nm (5 nm slit), λ_{em} = 500 - 530 nm (10 nm slit). Relative fluorescence unit values (R.F.U.) were calculated by substracting fluorescence unit values of negative non-transfected cultures. eGFP concentration was determined using a standard curve based on a linear correlation of a known concentration of eGFP (BioVision, Milpitas, CA, USA) and the associated fluorescence intensity in R.F.U. (Fig. S4):

$$\text{eGFP (mg/L)} = (\text{R.F.U.} - 6.7221)/59.144 \quad (1)$$

where eGFP is the estimated concentration of eGFP protein and R.F.U. is the measured eGFP fluorescence intensity in the samples.

A correlation was also established between R.F.U. from GageGFP transfected Sf9 cell supernatants and the content of fluorescent particles measured with the NTA:

$$\text{GageGFP nanoparticles (particles/mL)} = 3.96 \times 10^{8} \cdot \text{R.F.U.} \quad (2)$$

The Sf900III medium and a 0.1 mg/mL quinine sulphate solution were used as control patterns to normalize R.F.U. values between different experiments.

hSEAP quantification

The supernatant of hSEAP producing cells was harvested by centrifugation at 3000 x*g* for 5 min and cell pellets were disrupted under a 3-time freeze-thaw cycle for intracellular hSEAP measurement. The alkaline phosphatase activity was assessed with a colorimetric enzyme reaction using the QUANTI-Blue system (InvivoGen). To do this, 20 µL of sample were added to 200 µL of pre-warmed QUANTI-Blue solution and incubated for 1 h at 37ºC. The absorbance was measured in a Victor^3 spectrophotometer (PerkinElmer, Waltham, MA, USA) at a wavelength of 620 nm. Relative activity units (R.A.U.) were calculated by subtracting the absorbance of non-transfected cultures. hSEAP concentration was determined using a calibration curve based on a linear correlation of known hSEAP (InvivoGen) concentrations and the corresponding activity units in R.A.U.:

$$\text{hSEAP (mg/L)} = \text{R.A.U.} \times 2.9744 + 0.0615 \quad (3)$$

where hSEAP is the estimated concentration of the hSEAP protein and R.A.U. is the measured hSEAP activity units in the samples.

Enzyme-linked immunosorbent assay (ELISA)

HIV-1 p24 concentration from GageGFP transfected Sf9 cell supernatants and pellets was determined by HIV-1 p24 ELISA Kit (Sino Biological, Wayne, NJ, USA). Supernatants were harvested by centrifugation at 3000 x*g* for 5 min and cell pellets were disrupted as described in the previous section. Samples were incubated with SNCR buffer for 10 min at 70 °C and incubated with 1.5 % Triton X-100 for 10 min at 100 °C to disrupt the nanoparticles. The substrate solution was prepared by dissolving a SIGMA*FAST* OPD substrate tablet and one urea hydrogen peroxide tablet (Sigma Aldrich) in deionized water at a final concentration of 0.4 mg/mL. An HIV-1 p24 standard of known concentration was also included to determine GageGFP concentration. The reaction was stopped adding 625 mM H_2SO_4. The absorbance was measured at 492 nm with a reference wavelength at 630 nm in a Tecan Infinite 200 Pro reader (Tecan, Männedorf, Switzerland) as described by Reiter et al. [19]. p24 concentration values were corrected according to GageGFP molecular weight (87.7 kDa).

Cryo-Electron Microscopy

Morphology and qualitative particle size of DNA:PEI complexes as well as GageGFP supernatants from transfected Sf9 cells were visualised with a transmission electron microscope equipped with a cryotransfer holder. Briefly, 4 µL of sample was blotted onto EMR Lacey carbon films on 300 mesh copper grids or EMR Holey carbon films on 400 mesh copper grids (Micro to Nano, Wateringweg, Netherlands) for 3 s and 77 % relative air humidity. The grids were previously subjected to a glow discharge treatment in a PELCO easiGlow™ Discharge Cleaning System (PELCO, Fresno, CA, USA). The samples were subsequently plunged into liquid ethane at −180 °C using a Leica EM GP workstation (Leica, Wetzlar, Germany) and observed in a JEM-2011 TEM operating at 200 kV (Jeol Ltd., Akishima, Tokyo, Japan). Samples were maintained at −180 °C during imaging and pictures were taken using a CCD 895 USC 4000 multiscan camera (Gatan, Pleasanton, CA, USA).

Particle quantification by nanoparticle tracking analysis

The number of fluorescent and non-fluorescent particles present in GageGFP harvested supernatants at 48 hpt was measured using a NanoSight NS300 (Malvern Panalytical, Malvern, United Kingdom). Samples were diluted in 0.22 µm-filtered DPBS and continuously injected into the device chamber through a pump at an average concentration of 10^8 particles/mL (20 – 60 particles/frame). Videos of 60 s from independent triplicate measurement were analysed with the NanoSight NTA 3.2 software at room temperature.

Particle quantification using flow virometry

The production kinetics of fluorescent and non-fluorescent particles from GageGFP harvested supernatants was measured using a CytoFlex LX (Beckman Coulter, Brea, CA, USA) equipped with a 488 nm blue laser for fluorescent particle detection and a 405 nm laser/violet side scatter configuration for improved nanoparticle size resolution. Samples were diluted in 0.22 µm-filtered DPBS and triplicate measurements from independent samples were analysed with the CytExpert 2.3 software at room temperature.

VLP characterization through sucrose cushion ultracentrifugation

The supernatant of GageGFP transfected Sf9 cells at 48 hpt was sublayered with 5 mL of 25 % and 8 mL of 45 % (w/v) sucrose (Sigma) solution prepared in DPBS or DMEM (Thermo Fisher Scientific), respectively. 10 mL of supernatant was loaded in an ultracentrifuge tube (Beckman Coulter), filled to the top with sterile DPBS and centrifuged at 31000 rpm for 2.5 h at 4ºC (Beckman Optima L100XP, SW32ti rotor, Beckman Coulter). Samples were taken from each one of the ultracentrifugation fractions and the pellet was resuspended in 100 µL of sterile DPBS O/N. All samples were stored either at -4 or -80ºC.

DoE-based optimization of TGE

A three-variable Box-Behnken design was selected to find the optimal conditions for eGFP production (R.F.U.), transfection (% of eGFP positive cells) and cell viability (% of viable cells after transfection). Viable cell concentration at transfection (10^6 cell/mL), DNA/cell and PEI/cell

ratio (pg/cell) were chosen as the independent variables of the study. These variables were screened at three levels coded as: low level, -1; medium level, 0; high level, +1 (Table 1).

Table 1. Matrix design, response and ANOVA analysis for the Box-Behnken DoE variables. Run 13 was performed in triplicate as the centre point.

Coded levels	-1	0	1
Viable cell concentration (10^6 cell/mL)	10	20	30
DNA concentration (pg/cell)	0.5	1	1.5
PEI concentration (pg/cell)	1.5	2	2.5

	Variables			Responses		
Experimental run	[Cell][a]	[DNA]	[PEI]	Specific production (R.F.U.[b]/10^6 cells)	eGFP positive cells (%)	Viability (%)
1	-1	-1	0	109.5	38.0	93.8
2	1	-1	0	89.1	47.9	55.8
3	-1	1	0	197.3	22.7	85.6
4	1	1	0	150.3	33.0	83.1
5	-1	0	-1	147.9	20.7	96.7
6	1	0	-1	133.6	31.6	90.7
7	-1	0	1	146.6	45.5	88.4
8	1	0	1	118.0	45.0	48.7
9	0	-1	-1	119.8	46.5	87.1
10	0	1	-1	177.5	22.3	93.7
11	0	-1	1	99.1	59.1	30.1
12	0	1	1	124.5	50.2	62.5
13	0	0	0	130.6	55.0	84.8
13	0	0	0	140.1	50.1	82.4
13	0	0	0	120.6	52.0	78.9

Model	*F* test, *p*-value[c]	Lack of fit test, *p-value*[d]	R^2	Adjusted R^2
eGFP production (72 hpt)	0.048	0.053	84.9	64.8
eGFP positive cells (72 hpt)	<0.001	0.72	98.8	97.2
Viability (24 hpt)	<0.001	0.28	94.4	90.2

Model	eGFP production (72hpt)		eGFP positive cells (72 hpt)		Viability (24hpt)	
Parameters	Coefficient	*p*-value	Coefficient	*p*-value	Coefficient	*p*-value
Constant	848.550	<0.001	52.2367	<0.001	1.487	<0.001
[Cell]	-44.790	0.264	3.825	0.002	-0.732	<0.001
$[Cell]^2$	-122.000	0.063	-12.896	<0.001	0.4516	0.041
[DNA]	63.510	0.131	-7.913	<0.001	0.321	0.034
$[DNA]^2$	-160.710	0.024	-4.071	0.009	-0.388	0.070
[PEI]	14.930	0.695	9.838	<0.001	-1.077	<0.001
$[PEI]^2$	-100.460	0.109	-3.771	0.01	NS	>0.050
[Cell] x [DNA]	NS	>0.050	NS	>0.050	0.574	0.010
[Cell] x [PEI]	-140.220	0.034	-2.850	0.03	NS	>0.050
[DNA] x [PEI]	125.720	0.05	3.825	0.01	NS	>0.050

[a][Cell]: Viable cell concentration

[b]R.F.U.: relative fluorescent units

[c]*p*-value under 0.05 are considered as statistically significant with a 95% confidence.

[d]Lack of fit test, *p-value* above 0.05 imply that the hypothesis arguing that the model is suitable cannot be rejected.

NS: Non-significant term (*p-value* > 0.05)

The obtained results were fitted to a second-order polynomial equation by linear regression analysis for each response (Eq. 4):

$$Y = \beta_0 + \sum_{i=1}^{k} \beta_i \cdot X_i + \sum_{i=1}^{k} \beta_{ii} \cdot X_i^2 + \sum_{i=1}^{k} \sum_{j>1}^{k} \beta_{ij} \cdot X_i \cdot X_j + \varepsilon \quad (4)$$

where *Y* corresponds to each response under consideration (eGFP production, transfection and cell viability), β_0 is the model intercept term, β_i the linear coefficient, β_{ii} the quadratic coefficient, β_{ij} the interaction coefficient, X_i and X_j are the studied variables (viable cell concentration at transfection, DNA/cell and PEI/cell ratio) and ε is the experimental error. Data fitting for each response was performed in the R language environment (R Foundation for Statistical Computing, Vienna, Austria)

The best condition for TGE was found by simultaneously considering the three response functions obtained based on equation 4 by using a modified version of the *desirability* package in R. Different ranges were selected for each response according to experimental data and a weight value (*s*-value) was also chosen depending on the relevance given to the fitted equation (Eq. 5):

$$d_n = \begin{cases} 0 & if\ Y_n < LL \\ \left(\dfrac{Y_n - LL}{UL - LL}\right)^s & if\ LL \leq Y_n \leq UL \\ 1 & if\ Y_n > UL \end{cases} \quad (5)$$

where d_n is the desirability function for each equation, *s* refers to the relevance value given to the equation, Y_n is the fitted equation and *LL* and *UL* are de lower and upper limits of each equation, respectively. The different *n* desirability functions are then combined to find the conditions that maximise the Overall Desirability function (*OD*).

Statistical analyses

Statistical analyses of the different equations were performed using R software. The quality of the regression of the fitted equations was evaluated through R^2 and R^2_{adj} coefficients. An analysis of variance (ANOVA) *F*-test was used to determine the significance of the equations and each of the coefficients involved was assessed with a *t*-test. The lack-of-fit (LOF) test was used to evaluate differences between experimental and pure error of the fitted equations.

Results

Preliminary screening of transfection conditions

Several toxicity assays were carried out to define the appropriate DNA and PEI concentration ranges for Sf9 cells in Sf900III medium (Fig. S1). Initial series of transfection studies were performed at exponential phase (3 x 10^6 cell/mL) using the pIZTV5-eGFP plasmid but low transfections were achieved (< 20 %). At the same time, cell viability was compromised with increasing PEI concentrations. Medium replacement before transfection allowed increasing transfection efficiency (20 – 30 %) as well as cell viability after transfection. Remarkably, a substantial improvement in transfection efficacy was attained at high cell concentrations (30 – 40 %) being the strategy adopted in the following optimization studies (Fig. S2).

Study of DNA:PEI complexing on transient gene expression

It is widely accepted that the efficiency of DNA:PEI polyplexes on transfection is influenced by the solution used for complexation [20]. To this purpose, different solutions including ultrapure water, Sf900III medium and 150 mM NaCl were tested. Sequential addition of PEI and DNA to the cell culture (no complexing) was also investigated since it has been reported to work in different cell lines [21]. Best transfection efficiencies were achieved at 48 - 72 hours post transfection (hpt) with DNA:PEI incubation in ultrapure water and without DNA:PEI complexing (Fig. 1a – b). In these conditions, a decrease in cell growth rate compared to the other solutions was observed. Interestingly, cells transfected with pre-formed DNA:PEI polyplexes were more fluorescent in all cases compared to the no complexing condition (Fig. 1c). This was translated into a higher level of eGFP production in polyplexes pre-formed in ultrapure water though similar transfection efficiencies were attained without DNA:PEI complexing (Fig. 1d). Maximum intracellular eGFP production was accomplished at 72 hpt and barely no eGFP was detected in supernatant (Fig. 1d – e). According to these results, ultrapure water was selected as the incubation solution for polyplex formation since the best transfection efficiency and eGFP production was achieved.

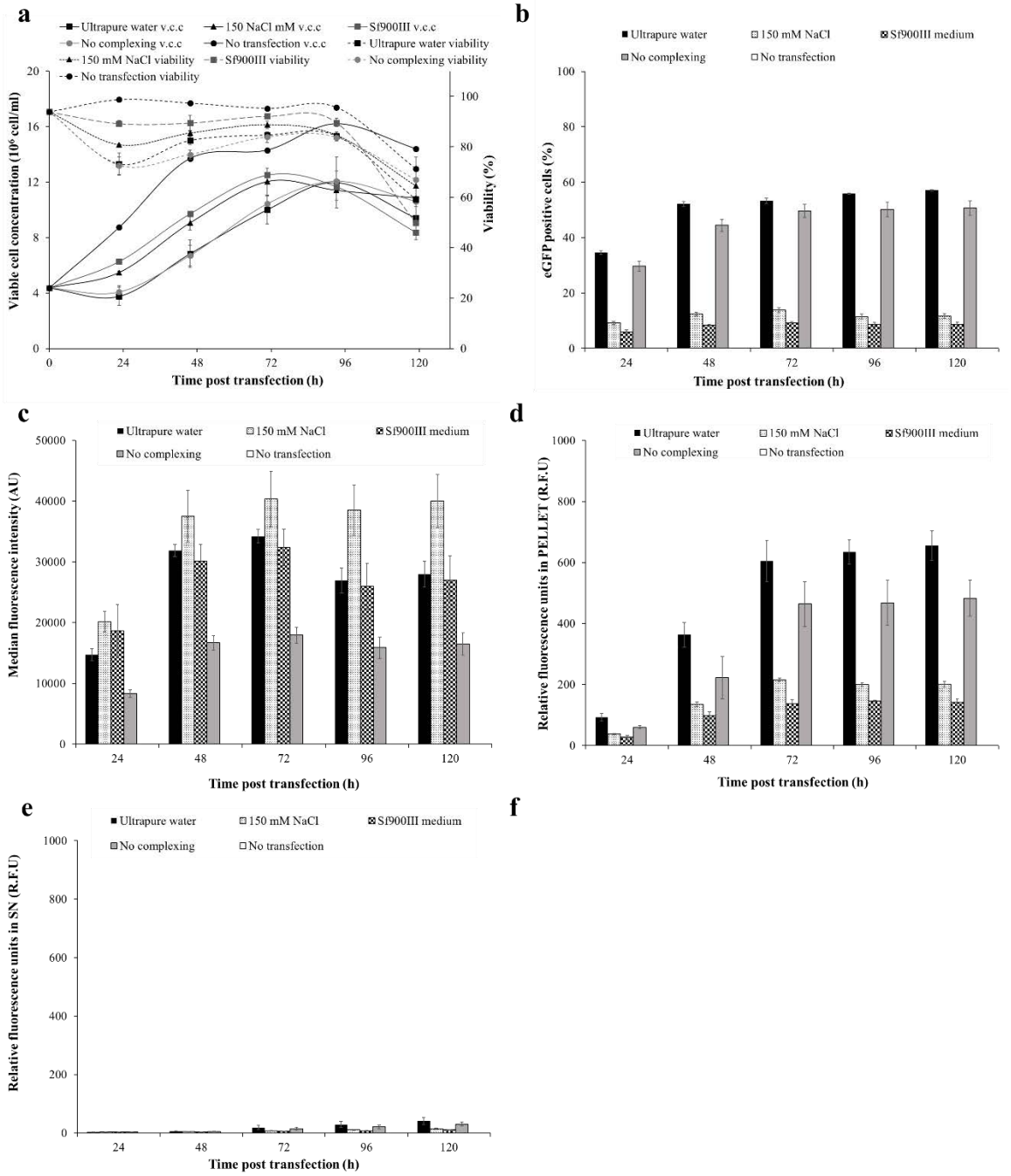

Figure 1. Transfection and eGFP production kinetics of Sf9 cells in batch culture with DNA:PEI polyplexes pre-formed in ultrapure water, 150 mM NaCl, Sf900III medium and direct addition of PEI + DNA (no complexing). (a) Cell growth and viability kinetics of transfected cultures. Exponentially growing cells were transfected at 20.0 x 10^6 cells/mL and diluted to 4.0 x 10^6 cells/mL after 1 h. (b - c) Transfection and median intensity of transfected cells by flow cytometry. (d – e) Intracellular and supernatant eGFP production measured with spectrofluorometry. Mean values ± standard deviation of triplicate experiments are represented.

The DNA:PEI incubation time was also assessed to determine the best conditions for an optimal transfection. To evaluate this, a transfection experiment with polyplexes incubated for <1, 10, 20 and 30 min in ultrapure water was performed. No differences were observed among the different

conditions tested (Fig. S3). In this sense, the strategy adopted for polyplex formation consisted in mixing DNA with PEI (incubation <1 min) and immediate addition to the concentrated culture. Cryo-EM was used to characterize the morphology and size of these polyplexes in native conditions (Fig. 2a – b). DNA:PEI polyplexes appeared as black electron-dense structures with an heterogeneous size comprised in the 0.2 – 1.5 µm range.

Transfection at high cell concentrations required the use of high PEI concentrations to maintain the PEI/cell ratio. To decrease the risk of cell damage upon prolonged exposure to these conditions, Sf9 concentrated cultures were transfected with polyplexes and incubated for 15, 30, 45 and 60 min before dilution to 4 x 10^6 cell/mL, with the aim to determine the shortest window of time that guaranteed best transfection conditions. No differences were observed in the transfection yield, but cell viability declined as the incubation time increased from 15 to 45 min (Fig. 2c – d). These results suggest that 15 min of DNA:PEI polyplex incubation with high concentrated cells is adequate to ensure the best level of transfection.

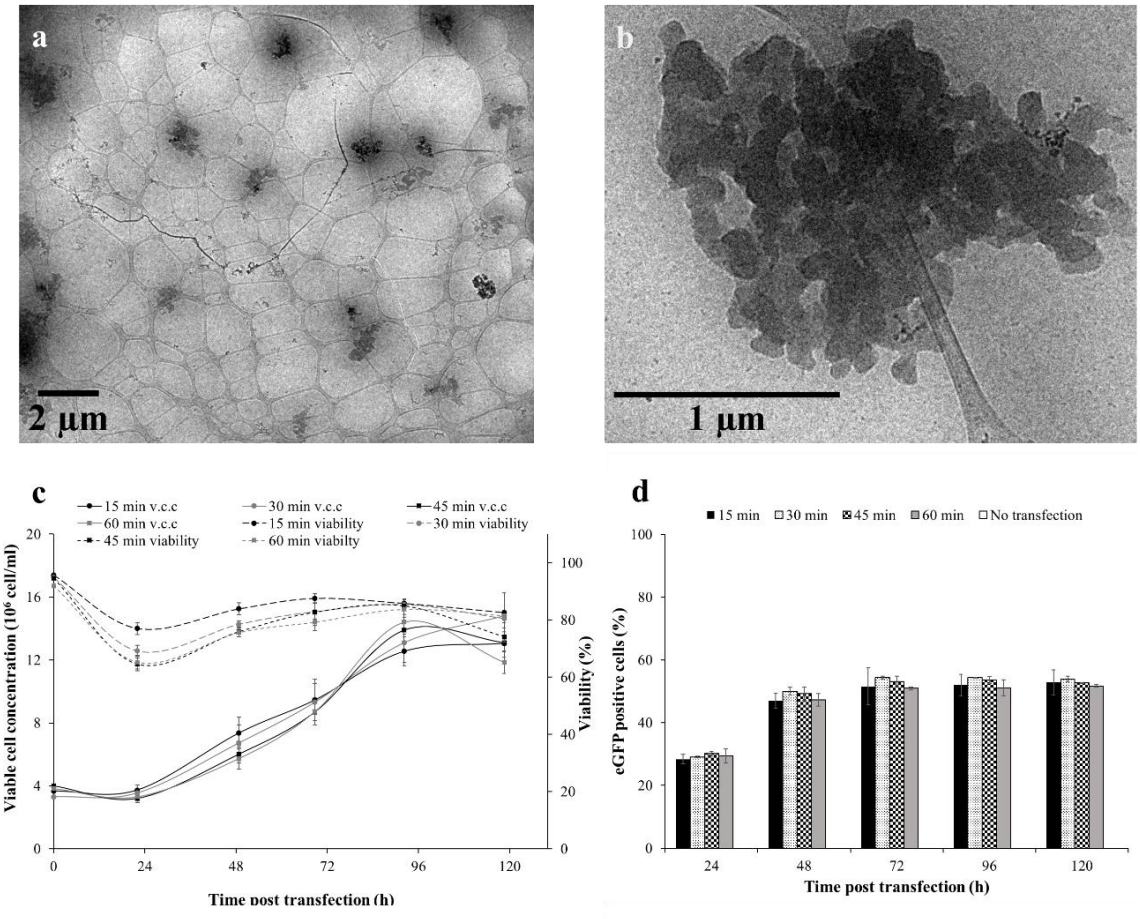

Figure 2. DNA:PEI polyplex characterization and their effect in high cell density cultures. (a - b) Cryo-electron microscopy images of DNA:PEI polyplexes pre-formed in ultrapure water for 10 min. (c - d) Cell growth and transfection kinetics of different incubation times between DNA:PEI complexes and high cell density cultures. Mean values ± standard deviation of triplicate experiments are represented.

Optimizing the transient gene expression process

After defining some variables affecting the transient gene expression process, a DoE approach was implemented to define the optimal conditions maximizing three different objective functions: transfection efficiency (%), viability after transfection (%) and eGFP production (R.F.U.). Viable cell concentration at transfection, DNA/cell and PEI/cell ratio were selected as the critical variables influencing the transient gene expression process as reported elsewhere [22]. The different experimental runs of the optimization process were performed with eGFP to facilitate product quantification.

A three-factor Box-Behnken design was generated with ranges for viable cell concentration, DNA/cell and PEI/cell ratio set as 10 – 30 x 10^6 cell/mL, 0.5 – 1.5 pg DNA /cell and 1.5 – 2.5 pg PEI/cell, respectively. The design matrix consisted in 15 experiments in which the central point was triplicated to account for pure experimental error (Table 1). Three different equations based on Eq. 4 were obtained for each one of the responses under study using the least squares regression method. Also, the statistical significance of each model equation was confirmed by ANOVA analysis (Table 1).

The best production conditions achieved at 72 hpt were at the highest DNA/cell and PEI/cell ratios (Fig. 3a – c). Indeed, a positive interaction between these two variables was observed. Noticeably, the equation model identified the 10 - 20 x 10^6 cell/mL experimental space as the most productive (Fig. 3c). In these conditions, the optimal condition for production was found as 12.9 x 10^6 cell/mL at transfection, 1.3 pg DNA/cell and 2.5 pg PEI/cell ratio. The best transfection efficiency at 72 hpt was obtained at the highest PEI/cell ratio and a viable cell concentration around the medium level (Fig. 3d – f). Interestingly, viable cell concentrations at transfection higher than 20 x 10^6 cell/mL exhibited worse transfection efficiencies although maintaining the same DNA/PEI and DNA/cell ratios. The optimal condition maximizing Sf9 cell transfection was found as 20.4

x 10^6 cell/mL, 0.8 pg DNA/cell and 2.5 pg PEI/cell ratio. Cell viability at 24 hpt was a critical step for transfection at high cell concentrations as demonstrated in previous sections. In this case, the variables most significantly influencing viability were viable cell concentration at transfection and PEI/cell ratio. Indeed, high PEI/cell ratios and viable cell concentrations proved to be detrimental for Sf9 cells (Fig. 3g – i). According to these results, the optimal conditions were determined as 10.0 x 10^6 cell/mL, 0.8 pg DNA/cell and 1.5 pg PEI/cell ratio.

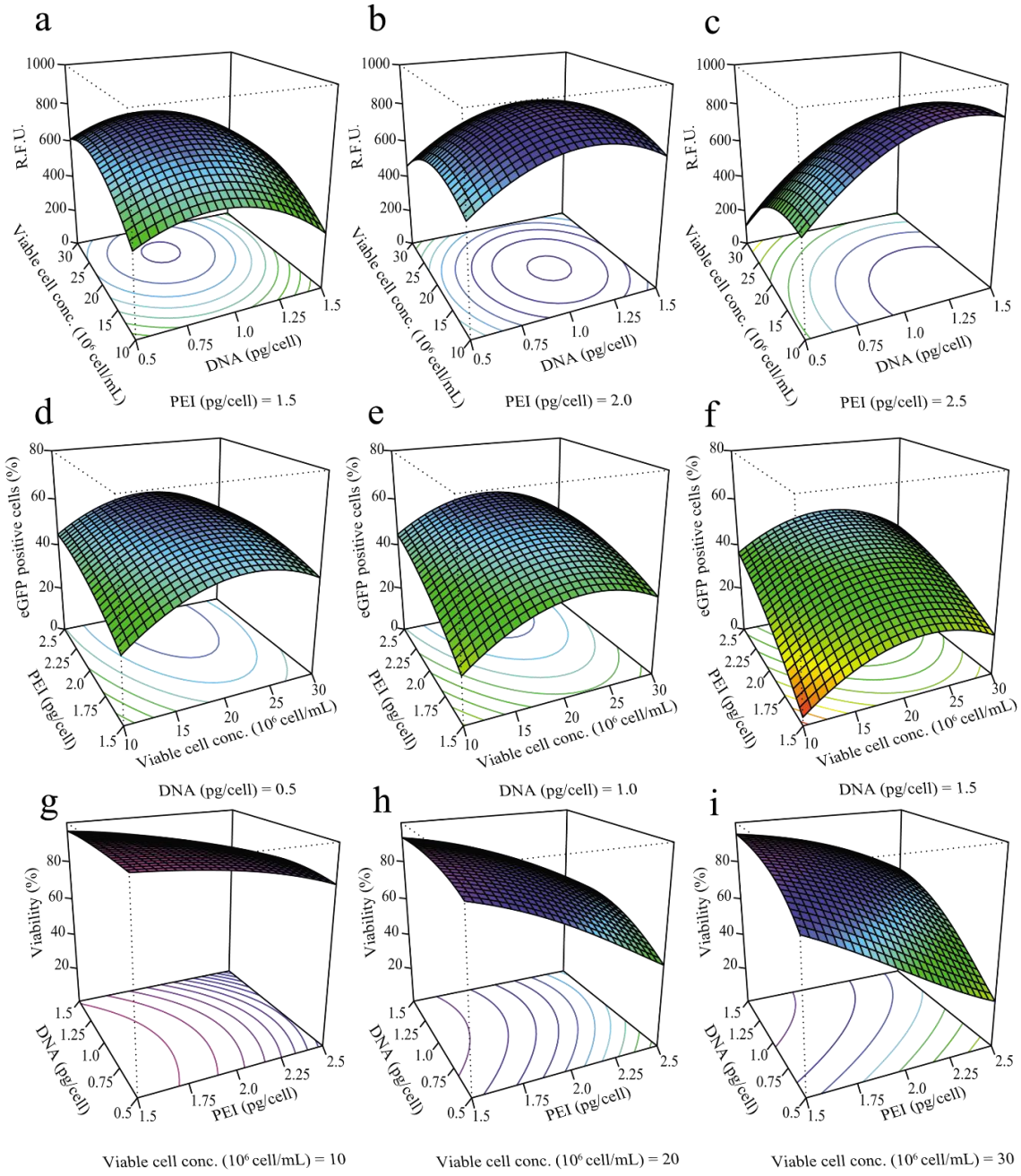

Figure 3. Response surface graphs from Box-Behnken DoE. (a - c) Intracellular eGFP production as a function of viable cell concentration, DNA/cell and PEI/cell ratios at 72 hpt. (d - f) Percentage of eGFP positive cells as a function of viable cell concentration, DNA/cell and PEI/cell ratios at 72 hpt. (g - i) Cell culture viabilities as a function of viable cell concentration, DNA/cell and PEI/cell ratios at 24 hpt. Three-dimensional graphs were constructed by depicting two variables at a time and maintaining the third one at a fixed level.

The evaluation of transient gene expression in Sf9 cells yielded different optimal conditions depending on the response under consideration. Then, a weighted-based equation approach was used to achieve a global optimal condition integrating the different responses. Weight assignation to each one of the equations was performed according to a priority criterion (*s*-value). Preference

was equally assigned to production and transfection (s = 2) while a lower restriction was given to cell viability after transfection (s = 1). Responses were then transformed to the d_n scale and combined into a unique overall desirability (*OD*) function to find a global TGE condition (Eq. 5). This process resulted in 17.6 x 10^6 cell/mL at transfection, 1.0 pg DNA/cell and 2.0 pg PEI/cell ratio with an *OD* score of 0.48. A sensitivity analysis was performed to confirm the robustness of the calculation (data not shown).

Sf9 cells as a platform to produce VLPs and other recombinant proteins

A confirmation experiment was conducted to verify the global optimal condition (Fig. 4). A maximum eGFP production of 11.7 ± 0.5 mg/L (723.4 ± 40.5 R.F.U.) and 51.7 ± 4.3 % transfection was obtained at 72 hpt, in agreement with the calculated prediction interval of the DoE (Table 2). Cell culture viability was 79.1 ± 6.7 % at 24 hpt, also in line with the DoE prediction (Fig. 4a).

Table 2. Experimental validation of the optimal condition and comparison to model predictions.

Response	Experimental	Model prediction
eGFP positive cells (%)	51.7 ± 4.3	52.0 ± 2.1
eGFP production (mg/L)	11.7 ± 0.5	13.7 ± 1.8
Viability (%)	79.1 ± 6.7	83.0 ± 5.5

To assess the general applicability of the optimized transient gene expression system here presented, other proteins with different structural complexities were assessed. Besides the intracellular eGFP used for process optimization, the production of secreted hSEAP and the HIV-1 GageGFP VLP was evaluated. eGFP and hSEAP production peaked at 72 hpt, with the majority of eGFP retained intracellularly whereas hSEAP (23.6 ± 2.3 mg/L) was mainly secreted to the supernatant (Fig. 4c). On the other hand, a continuous increase in GageGFP production was observed after transfection in the supernatant, with a significant amount of the polyprotein accumulated in the intracellular space. The sum of intracellular and extracellular GageGFP production reached a maximum between 48 – 72 hpt (47.9 ± 12.1 R.F.U.). Confocal microscopy analysis of eGFP and GageGFP transfected Sf9 cells showed the distinctive features of each

protein (Fig. 4d – e). Indeed, all the green signal was localized intracellularly in eGFP producing cells. Conversely, yellow regions were observed in the membrane of GageGFP transfected cells resulting from GageGFP (green) and cell membrane (red) co-localization, a characteristic indication of VLP formation.

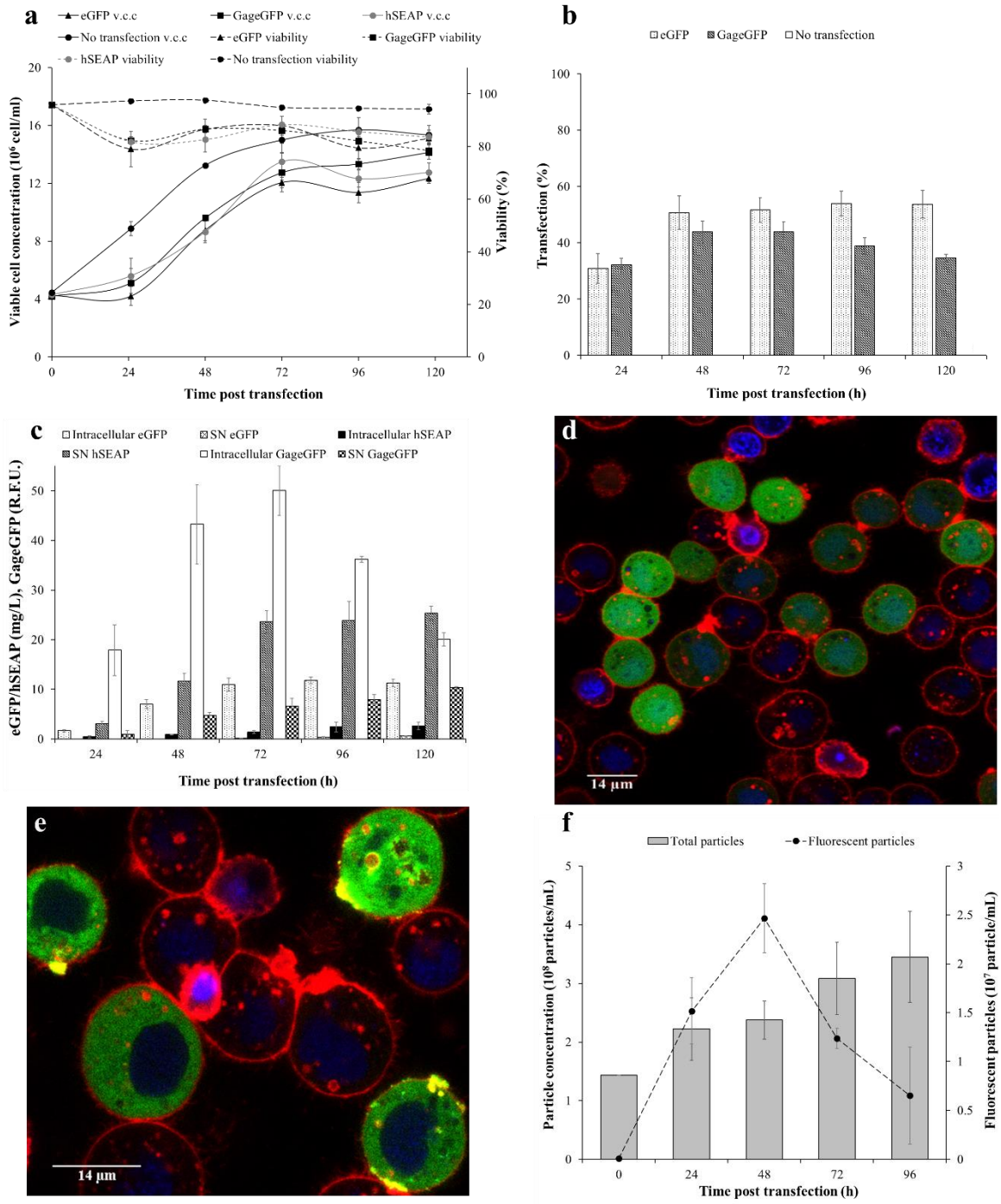

Figure 4. Validation of the global optimal conditions and comparison with hSEAP and GageGFP. (a) Cell growth and viability kinetics of transfected cultures with eGFP, hSEAP and GageGFP. Exponentially growing cells were transfected at 17.6 x 10^6 cells/mL and diluted to 4.0 x 10^6 cells/mL after 15 min. (b – c) Transfection and intracellular/extracellular production of the different proteins. (d – e) Confocal fluorescence microscopy image of eGFP (d) and GageGFP (e) transfected Sf9 cells. Cell nucleus was stained with Hoechst (blue) and membrane was stained with CellMask™ (red). (f) Nanoparticle quantification of GageGFP transfected cells using flow virometry. The average values of triplicate experiments are represented.

A more thorough characterization was conducted to assess the GageGFP VLP production kinetics. Flow virometry revealed that the maximal fluorescent particle concentration was attained at 48 hpt which differed from the data analyzed by spectrofluorometry (Fig. 4f). Free GageGFP release could explain the increase of fluorescence in the supernatant but not in the form of assembled particles. An increase in extracellular vesicle (EV) production was also detected by flow virometry and NTA (Table 3), which are known to be produced as a mechanism of cell-to-cell communication in different cell lines [23]. According to these results, 48 hpt proved to be the best option for VLP harvesting since the highest ratio of VLP to extracellular vesicles was obtained. In these conditions, VLP quantification using NTA yielded $1.9 \pm 0.8 \times 10^9$ fluorescent particles/mL.

Table 3. GageGFP production in harvested supernatants and cell lysates at 48 hpt using different quantification methodologies.

Quantification method	Fluorescent particles/mL	Total particles/ mL	Supernatant	Intracellular
NTA (particles/mL)	$1.9 \pm 0.8 \cdot 10^9$	$7.5 \pm 0.1 \cdot 10^{10}$	-	-
Flow virometry (particles/mL)	$2.5 \pm 0.4 \cdot 10^7$	$2.4 \pm 0.3 \cdot 10^8$	-	-
ELISA (ng/mL)	-	-	23.1 ± 5.8	211.1 ± 25.7
Fluorometry (R.F.U.)	$1.5 \pm 0.2 \cdot 10^{9a}$	-	4.8 ± 0.6	43.1 ± 11.5

[a]This is the resulting value of correlating R.F.U. to NTA (eq. 2)

Characterization of VLP production

GageGFP harvested supernatants at 48 hpt were analyzed using cryo-EM (Fig. 5a). Representative micrographs showed the presence of spherical virus-like particles surrounded by a lipid envelope with a diameter ranging 100 – 200 nm. EVs were also observed as smaller round-shaped structures (< 100 nm) and less electron-dense in comparison to VLPs, most likely corresponding to exosomes [24].

A final characterization of the harvested supernatant was performed to determine the efficiency of Sf9 cells at assembling GageGFP in the form of VLPs (VLP fluorescence/ total fluorescence).

To evaluate this, the GageGFP supernatants were ultracentrifuged in a double 25 – 45 % sucrose cushion and each of the resulting fractions was analyzed using a spectrofluorometer (Fig. 5b). The 80 % of the measured fluorescence signal was in the form of VLPs (25 %, 25 – 45 %, 45 % fractions) whereas the remaining 20 % corresponded to unassembled GageGFP monomer (SN, SN – 25 %) or was associated to cell debris (Pellet). Interestingly, the GageGFP correlation between fluorescence and VLPs (Eq. 2) resulted in 1.5 ± 0.2 x 10^9 VLP/mL, which was in agreement with the NTA measurement. This data indicated that VLP concentration could be accurately calculated using spectrofluorometry which has been demonstrated to be a rapid and cost-effective quantification methodology [25].

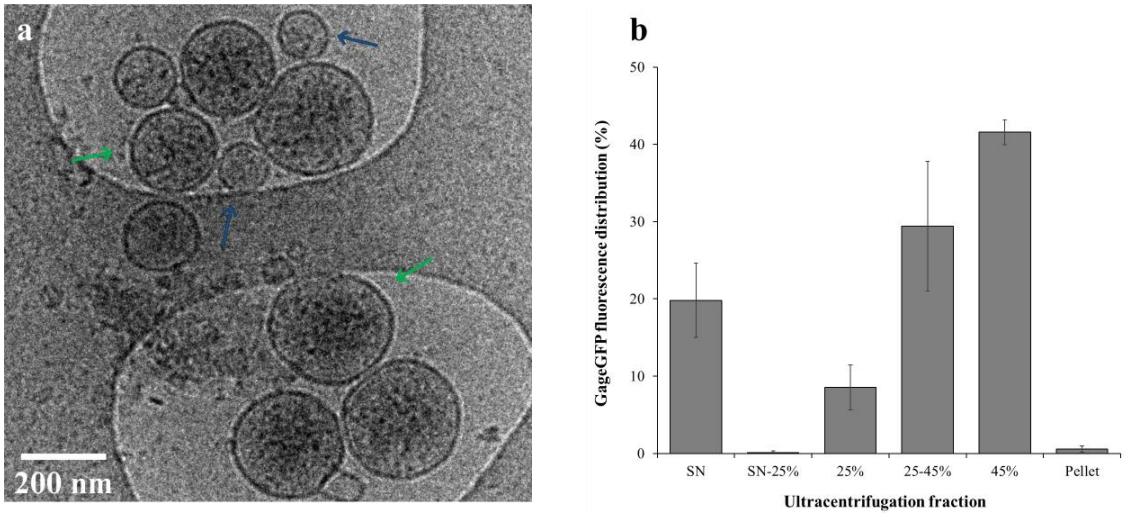

Figure 5. GageGFP supernatant characterization. (a) Cryo-electron microscopy images of transiently transfected Sf9 cells with GageGFP at 48 hpt showing the presence of VLPs (green) and EVs (blue). (b) Fluorescence distribution of GageGFP harvested supernatant at 48 hpt after double sucrose cushion ultracentrifugation. Mean values ± standard deviation of triplicate experiments are represented.

Discussion

The insect cell/BEVS has proven to be a powerful tool for the expression of various recombinant proteins and complex nanoparticles. However, there are several limitations to this system associated to the lytic nature of infection that can influence product quality [26]. Actually, production of complex nanoparticles such as VLPs can be compromised to some extent by the presence of baculovirus-derived proteins like GP64 [27]. Although some efforts have been devoted to remove the expression of this protein [28], the baculovirus itself still hampers VLP

separation at the downstream stage [29]. Therefore, the use of alternative methodologies is of general interest. Here, we describe a robust transient gene expression method for the Sf9 cell line in a low-hydrolysate medium based on the transfection reagent polyethylenimine.

Initial efforts to transfect Sf9 cells were performed at low cell densities but resulted in poor transfection efficiencies. This cell line proved to be resistant to PEI transfection using standard approaches otherwise successfully applied in mammalian cells [30,31]. In this sense, the development of culture media allowing Sf9 cell transfection in these conditions would be desirable in the future. Better transfection yields were obtained after medium replacement prior to transfection and using high cell densities. Medium replacement has worked in several cases arguing that negatively-charged byproducts are removed, thus avoiding their interference with DNA:PEI polyplexes [32,33]. Also, some benefit has been reported with transfection at high cell densities since it is possible to increase the effective PEI concentration while maintaining a non-toxic PEI/cell ratio [34,35]. Interestingly, this work demonstrated that part of the deleterious effect of high PEI concentrations could be mitigated by reducing the time of polyplex incubation with cell cultures.

A thorough study of the DNA:PEI polyplex formation was conducted to optimize the conditions for transfection. The incubation solution for polyplex formation proved to be essential. The Sf900III medium and the 150 mM NaCl solution were not efficient in delivering the polyplexes to the cells probably due to the fast aggregation kinetics between DNA and PEI [36]. In fact, big polyplexes can hinder the uptake of DNA by the cells as reported elsewhere [37]. Ultrapure water and direct addition of PEI and DNA showed the best transfection yields. This is in agreement with the optimal polyplex formation conditions recently described for PEI-based TGE of the Hi5 insect cell line [15]. However, DNA:PEI polyplexes were more size heterogeneous in the optimal transfection conditions for Sf9 compared to Hi5 cells, probably owing to the higher effective concentrations of DNA and PEI. The effect of incubation time between DNA and PEI in ultrapure water was also explored resulting in similar transfection outcomes in all the conditions tested. These findings are in accordance with the stability attributed to DNA:PEI polyplexes pre-formed in water [14].

Several key parameters were monitored during TGE optimization using DoE. Cell viability after transfection, eGFP production and transfection were considered as crucial for proper process development. A multiple response optimization approach was applied to find a global TGE condition based on the three equations from the Box-Behnken DoE. Using this strategy, an optimal DNA/PEI ratio of 1:2 was found for Sf9 cells, similar to that reported with other animal cell lines [38,39].

The maximum yield of eGFP achieved was 11.7 ± 0.5 mg/L at 3 days post transfection, a 2 and 2.7-fold increase compared to Hi5 and HEK293SF cells, respectively [15]. The eGFP specific productivity was 0.6 µg/10^6 transfected cell per day in these conditions, 2-fold higher with respect to the recently published transient eGFP production protocol for Sf9 cells with the lipofectin reagent [40]. Different results were observed when comparing to Sf9 baculovirus infection, with more than 10-fold increase [41] or 6-fold decrease [42] in eGFP specific productivities. Regarding hSEAP, Sf9 cells proved to be more efficient in producing this secreted protein compared to eGFP, with a specific productivity of 1.1 ± 0.1 µg/10^6 transfected cell per day. The maximum hSEAP yield obtained (23.6 ± 2.3 mg/L) was in the range of the 39 mg/L achieved using baculovirus infection in Sf9 cells [43].

From the perspective of new generation vaccines, we tested the utility of this platform to produce HIV-1-based VLPs. The complexity associated to the production of GageGFP could be clearly observed when comparing the fluorescence yields obtained with eGFP. Indeed, a 15-fold increase in eGFP production (723.4 ± 40.5 R.F.U.) was achieved compared to GageGFP (47.9 ± 12.1 R.F.U.). The budding process step required for GageGFP VLP formation was found to be the bottleneck as demonstrated by the intracellular/extracellular spectrofluorometry and ELISA quantification (Table 3). Similar results have been observed in the production of multimeric nanoparticles in mammalian cells [44], highlighting the difficulties for cells to process these complex polyproteins. Still, the evaluation of VLP assembling by analytical ultracentrifugation revealed that the Sf9 cell line was highly efficient since most of the polyprotein was in the form of assembled nanoparticles. Native visualization of these nanoparticles using cryo-EM corroborated the correct morphology and structure of GageGFP VLPs but also the concomitant

expression of extracellular vesicles. Strategies based on ion exchange or affinity chromatography should allow to separate both specimens as recently reported for other animal-derived VLPs [19,45]. In these conditions, a competitive production of $1.9 \pm 0.8 \times 10^9$ GageGFP VLP/mL was obtained at 2 days post transfection. These results proved to be in the range of GageGFP VLP production in HEK 293 mammalian cells by TGE [39]. Moreover, these conditions allowed for a faster and also higher production by 3.9-fold in comparison to recently reported Gag VLP production in Sf9 stable cell lines [46]. These results represent an important advance to existing insect cell-based production platforms devoid of baculovirus, with a potential applicability to produce an ample variety of recombinant products.

Acknowledgments

The authors would like to thank Dr. Julià Blanco (Irsi Caixa, Badalona, Spain) and Dr. Paula Alves (Instituto de Biologia Experimental e Tecnológica, Oeiras, Portugal) for providing the pGageGFP and pITV5-eGFP plasmids, respectively. We would also like to thank Jorge Fomaro and Ángel Calvache (Beckman Coulter) for ceding the CytoFelx LX flow cytometer. The help of Núria Barba and Mónica Roldán in confocal microscopy and Martí de Cabo with the Cryo-EM (Servei de Microscòpia, UAB) are also acknowledged. The support of José Amable Bernabé (Institut de Ciència de Materials de Barcelona, CSIC), Manuela Costa (Servei de Cultius Cel·lulars, Producció d'Anticossos i Citometria, UAB) and Sahar Masoumeh (University of Natural Resources and Life Sciences, Vienna, Austria) with NTA, flow cytometry and ELISA quantification, respectively, is appreciated. Eduard Puente-Massaguer is a recipient of an FPU grant from Ministerio de Educación, Cultura y Deporte of Spain (FPU15/03577). The research group is recognized as 2017 SGR 898 by Generalitat de Catalunya.

Compliance with Ethical Standards

Conflict of interest

The authors declare that they have no competing interests.

Ethical approval

This article does not contain any studies with human participants performed by any of the authors.

References

[1] J.M. Gutierrez, N.E. Lewis, Optimizing eukaryotic cell hosts for protein production through systems biotechnology and genome-scale modeling, Biotechnol. J. 10 (2015) 939–949.

[2] L. Ikonomou, Y.-J. Schneider, S.N. Agathos, Insect cell culture for industrial production of recombinant proteins, Appl. Microbiol. Biotechnol. 62 (2003) 1–20.

[3] S. George, A.M. Jauhar, J. Mackenzie, S. Kieβlich, M.G. Aucoin, Temporal characterization of protein production levels from baculovirus vectors coding for GFP and RFP genes under non-conventional promoter control, Biotechnol. Bioeng. 112 (2015) 1822–1831.

[4] E. Carpentier, D. Lebesgue, A.A. Kamen, M. Hogue, M. Bouvier, Y. Durocher, Increased Production of Active Human β2-Adrenergic/Gαs Fusion Receptor in Sf-9 Cells Using Nutrient Limiting Conditions, Protein Expr. Purif. 23 (2001) 66–74.

[5] L. Nika, J. Wallner, D. Palmberger, K. Koczka, K. Vorauer-Uhl, R. Grabherr, Expression of full-length HER2 protein in Sf 9 insect cells and its presentation on the surface of budded virus-like particles, Protein Expr. Purif. 136 (2017) 27–38.

[6] S.-Y. Lin, Y.-C. Chung, Y.-C. Hu, Update on baculovirus as an expression and/or delivery vehicle for vaccine antigens, Expert Rev. Vaccines. 13 (2014) 1501–1521.

[7] M. Bleckmann, S. Schmelz, C. Schinkowski, A. Scrima, J. van den Heuvel, Fast plasmid based protein expression analysis in insect cells using an automated SplitGFP screen, Biotechnol. Bioeng. 113 (2016) 1975–1983.

[8] S. Gutierrez-Granados, L. Cervera, A.A. Kamen, F. Godia, Advancements in mammalian cell transient gene expression (TGE) technology for accelerated production of biologics., Crit. Rev. Biotechnol. 0 (2018) 1–23.

[9] M. Lu, R.R. Johnson, K. Iatrou, Trans-activation of a cell housekeeping gene promoter by the IE1 gene product of baculoviruses, Virology. 218 (1996) 103–113.

[10] M.B. Keith, P.J. Farrell, K. Iatrou, L. a Behie, Screening of transformed insect cell lines for recombinant protein production., Biotechnol. Prog. 15 (1999) 1046–52.

[11] S. Geisse, Reflections on more than 10 years of TGE approaches, Protein Expr. Purif. 64 (2009) 99–107.

[12] X. Shen, A.K. Pitol, V. Bachmann, D.L. Hacker, L. Baldi, F.M. Wurm, A simple plasmid-based transient gene expression method using High Five cells, J. Biotechnol. 216 (2015) 67–75.

[13] K. Mori, H. Hamada, T. Ogawa, Y. Ohmuro-matsuyama, T. Katsuda, H. Yamaji, Efficient production of antibody Fab fragment by transient gene expression in insect cells, J. Biosci. Bioeng. 124 (2017) 221–226.

[14] X. Shen, D.L. Hacker, L. Baldi, F.M. Wurm, Virus-free transient protein production in Sf9 cells, J. Biotechnol. 171 (2013) 61–70.

[15] E. Puente-Massaguer, M. Lecina, F. Gòdia, Nanoscale characterization coupled to multi-parametric optimization of Hi5 cell transient gene expression, Appl. Microbiol. Biotechnol. 102 (2018) 10495–10510.

[16] M. Bleckmann, M.H.-Y. Fritz, S. Bhuju, M. Jarek, M. Schürig, R. Geffers, V. Benes, H. Besir, J. van den Heuvel, Genomic Analysis and Isolation of RNA Polymerase II Dependent Promoters from Spodoptera frugiperda, PLoS One. 10 (2015) e0132898.

[17] M. Lecina, A. Soley, J. Gràcia, E. Espunya, B. Lázaro, J.J. Cairó, F. Gòdia, Application of on-line OUR measurements to detect actions points to improve baculovirus-insect cell cultures in bioreactors, J. Biotechnol. 125 (2006) 385–394.

[18] L. Hermida-Matsumoto, M.D. Resh, Localization of human immunodeficiency virus type 1 Gag and Env at the plasma membrane by confocal imaging., J. Virol. 74 (2000) 8670–8679.

[19] K. Reiter, P.P. Aguilar, V. Wetter, P. Steppert, A. Tover, A. Jungbauer, Separation of virus-like particles and extracellular vesicles by flow-through and heparin affinity chromatography, J. Chromatogr. A. 1588 (2019) 77–84.

[20] E.V.B. Van Gaal, R. Van Eijk, R.S. Oosting, R.J. Kok, W.E. Hennink, D.J.A. Crommelin, E. Mastrobattista, How to screen non-viral gene delivery systems in vitro?, J. Control. Release. 154 (2011) 218–232.

[21] D.L. Hacker, D. Kiseljak, Y. Rajendra, S. Thurnheer, L. Baldi, F.M. Wurm, Polyethyleneimine-based transient gene expression processes for suspension-adapted HEK-293E and CHO-DG44 cells, Protein Expr. Purif. 92 (2013) 67–76.

[22] B.C. Thompson, C.R.J. Segarra, O.L. Mozley, O. Daramola, R. Field, P.R. Levison, D.C. James, Cell line specific control of polyethylenimine-mediated transient transfection optimized with "Design of experiments" methodology, Biotechnol. Prog. 28 (2012) 179–187.

[23] D.G. Meckes, N. Raab-Traub, N. Raab-Traub, Microvesicles and viral infection., J. Virol. 85 (2011) 12844–54.

[24] S. El Andaloussi, I. Mäger, X.O. Breakefield, M.J.A. Wood, Extracellular vesicles: Biology and emerging therapeutic opportunities, Nat. Rev. Drug Discov. 12 (2013) 347–357.

[25] S. Gutiérrez-Granados, L. Cervera, F. Gòdia, J. Carrillo, M.M. Segura, Development and validation of a quantitation assay for fluorescently tagged HIV-1 virus-like particles, J. Virol. Methods. 193 (2013) 85–95.

[26] F. Liu, X. Wu, L. Li, Z. Liu, Z. Wang, Use of baculovirus expression system for generation of virus-like particles: Successes and challenges, Protein Expr. Purif. 90 (2013) 104–116.

[27] W.-Y. Luo, S.-Y. Lin, K.-W. Lo, C.-H. Lu, C.-L. Hung, C.-Y. Chen, C.-C. Chang, Y.-C. Hu, Adaptive immune responses elicited by baculovirus and impacts on subsequent transgene expression in vivo., J. Virol. 87 (2013) 4965–73.

[28] L.C.S. Chaves, B.M. Ribeiro, G.W. Blissard, Production of GP64-free virus-like particles from baculovirus-infected insect cells, J. Gen. Virol. 99 (2018) 265–274.

[29] T. Vicente, A. Roldão, C. Peixoto, M.J.T.T. Carrondo, P.M. Alves, Large-scale production and purification of VLP-based vaccines, J. Invertebr. Pathol. 107 (2011) S42–S48.

[30] M. Derouazi, P. Girard, F.F. Van Tilborgh, K. Iglesias, N. Muller, M. Bertschinger, F.M. Wurm, Serum-free large-scale transient transfection of CHO cells, Biotechnol. Bioeng. 87 (2004) 537–545.

[31] P.L. Pham, S. Perret, H.C. Doan, B. Cass, G. St-Laurent, A. Kamen, Y. Durocher, Large-

scale transient transfection of serum-free suspension-growing HEK293 EBNA1 cells: Peptone additives improve cell growth and transfection efficiency, Biotechnol. Bioeng. 84 (2003) 332–342.

[32] Y. Rajendra, D. Kiseljak, S. Manoli, L. Baldi, D.L. Hacker, F.M. Wurm, Role of non-specific DNA in reducing coding DNA requirement for transient gene expression with CHO and HEK-293E cells, Biotechnol. Bioeng. 109 (2012) 2271–2278.

[33] J. Ye, V. Kober, M. Tellers, Z. Naji, P. Salmon, J.F. Markusen, High-level protein expression in scalable CHO transient transfection, Biotechnol. Bioeng. 103 (2009) 542–551.

[34] G. Backliwal, M. Hildinger, V. Hasija, F.M. Wurm, High-density transfection with HEK-293 cells allows doubling of transient titers and removes need for a priori DNA complex formation with PEI, Biotechnol. Bioeng. 99 (2008) 721–727.

[35] M. Stuible, A. Burlacu, S. Perret, D. Brochu, B. Paul-Roc, J. Baardsnes, M. Loignon, E. Grazzini, Y. Durocher, Optimization of a high-cell-density polyethylenimine transfection method for rapid protein production in CHO-EBNA1 cells, J. Biotechnol. 281 (2018) 39–47.

[36] Y. Sang, K. Xie, Y. Mu, Y. Lei, B. Zhang, S. Xiong, Y. Chen, N. Qi, Salt ions and related parameters affect PEI-DNA particle size and transfection efficiency in Chinese hamster ovary cells., Cytotechnology. 67 (2015) 67–74.

[37] I. González-Domínguez, N. Grimaldi, L. Cervera, N. Ventosa, F. Gòdia, Impact of physicochemical properties of DNA/PEI complexes on transient transfection of mammalian cells, N. Biotechnol. 49 (2019) 88–97.

[38] M. Bertschinger, A. Schertenleib, J. Cevey, D.L. Hacker, F.M. Wurm, The kinetics of polyethylenimine-mediated transfection in suspension cultures of Chinese hamster ovary cells., Mol. Biotechnol. 40 (2008) 136–43.

[39] L. Cervera, S. Gutiérrez-Granados, M. Martínez, J. Blanco, F. Gòdia, M.M. Segura, Generation of HIV-1 Gag VLPs by transient transfection of HEK 293 suspension cell cultures using an optimized animal-derived component free medium, J. Biotechnol. 166

(2013) 152–165.

[40] M. Bleckmann, M. Schürig, F.F. Chen, Z.Z. Yen, N. Lindemann, S. Meyer, J. Spehr, J. Van Den Heuvel, Identification of essential genetic baculoviral elements for recombinant protein expression by transactivation in Sf21 insect cells, PLoS One. 11 (2016) 1–19.

[41] F. Monteiro, V. Bernal, X. Saelens, A.B. Lozano, C. Bernal, A. Sevilla, M.J.T. Carrondo, P.M. Alves, Metabolic profiling of insect cell lines: Unveiling cell line determinants behind system's productivity, Biotechnol. Bioeng. 111 (2014) 816–828.

[42] F. Fernandes, J. Vidigal, M.M. Dias, K.L.J. Prather, A.S. Coroadinha, A.P. Teixeira, P.M. Alves, Flipase-mediated cassette exchange in Sf9 insect cells for stable gene expression, Biotechnol. Bioeng. 109 (2012) 2836–2844.

[43] L. Ikonomou, G. Bastin, Y. Schneider, S. Agathos, Design of an efficient medium for insect cell growth and recombinant protein production, Vitr. Cell. & Dev. Biol. - Anim. 37 (2001) 549–559.

[44] L. Cervera, I. González-Domínguez, M.M. Segura, F. Gòdia, Intracellular characterization of Gag VLP production by transient transfection of HEK 293 cells, Biotechnol. Bioeng. 114 (2017) 2507–2517.

[45] P. Steppert, D. Burgstaller, M. Klausberger, E. Berger, P. Pereira, T.A. Schneider, P. Kramberger, A. Tover, K. Nöbauer, E. Razzazi-fazeli, A. Jungbauer, Purification of HIV-1 gag virus-like particles and separation of other extracellular particles, J. Chromatogr. A. 1455 (2016) 93–101.

[46] J. Vidigal, B. Fernandes, M.M. Dias, M. Patrone, A. Roldão, M.J.T. Carrondo, P.M. Alves, A.P. Teixeira, RMCE-based insect cell platform to produce membrane proteins captured on HIV-1 Gag virus-like particles, Appl. Microbiol. Biotechnol. 102 (2018) 655–666.

Supplementary material

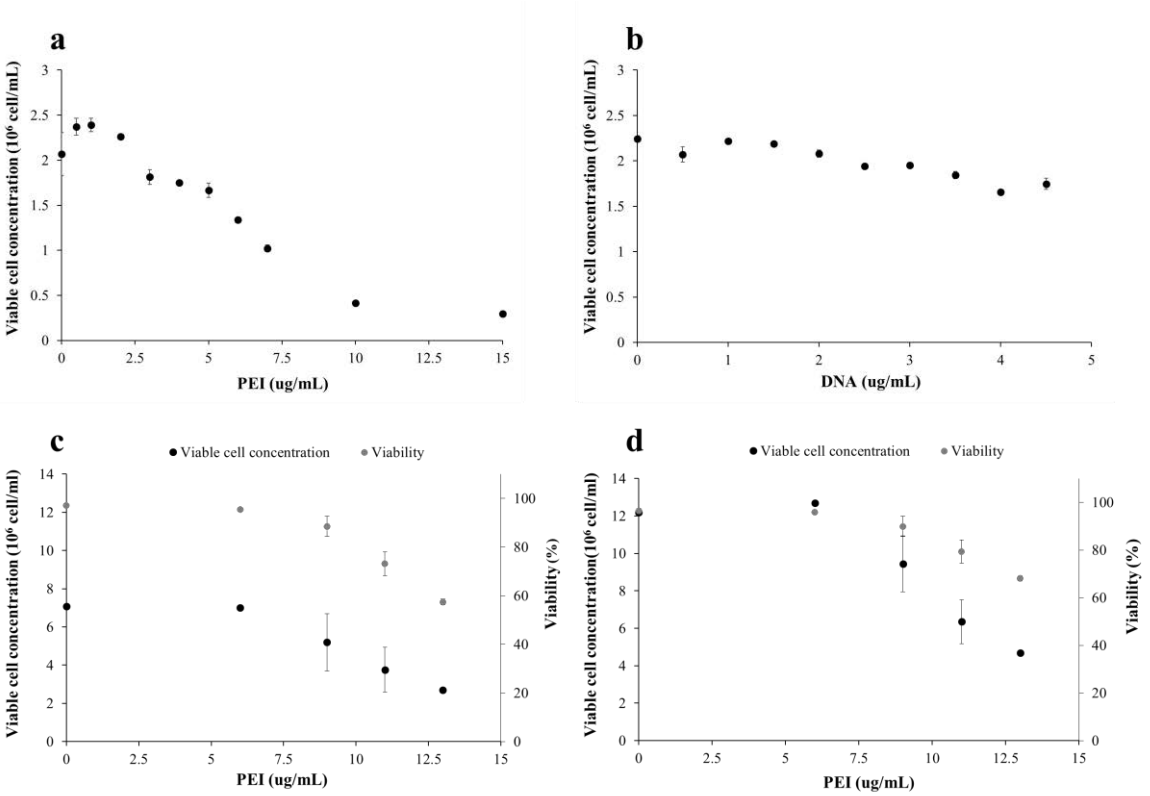

Figure S1. Toxicity experiments for linear 25 kDa PEI and plasmid DNA. (a - b) 96-well plate toxicity assays for PEI (a) and plasmid DNA (b). Cells were seeded at 0.5 x 10^6 cell/mL and measured at 48 h after different quantities of DNA or PEI were added. Cell concentration was measured by the CellTiter 96® AQueous one solution cell proliferation assay (Promega, Madison, WI, USA) according to manufacturer's instructions. (c – d) Toxicity assays for PEI at Erlenmeyer flask scale. Cells were seeded at 3.0 x 10^6 cell/mL and measured at 24 h (c) and 48 h (d) after the addition of different quantities of PEI. Viable cell concentration and viability were measured with the NC-3000 nucleocounter. Mean values ± standard deviation of triplicate experiments are represented.

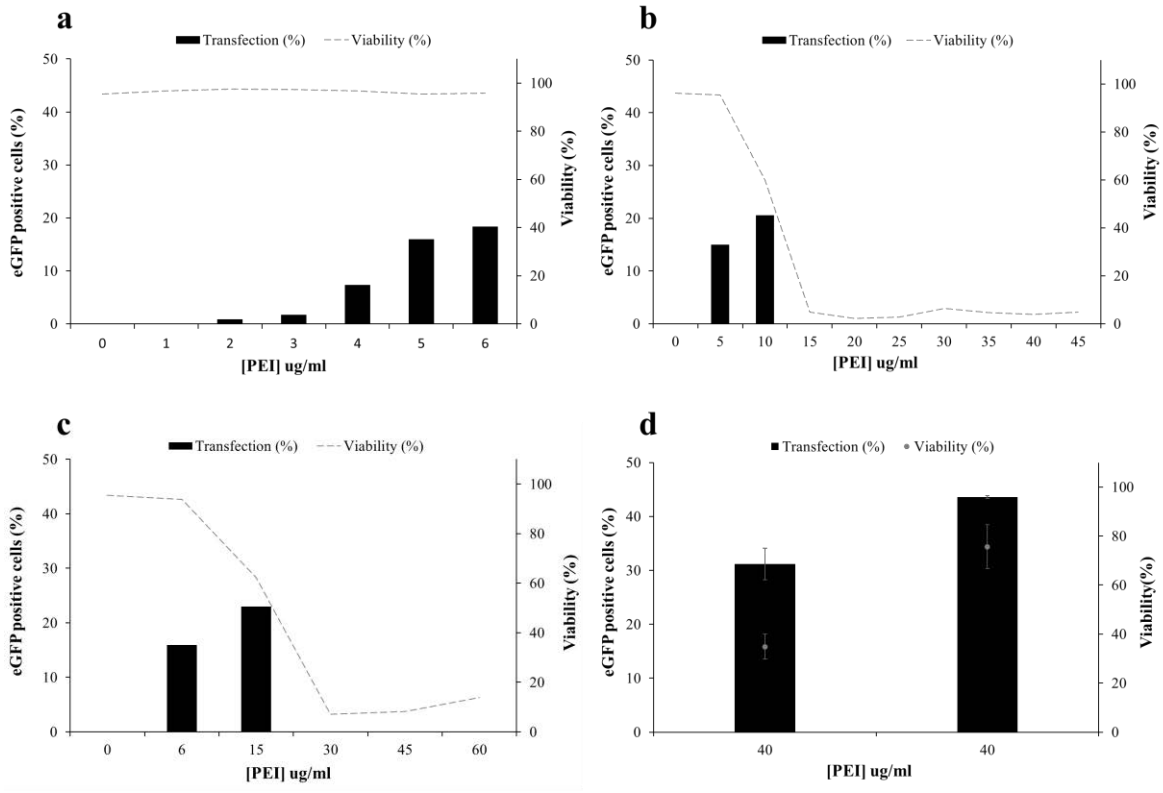

Figure S2. Screening of Sf9 transfection conditions at 48 hpt. (a - b) Series of transfection experiments at increasing PEI concentrations. Cells were transfected at 3.0 x 10^6 cell/mL and a DNA concentration of 3 µg/mL. (c) Transfection experiments with medium exchange before transfection. (d) High cell density transfection experiments performed at 10 - 20 x 10^6 cell/mL and a DNA concentration of 20 µg/mL. Cell viability was measured with the NC-3000 nucleocounter. Mean values ± standard deviation of triplicate experiments are represented.

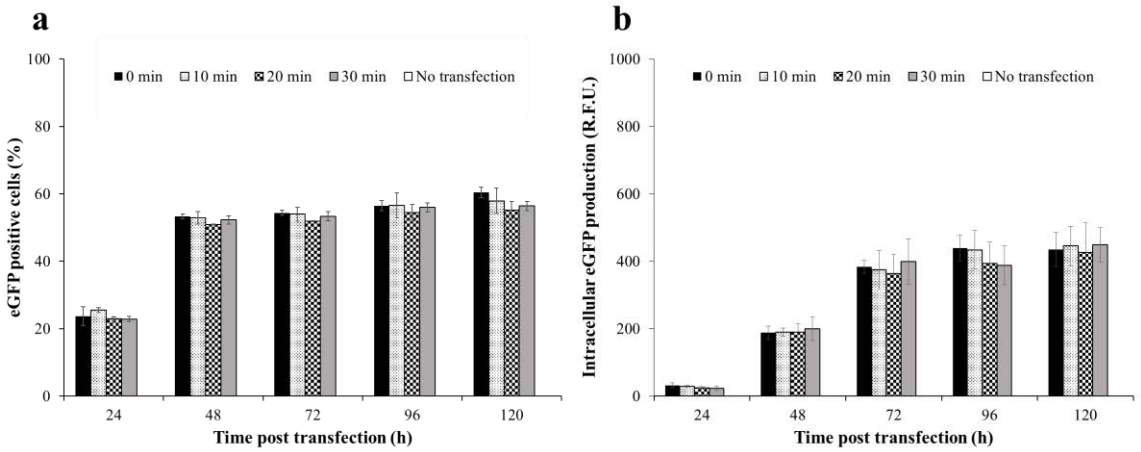

Figure S3. Analysis of eGFP expression in transfected cells using DNA and PEI mixture preformed with different incubation times. (a - b) Transfection and intracellular eGFP production using polyplexes pre-formed in ultrapure water for < 1, 10, 20, 30 min. Mean values ± standard deviation of triplicate experiments are represented.

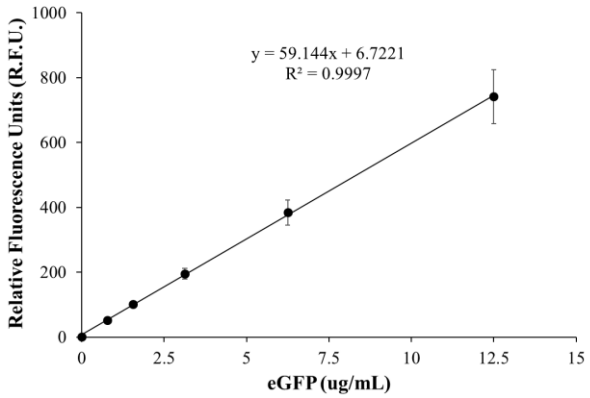

Figure S4. Linear relation between relative fluorescence units (R.F.U.) anf eGFP concentration (mg/L). Mean values ± standard deviation of triplicate experiments are represented.

Chapter 3 – Part II

Nanoscale characterization coupled to multi-parametric optimization of Hi5 cell transient gene expression

Part of this chapter is published in Applied Microbiology and Biotechnology, vol. 102, 2018

Eduard Puente Massaguer, Martí Lecina and Francesc Gòdia

Abstract

Polyethylenimine (PEI)-based transient gene expression (TGE) is nowadays a well-established methodology for rapid protein production in mammalian cells, but it has been used to a much lower extent in insect cell lines. A fast and robust TGE methodology for suspension Hi5 (*Trichoplusia ni*) cells is presented. Significant differences in size and morphology of DNA:PEI polyplexes were observed in the different incubation solutions tested. Moreover, minimal complexing time (< 1 min) between DNA and PEI in 150 mM NaCl solution provided the highest transfection efficiency. Nanoscopic characterization by means of cryo-EM revealed that DNA:PEI polyplexes up to 300 – 400 nm were the most efficient for transfection. TGE optimization was performed using eGFP as model protein by means of the combination of advanced statistical designs. A global optimal condition of 1.5 x 10^6 cell/mL, 2.1 µg/mL of DNA and 9.3 µg/mL PEI was achieved through weighted-based modelling of transfection, production and viability responses. Under these conditions, a 60 % transfection and 0.8 ± 0.1 µg/10^6 transfected cell·day specific productivity was achieved. The optimal transfection conditions were tested to produce diverse recombinant products, including hSEAP and GageGFP. The TGE protocol developed for Hi5 cells provides a promising baculovirus-free and worthwhile approach to produce a wide variety of recombinant proteins in a short period of time.

Keywords: High Five cells, polyethylenimine, transient gene expression, cryo-electron microscopy, dynamic light scattering, Design of Experiments

Abbreviations: AAV, adeno-associated virus; ANOVA, Analysis of variance; BEVS, Baculovirus expression vector system; Cryo-EM, Cryo-electron microscopy; DLS, dynamic light scattering; DoE, Design of Experiments; eGFP, enhanced green fluorescent protein; Gene of interest, GOI; HIV, human immunodeficiency virus; hpt, hours post transfection; hSEAP, human placental alkaline phosphatase; kcps, kilocounts per second; LOF, Lack-of-Fit; NTA, Nanoparticle tracking analysis; PEI, Polyethylenimine; RSM, response surface methodology; SN, Supernatant; TGE, Transient gene expression; VLP, Virus-like particle.

Introduction

The emergence of high-throughput techniques has brought under the spotlight the need for efficient and productive hosts to screen for a large number of protein candidates. CHO and HEK293 mammalian cell lines commonly serve to this purpose since they efficiently produce complex protein structures with adequate post-translational modifications [1]. Likewise, insect cells have also proven to be useful systems to produce difficult-to-express proteins maintaining their biological activity [2]. Furthermore, insect cells are capable to grow to high cell densities and they also have less strict culture requirements. Sf21 and Sf9 from *Spodoptera frugiperda*, Hi5 (High Five) and Tna38 from *Trichoplusia ni* are the most extensively used insect cell lines. In general terms, *Trichoplusia ni*-derived cell lines are the platforms selected for protein production since higher specific productivities are achieved compared to Sf9 and Sf21 cell lines. Typically, the baculovirus expression vector system (BEVS) is the preferred production methodology with regards to protein expression in insect cells. While the baculovirus-insect cell system has been successfully applied for the production of a number of target proteins, a long-time is still required from the cloning of the gene of interest (GOI) to obtain the baculovirus working stock [3]. Besides, several limitations of this system have been encountered with virus-like particles at the downstream phase due to co-purification of the two specimens [4]. A lack of consistency in the production of adeno-associated viruses (AAV) has also been reported and attributed to instability of the AAV cassette in baculoviruses during the expansion phase [5].

Growing interest has emerged on exploiting the benefits of insect cell lines for protein production devoid of BEVS methodology. Stable expression based on the transfection of plasmid DNA encoding for the GOI with subsequent antibiotic based selection has been evaluated for different proteins with variable results [6,7]. However, stable gene expression is time-consuming when several GOI have to be evaluated. In the same line, selecting a high producer clone from the stable expressing cell population entails a lot of effort which limits to a certain extent the applicability of this system for short-term applications [8].

Transient gene expression (TGE) is a methodology that enables rapid protein production in sufficient levels to be used in pre-clinical and early-clinical phases [9]. TGE has been extensively

used in mammalian cells but less is known for its application to insect cell lines. First attempts were performed in serum-containing adherent cultures by means of liposome-derived reagents and low titers were obtained [10,11]. However, the use of these transfection carriers hindered the scaling-up of the process in terms of cost-efficiency and have been gradually relegated to stable gene expression. Alternatively, attention has been focused on using bulk chemicals such as polyethylenimine (PEI) to evaluate TGE in suspension cultures, with successful results in the field of mammalian cells.

In parallel, many efforts have been directed to developing serum-free fully chemically-defined media that support high insect cell densities, but difficulties are encountered when replacing yeast hydrolysates. Recent studies have addressed PEI-based TGE of Hi5 cells but a lack of consistency due to the use of high hydrolysate containing media was reported [12,13]. This lot-to-lot variability greatly hinders the standardization and characterization of the transient transfection process which may explain the few information available regarding the driving forces that mediate TGE in insect cells.

In this study, a robust and reproducible transient transfection method for suspension-adapted Hi5 cells using PEI is described. Characterization of the DNA:PEI complexes that mediate transient transfection was thoroughly evaluated by means cryo-electron microscopy (Cryo-EM) and dynamic light scattering techniques. Several incubation solutions and different times of DNA:PEI complex formation were also studied as factors potentially influencing the physical properties of transient transfection. Finally, advanced statistically response surface methodologies (RSM) coupled to weighted-based modelling of different responses were successfully applied towards defining an optimum transfection condition for Hi5 cells.

Materials and Methods

Cell line, media and culture conditions

The lepidopteran insect cell line used in this work is *Trichoplusia ni* BTI-TN-5B1-4 (High Five, cat. num. B85502, Thermo Fisher Scientific). Four different serum-free commercial media formulations for Hi5 cells were tested for the following parameters: cell growth, transfection and

enhanced green fluorescent (eGFP) production. These include EX-CELL 405 (SAFC Biosciences, Saint Louis, MO, USA), Express Five SFM (Thermo Fisher Scientific, Waltham, MA, USA), Insect Xpress (Lonza, Verviers, Belgium) and Sf900III (Thermo Fisher Scientific, Grand Island, NY, USA). Cells were previously adapted to each medium prior to experimentation. Cell passaging was performed three times a week at a density of 2-4 x 10^5 cells/mL in 125-mL disposable polycarbonate Erlenmeyer flasks (Corning, Steuben, NY, USA) in 15 mL medium. All cultures were shaken at 130 rpm using an orbital shaker (Stuart, Stone, UK) and were maintained at 27°C.

Cell count and viability were measured with Nucleocounter NC-3000 (Chemometec, Allerod, Denmark) for 5 - 6 days. Maximum specific growth rates, μ_{max} (h^{-1}), and duplication times, $t_{1/2}$ (h) were determined from the data corresponding to the exponential growth phase.

Plasmid vectors

The plasmid vector used in the optimization of transient gene expression in Hi5 cells is the pIZTV5-eGFP (cat. num. V801001, Thermo Fisher Scientific) which harbours the immediate-early OPIE2 promoter from *Orgya pseudotsugata* multicapsid nucleopolyhedrosis virus (*Op*MNPV). The Sh *ble* resistance gene of this plasmid was fused in frame to a GFP in origin. The GFP portion of the Sh *ble* gene was removed by PCR cloning in order to eliminate fluorescence interference signals between GFP and eGFP. Briefly, pIZTV5-eGFP plasmid with the GFP gene at the Sh *ble* gene was PCR amplified using the following primer pair: GFPremove_fw: 5'-CGTAAGATCTCGCCATGGTTTAGTTCCTCAC-3' and GFPremove_rev: 5'-CGTAAGATCTATGGATGCCAAGTTGACCAG-3', then the PCR product was digested with *Bgl*II and ligated with T4 DNA ligase.

The production of other recombinant products was also tested using the optimal condition obtained with pIZTV5-eGFP plasmid. These include the truncated form of human placental alkaline phosphatase (hSEAP) and the human immunodeficiency virus (HIV-1) Gag fused in frame to the eGFP (GageGFP). All these genes were cloned into the pIZTV5 vector as previously described in part I of this chapter.

Standard transfection protocol

eGFP was produced by transient transfection of Hi5 cells with pIZTV5-eGFP plasmid DNA using 25 kDa linear polyethylenimine (PEI, PolySciences, Warrington, PA, USA). Linear PEI 25 kDa was prepared in ultrapure water at a concentration of 1 mg/mL with pH of 7 and was sterilized by filtration. The standard transfection protocol was defined according to preliminary experiments and was further optimized as detailed in the "Results" section. Prior to transfection, medium exchange was performed to exponentially growing cells by centrifugation at 300 x*g* during 5 min. Cells were resuspended to 1 x 10^6 cell/mL in 15 mL medium. DNA and PEI complex formation was performed in 1mL incubation solution with DNA at 1 µg/10^6 cell added first and vortexed during 10 s; then PEI at 3 µg/10^6 cell was added to DNA and vortexed for 10 s. Dulbecco's Phosphate-Buffered Saline (DPBS, Thermo Fisher Scientific, Logan, UT, USA) was selected as the DNA:PEI complexing solution for the medium screening phase but other solutions were also tested. These solutions include NaCl (Sigma-Aldrich, Saint Louis, MO, USA) and ultrapure water (Merck Millipore, Burlington, MA, USA). After 15 minutes of incubation at room temperature, the mixture was added to the culture. The percentage of eGFP and GageGFP expressing cells was assessed by flow cytometry using a BD FACS Canto II flow cytometer (BD Biosciences, San José, CA, USA) at different hours post transfection (hpt).

Fluorescence confocal microscopy

The visualization of GageGFP and eGFP producer cells was performed using a TCS SP5 confocal microscope (Leica, Wetzlar, Germany). Transfected cells were dyed with 0.05% v/v of CellMask™ and 0.1% v/v of Hoechst (Thermo Fisher Scientific, Eugene, OR, USA) in order to stain the lipid membrane and cell nucleus respectively. A washing step was performed by centrifuging the cells at 300 x*g* during 5 min and resuspending the pellet in fresh Sf900III medium. Samples were placed in 35 mm glass bottom Petri dishes with 14 mm microwell (MatTek Corporation, Ashland, MA, USA) for visualization.

Cryo-electron microscopy

Morphology and qualitative particle size distribution of DNA:PEI complexes formed in different solutions was studied with a cryo-transmission electron microscope (TEM). Briefly, 2 µL of sample was blotted onto carbon copper or holey carbon 200 mesh copper (Quantifoil Micro Tools, Großlöbichau, Germany) grids previously subjected to a glow discharge treatment in a PELCO easiGlow™. Discharge Cleaning System (PELCO, Fresno, CA, USA). The samples were subsequently plunged into liquid ethane at −180 °C using a Leica EM GP workstation (Leica, Wetzlar, Germany) and observed in a JEM-2011 TEM operating at 200 kV (Jeol Ltd., Akishima, Tokyo, Japan). Samples were maintained at −180 °C during imaging and pictures were taken using a CCD 895 USC 4000 multiscan camera (Gatan, Pleasanton, CA, USA).

Determination of DNA:PEI complex size

DNA:PEI average complex size distribution was evaluated with a Zetasizer Nano ZS dynamic light scattering (DLS) instrument (Malvern instruments, Malvern, UK) with a He/Ne 633 nm laser at 173°. The hydrodynamic diameter and polydispersity index (PDI) were calculated with cumulative fit correlation at 25 °C and 0.8872 cP. DNA:PEI complexes were prepared as described previously and placed in disposable plastic cuvettes followed by automated experimental data collection with Zetasizer Nano software (Malvern instruments, Malvern, UK). Complex formation was observed up to 1 µm average DNA:PEI complex size which is the upper detection threshold of the DLS equipment. The kilocounts per second (kcps) were also monitored and compared between samples according to the standardized values given by the Zetasizer Nano software.

eGFP and GageGFP quantification

eGFP and GageGFP producing cells were harvested by centrifugation at 3000 x*g* for 5 min. Pelleted cells were then subjected to a three freeze-thaw cycles (2h freezed at -20ºC and thawed at 37ºC for 0.5 h). Samples were vortexed for 5 seconds between cycles. Lysed pellets were resuspended in 0.5 mL of TMS buffer (50 mM Tris-HCl, 150 mM NaCl, 2 mM $MgCl_2$, pH 8.0)

and centrifuged at 13700 x*g* during 20 min. The eGFP green fluorescence was measured with a Cary Eclipse fluorescence spectrophotometer (Agilent Technologies, Santa Clara, CA, USA) at room temperature set as follows: λ_{ex} = 488 nm (5 nm slit), λ_{em} = 500 - 530 nm (10 nm slit). Relative fluorescence units (R.F.U) were calculated by substracting the fluorescence unit of non-transfected cultures. eGFP mass concentration was determined using a standard curve by a linear correlation of a known concentration of eGFP (BioVision, Milpitas, CA, USA) and the associated fluorescence intensity in R.F.U:

$$\text{eGFP (mg/L)} = (\text{R.F.U} - 1.0122)/32.564 \quad (1)$$

where eGFP is the estimated concentration of eGFP protein and R.F.U is the measured eGFP fluorescence intensity in the samples.

R.F.U. from GageGFP transfected Hi5 cell supernatants were also converted to GageGFP VLPs according to Gutiérrez-Granados et al. [14]:

$$\text{GageGFP nanoparticles (particles/mL)} = 1.53 \cdot 10^8 \text{ x R.F.U.} \quad (2)$$

The Sf900III medium and a 0.1 mg/mL quinine sulphate solution were used as control patterns to normalize R.F.U values between different experiments.

hSEAP quantification

Transiently transfected Hi5 cells with pIZTV5-hSEAP were harvested by centrifugation at 3000 x*g* for 5 min and cell pellets were disrupted under a 3-time freeze-thaw cycle for intracellular hSEAP quantification. The hSEAP concentration was measured based on the alkaline phosphatase activity of a colorimetric enzyme reaction (QUANTI-Blue system, InvivoGen). Shortly, 20 µL of sample were added to 200 µL of pre-warmed QUANTI-Blue solution and incubated for 1 h at 37ºC. The absorbance was measured in a Victor^3 spectrophotometer (PerkinElmer, Waltham, MA, USA) at a wavelength of 620 nm. Relative activity units (R.A.U.) were calculated by subtracting the absorbance corresponding to non-transfected cultures. hSEAP concentration was determined using a calibration curve based on a linear correlation of known hSEAP (InvivoGen) concentrations and the corresponding activity units in R.A.U.:

$$\text{hSEAP (mg/L)} = \text{R.A.U. x } 2.9744 + 0.0615 \quad (3)$$

where hSEAP is the calculated concentration of hSEAP protein and R.A.U. are the hSEAP activity units measured in the samples.

p24 Enzyme-linked immunosorbent assay (ELISA)

GageGFP containing supernatants and pellets were analysed to determine the content of HIV-1 p24 (Sino Biological, Wayne, NJ, USA). Briefly, supernatants were obtained by centrifugation at 3000 x *g* for 5 min and the collected cell pellets were disrupted as previously described. The different samples were analysed as described in part I of this chapter. The p24 (24 kDa) concentration values obtained in the ELISA were corrected considering the GageGFP molecular weight (87.7 kDa).

Flow virometry

Fluorescent and non-fluorescent particles from GageGFP harvested supernatants were measured using a CytoFlex LX (Beckman Coulter, Brea, CA, USA) equipped with a 488 nm blue laser for fluorescent particle detection and a 405 nm laser/violet side scatter configuration for improved nanoparticle size resolution. Samples were diluted in 0.22 µm-filtered DPBS and triplicate measurements from independent samples were analysed with the CytExpert 2.3 software at room temperature.

Nanoparticle tracking analysis

Nanoparticles in GageGFP harvested supernatants were also quantified using a NanoSight NS300 (Malvern Panalytical, Malvern, United Kingdom). Samples were diluted in 0.22 µm-filtered DPBS and continuously injected into the device chamber through a pump at an average concentration of 10^8 particles/mL (20 – 60 particles/frame). Videos of 60 s from independent triplicate measurement were analysed with the NanoSight NTA 3.2 software at room temperature.

VLP characterization by analytical ultracentrifugation

Supernatant containing GageGFP VLPs from transfected Hi5 cells at 72 hpt was centrifuged in a double sucrose (Sigma) cushion of 25 % and 45 % (w/v) prepared in DPBS and DMEM (Thermo

Fisher Scientific), respectively. 10 mL of supernatant were loaded in an ultracentrifuge tube (Beckman Coulter), filled to the top with sterile DPBS and centrifuged at 31000 rpm for 2.5 h at 4ºC (Beckman Optima L100XP, SW32ti rotor, Beckman Coulter). Samples were taken from each one of the ultracentrifugation fractions and the pellet was resuspended in 100 µL of sterile DPBS O/N. All samples were stored either at -4 or -80ºC.

Optimization of transient transfection using DoE

Transient transfection was optimized to maximize eGFP specific production using Design of experiments methodology (DoE). In addition, the percentage of eGFP positive cells and cell culture viability were also measured and considered as responses towards completely defining the transient transfection process with the final aim of finding a global process optimum. Viable cell concentration at the time of transfection, DNA and PEI concentration were the independent variables selected for optimization.

Box-Behnken design

A Box-Behnken design was used in order to define the optimal condition for each response and the independent variables to be studied. The three variables were screened at three levels coded as follows: low level, -1; medium level, 0; high level, +1; as indicated in Table 1.

Table 1. Matrix design, response and ANOVA analysis for Box-Behnken experimental design of the different variables. Run 13 was performed in triplicate as it is the centre point.

Coded levels	-1	0	1
Viable cell concentration (10^6 cell/mL)	1	2	3
DNA concentration (mg/L)	1	2	3
PEI concentration (mg/L)	5	8	11

	Variables			Responses		
Experimental run	[Cell][a]	[DNA]	[PEI]	Specific production (R.F.U[b]/10^6 cells)	eGFP positive cells (%)	Viability (%)
1	-1	-1	0	50.02	62.00	83.70
2	1	-1	0	65.56	35.80	68.30
3	-1	1	0	77.46	53.20	75.70
4	1	1	0	107.66	52.90	61.80
5	-1	0	-1	63.64	58.20	82.60
6	1	0	-1	103.81	44.60	63.20
7	-1	0	1	70.10	54.50	75.70
8	1	0	1	110.88	49.80	71.50
9	0	-1	-1	95.38	32.40	58.90
10	0	1	-1	133.86	47.20	67.50
11	0	-1	1	92.60	52.20	73.50
12	0	1	1	131.13	52.30	76.30
13	0	0	0	173.51	45.90	68.40
13	0	0	0	156.47	47.80	68.10
13	0	0	0	163.80	51.70	66.30

Model	*F* test, *p*-value[c]	Lack of fit test, *p-value*[d]	R^2
Specific production (72 hpt)	<0.001	0.736	0.981
eGFP positive cells (48 hpt)	0.007	0.251	0.842
Viability (72 hpt)	0.009	0.053	0.772

Model	Viability (72hpt)		eGFP positive cells (48 hpt)		Specific production (72hpt)	
Parameters	Coefficient	*p*-value	Coefficient	*p*-value	Coefficient	*p*-value
Constant	68.429	<0.001	47.071	<0.001	164.592	<0.001
[Cell]	-6.625	0.002	-5.600	0.004	15.837	<0.001
$[Cell]^2$	4.384	0.079	4.304	0.074	-57.779	<0.001
[DNA]	-0.388	0.804	2.900	0.077	18.316	<0.001
$[DNA]^2$	NS	>0.050	NS	>0.050	-31.640	<0.001
[PEI]	3.100	0.071	3.300	0.050	1.004	0.701
$[PEI]^2$	NS	>0.050	NS	>0.050	-19.708	<0.001
[Cell] x [DNA]	NS	>0.050	6.475	0.013	NS	>0.050
[Cell] x [PEI]	3.800	0.110	NS	>0.050	NS	>0.050
[DNA] x [PEI]	NS	>0.050	-3.675	0.107	NS	>0.050

[a][Cell]: Viable cell concentration

[b]R.F.U: relative fluorescent units

[c]*p*-value under 0.05 are considered as statistically significant with a 95% confidence.

[d]Lack of fit test, *p-value* above 0.05 imply that the hypothesis arguing that the model is suitable cannot be rejected.

NS: Non-significant term (*p-value* > 0.05)

The obtained results were fitted to a second-order polynomial equation by linear regression analysis for each response (Eq. 2):

$$Y = \beta_0 + \sum_{i=1}^{k} \beta_i \cdot X_i + \sum_{i=1}^{k} \beta_{ii} \cdot X_i^2 + \sum_{i=1}^{k} \sum_{j>1}^{k} \beta_{ij} \cdot X_i \cdot X_j + \varepsilon \quad (2)$$

where Y is the response variable (eGFP specific production in R.F.U/10^6 transfected cells, percentage of eGFP positive cells or cell culture viability in percentage), β_0 is the model intercept term, β_i the linear coefficient, β_{ii} the quadratic coefficient, β_{ij} the interaction coefficient, X_i and X_j are the studied variables (Viable cell concentration at the time of transfection, DNA and PEI concentration) and ε is the experimental error. The different model equations based on model Eq. 2 were obtained using the R Software (R Development Core Team, Vienna, Austria) by means of the *Frf2*, *car* and *RcmdrPlugin DoE* packages [15]. These equations were used to predict the optimal values of the independent variables using the L-BFGS-B quasi-Newton algorithm

implemented in the *optimx* package of the R software. Three-dimensional plots were generated with the *gplots* package to facilitate model interpretation and were readapted with Adobe Illustrator CS6 (Adobe Systems Incorporated, San José, CA, USA).

Multiple response optimization using desirability functions

The best overall condition considering the three model equations was determined using the *desirability* package from the R software. However, several modifications in the basic code of this package were implemented in order to successfully apply this methodology. The design space was fixed as circular because of the Box-Behnken design used for the optimization and values outside this space were not considered. Different ranges were selected for each response according to the experimental data and a relevance value (*s* value) was also chosen depending on the importance of the model equation (Eq. 3):

$$d_n = \begin{cases} 0 & if\ Y_n < LL \\ \left(\frac{Y_n - LL}{UL - LL}\right)^s & if\ LL \leq\ Y_n \leq UL \\ 1 & if\ Y_n > UL \end{cases} \qquad (3)$$

where d_n is the desirability response function for each model equation in [0 – 1] scale, *s* accounts for the relevance value given to the equation, Y_n is the model equation (in this case n = 3), *LL* and *UL* are de lower and upper limits of each equation, respectively. Greater *s* values make the desirability value d_n more difficult to be satisfied and are associated to the most important model equations. The different *N* desirability functions are then combined to achieve an Overall Desirability function *OD* (Eq. 4):

$$OD = dmax\left(\prod_{1}^{N} d_n\right)^{1/N} \qquad (4)$$

where *OD* is the overall desirability to be maximized, d_n is the desirability response function for each model equation in [0 – 1] scale and *N* is the number of desirability functions. The *OD* value is the output of applying the geometric mean to the *N* desirability functions which has the property that if any model equation is undesirable (d_n = 0), the overall desirability is also not satisfied (*OD*

= 0). After defining the different items that integrate the *desirability* code, an iteration process seeks for the best *OD* ending when the best condition maximizing the *OD* is found.

Statistical analyses

Statistical analyses of the different models were performed using R Software by means of the *car*, *MASS* and *faraway* packages. The quality of the regression of the model equations was evaluated by the coefficients R^2 and R^2_{adj}. The overall significance of the model was determined by analysis of variance (ANOVA) *F*-test whereas the significance of each coefficient was determined by the corresponding *t*-test. The lack-of-fit (LOF) test was used to evaluate differences between experimental and pure error of the models. Normality of the residuals was evaluated by means of the Shapiro-Wilk test whereas constant variance of the residuals was assessed by means of the Breusch-Pagan test.

Results

Media screening for cell growth and transfection efficiency

Four different serum-free commercially available media were selected for Hi5 cell culture in suspension [16,17]. All formulations tested (EX-CELL 405, Express Five SFM, Insect Xpress and Sf900III) are serum-free. The first three media contain hydrolysates to a certain extent whereas Sf900III is the only medium with low-hydrolysate content and animal origin-free compounds [18]. Nonetheless, the exact composition of the media is proprietary of the manufacturers. In preliminary experiments, cell growth of Hi5 cells in the different formulations was evaluated in batch culture (Fig. 1A). Unexpectedly, cells did not adapt to grow in Express Five SFM and therefore this medium was not included in further experiments. For all other media, cells maintained a high viability (> 90%) until 96h coinciding with maximum cell density. Insect Xpress medium supported the highest maximum cell concentration ($5.0 \pm 0.1 \times 10^6$ cells/mL) with a doubling time of 15.5 ± 0.4 h. Hi5 cells grew up to $4.5 \pm 0.3 \times 10^6$ cells/mL with a doubling time of 20.5 ± 0.5 h in Sf900III medium whereas $3.6 \pm 0.3 \times 10^6$ cells/mL and a doubling time of 17.8 ± 1.8 h was achieved in EX-CELL 405 medium.

Intracellular eGFP production upon transfection with the standard protocol was also studied through sampling every 24 h during 5 days. Transfection was performed with DNA and PEI pre-complexation in DPBS for 15 min. The percentage of eGFP positive cells peaked at 48 hpt in all media formulations, being highest in Sf900III (~35 %) while ~21 and ~23 % transfection was achieved in Insect Xpress and EX-CELL 405, respectively (Fig. 1C). The percentage of eGFP positive cells was maintained in Sf900III up to 96 hpt whereas it decreased in the other two media beyond 48 hpt.

Green fluorescent cells were visualized under confocal fluorescence microscoe at 48 hpt. Green fluorescence due to eGFP expression was observed in the cytoplasm of transfected cells (Fig. 1B). Then, the kinetics of eGFP expression upon transient transfection was evaluated by monitoring intra and extracellular fluorescence intensity at different times post-transfection. Maximum eGFP production was obtained in all media at 72 hpt, being the highest in Sf900III (~150 R.F.U) as shown in Fig. 1D. In contrast, lower production levels were reached both in Insect Xpress (~100 R.F.U) and EX-CELL 405 with ~60 R.F.U. Barely no eGFP expression was detected in the supernatant of the different media formulations until 96 hpt (Fig. 1E) and only low amounts were detected afterwards coinciding with the drop in cell viability. In this sense, protein leakage from death cells could explain the presence of eGFP in the supernatant which is supported by the decrease in intracellular eGFP from 96 hpt on. Distinct agitation conditions during transfection (80, 130, 150, 170 rpm) were also evaluated with no significant differences neither in the transfection percentage nor in eGFP production (data not shown).

Sf900III was the medium selected for further optimization experiments since it showed the best transfection and production levels and also good cell growth. Of note, this medium is devoid of animal-derived compounds and also has a low-hydrolysate content. These features contribute to diminish experimental variation due to lot-to-lot variability and makes it an interesting platform towards defining a robust bioprocess.

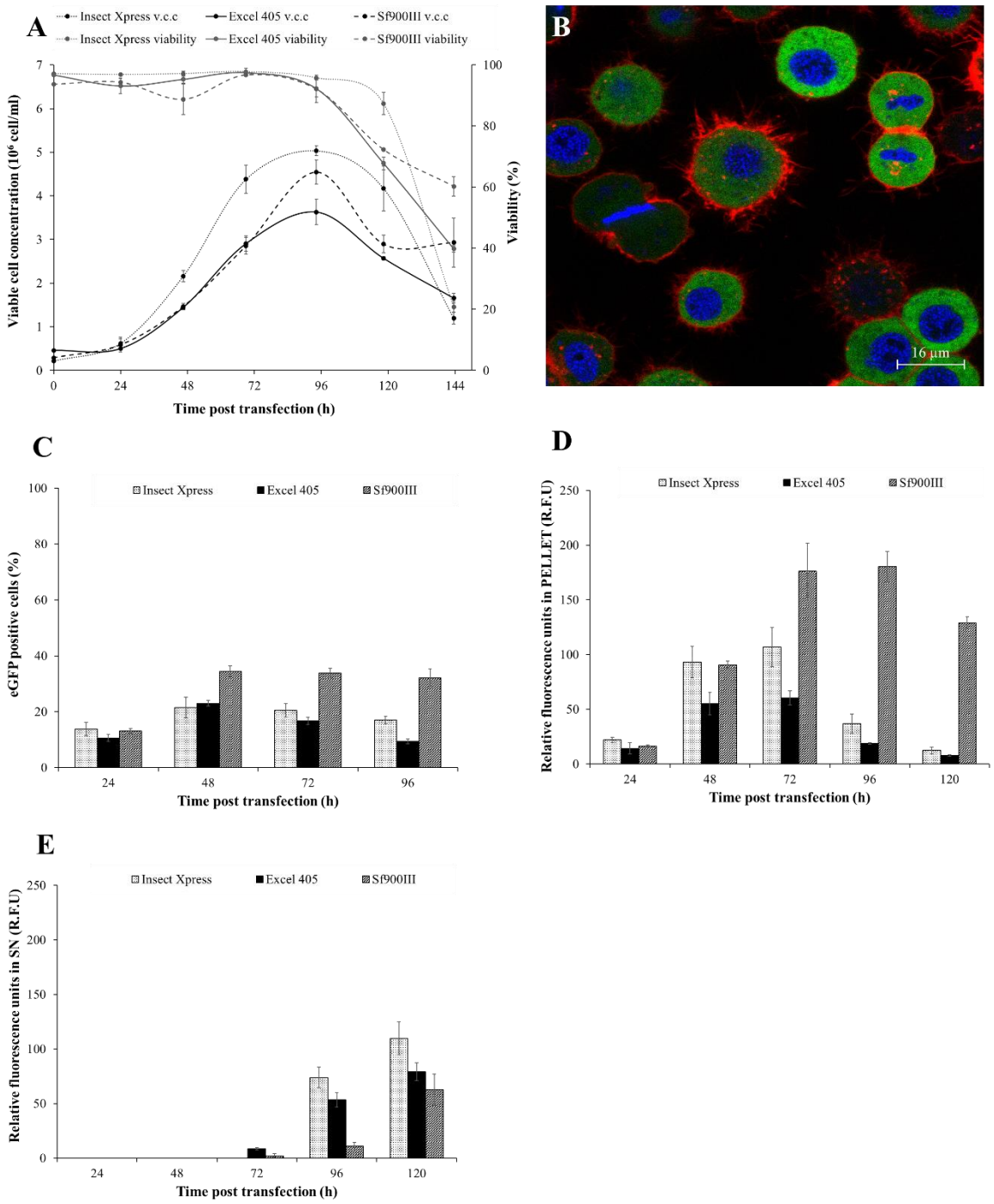

Figure 1. Growth and transfection kinetics of High Five cells in batch culture in different media. (A) Exponentially growing cells were seeded at 0.3 x 10^6 cells/mL in 125-mL flasks. Cell density and viability were determined every 24 h in each culture media. Mean values ± standard deviation of triplicate experiments are represented. (B) Confocal fluorescence microscopy image of Hi5 producer cells at 48 hpt. Cell nucleus was stained with Hoechst (blue) and membrane was stained with CellMask™ (red). Green fluorescence refers to the production of intracellular eGFP molecules. (C-E) Transfection and production of intracellular eGFP in different culture media. Exponentially growing cells were transfected at 1.0 x 10^6 cells/mL in 125-mL flasks. Hi5 cells transfection efficiency (C), intracellular eGFP production in pellet (D) and supernatant in relative fluorescence units (E) were measured. Mean values ± standard deviation of triplicate experiments are represented.

Size of Hi5 cells adapted to grow in Sf900III was measured under a confocal microscope resulting in a diameter of 16.3 ± 2.2 μm (50 cells were measured). This value was in good agreement with the results obtained by [19] for Hi5 cells adapted to Express Five medium (16.3 μm). Therefore, Hi5 cell size does not probably change in a significant manner with regards to the culture medium used.

Selection of the DNA:PEI complexing solution

Different solutions were investigated for Hi5 cells transient transfection according to their use as DNA:PEI complexing media [20,21]. These incubation solutions include 3 and 150 mM NaCl, DPBS, ultrapure water and the cell culture medium Sf900III. Cell transfection with previous DNA:PEI complexation in the different incubation solutions was performed according to the standard transfection protocol. Direct transfection without prior pre-complexation was also evaluated since it has been reported to be efficient in a variety of cell lines [22,23]. To this purpose, sequential addition of PEI followed by DNA was carried out since the opposite combination has shown little efficiency on transfection as described elsewhere [24]. Flow cytometry analysis showed comparable transfection efficiencies around 30 - 35% in 3 and 150 mM NaCl solutions and DPBS at 48 hpt, being the highest in 150 mM NaCl (Fig. 2A). Lower transfection efficiencies of ~20 - 25% were obtained with DNA:PEI complexes pre-formed in water and Sf900III medium whereas addition of PEI and DNA without prior pre-complexation resulted in the worst overall condition (~10%).

Assessment of eGFP expression at 72 hpt revealed that maximum eGFP production was obtained in the incubation solutions with the highest salt content (Fig. 2B). Conversely, smaller production levels where achieved both in 3 mM NaCl and ultrapure water while no pre-complexation of DNA and PEI showed the lowest production. Interestingly, there was no correlation between transient transfection efficiency and eGFP production. According to these results, 150 mM NaCl was selected as the DNA and PEI incubation solution since it showed the best transfection yield and a good production level of eGFP.

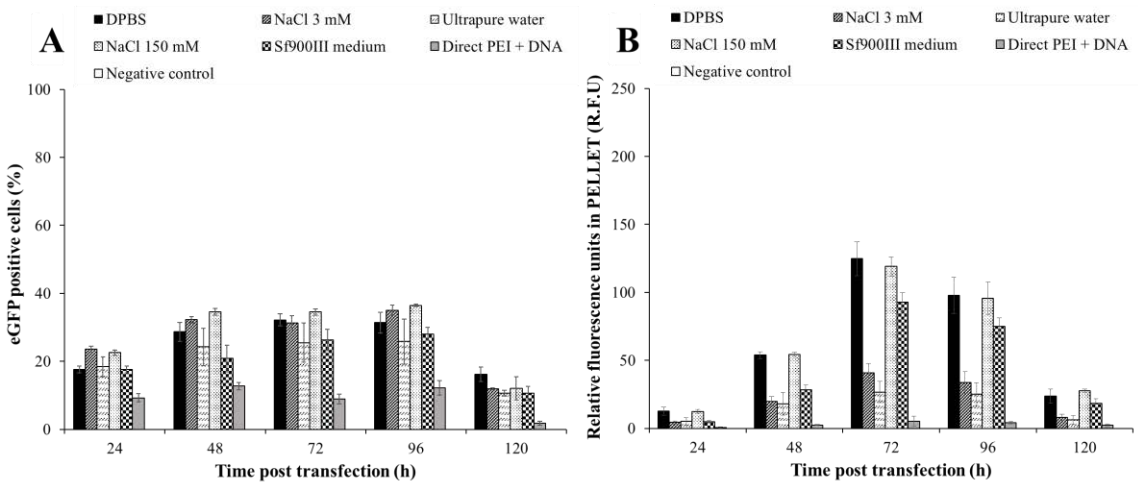

Figure 2. Transfection and eGFP production kinetics of High Five cells in batch culture in Sf900III medium with DNA:PEI complexes pre-formed in NaCl 3 and 150 mM, DPBS, Sf900III, ultrapure water and direct addition of PEI + DNA. (A) Hi5 cells transfection efficiency. Exponentially growing cells were transfected at 1.0 x 10^6 cells/mL in 125-mL flasks. (B) eGFP production in pellet in relative fluorescence units. A negative control consisting in DNA addition was also included. Mean values ± standard deviation of triplicate experiments are represented.

Characterization of DNA:PEI complexing process

DNA:PEI complexes pre-formed in the different incubation solutions were examined with DLS to better characterizing the nature of the species that mediated transfection and production in Hi5 cells. PEI and pIZTV5-eGFP solutions were mixed according to the standard transfection protocol in different complexing solutions: Sf900III medium, 3 and 150 mM NaCl, DPBS and ultrapure water. The whole population of complexes incubated in Sf900III, 150 mM NaCl and DPBS experienced a dynamic shift of increasing in size during the time period tested (Fig. 3A). Interestingly, similar aggregation patterns were observed between 150 mM NaCl and DPBS. Polyplexes incubated in 150 mM NaCl exhibited a higher polydispersity and grew up to 1 µm within 25 min whereas in DPBS this complex size was attained in 35 min. Polyplexes seemed to stabilize at size of approximately 1 µm since higher structures could not be efficiently tracked due to DLS equipment limitations. DNA:PEI complexes incubated in Sf900III medium revealed the coexistence of two populations where the smaller one decreased over time whilst the higher population increased (Figure S1). This would be mainly attributed to the aggregation of smaller polyplexes that triggered the formation of higher structures. On the contrary, a very slow

aggregation tendency was observed in ultrapure water and 3 mM NaCl. In both solutions, two different populations were encountered but no clear aggregation tendencies were observed in any of them over the studied time period. A smaller DNA:PEI complex population was clearly more abundant in these two solutions, stabilizing at 50-60 nm in 3 mM NaCl and at 60-70 nm in ultrapure water. The kilocounts per second (kcps) decreased over time in all the incubation solutions, especially in those with the highest salt content (Fig. 3B). Ultrapure water and 3mM NaCl solutions showed a faint decline in the kcps over time which was in agreement with DNA:PEI complex size stabilization previously described. This phenomenon could be in turn related either with an aggregation or precipitation process of DNA:PEI complexes but the latter was discarded since no sample precipitation was observed. Besides, 150 mM NaCl, Sf900III medium and to a lesser extent DPBS were the complexing solutions with highest kcps during the time range tested. Higher kcps values could be a consequence of an increase in either the number or size of DNA:PEI complexes or both. It could be then argued that bigger structures were present in 150 mM NaCl, Sf900III medium and DPBS but not ascertainment of also higher concentration of complexes could be made.

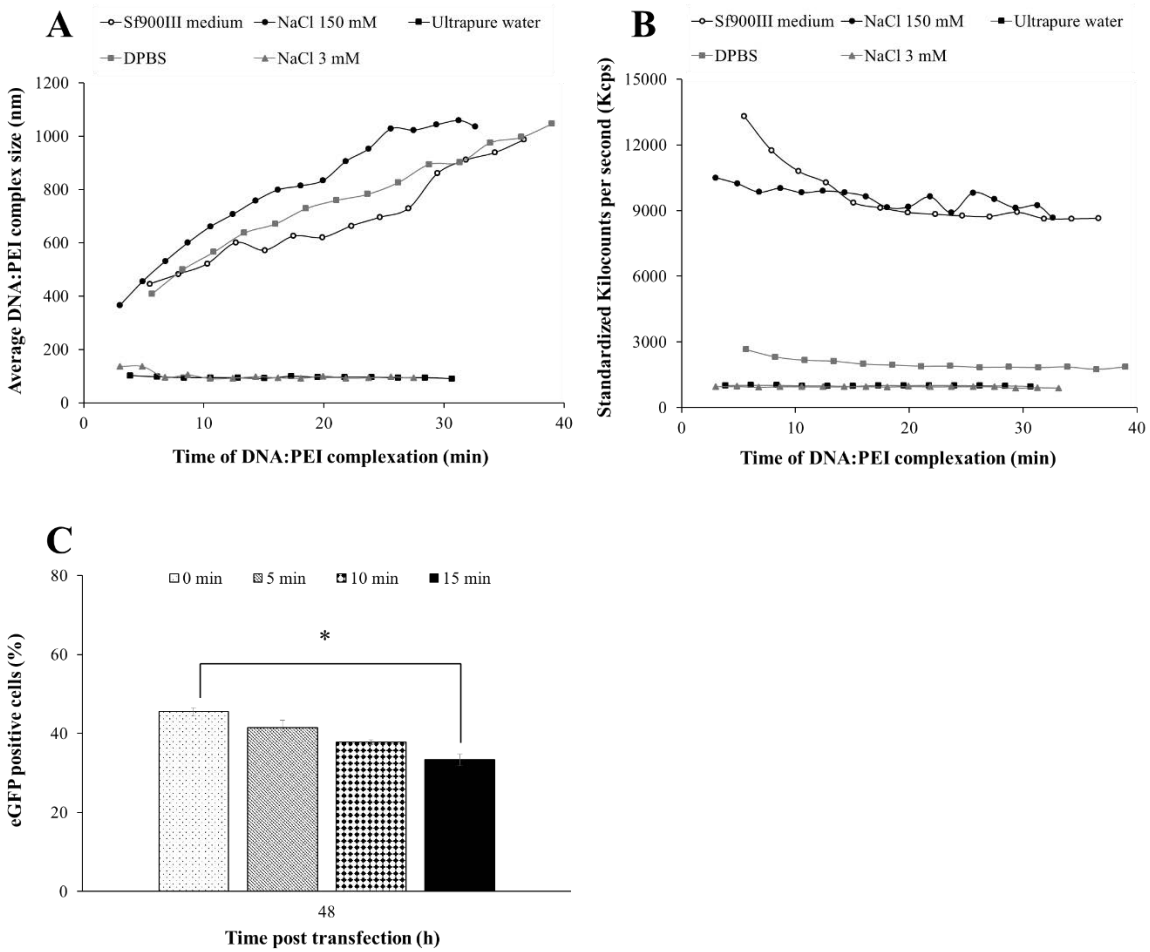

Figure 3. DNA:PEI complex kinetics in different solutions. (A-B) DLS measurement of mean DNA:PEI complex size (nm) and kilocounts per second (kcps) in NaCl 3 and 150 mM, ultrapure water, DPBS and Sf900III medium. (C) Hi5 cells transfection efficiency upon transfection with DNA:PEI complexes pre-formed in NaCl 150 mM during various incubation times. Mean values ± standard deviation of triplicate experiments are represented.

Addition of DNA to the different incubation solutions did not trigger any aggregation process, but 100-200 nm particle formation was observed in Sf900III (Figure S2). PEI addition triggered an aggregation process only in Sf900III medium, indicating PEI interactions with negatively charged medium compounds other than DNA. (Figure S3).

Morphology of DNA:PEI complexes in the different incubation solutions was also studied by means of Cryo-EM. Organization of DNA and PEI into particles was observed in all the incubation solutions (Fig. 4). These complexes appeared as black nearly round electron-dense structures which could be clearly identified in Sf900III medium, 150 mM NaCl and DPBS. In these solutions, DNA:PEI polyplexes seem to be formed by the aggregation of smaller pieces of complexes of around 200-400 nm and grew up to > 1 µm structures. Otherwise, DNA:PEI

complexes smaller than 100 nm were observed both in ultrapure water and 3 mM NaCl (Fig. 4C-D). In these two solutions, small complexes were accompanied by bigger less dense stains that could be related to unbound DNA as compared to DNA control samples (Figure S4). Moreover, PEI addition to each incubation solution did not unleash particle formation except for Sf900III medium which is in agreement with the results obtained with DLS (Figure S5).

DNA and PEI complex formation kinetics uncovered that incubation time between the two species could influence the transfection of Hi5 cells. To value this, a transfection experiment with DNA:PEI complexes pre-formed in 150 mM NaCl during different incubation times (< 1, 5, 10 and 15 min) was performed. A staggered increase in transfection was achieved as the incubation time between DNA and PEI decreased which corresponded to small DNA:PEI polyplexes (Fig. 3C). Smaller DNA:PEI complexes up to 300 – 400 nm were observed during < 1 min incubation compared to DNA:PEI complexes incubated during 15 min (Fig. 4E-F).

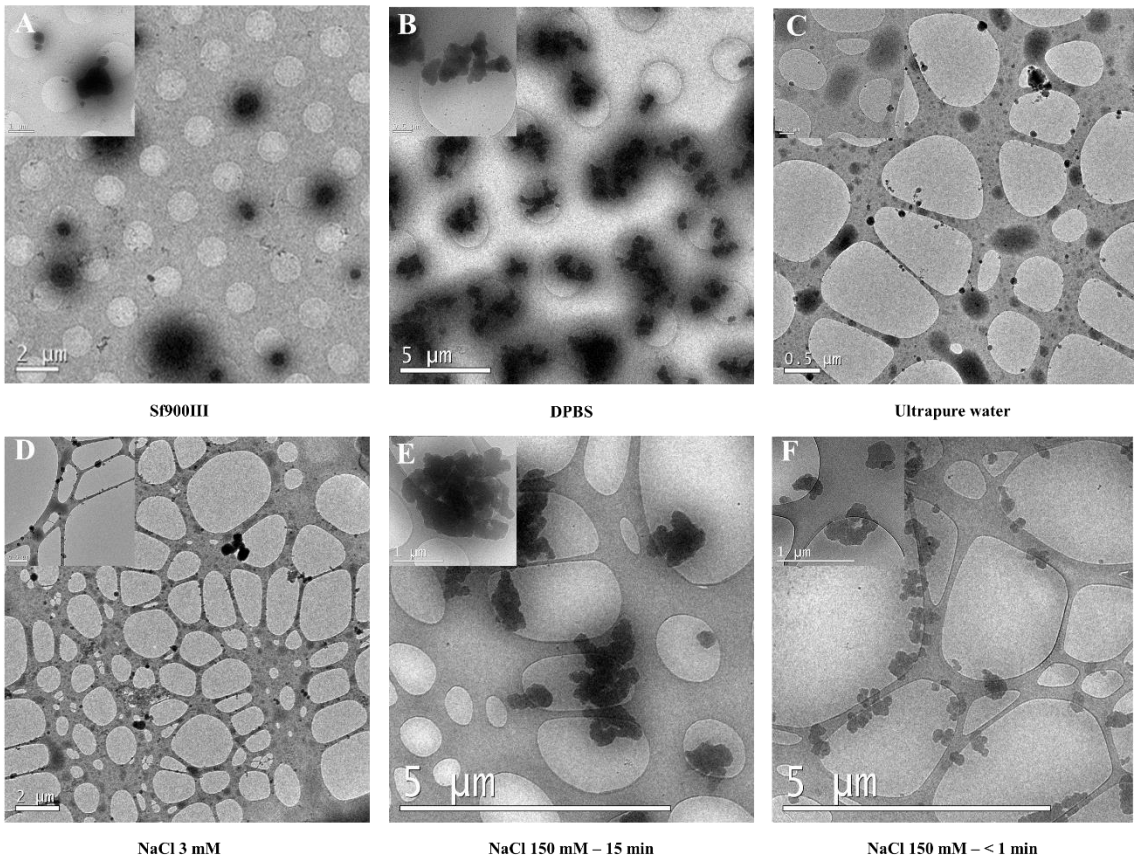

Figure 4. Cryo-electron microscopy images of DNA:PEI complexes in different incubation solutions. (A-E) DNA:PEI complexes incubated during 15 min in Sf900III, DPBS, ultrapure water, NaCl 3 mM and NaCl 150 mM, respectively. (F) DNA:PEI complexes incubated in NaCl 150 mM and subsequently added to cell culture (< 1 min).

Optimization of transient eGFP production by DoE

Different variables affecting the transfection of Hi5 cells were evaluated in the previous sections in order to diminish the number of parameters to be evaluated by means of more elaborated statistical techniques. DNA, PEI and cell concentration at the time of transfection were selected as the most influencing variables on eGFP transfection and production as previously reported for other cell lines [25,26]. To this purpose, a DoE-based approach was used to achieve an optimum condition with a reduced number of experiments in a reasonable time.

Additionally, variability caused by nuisance factors within the same experiment and between different experiments was carefully considered. As an illustration of this phenomenon, it was observed that a high cell passage number of >30 after thawing entailed a decrease of about 10-20% in transfection of Hi5 cells (data not shown) which could interfere with the interpretation of the relevant variables. As a consequence, the cell age window was carefully monitored in all

experiments, assuring that cells were not cultured beyond 20 passages. Similar performances were also reported in [27]. Of note, different Sf900III medium lots and distinct PEI 25 kDa stocks were used along the experimentation phase without relevant variation in the outcomes.

Response surface methodology and experimental space boundaries

A three-factor, three-level Box-Behnken design was selected to optimize DNA, PEI and cell concentration at transfection as it is an efficient methodology regarding the number of experimental runs to be performed and the statistically relevant information that can be obtained [28]. The range for cell concentration was chosen according to the cell growth exponential phase of Hi5 cells in Sf900III medium whereas DNA concentration was selected based on literature [29,30]. In the case of PEI, concentration ranges were picked based on empirical toxicity assays (Figure S6). Since PEI had a toxicity effect on cells, the upper limit was set at 11 µg/mL and the lower at 5 µg/mL. Working ranges for each variable at different levels -1, 0 and +1 are presented in Table 1.

Box-Behnken design matrix consisted in 15 experiments in which the central point was triplicated to account for the pure experimental error. Cells seeded at 0.3 x 10^6 cell/mL were amplified during 48 h and then subjected to a medium exchange to fresh Sf900III medium prior to transfection with 1 mL of DNA:PEI complexes minimally incubated (< 1 min) in 150 mM NaCl. Specific production (R.F.U/10^6 cell), transient transfection (% of eGFP positive cells) and viability (% of viable cells) were evaluated as responses in this study (Table 1). The data were fitted to a second-order polynomial model by the least squares method and a different model was obtained for each one of the response variables based on Eq. 2. The statistical significance of each model equation was confirmed by ANOVA analysis as depicted in Table 1. Model equation were subjected to a refinement process to eliminate non-statistically significant terms (NS) based on the hierarchy principle [31].

Three-dimensional plots were built according to model equations in order to detect synergies between DNA, PEI and viable cell concentration (Fig. 5A-I). Noticeably, the three independent variables had a strong influence on specific production being viable cell concentration at

transfection the most relevant one (Table 1). In all cases, DNA, PEI and cell concentrations close to the space boundaries of the design revealed a decreased outcome in terms of eGFP specific production. Hi5 cells transfected at mid concentration (level = 0) showed the highest production rate. In this sense, the optimum condition maximizing specific production for the three variables was located in the central region of the design space (Fig. 5A-C) which corresponded to 2.3 µg/mL of DNA, 8.1 µg/mL of PEI and 2.1 x 10^6 cell/mL at the time of transfection.

A different behavior was observed regarding transient transfection efficiency, being viable cell concentration the most significant variable and to a lesser extend DNA and PEI concentrations (Fig. 5D-F). In fact, the lower the cell concentration the higher the transfection efficiency, which was more pronounced with low amounts of DNA and high concentrations of PEI (Fig 5D). A statistically significant interaction between cell and DNA concentration was identified (*p*-value = 0.013, see Table 1) and indications of a possible interaction between DNA and PEI were also encountered. Also, high DNA concentrations did not trigger efficient Hi5 cell transfection with any PEI combination tested probably due to an imbalance in DNA:PEI complex formation (Fig. 5F). Then, the optimum condition maximizing transient transfection was found as 1 µg/mL of DNA, 11 µg/mL of PEI and 1 x 10^6 cell/mL at the time of transfection.

The effect of DNA, PEI and cell concentration on culture viability was also monitored to better understand cell state at the time of harvest. Viable cell concentration at the time of transfection was the most influencing variable whereas PEI and DNA concentration had little and no effect, respectively. Cells transfected at a higher concentration showed an earlier decline in cell viability when compared to Hi5 cells transfected at a low concentration (Fig. 5G-I). Interestingly, high PEI concentrations within the design range exhibited a slight beneficial effect on viability of high concentrated cells. This could be attributed to better transfection efficiencies obtained at high PEI concentrations with a reduced growth rate of transfected cells compared to non-transfected cells. On the contrary, DNA concentration did not impact on cell viability as observed in Fig. 5G-I where DNA concentration increases from 1 to 3 µg/mL and viability remained unchanged. In this case, the optimum for DNA, PEI and cell concentration was 1 µg/mL of DNA, 5 µg/mL of PEI and 1 x 10^6 cell/mL.

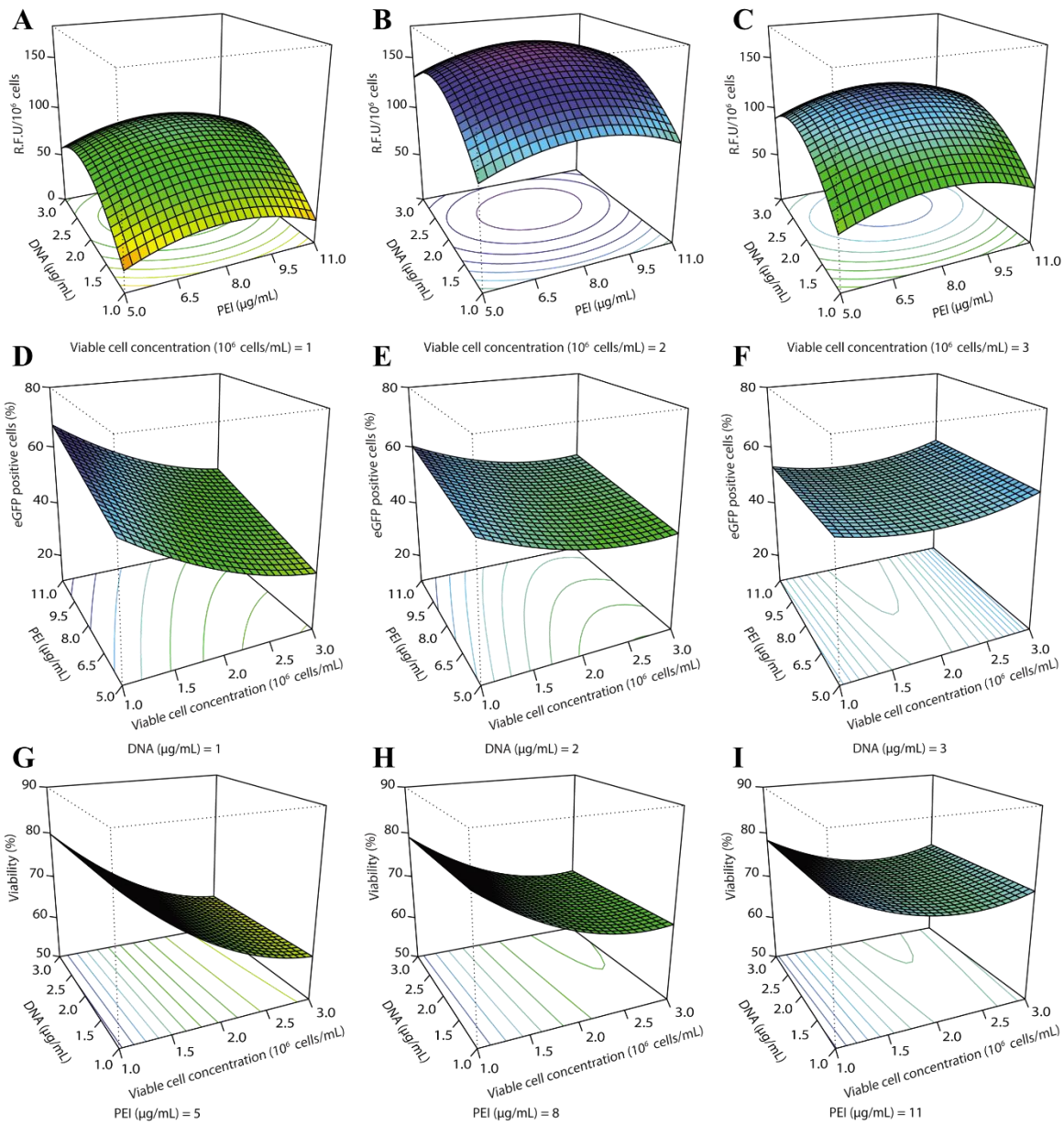

Figure 5. Response surface graphs based on Box-Behnken experimental results. (A-C) Specific production of cell culture lysates as a function of DNA, PEI and viable cell concentration at 72 hpt. (D-F) Percentage of eGFP positive cells as a function of DNA, PEI and viable cell concentration at 48 hpt. (G-I) Cell culture viabilities as a function of DNA, PEI and viable cell concentration of DNA, PEI and viable cell concentration at 72 hpt. The three-dimensional graphs were constructed by depicting two variables at a time and maintaining the third one at a fixed level.

Multiple response optimization with desirability functions

The assessment of Hi5 cells transient transfection by means of monitoring several responses yielded different optimal conditions in each of the model equations. The purpose was to obtain an overall transfection condition integrating the different responses in order to avoid situations involving high transfection efficiencies but low productivities or vice versa. To do this, a weighted-based modelling approach of the three responses consisting in the application of desirability functions was implemented. Weight assignation to the responses (s – value) was performed according to the priority given to each of the modelled equations. In this regard, preference was assigned to the percentage of transfection (s = 2) and specific production (s = 1.5) whilst cell viability at harvest time was considered as easily to be accomplished (s = 1). The transformed d_n responses were then combined in a unique overall desirability (*OD*) function and the best condition maximizing *OD* was found by applying Eq. 4. The combination of the three responses resulted in 2.1 µg/mL of DNA, 9.3 µg/mL of PEI and 1.5 x 10^6 cell/mL as the global optimum condition with an *OD* score of 0.47. A sensitivity analysis was also performed by changing the *s* values of the different equations resulting in very similar optimum conditions that confirmed the robustness of the calculation (data not shown).

Validation of the optimized model

A confirmation experiment was carried out to corroborate the optimal condition predicted by the combination of RSM and desirability functions (Fig. 6). Under these conditions, the experimental output was a maximum eGFP production of 5.8 ± 0.5 mg/L and 58.1 ± 0.9 % transfection which was within the calculated prediction interval of the overall optimum (Table 2). Cell culture viability was 80.6 ± 0.6 % at the time of maximum production (72 hpt) in good agreement with model prediction (Fig. 6A). eGFP specific productivity was calculated as 0.8 ± 0.1 µg/10^6 transfected cell·day in the optimal condition.

Table 2. Experimental validation of the optimal condition and comparison to model predictions.

Response	Experimental	Model prediction
eGFP positive cells (%)	58.1 ± 0.9	52.0 ± 10
Specific production (mg/L)	5.5 ± 0.5	6.0 ± 0.8
Viability (%)	80.6 ± 0.6	73.2 ± 10.2

Comparison between Hi5 and HEK293SF transient gene expression

Finally, the optimal transfection condition was compared to the optimum obtained in a previous work with mammalian HEK293SF cells [30], a stablished cell line for protein production by means of TGE [27,29]. Maximum Hi5 viable cell concentration and transfection (~60%) was achieved at 48 hpt whereas HEK293SF cells did between 72-96 hpt (~70%). The same trend was observed for maximum eGFP production, in this case 72 and 96 hpt for Hi5 and HEK293SF cell lines, respectively (Fig. 6C). In these conditions, HEK293SF cells yielded a maximum eGFP production of 4.3 ± 0.4 mg/L.

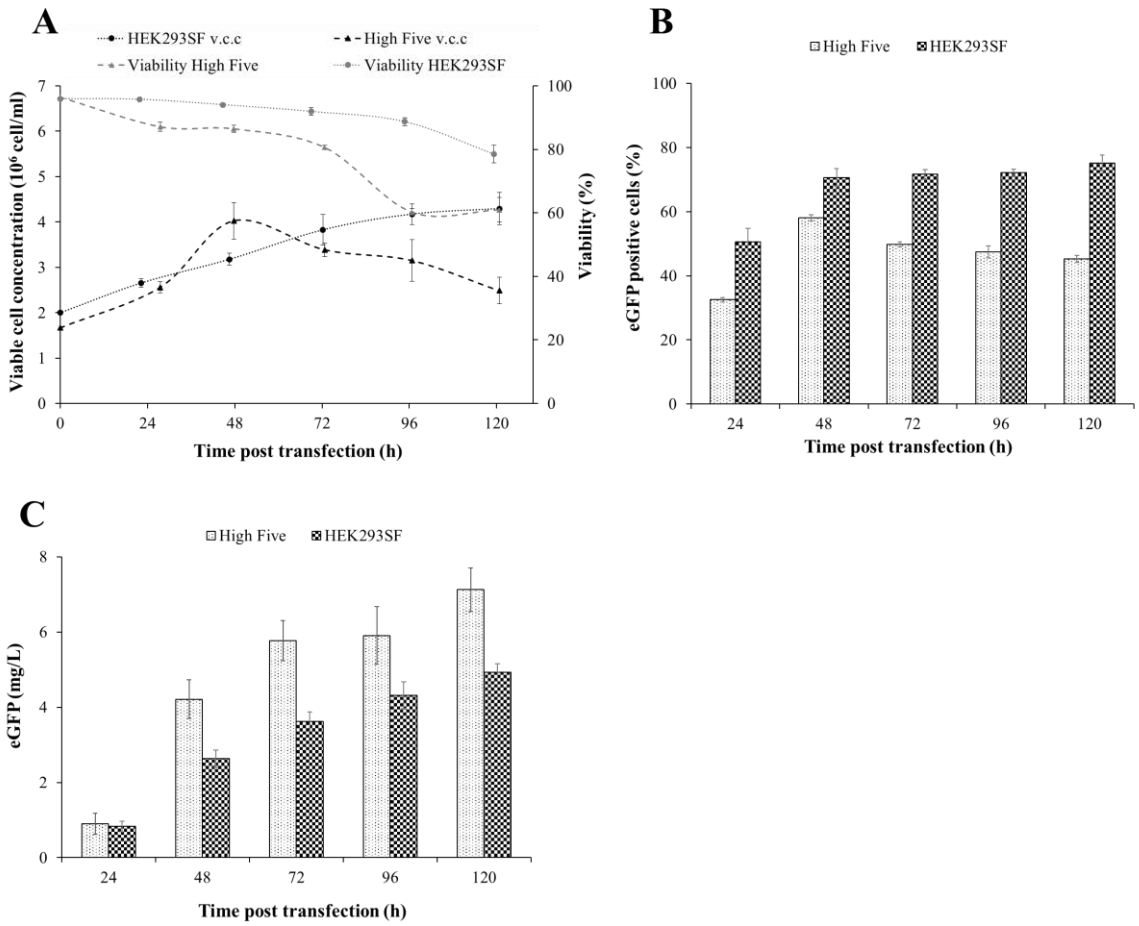

Figure 6. Model validation and comparison to HEK293SF cell line. (A) Cell growth of Hi5 and HEK293SF cell lines transfected at their optima, respectively. (B) C Percentage of eGFP positive cells. (C) Intracellular eGFP concentration in cell culture pellets. Cell density, viability, % eGFP positive cells and eGFP production were measured daily. Mean values ± standard deviation of triplicate experiments are represented.

Production of different recombinant products

The optimal transfection condition obtained based on the combination of DoE and desirability functions was used in the production of diverse recombinant products besides eGFP, including hSEAP and GageGFP. Maximal viable cell concentration was achieved at 48 hpt for hSEAP while Hi5 cells peaked at 72 hpt regarding GageGFP production (Fig. 7).

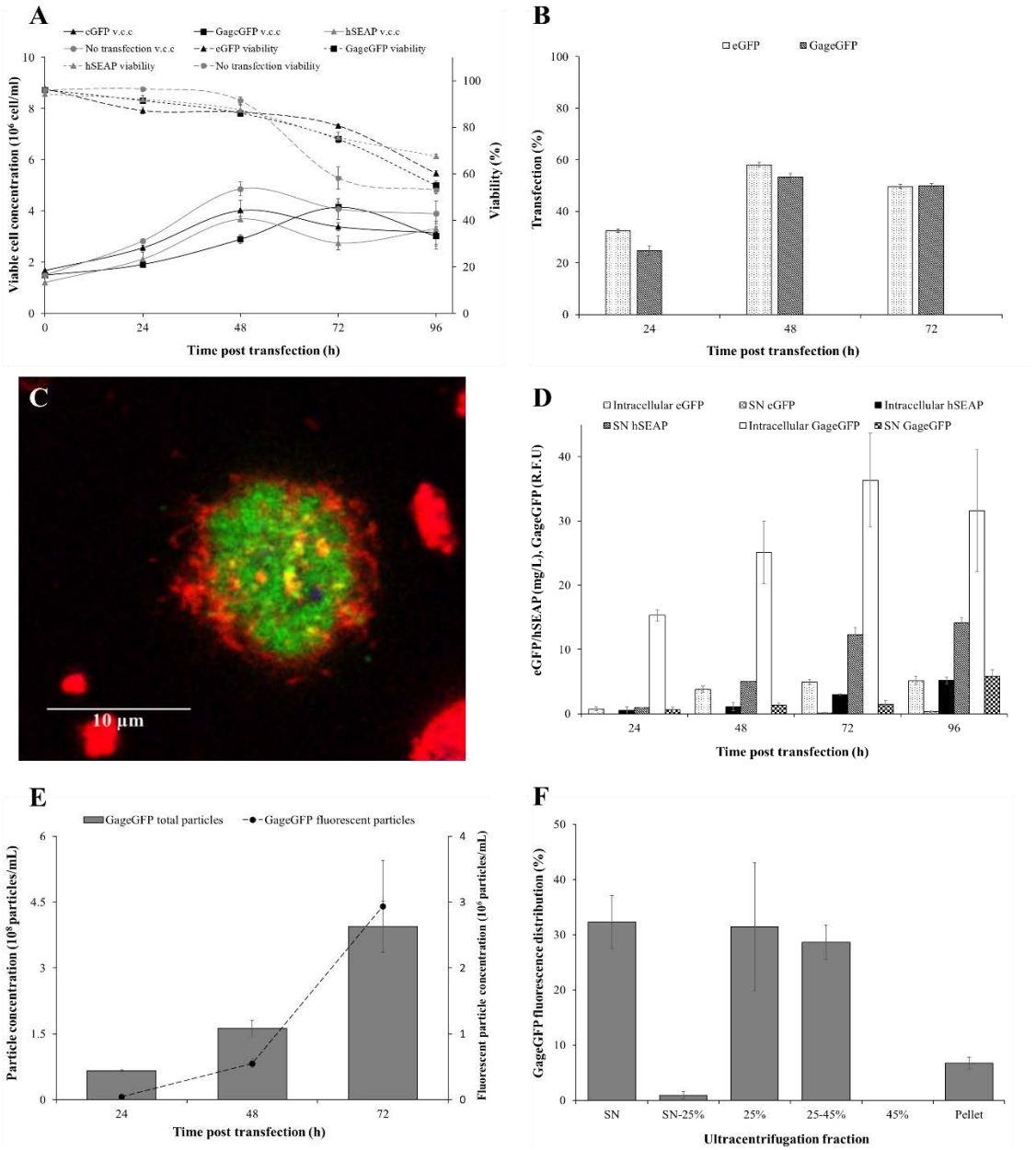

Figure 7. Production of eGFP, hSEAP and GageGFP in Hi5 cells using TGE. (A - B) Cell growth, viability and transfection kinetics. Exponentially growing cells were transfected at 1.5 x 10^6 cells/mL. (C) Confocal microscopy image of Hi5 cells transfected with pIZTV5-GageGFP. Cell membrane was stained with CellMask™ (red) and cell nucleus with Hoechst (blue). Percentage of eGFP positive cells. (D) Intra and extracellular production levels of different recombinant products. (E) GageGFP nanoparticle production kinetics quantification by flow virometry. (F) GageGFP fluorescence distribution in the different fractions after ultracentrifugation.

The fusion of eGFP allowed to detect the interaction of GageGFP with the transfected Hi5 cell membrane using confocal microscopy (Fig. 7C). These regions appeared as yellow dots arising from the colocalization of GageGFP (green) with the lipid bilayer stained with CellMask™ (red). The highest hSEAP concentration was attained at 72 hpt (15.3 ± 1.3 mg/L), with most of the protein secreted to the supernatant. Similarly, a maximal GageGFP production of 37.8 ± 7.9

R.F.U. was obtained at 72 hpt. A remarkable proportion of the GageGFP produced remained intracellularly and never budded from the cells (Fig. 7D).

A more comprehensive analysis was performed by means of flow virometry. Using this technique, the nanoparticle production kinetics could be directly tracked in GageGFP supernatants (Fig. 7E). The highest number of GageGFP VLPs was attained at 72 hpt, coinciding with the fluorescence peak measured by spectrofluorometry. In these conditions, nanoparticle quantification using NTA resulted in a maximum concentration of $3.6 \pm 1.0 \times 10^8$ fluorescent particle/mL (Table 3).

Table 3. GageGFP production in harvested supernatants and cell lysates at 72 hpt using different quantification methodologies.

Quantification method	Fluorescent particles/mL	Total particles/ mL	Supernatant	Intracellular
NTA (particles/mL)	$3.6 \pm 1.0 \cdot 10^8$	$2.4 \pm 0.3 \cdot 10^{11}$	-	-
Flow virometry (particles/mL)	$2.9 \pm 0.7 \cdot 10^6$	$4.0 \pm 0.6 \cdot 10^8$	-	-
ELISA (ng/mL)	-	-	10.0	238.4
Fluorometry (R.F.U.)	$1.4 \pm 0.6 \cdot 10^{8a}$	-	1.5 ± 0.6	36.3 ± 7.3

[a]This is the resulting value of correlating R.F.U. to VLP concentration (eq. 2)

The optimal harvesting condition for GageGFP VLP production was analyzed by analytical ultracentrifugation aiming to assess the VLP assembling efficiency of Hi5 cells (Fig. 7F). Around 60 % of the fluorescence in the supernatant was attributed to VLPs (25 %, 25 – 45 %, 45 %) while the rest was associated to non-assembled GageGFP monomer (SN and SN – 25 %) and cell debris (Pellet). Considering that 60 % of the fluorescence in the supernatant corresponded to VLPs, the number of GageGFP VLPs was calculated as $1.4 \pm 0.6 \times 10^8$ fluorescent particle/mL based on Eq. 2, in agreement with the NTA quantification (Table 3).

Discussion

The development of production strategies in insect cells devoid of baculovirus is gaining increasing interest. Transient gene expression has been successfully used for the expression of a

variety of proteins in different mammalian cell lines [9]. Among the available transfection methodologies, liposome-based reagents or electroporation methods do not guarantee the scalability or cost efficiency of the process and have been gradually relegated to the generation of stable cell lines [7]. In this regard, affordable transfection carriers such as polyethylenimine have become the gold standard for transient transfection purposes.

Recently, some publications have addressed PEI-based transient transfection in Hi5 cells reaching ~150 mg/L of TNFR:Fc [12] and ~120 mg/L Fab fragment [13] with specific productivities ranging from 7.1 to 8.7 μg/10^6 transfected cell·day, respectively. Difficulties were found to compare existing transfection methodologies since the output considerably depends on the target recombinant protein, plasmid promoter, codon-optimization, enhancer regions and post-regulatory elements [32,33]. For example, a 10-fold difference in specific productivity is observed for the production of TNFR:Fc (3.5 μg/10^6 transfected cell·day) and eGFP (0.3 μg /10^6 transfected cell·day) in the same host [24,34]. In this regard, differences in specific productivity of the system here presented with the aforementioned publications could be attributed to the expression of different proteins. Interestingly, a 2-fold increase in specific productivity was achieved in this system in comparison to the most recent published transient eGFP production in Sf9 insect cells [34,35]. Also, 1.3-fold overall eGFP production was obtained compared to HEK293SF cells, a 2.3-fold increase in specific productivity considering the optimal harvest time for each cell line (0.4 μg/10^6 transfected cell·day). The TGE method here proposed resulted in more than 20-fold increase in eGFP specific productivity compared to Hi5 cell with the BEVS [36], but a 5-fold decrease as regards Sf9 baculovirus production [8]. In the case of hSEAP, 1.9 ± 0.2 μg/10^6 transfected cell·day were attained under the optimal production conditions, a 1.7-fold increase in specific productivity compared to PEI mediated TGE in Sf9 cells. The overall hSEAP production here reported (15 ± 1.3 mg/L) is similar to the 12.9 mg/L [37] and 3.9-fold lower [38] for baculovirus infected Hi5 cells, respectively.

The complexity associated to the production of GageGFP VLPs could be appreciated in comparison to the eGFP protein. A total of 37.8 ± 7.9 R.F.U. were achieved for GageGFP whereas 322.2 ± 25.8 R.F.U. were produced for eGFP, representing an 8.5-fold increase in fluorescent

protein production. The different production levels obtained for these two different recombinant products indicate that protein complexity is highly influential in the final protein outcome. Similar results were reported in the HEK 293 mammalian cell line when comparing the production of simple reporter proteins to complex nanoparticles [39].

Existing PEI-based TGE methods of Hi5 cells use animal-compound and high-hydrolysate content culture media that could entail several limitations in terms of reproducibility and standardization in the production of biologicals [12]. Thereof, the properties of DNA:PEI complexes could be subjected to lot-to-lot variations in the culture media which would compromise the applicability of this system. This variability hinders the appropriate characterization of TGE in insect cells and consequently many variables influencing transfection remain undefined. Here, the use of an animal origin-free and low-hydrolysate containing medium favoured to better understand the synergies between several variables affecting TGE and should also contribute to develop more reproducible bioprocessing methodologies.

Dynamic light scattering and cryo-electron microscopy were used to determine several properties of DNA and PEI complexing process. In general lines, DLS provided information about the mean size of DNA:PEI complexes and the co-existence of more than one population. Polyplexes pre-formed in Sf900III, 150 mM NaCl and DPBS showed a mean size population increase with longer incubation times between DNA and PEI. On the contrary, DNA and PEI incubation in ultrapure water and 3 mM NaCl did not trigger any aggregation process during time period tested. The latter confirmed that the presence of salt in the incubation solutions enhanced the aggregation of DNA and PEI [40]. Furthermore, smaller polyplexes present in the incubation solutions with lower salt content (ultrapure water and 3 mM NaCl) displayed similar transfection efficiencies to those pre-formed in the solutions with higher salt content (Sf900III, 150 mM NaCl and DPBS). This unveiled that small DNA:PEI polyplexes were the ones governing efficient transfection of Hi5 cells, similarly to recent evidences found in other cell types [21].

Interestingly, there was no correlation between transient transfection efficiency and eGFP production. For instance, DNA:PEI complex formation in 3 mM NaCl showed a similar transfection efficiency compared to 150 mM NaCl but approximately only one third of the

production in 150 mM NaCl was achieved in the former. The opposite occurred with DNA:PEI complex formation in Sf900III, where a smaller transfection efficiency compared to 3 mM NaCl was obtained but more than 2-fold eGFP production was reached. This could be attributed to a better condensing capability of DNA in complexes pre-formed in higher salt-containing solutions compared to the small complexes obtained in low salt conditions. The former could probably load more DNA and boost the production of eGFP which could be evidenced with higher fluorescence intensities of transfected cells. In this sense, salt content in the solution of DNA and PEI polyplex formation was revealed as an important variable strongly influencing protein expression.

Cryo-EM helped to gain insight into the morphology of these particles considering recent studies highlighting the relevance of this property in DNA and drug delivery approaches [41,42]. The advantage of using Cryo-EM was the visualization of different structure typologies and particle assemblies in aqueous solution that is generally the natural occurring process. In fact, other systems like Scanning or Transmission Electron Microscopy involve a sample pre-treatment with either drying or staining that may complicate the resolution of the specimen under evaluation. Cryo-EM revealed the presence of polyplexes higher than 1 µm which could not be efficiently detected by DLS and also confirmed the existence of diverse DNA:PEI complex populations in the different incubation solutions tested. These results differ from previous reported observations [43] where DNA:PEI complexes structures higher than 1 µm could not be described in detail.

Optimization of viable cell concentration at time of transfection, DNA and PEI concentrations was performed by means of a DoE-based approach, a methodology that enables to achieve an optimal condition with a reduced number of experiments in a reasonable time [23,28]. These three variables were used to monitor and model the three responses under consideration obtaining different optimal conditions. In fact, low cell concentrations improved the transfection yield whereas specific protein production increased at high cell concentrations. Strategies involving graphical optimization and the application of desirability functions were firstly considered towards the obtaining of a global optimal condition. Graphical optimization is a tedious methodology when more than two responses are to be optimized [44], consequently the mathematical-based approach on desirability functions was finally selected [45]. This technique

consisted in transforming each model equation to a dimensionless desirability scale d_n ranging from zero (undesirable response) to one (optimal response) as depicted in Eq. 3. Besides, each equation was given a weight (*s* value) according to the importance of each response. Low *s* values made the equation to more easily satisfy desirability maximization whereas large *s* values narrowed the possible responses satisfying this criterion. The transformed d_n responses were then combined in a unique overall desirability (*OD*) function and the best condition maximizing *OD* was found by applying Eq. 4. Of note, the target of this optimization procedure was to find the best condition but not to get an *OD* = 1 since the latter is completely dependent on the shape of the responses and space boundaries [46]. Similar approaches combining the use of DoE and desirability functions were found [47,48] but here we demonstrate that this methodology is also applicable in a license-free software environment.

In conclusion, a robust and reproducible baculovirus-free transient gene expression methodology of Hi5 cells is presented. Characterization of DNA:PEI complexes by means of Cryo-EM and DLS techniques revealed that up to 300-400 nm size polyplexes were the most efficient in transfecting Hi5 cell line. Also, DNA:PEI complex formation in 150 mM NaCl under minimal complexing time (< 1 min) was proven as the best transfection and production condition. An optimal transfection condition was achieved by means of combining RSM and desirability functions which represents the first study dealing with multi-parametric optimization in TGE. The developed Hi5 cell line TGE protocol provides an alternative to mammalian cell lines to rapidly screen a wide variety of recombinant proteins within 3 days of transfection. Future efforts towards scale-up of this process should allow the development of a rapid, efficient and flexible protein production platform for therapeutic, diagnostic or structural biology purposes.

Acknowledgments

The authors would like to thank Dr. Paula Alves (Instituto de Biologia Experimental e Tecnológica, Oeiras, Portugal) for providing the BTI-TN-5B1-4 cell line and pITV5-eGFP plasmid vector. We would also like to thank Jorge Fomaro and Ángel Calvache (Beckman Coulter) for ceding the CytoFelx LX flow cytometer. We appreciate the support of Martí de Cabo,

Mónica Roldán and Nuria Barba from Servei de Microscòpia of UAB for his support with the cryo-EM and confocal microscopy, respectively. The help of Llorenç Badiella (Servei d'Estadística Aplicada, UAB) in developing the R code and on statistical analysis is also acknowledged. The help of José Amable Bernabé (Institut de Ciència de Materials de Barcelona, CSIC), Manuela Costa (Servei de Cultius Cel·lulars, Producció d'Anticossos i Citometria, UAB) and Dr. Salvador Bartolomé (Departament de Bioquímica i de Biologia Molecular, UAB) for the assistance with DLS, cytometry and fluorometry, respectively, are also appreciated. The support of Sahar Masoumeh in ELISA quantification is also appreciated. Eduard Puente-Massaguer is a recipient of an FPU grant from Ministerio de Educación, Cultura y Deporte of Spain (FPU15/03577). The research group is recognized as 2017 SGR 898 by Generalitat de Catalunya.

Compliance with Ethical Standards

Conflict of interest

The authors declare that they have no competing interests.

Ethical approval

This article does not contain any studies with human participants performed by any of the authors.

References

[1] G. Walsh, R. Jefferis, Post-translational modifications in the context of therapeutic proteins, Nat. Biotechnol. 24 (2006) 1241–1252.

[2] F. Fernandes, A.P. Teixeira, N. Carinhas, M.J.T. Carrondo, P.M. Alves, Insect cells as a production platform of complex virus-like particles., Expert Rev. Vaccines. 12 (2013) 225–36.

[3] S. Roest, S. Kapps-Fouthier, J. Klopp, S. Rieffel, B. Gerhartz, B. Shrestha, Transfection of insect cell in suspension for efficient baculovirus generation, MethodsX. 3 (2016) 371–377.

[4] F. Liu, X. Wu, L. Li, Z. Liu, Z. Wang, Use of baculovirus expression system for generation of virus-like particles: Successes and challenges, Protein Expr. Purif. 90 (2013) 104–116.

[5] N. Clément, J.C. Grieger, Manufacturing of recombinant adeno-associated viral vectors for clinical trials, Mol. Ther. - Methods Clin. Dev. 3 (2016) 16002.

[6] Z. Shoja, M. Tagliamonte, S. Jalilvand, Y. Mollaei-Kandelous, A. De stradis, M.L. Tornesello, F. M. Buonaguro, L. Buonaguro, Formation of Self-Assembled Triple-Layered Rotavirus-Like Particles (tlRLPs) by Constitutive Co-Expression of VP2, VP6, and VP7 in Stably Transfected High-Five Insect Cell Lines, J. Med. Virol. 87 (2015) 102–111.

[7] J. Vidigal, B. Fernandes, M.M. Dias, M. Patrone, A. Roldão, M.J.T. Carrondo, P.M. Alves, A.P. Teixeira, RMCE-based insect cell platform to produce membrane proteins captured on HIV-1 Gag virus-like particles, Appl. Microbiol. Biotechnol. 102 (2018) 655–666.

[8] F. Fernandes, J. Vidigal, M.M. Dias, K.L.J. Prather, A.S. Coroadinha, A.P. Teixeira, P.M. Alves, Flipase-mediated cassette exchange in Sf9 insect cells for stable gene expression, Biotechnol. Bioeng. 109 (2012) 2836–2844.

[9] S. Gutierrez-Granados, L. Cervera, A.A. Kamen, F. Godia, Advancements in mammalian cell transient gene expression (TGE) technology for accelerated production of biologics., Crit. Rev. Biotechnol. 0 (2018) 1–23.

[10] P. Royl, Transient expression in insect cells using a recombinant baculovirus synthesising

bacteriophage T7 RNA polymerase, Nucleic Acids Res. 23 (1995) 188–191.

[11] M. Lu, R.R. Johnson, K. Iatrou, Trans-activation of a cell housekeeping gene promoter by the IE1 gene product of baculoviruses, Virology. 218 (1996) 103–113.

[12] X. Shen, A.K. Pitol, V. Bachmann, D.L. Hacker, L. Baldi, F.M. Wurm, A simple plasmid-based transient gene expression method using High Five cells, J. Biotechnol. 216 (2015) 67–75.

[13] K. Mori, H. Hamada, T. Ogawa, Y. Ohmuro-matsuyama, T. Katsuda, H. Yamaji, Efficient production of antibody Fab fragment by transient gene expression in insect cells, J. Biosci. Bioeng. 124 (2017) 221–226.

[14] S. Gutiérrez-Granados, L. Cervera, F. Gòdia, J. Carrillo, M.M. Segura, Development and validation of a quantitation assay for fluorescently tagged HIV-1 virus-like particles, J. Virol. Methods. 193 (2013) 85–95.

[15] S. Kuhnt, N. Rudak, Simultaneous Optimization of Multiple Responses with the R Package JOP, J. Stat. Softw. 54 (2013) 1–23.

[16] L.A. Palomares, M. Realpe, O.T. Ramírez, An Overview of Cell Culture Engineering for the Insect Cell-Baculovirus Expression Vector System (BEVS), in: Anim. Cell Cult., Springer, Cham, 2015: pp. 501–519.

[17] J. Osz-Papai, L. Radu, W. Abdulrahman, I. Kolb-Cheynel, N. Troffer-Charlier, C. Birck, A. Poterszman, Insect cells-baculovirus system for the production of difficult to express proteins, in: Methods Mol. Biol., Humana Press, New York, NY, 2015: pp. 181–205.

[18] L.C.L. Chan, S. Reid, Development of serum-free media for lepidopteran insect cell lines, in: Methods Mol. Biol., Humana Press, New York, NY, 2016: pp. 161–196.

[19] L. Sander, A. Harrysson, Using cell size kinetics to determine optimal harvest time for Spodoptera frugiperda and Trichoplusia ni BTI-TN-5B1-4 cells infected with a baculovirus expression vector system expressing enhanced green fluorescent protein, Cytotechnology. 54 (2007) 35–48.

[20] E.V.B. Van Gaal, R. Van Eijk, R.S. Oosting, R.J. Kok, W.E. Hennink, D.J.A. Crommelin, E. Mastrobattista, How to screen non-viral gene delivery systems in vitro?, J. Control.

Release. 154 (2011) 218–232.

[21] A. Raup, H. Wang, C. V. Synatschke, V. Jérôme, S. Agarwal, D. V. Pergushov, A.H.E. Müller, R. Freitag, Compaction and Transmembrane Delivery of pDNA: Differences between l-PEI and Two Types of Amphiphilic Block Copolymers, Biomacromolecules. 18 (2017) 808–818.

[22] D.L. Hacker, D. Kiseljak, Y. Rajendra, S. Thurnheer, L. Baldi, F.M. Wurm, Polyethyleneimine-based transient gene expression processes for suspension-adapted HEK-293E and CHO-DG44 cells, Protein Expr. Purif. 92 (2013) 67–76.

[23] S. Gutierrez-Granados, L. Cervera, M. de las M. Segura, J. Wolfel, F. Godia, Optimized production of HIV-1 virus-like particles by transient transfection in CAP-T cells, Appl. Microbiol. Biotechnol. 100 (2016) 3935–3947.

[24] X. Shen, D.L. Hacker, L. Baldi, F.M. Wurm, Virus-free transient protein production in Sf9 cells, J. Biotechnol. 171 (2013) 61–70.

[25] B.C. Thompson, C.R.J. Segarra, O.L. Mozley, O. Daramola, R. Field, P.R. Levison, D.C. James, Cell line specific control of polyethylenimine-mediated transient transfection optimized with "Design of experiments" methodology, Biotechnol. Prog. 28 (2012) 179–187.

[26] J. Fuenmayor, L. Cervera, S. Gutiérrez-Granados, F. Gòdia, Transient gene expression optimization and expression vector comparison to improve HIV-1 VLP production in HEK293 cell lines, Appl. Microbiol. Biotechnol. 102 (2018) 165–174.

[27] F. Bollin, V. Dechavanne, L. Chevalet, Design of experiment in CHO and HEK transient transfection condition optimization, Protein Expr. Purif. 78 (2011) 61–68.

[28] D.C. Montgomery, Design and Analysis of Experiments, 5th ed., John Wiley & Sons Inc., Arizona, 2012.

[29] G. Backliwal, M. Hildinger, V. Hasija, F.M. Wurm, High-density transfection with HEK-293 cells allows doubling of transient titers and removes need for a priori DNA complex formation with PEI, Biotechnol. Bioeng. 99 (2008) 721–727.

[30] L. Cervera, S. Gutiérrez-Granados, M. Martínez, J. Blanco, F. Gòdia, M.M. Segura,

Generation of HIV-1 Gag VLPs by transient transfection of HEK 293 suspension cell cultures using an optimized animal-derived component free medium, J. Biotechnol. 166 (2013) 152–165.

[31] J.L. Peixoto, Hierarchical Variable Selection in Polynomial Regression Models, Am. Stat. 41 (1987) 311.

[32] M. Lu, P.J. Farrell, R. Johnson, K. Iatrou, A baculovirus (Bombyx mori nuclear polyhedrosis virus) repeat element functions as a powerful constitutive enhancer in transfected insect cells, J. Biol. Chem. 272 (1997) 30724–30728.

[33] R. Román, J. Miret, F. Scalia, A. Casablancas, M. Lecina, J.J. Cairó, Enhancing heterologous protein expression and secretion in HEK293 cells by means of combination of CMV promoter and IFNα2 signal peptide, J. Biotechnol. 239 (2016) 57–60.

[34] M. Bleckmann, M. Schürig, F.F. Chen, Z.Z. Yen, N. Lindemann, S. Meyer, J. Spehr, J. Van Den Heuvel, Identification of essential genetic baculoviral elements for recombinant protein expression by transactivation in Sf21 insect cells, PLoS One. 11 (2016) 1–19.

[35] S. Radner, P.H.N. Celie, K. Fuchs, W. Sieghart, T.K. Sixma, M. Stornaiuolo, Transient transfection coupled to baculovirus infection for rapid protein expression screening in insect cells, J. Struct. Biol. 179 (2012) 46–55.

[36] F. Monteiro, V. Bernal, X. Saelens, A.B. Lozano, C. Bernal, A. Sevilla, M.J.T. Carrondo, P.M. Alves, Metabolic profiling of insect cell lines: Unveiling cell line determinants behind system's productivity, Biotechnol. Bioeng. 111 (2014) 816–828.

[37] T.R. Davis, K.M. Trotter, R.R. Granados, H.A. Wood, Baculovirus Expression of Alkaline Phosphatase as a Reporter Gene for Evaluation of Production, Glycosylation and Secretion, Nat. Biotechnol. 10 (1992) 1148–1150.

[38] L. Ikonomou, G. Bastin, Y. Schneider, S. Agathos, Design of an efficient medium for insect cell growth and recombinant protein production, Vitr. Cell. & Dev. Biol. - Anim. 37 (2001) 549–559.

[39] L. Cervera, S. Gutiérrez-Granados, N.S. Berrow, M.M. Segura, F. Gòdia, Extended gene expression by medium exchange and repeated transient transfection for recombinant

protein production enhancement, Biotechnol. Bioeng. 112 (2015) 934–946.

[40] Y. Sang, K. Xie, Y. Mu, Y. Lei, B. Zhang, S. Xiong, Y. Chen, N. Qi, Salt ions and related parameters affect PEI-DNA particle size and transfection efficiency in Chinese hamster ovary cells., Cytotechnology. 67 (2015) 67–74.

[41] Z. Chu, S. Zhang, B. Zhang, C. Zhang, C.-Y. Fang, I. Rehor, P. Cigler, H.-C. Chang, G. Lin, R. Liu, Q. Li, Unambiguous observation of shape effects on cellular fate of nanoparticles, Sci. Rep. 4 (2015) 4495.

[42] L. Chen, S. Xiao, H. Zhu, L. Wang, H. Liang, Shape-dependent internalization kinetics of nanoparticles by membranes, Soft Matter. 12 (2016) 2632–2641.

[43] R.M. Glaeser, How good can cryo-EM become?, Nat. Methods. 13 (2016) 28–32.

[44] M.A. Bezerra, R.E. Santelli, E.P. Oliveira, L.S. Villar, L.A. Escaleira, Response surface methodology (RSM) as a tool for optimization in analytical chemistry, Talanta. 76 (2008) 965–977.

[45] G. Derringer, R. Suich, Simultaneous optimization of several response variables, J. Qual. Technol. 12 (1980) 214–219.

[46] L. Vera Candioti, M.M. De Zan, M.S. Cámara, H.C. Goicoechea, Experimental design and multiple response optimization. Using the desirability function in analytical methods development, Talanta. 124 (2014) 123–138.

[47] C. Paillet, G. Forno, N. Soldano, R. Kratje, M. Etcheverrigaray, Statistical optimization of influenza H1N1 production from batch cultures of suspension Vero cells (sVero), Vaccine. 29 (2011) 7212–7217.

[48] R. Islam, R. Sparling, N. Cicek, D. Levin, Optimization of Influential Nutrients during Direct Cellulose Fermentation into Hydrogen by Clostridium thermocellum, Int. J. Mol. Sci. 16 (2015) 3116–3132.

Supplementary material

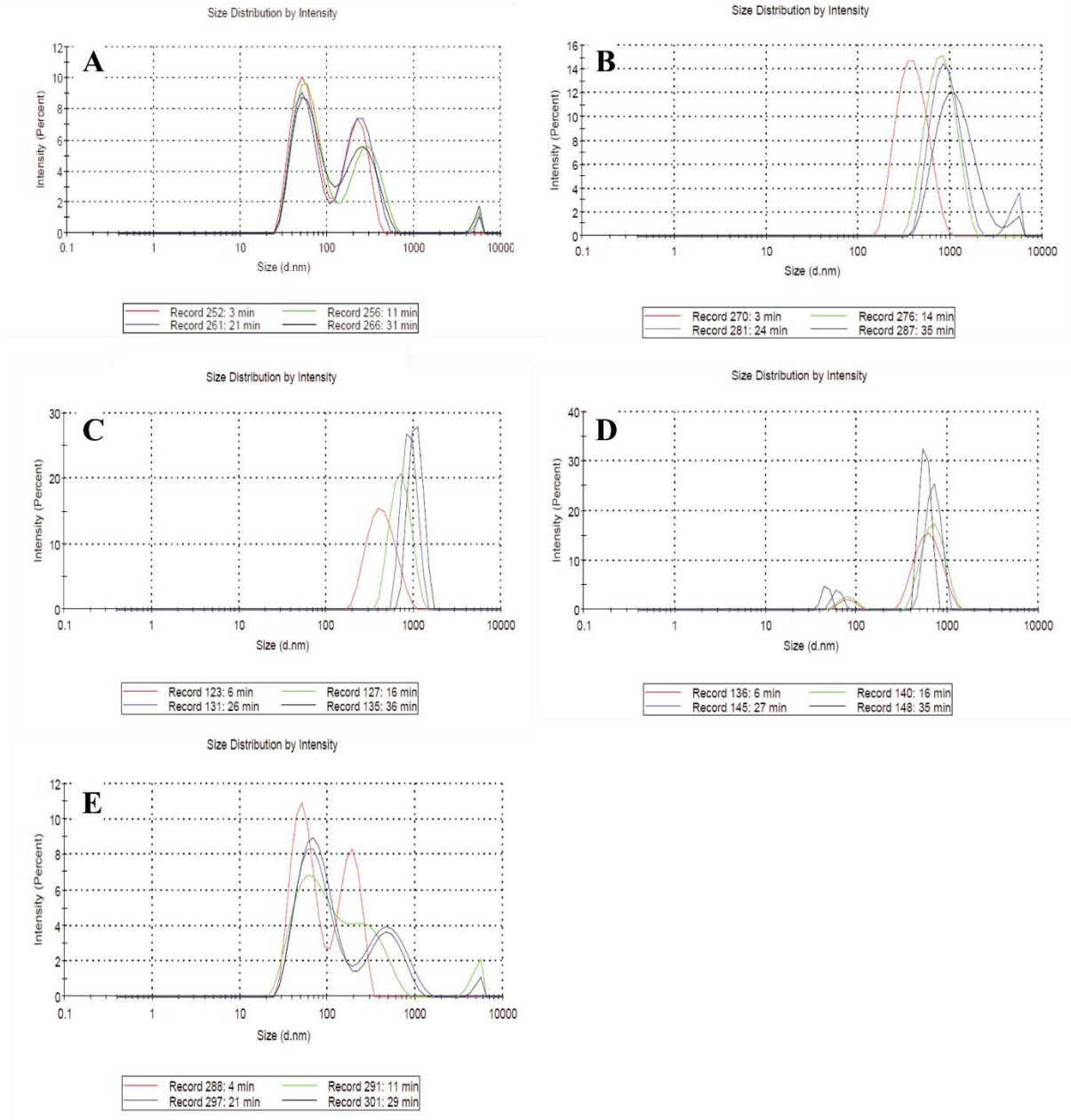

Figure S1. Intensity-based mean hydrodynamic diameter of DNA:PEI polyplex formation over time measured with dynamic light scattering. (A) 3 mM NaCl (Atn:10). (B) 150 mM NaCl (Atn:7). (C) DPBS (Atn:8). (D) Sf900III medium (Atn:7). (E) Ultrapure water (Atn:10). *Atn*: DLS attenuator.

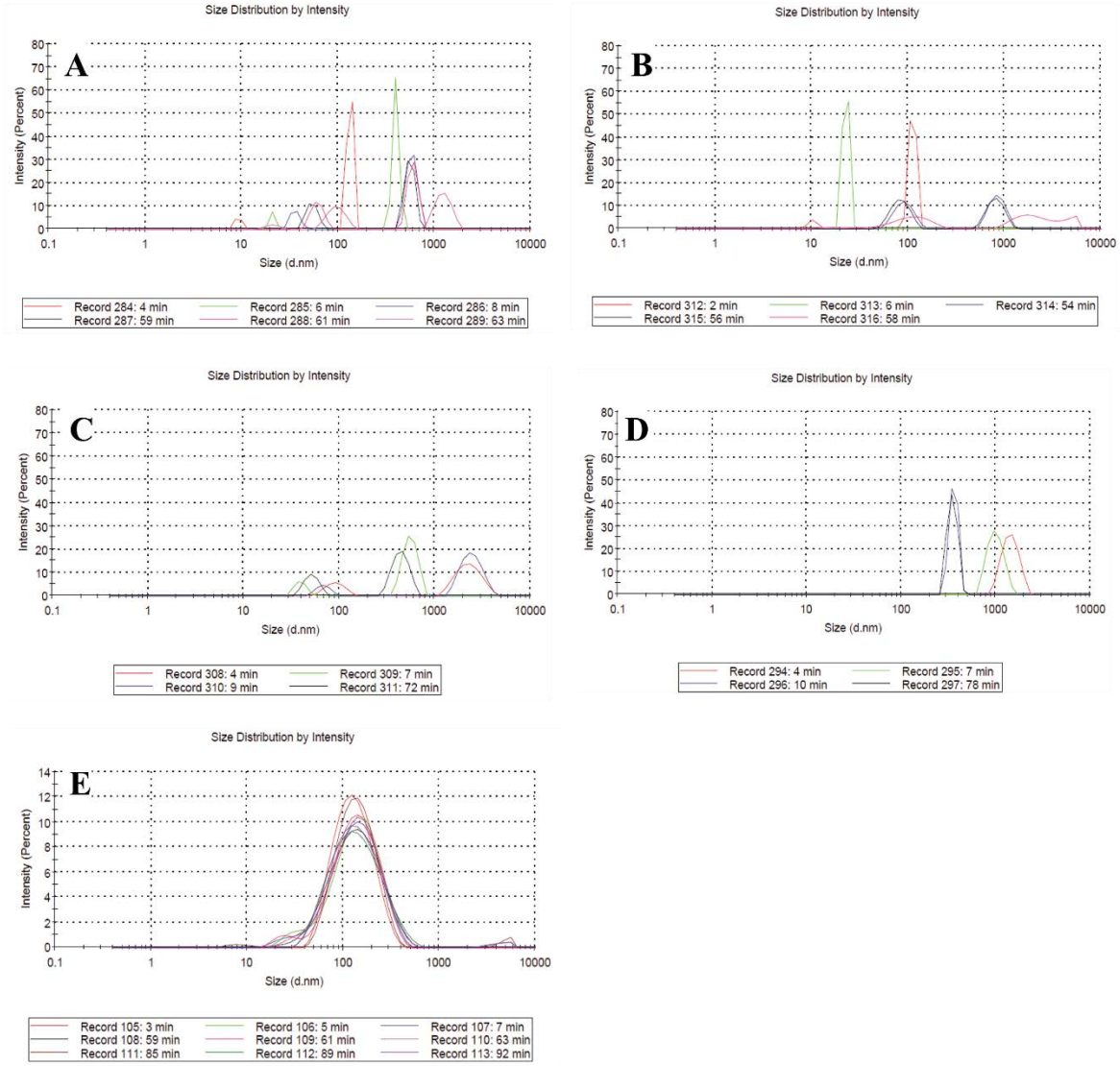

Figure S2. Intensity-based mean hydrodynamic diameter of DNA adition to the different incubation solutions over time measured with dynamic light scattering. (A) 3 mM NaCl (Atn:11). (B) 150 mM NaCl (Atn:11). (C) DPBS (Atn:11). (D) Sf900III medium (Atn:10). (E) Ultrapure water (Atn:11). *Atn*: DLS attenuator.

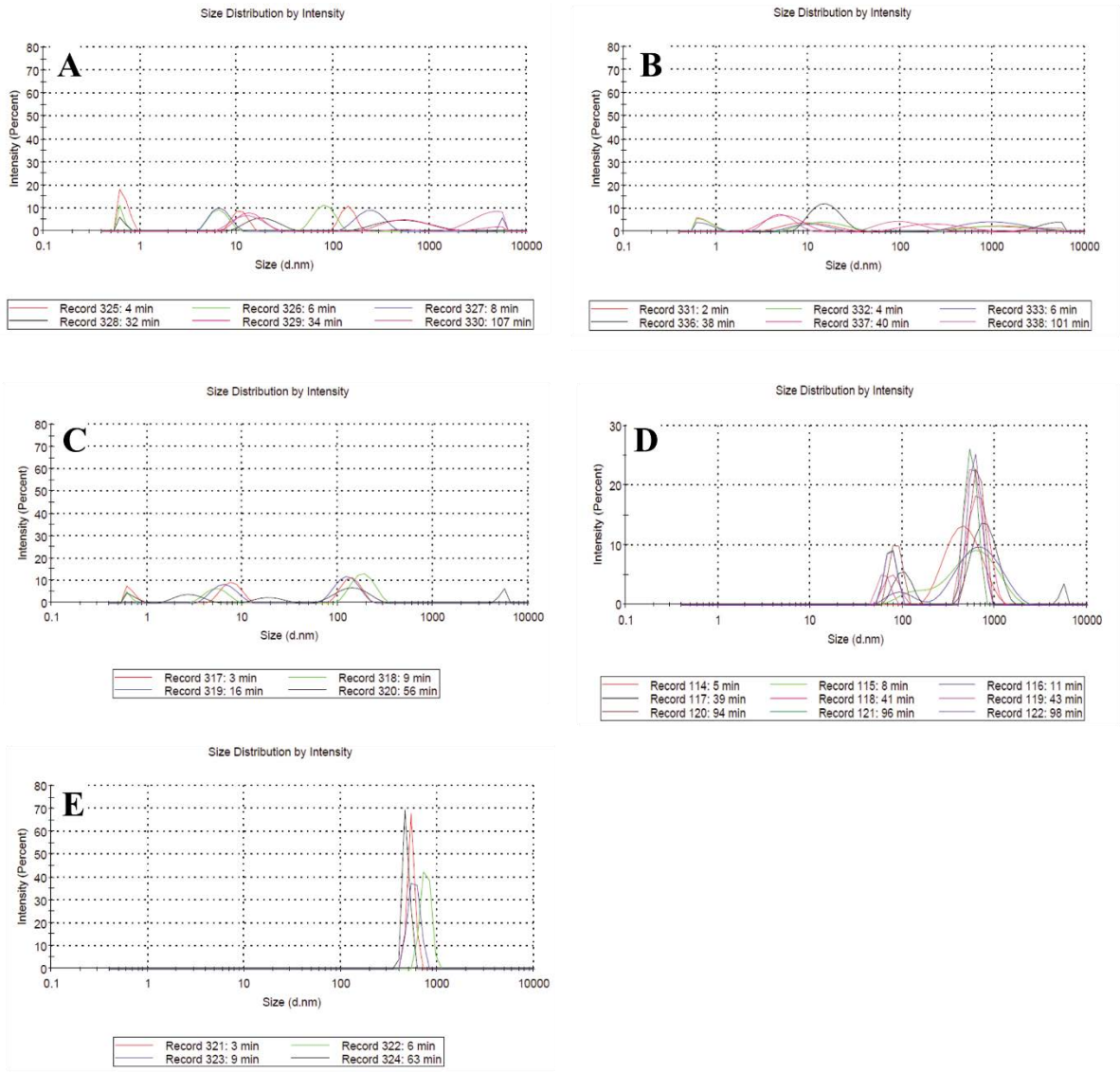

Figure S3. Intensity-based mean hydrodynamic diameter of PEI adition to the different incubation solutions over time measured with dynamic light scattering. (A) 3 mM NaCl (Atn:11). (B) 150 mM NaCl (Atn:11). (C) DPBS (Atn:11). (D) Sf900III medium (Atn:7). (E) Ultrapure water (Atn:11). *Atn*: DLS attenuator.

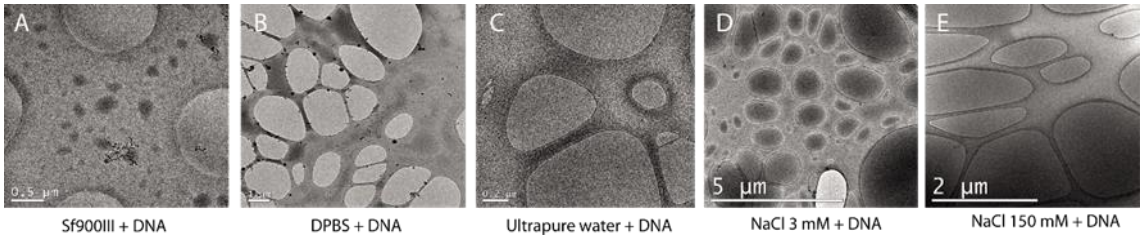

Figure S4. Cryo-EM images of DNA adition to the different incubation solutions at 5 min incubation.

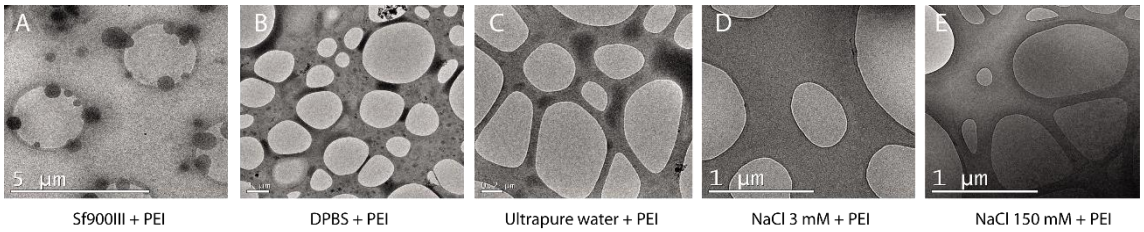

Figure S5. Cryo-EM images of PEI adition to the different incubation solutions at 5 min incubation.

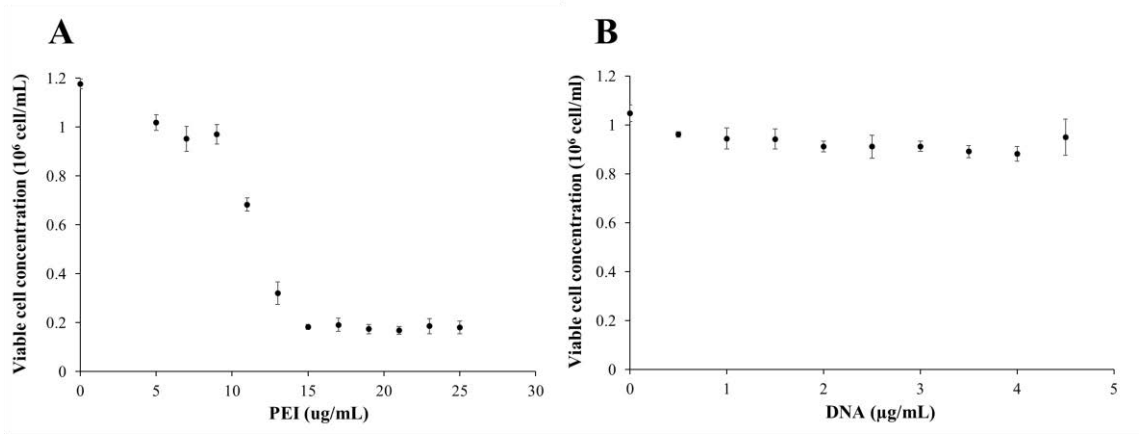

Figure S6. Toxicity assays of PEI 25kDa and pIZTV5-eGFP DNA on Hi5 cells in Sf900III medium. Briefly, 100 µL of Hi5 cells at 0.3 x 10^6 cell/mL were seeded in each well of a 96-well plate and 10 µL of PEI or DNA at different concentrations was added into each of the wells. After 48h, a Cell Titer 96® AQ_{ueous} One Solution Cell Proliferation Assay (Promega, Madison, WI, USA) was used to determine the effect of the different PEI and DNA concentrations on cell growth. Mean values ± standard deviation of triplicate experiments are represented.

Chapter 4

Generation of stable insect cell pools for the production of GageGFP VLPs

Eduard Puente Massaguer, Paula Grau-García, Martí Lecina and Francesc Gòdia

Abstract

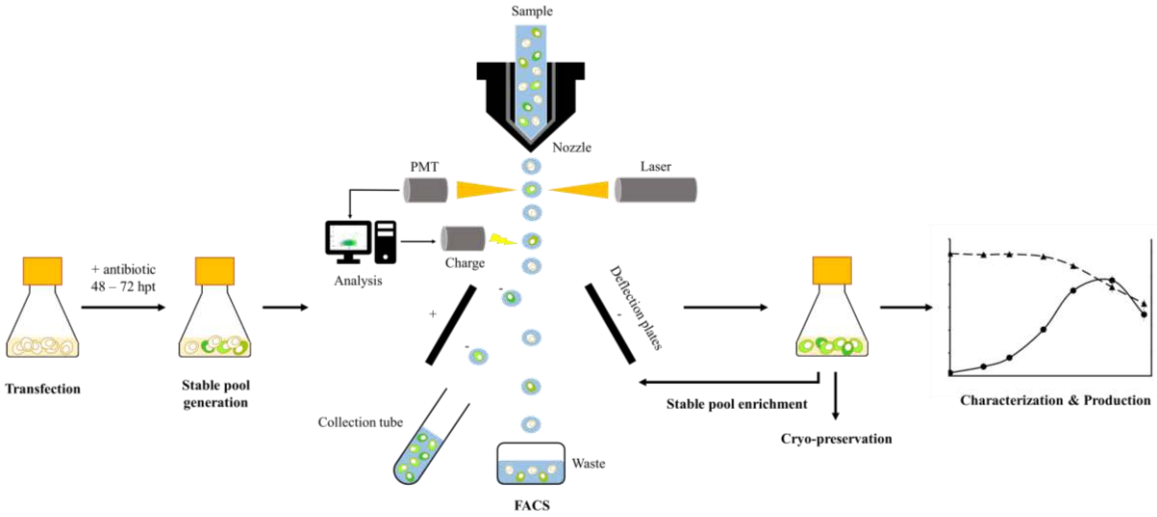

Stable cell pools have emerged as a strategy to stably express recombinant products. The reduced timeline required for their development and the capacity to achieve similar production yields to those achieve by clonal cell lines make them an interesting approach. In this chapter, stable insect cell pools were developed to produce recombinant products with different complexities: the mCherry intracellular protein and HIV-1 GageGFP virus-like particles (VLPs). Random integration coupled to fluorescence-activated cell sorting (FACS) were applied to generate the stable cell pools and to select the high producer cell within each pool, respectively. The complete generation process from transfection to stable production took 7 weeks for High Five cells and 10 weeks for Sf9 cells. Sf9 stable cell pools achieved a 1.4-fold increase in mCherry concentration (37.4 ± 4.5 mg/L) whereas High Five cells attained higher VLP titers by 3.7-fold (14.9 ± 1.4 x 10^5 VLP/mL). The stability of the cell pools here developed was successfully evaluated during the time course of a month. This study highlights the use of insect cell pools to stably produce a variety of recombinant products in a reduced window of time.

Keywords: Sf9 cells, High Five cells, stable cell pool, virus-like particle, fluorescence-activated cell sorting

Abbreviations: eGFP, enhanced green fluorescent protein; EV, Extracellular vesicle; FACS, fluorescence-activated cell sorting; FBS, fetal bovine serum; GOI, gene of interest; HIV, human immunodeficiency virus; VLP, Virus-like particle.

Introduction

Transient gene expression (TGE) is widely used to screen different genes of interest (GOI) and to produce enough amounts of a recombinant product in short timeframe [1]. It is based on the transient episomal expression of a plasmid DNA/s that have been introduced into the cells, but this expression is lost over time. Therefore, TGE is very adequate at early stages of the development of biopharmaceutical products, but when the target recombinant product has been selected among different candidates and the production at bioreactor scale is required, TGE has a series of drawbacks [2]. These limitations encompass the production of high amounts of DNA and an added step of maneuverability due to the need to introduce DNA in combination to a transfection reagent, thus increasing batch-to-batch variability and eventually the manufacturing costs. Furthermore, there exists the possibility that the medium used for cell growth is incompatible with transfection, which would require a partial or complete medium replacement prior to transfection [3,4]. Stable gene expression (SGE) consists in the expression of a GOI/s based on the integration of a plasmid DNA/s into genome of the cells. This process can be performed via targeted and non-targeted integration methodologies. Target integration groups a series of methods that direct plasmid DNA to genome loci with high transcription rates and low gene silencing [5,6]. This is also possible in non-targeted integration techniques, but the efficiency is lower. Non-targeted random integration is an extensively used approach to develop stable expression systems and it basically allows to introduce one or more copies of DNA through the cell genome [7,8]. Both techniques of DNA integration into the genome are followed by a phase in which the stably producing phenotype is selected over the others based on the addition of a selective pressure into the cell culture media. At this point, the classical procedure is to screen for individual clones that have the highest growing and producing capabilities, with better chances for targeted integration techniques. Limiting dilution and more recently fluorescence-activated cell sorting (FACS) are common techniques employed to this purpose with the final goal to stablish a phenotypic and genotypic homogenic system for protein production [9]. This process can be time-consuming since the higher the clones screened, the better the chances to find a high

producer cell. Nevertheless, several studies have reported that different expression patterns are also observed within cells derived from a clonal cell line [10,11]. Then, it is not clear if the efforts needed to develop a stable cell line are sufficiently justified. Stable cell pools have emerged as a valuable approach for stable protein production [12,13]. In this case, the timeline from transfection to production is substantially reduced and production titers are similar to those achieved with stable cell lines.

So far, most of the studies conducted for the development of stable cell pools have been performed in CHO cells [13,14]. Nonetheless, Insect cell lines have proven to be a robust system with success in the production of different recombinant products [15]. These cells provide the means to generate adequate post-translational modifications, have low culture requirements, show a fast cell growth, and possess a high safety level due to the absence of known human pathogens. Among them, *Dipteran* S2 cells have been used for stable production of recombinant proteins [16], but *Lepidopteran* Sf9 and High Five cells have also shown good promise [17,18].

In this work, the generation of stable Sf9 and High Five insect cell pools was investigated for the production of two recombinant products with different complexities, the mCherry intracellular protein and HIV-1 Gag virus-like particles (VLPs). To facilitate VLP quantification, the Gag polyprotein was fused in frame to eGFP. Random DNA integration was used in combination to FACS to select the high producers within each stable cell pool. A final characterization of cell pool stability was performed to assess that recombinant protein expression was maintained over time.

Materials and methods

Cell lines and culture conditions

The BTI-TN-5B1-4 cells (High Five, cat. num. B85502, Thermo Fisher Scientific, Grand Island, NY, USA) and Sf9 cells (cat. num. 71104, Merck, Darmstadt, Germany) were adapted to grow in

the Sf900III medium (Thermo Fisher Scientific). Both insect cells were subcultured three times a week in 125 mL disposable polycarbonate Erlenmeyer flasks (Corning, Steuben, NY, USA) at a density of 2 - 4 x 10^5 cells/mL for High Five cells and 4 - 6 x 10^5 cells/mL for Sf9 cells. All cultures were grown in an orbital shaker at 130 rpm (Stuart, Stone, UK) and maintained in an incubator at 27 °C.

For cell selection, the medium was supplemented with the antibiotic zeocin (InvivoGen, San Diego, CA, USA) according to toxicity assays. Zeocin selection was kept until the viability of the culture was completely recovered, but a minimum of 4 weeks of zeocin addition to the culture was maintained to ensure that the expression of mCherry or GageGFP was not episomal but from stable integration.

Cell count and viability were measured with the automated cell counter Nucleocounter NC-3000 (Chemometec, Allerød, Denmark). Stable cell pools were also observed under a TCS SP5 confocal microscope (Leica, Wetzlar, Germany) for qualitative analysis of mCherry and GageGFP expression. Cell nuclei were stained in blue dye with 0.1 % v/v of Hoechst (Thermo Fisher Scientific). Dye excess was removed by mild centrifugation at 300 x*g* for 5 min and cell resuspension in fresh Sf900III medium. Afterwards, samples were placed in 35 mm glass bottom Petri dishes with 14 mm microwell (MatTek Corporation, Ashland, MA, USA) for visualization.

Plasmid construction and transfection

The pIZTV5-GageGFP plasmid coding for a Rev-independent HIV-1 Gag fused in frame to the enhanced green fluorescent protein eGFP (NIH AIDS Reagent Program, cat. num. 11468) [19] was constructed as described in Chapter 3. The pIZTV5-mCherry plasmid coding for the intracellular fluorescent mCherry protein was generated from PCR cloning of the *mCherry* gene from the pPEU3 plasmid [20] with the following primer pair: forward 5'-CGTAAAGCTTATTTACAATCAAAGGAGATATACCA-3' and reverse 5'-CGTAGCGGCCGCCTACTTGTACAGCTCGTCCATGC-3'. The amplified fragment and the

pIZTV5-his plasmid (Thermo Fisher Scientific) were digested with *Hin*dIII and *Not*I and ligated into the pIZTV5-mCherry. Fragments containing the sequences of interest were ligated, obtaining the pVL1393-GageGFP transfer plasmid. Both plasmid DNA encode for the bleomycin resistance protein which confers resistance to zeocin.

Both insect cells were transfected using Cellfectin® II (Thermo Fisher Scientific) as reported by Vidigal and co-workers [21]. Briefly, 0.3 µg/10^6 cell of pIZTV5-mCherry or pIZTV5-GageGFP and 8 µL/10^6 cell of Cellfectin II were separately added to 500 µL of non-supplemented Grace's insect medium (Thermo Fisher Scientific), vortexed for 5 s and incubated at RT for 30 min. Then, both solutions were mixed, vortexed for 5 s and added to cells. Zeocin selection was started at 48 and 72 hpt for High Five and Sf9 cells, respectively.

The percentage of mCherry or GageGFP positive cells was evaluated in a BD FACS Canto II flow cytometer and analyzed with the BD FACSDIVA software (BD Biosciences, San Jose, CA, USA). The number of mCherry and GageGFP positive cells was determined in the PerCP-Cy5-A and FITC-A PMT detectors, respectively.

Fluorescence-activated cell sorting

Stable pool enrichment with high producer cells was performed by three rounds of fluorescence-activated cell sorting (FACS) in a BD FACSJazz™ (BD Biosciences) equipped with two lasers (488 nm and 635 nm). The threshold was set to select the 30 % of most fluorescent cells during the first two rounds of FACS, and the final round was used to remove the lowest fluorescent cells (50 – 80 %). Shortly, mCherry and GageGFP stable producing cell pools were grown to 2 x 10^6 cell/mL for High Five and 3 x 10^6 cell/mL for Sf9 cells before sorting. 1 % of Pluronic F-68 100*X* and 1*X* from a 100*X* solution of antibiotic-antimycotic (Thermo Fisher Scientific) were added to the cell culture to minimize the effect of shear stress and avoid contamination. The sheath fluid was DPBS (Thermo Fisher Scientific) at constant pressure of 27 psi and the sorting rate was maintained in the range of 500 to 2000 cell/s. 2 x 10^6 cell cells were collected in fresh Sf900III

medium supplemented with 2 % FBS and 1*X* of antibiotic-antimycotic. After sorting, cells were centrifuged at 300 x*g* for 5 min to remove the sheath fluid and resuspended at a final concentration of 0.5 x 10^6 cell/mL in 6-well plate with fresh Sf900III medium containing 5 % FBS, zeocin and 1*X* of antibiotic-antimycotic. Then, cells were maintained in the incubator at 150 rpm for 1 week. Zeocin was removed from cell culture after the different rounds of FACS were performed.

Spectrofluorometry

Intracellular GageGFP and mCherry production were evaluated based on the fluorescence levels from stable pools. Cell pellets were recovered by centrifugation 3000 x*g* for 5 min and disrupted by means of three freeze-thaw cycles (2.5 h at -20 °C and 0.5 h at 37 °C) and vortexed 5s 3 times between cycles. Lysed pellets were then resuspended in TMS buffer (50 mM Tris-HCl, 150 mM NaCl, 2 mM $MgCl_2$, pH 8.0) and centrifuged at 13700 x*g* for 20 min. GageGFP fluorescence was measured with a Cary Eclipse spectrophotometer (Agilent Technologies, Santa Clara, CA, USA) at RT as follows: λex = 488 nm (slit = 5), λem= 500 – 530 nm (slit = 10). For mCherry fluorescence measurement, the equipment settings were as follows: λex = 587 nm (slit = 5), λem= 600 – 630 nm (slit = 10) Relative fluorescence units (R.F.U) were calculated by measuring the difference between stable producing pools and non-expressing controls. mCherry concentration was determined using a standard curve based on the linear correlation between known mCherry concentrations (BioVision, Milpitas, CA, USA) and their associated fluorescence R.F.U.:

$$\text{mCherry (mg/L)} = (\text{R.F.U.} - 55.008)/9.0401 \qquad (1)$$

The Sf900III medium and a 0.1 mg/mL quinine sulphate solution were used as controls to normalize de R.F.U. between samples from different experiments.

Nanoparticle quantification

The concentration of GageGFP VLPs and extracellular vesicles were assessed by flow virometry in a CytoFlex LX (Beckman Coulter) equipped with a 488 nm blue laser for fluorescent particle detection and a 405 nm laser/violet side scatter configuration for improved nanoparticle size resolution. Samples were diluted in 0.22 µm-filtered DPBS and analyzed with the CytExpert 2.3 software.

A HIV-1 p24 enzyme-linked immunosorbent assay (ELISA) (Sino Biological, Wayne, NJ, USA) was also used to quantify GageGFP polyprotein concentrations in the supernatant. The protocol used is described in chapter 3. The p24 concentration values were corrected based on GageGFP molecular weight (87.7 kDa).

Results and discussion

Toxicity assays

Different zeocin concentrations were tested for stable pool generation in High Five and Sf9 cells. The concentration range was defined according to preliminary experiments of this antibiotic with both cells (data not shown) and was set from 50 to 500 µg/mL (Figure 1). zeocin displays a combined mechanism of action based on intercalation into DNA and the induction of DNA double strand breaks [22,23].

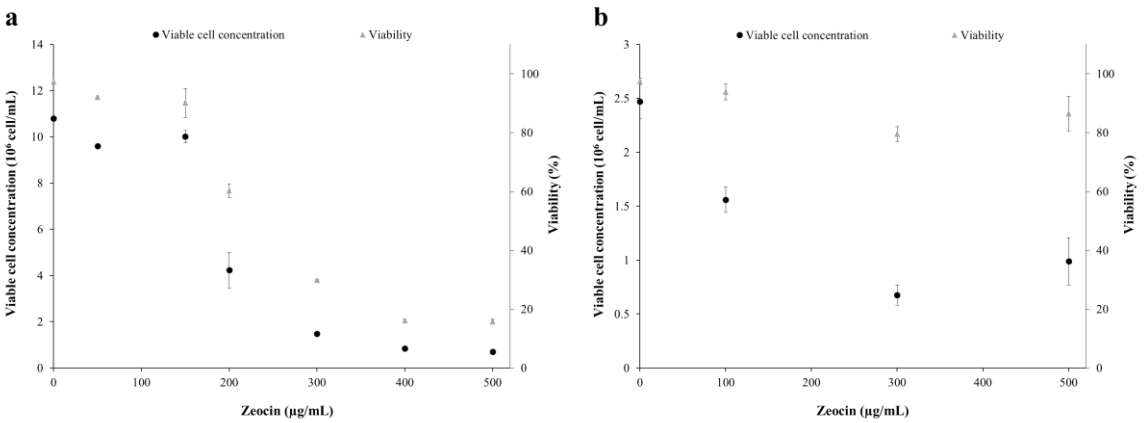

Figure 1. Zeocin toxicity assay in Sf9 (a) and High Five cells (b). Viable cell concentration and viability in 10 mL of cell culture in Erlenmeyer flasks at 48 h post addition of the antibiotic. Sf9 cells were seeded at 4.0 x 10^6 cell/mL and High Five cells at 0.5 x 10^6 cell/mL. Results from triplicate experiments are represented.

Zeocin addition to Sf9 cell cultures triggered cell death at increasing concentrations as observed by the decline in cell viability and in viable cell concentration. On the other hand, zeocin activity in High Five cells arrested their growth but cell viability was not significantly affected, possibly indicating a delayed action of zeocin in this cell line [24]. Addition of 300 µg/mL of zeocin was selected as the condition for stable pool generation in both cell lines since higher antibiotic concentrations did not show a significant difference.

Stable cell pool generation

Transfected cells with pIZTV5-mCherry and pIZTV5-GageGFP were left to grow until 48 hpt for High Five cells and 72 hpt for Sf9 cells in Sf900III medium. Initial drop in cell viability was caused by the transfection process itself while subsequent declines in cell viability were produced by the addition of zeocin. During the development process of the stable cell pools, no relevant differences were observed in the time required to stably express GageGFP or mCherry within the same cell lineage (Figure 2).

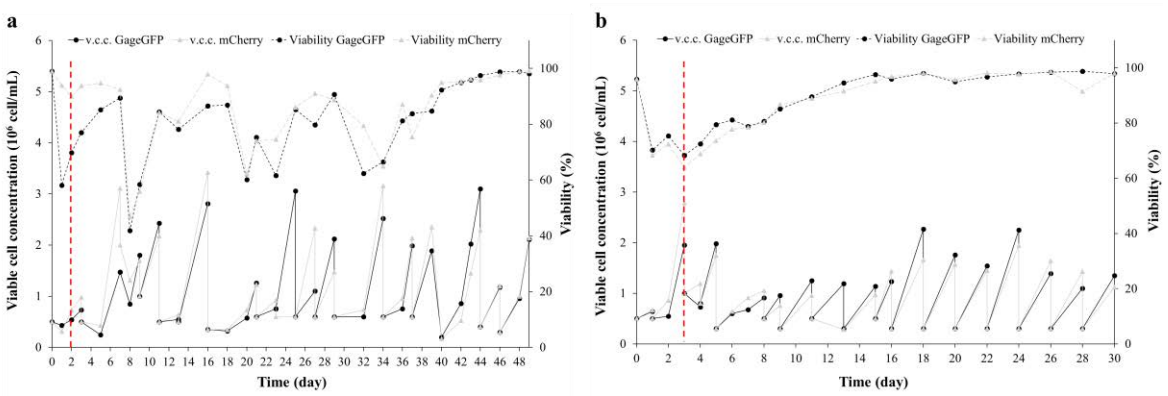

Figure 2. Time line of mCherry and GageGFP stable cell pool generation in Sf9 (a) and High Five cells (b) from transfection. The dashed red-line indicates the moment of zeocin addition, which was added at a final concentration of 300 µg/mL and kept at this concentration in every subculture.

High Five cells exhibited an initial decline in cell viability to 60 – 70 % that lasted one week and then cells experimented a progressive recuperation. For Sf9 cells, more variability in cell viability was observed during the first month under selection and after that cell viability started to raise. The accelerated cell growth kinetics of High Five cells resulted in faster accomplishment of cell pool stability in comparison to Sf9 cells. It took approximately 2 weeks for High Five cells to completely recover cell viability, but cells were left for 4 weeks under culture to ensure stable plasmid integration into cell genome. In the case of Sf9 cells, 7 weeks were required to recover cell viability in the transfected cell cultures under selective pressure. These difference in the time needed for stable pool expression in both cell lines were not that remarkable when comparing the number of subcultures performed in for each cell lineage. During the 7 weeks required to develop the stable Sf9 pools, cells were subculture 15 times, while 16 cell passages were required for High Five cells to obtain the stable cell pools during the 4 weeks that were maintained in culture.

Stable pool enrichment by FACS

The initial stable cell pools (unsorted) were a mix of various cell types, encompassing cells that had integrated one or several copies of each plasmid and others that had only integrated the resistance gene. At the end of the development of each stable cell pool, the percentage of stably expressing Sf9 cells was 53.1 % for GageGFP and 74.1 % for mCherry whereas for Hi5 stable

pools it was 45.6 % and 47.8 %, respectively. To this purpose, FACS was used to remove the non-producing cells and select the high producer cell population in each pool (Figure 3).

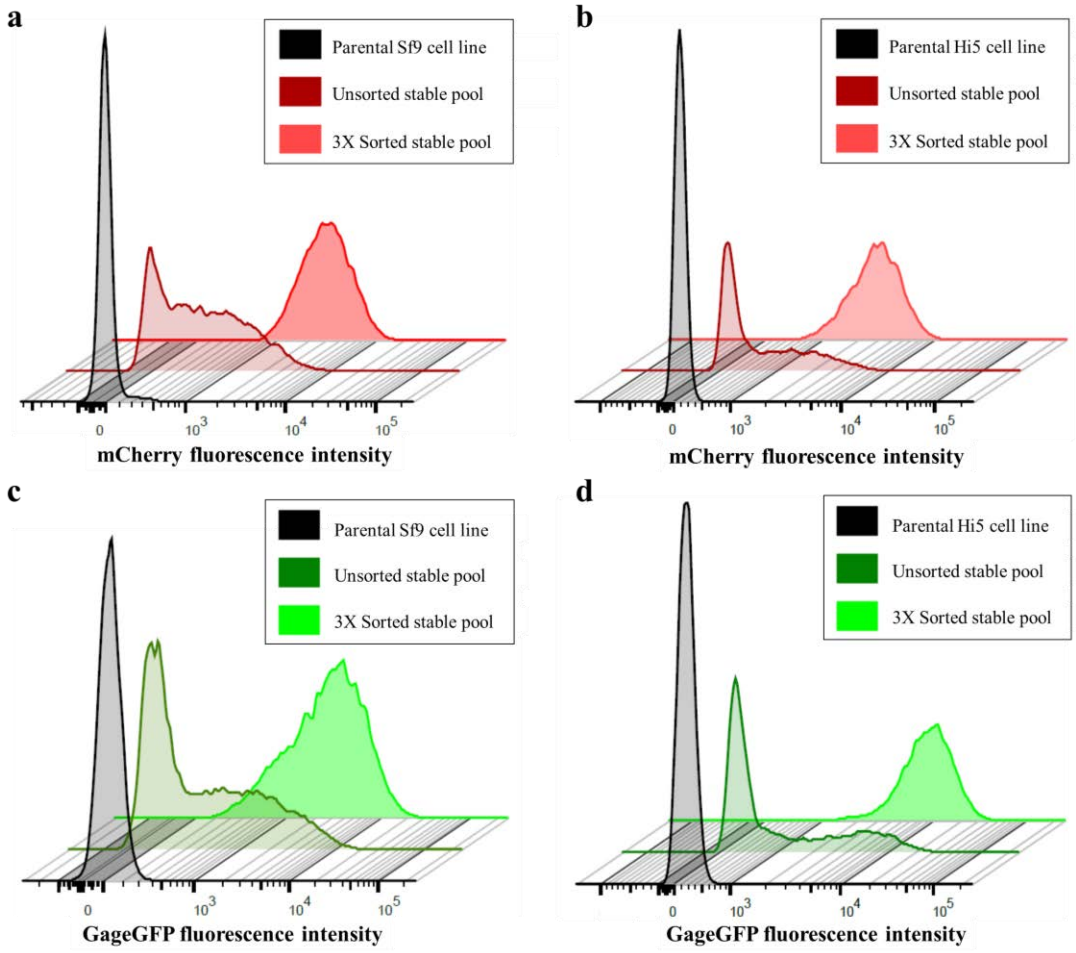

Figure 3. Histograms comparing the average fluorescence intensity from parental cells, unsorted stable cell pools and stable cell pools after three rounds of sorting. (a) Sf9 mCherry, (b) High Five mCherry, (c) Sf9 GageGFP and (d) Hi5 GageGFP. Average mCherry fluorescence intensity was measured in the PerCP detector whereas GageGFP fluorescence was evaluated in the FITC detector.

Three rounds of FACS enrichment for each stable cell pool were performed to maximize the number of high producing cells in each pool. After the three rounds of sorting, the average fluorescence intensity from each cell pool was significantly improved (Table 1). An 8.1 and 3.4-fold improvement in GageGFP average fluorescence intensity was obtained, whereas a 4.5 and 4.1-fold increase in mCherry average fluorescence intensity were achieved for Sf9 and High Five stable pools, respectively. This strategy has also been applied to enrich stably producing pools of monoclonal antibodies in CHO cells [25,26] and fluorescent proteins in insect cells [27,28].

Table 1. Average fluorescence intensity values for mCherry and GageGFP unsorted stable pools and after three rounds of FACS. Values are expressed in arbitrary units.

	Hi5		Sf9	
Condition	mCherry	GageGFP	mCherry	GageGFP
Unsorted stable pool	62	200	109	77
3X sorted stable pool	255	894	367	625

After FACS, the 8.6 % and 4.9 % most producing cells of the unsorted mCherry stable pool were selected and the 12.7 % and 7.8 % of the unsorted GageGFP stable pool for High Five and Sf9 cells, respectively.

Stable pool characterization

Cell growth and maintenance of sorted cell population in the enriched stable pools was evaluated (Figure 4). Stable protein production did not affect the maximum cell concentration attained by mCherry and GageGFP stable pools in comparison to parental Sf9 cells. Indeed, maximum cell concentration increased in both stable pools, probably due to the longer period in which the stables pools were cultured in Sf900III medium resulting in a better adaptation to this medium. On the contrary, maximum viable cell concentration decreased in mCherry and GageGFP High Five stable pools compared to parental cells. In this case, parental High Five cells were left for two months in culture to adapt them to the Sf900III medium since it is developed for Sf9 cells. In turn, this adaptation process could cause that a longer exposure to Sf900III did not improve the performance of High Five cells in this medium. Thus, the constitutive production of a heterologous protein could re-direct some of the employed for cell growth to protein production causing a decrease in the final maximum cell density. A similar behavior in cell growth kinetics has also been observed in the development of stable Sf9 cell lines [21].

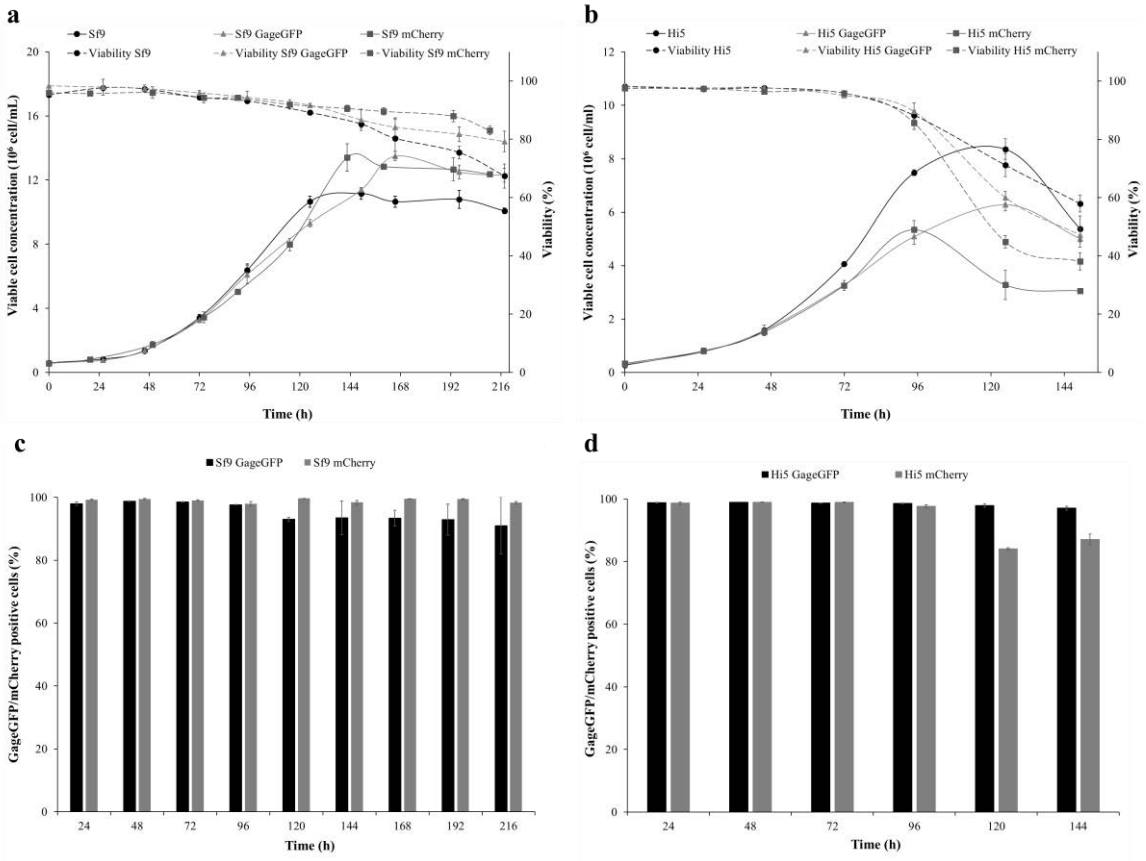

Figure 4. Cell growth profile and percentage of fluorescent cells of stable cell pools and parental cell lines. Viable cell concentration and viability of mCherry, GageGFP stable pools and parental cells for Sf9 (a) and High Five cells (b). Sf9 and High Five cells were seeded at 0.5 and 0.3 x 10^6 cell/mL, respectively. Analysis of the percentage of fluorescent cells of GageGFP and mCherry Sf9 (c) and High Five (d) stable pools by flow cytometry.

Comparison of doubling times in the different Sf9 cell conditions showed no difference between GageGFP stable pools and parental cells but did exhibit an increase for mCherry stable pools, possibly related to the metabolic burden triggered by the production of the recombinant protein (Table 2). Despite no significant differences were observed between parental and Sf9 GageGFP stable pools, it is evident that the pace of the latter is substantially reduced by the end of the exponential phase (120 h) in comparison to parental cells. This could indicate that the pressure exerted to produce GageGFP could also be affecting the cell growth of the GageGFP stable pool from 120 h onwards. Regarding High Five cells, the doubling time increased in both stable pools compared to parental cells, indicating a deceleration in cell growth due to the production of GageGFP and mCherry.

Table 2. Comparison of doubling times between parental cell lines, mCherry and GageGFP stable pools.

Cell line	Condition	Doubling time (h)
Hi5	Parental cell line	18.6 ± 0.2
	GageGFP stable pool	20.4 ± 0.8
	mCherry stable pool	22.1 ± 1.0
Sf9	Parental cell line	23.0 ± 0.2
	GageGFP stable pool	22.7 ± 0.3
	mCherry stable pool	26.5 ± 2.0

The percentage of fluorescent cells was maintained up to 120 h in both cases. As from 120 h, a decrease was observed, which was more pronounced for the Sf9 GageGFP compared to the mCherry stable pool, whereas for High Five cells it was more relevant for the mCherry than for the GageGFP stable pool. Analysis of cell viability indicated that the decline in the number of fluorescent cells coincided with the decrease in cell viability, which was more pronounced for the GageGFP pool in Sf9 cells and for the mCherry pool for High Five cells. Inspection of the different stable pools by confocal microscopy showed the expression of GageGFP (green) and mCherry (magenta). Different fluorescence intensities could be observed within the same stable pool, thus indicating heterogeneity in the production levels of the cells conforming each pool (Figure 5).

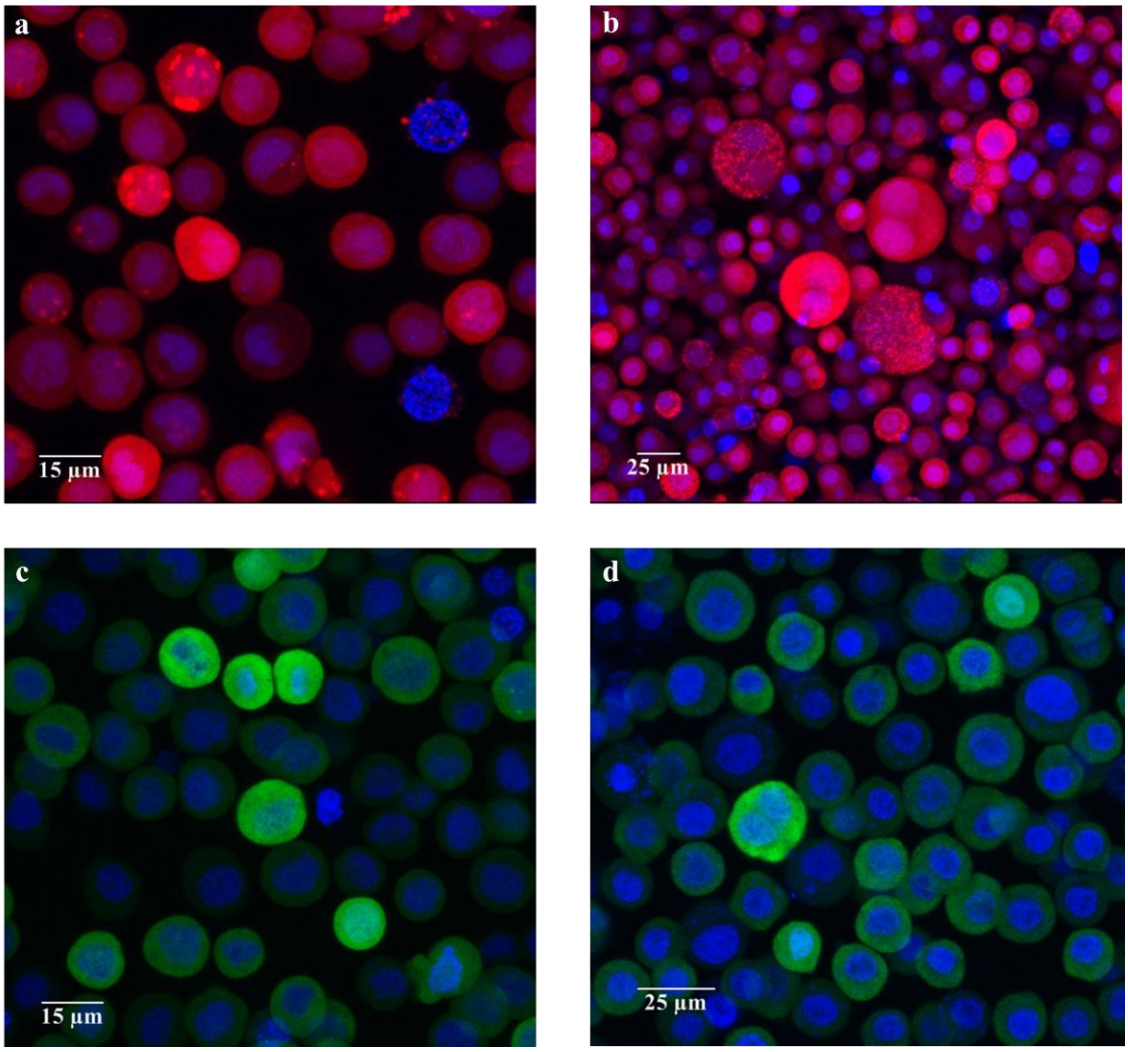

Figure 5. Confocal microscopy three dimensional images of stable cell pools. mCherry and GageGFP stable pools for Sf9 (a, c) and High Five cells (b, d) at 96 and 48 h, respectively. The nuclei of GageGFP (green) and mCherry (magenta) producing cells was stained with Hoechst (blue).

Intracellular mCherry production levels steadily increased up to 144 h and 120 h for Sf9 and High Five cells, respectively (Figure 6a - b). mCherry could also be measured in the supernatant of stable cell pools mainly at the end of the production curve, which could be attributed to protein leakage from dead cells. mCherry intracellular production peaked at 144 h in Sf9 cells (283.4 ± 41.0 R.F.U.) and 120 h for High Five cells (187.5 ± 4.8 R.F.U.), corresponding to 37.4 ± 4.5 and 26.8 ± 0.5 mg/L of mCherry (Eq. 1). Sf9 stable pools reached a 1.4-fold increase in mCherry production but High Five cells attained a 1.5-fold increase in specific production (4.7 ± 0.4 mg/10^6 cell). The mCherry production titers obtained in this work were in the range of other fluorescent proteins produced with baculovirus-free systems. For instance, a 47.9 ± 4.1 mg/L of eGFP were

reported in a Sf9 clonal cell line [29] and 50 mg/L of purified GFP were produced by transient gene expression (TGE) in HEK 293-EBNA1 cells [30]. Also, these mCherry titers show superior results than eGFP production by TGE in Sf9 and High Five cells as reported in chapter 3. Comparison to the baculovirus expression vector system (BEVS) yielded different outcomes. On the one hand, Monteiro and co-workers report lower GFP specific productivities around 0.02 $\mu g/10^6$ cell for Sf9 cells and about 0.15 $\mu g/10^6$ cell for High Five cells [31] while a 1.8 and 2.5-fold increase in GFP production compared to Sf9 and High Five stable mCherry pools, respectively, is shown by Fernandes and co-authors (67.9 ± 5.7 mg/L) [29].

Regarding the production of GageGFP VLPs, intracellular GageGFP fluorescence levels grow until 120 h for both insect cells lines whereas VLP titers increased up to end of the experiment (Figure 6c – d). However, the VLP production rate decreased in Sf9 cells from 144 h onwards, which could indicate that extending the production phase might not be worth considering. Then, considering a good compromise between VLP production and cell viability at harvest, the harvest times were defined as 144 h and 120 h for Sf9 and High Five cells, respectively. In these conditions, a maximum VLP production of 4.0 ± 0.1 x 10^5 VLP/mL was obtained for Sf9 cells while 14.9 ± 1.4 x 10^5 VLP/mL was achieved in High Five cells, representing a 3.7-fold increase in VLP production and an 8-fold in VLP specific production over the Sf9 stable pool. VLP quantification in the supernatant by ELISA yielded 12.5 and 14.8 ng/mL of GageGFP for Sf9 and High Five cells, respectively. Interestingly, significant co-production of other nanoparticles such as extracellular vesicles (EVs) was also detected in both stable GageGFP pools, being 4.4 ± 0.6 x 10^8 total nanoparticles/mL for Sf9 cells and 7.5 ± 0.9 x 10^8 total nanoparticles/mL for High Five cells.

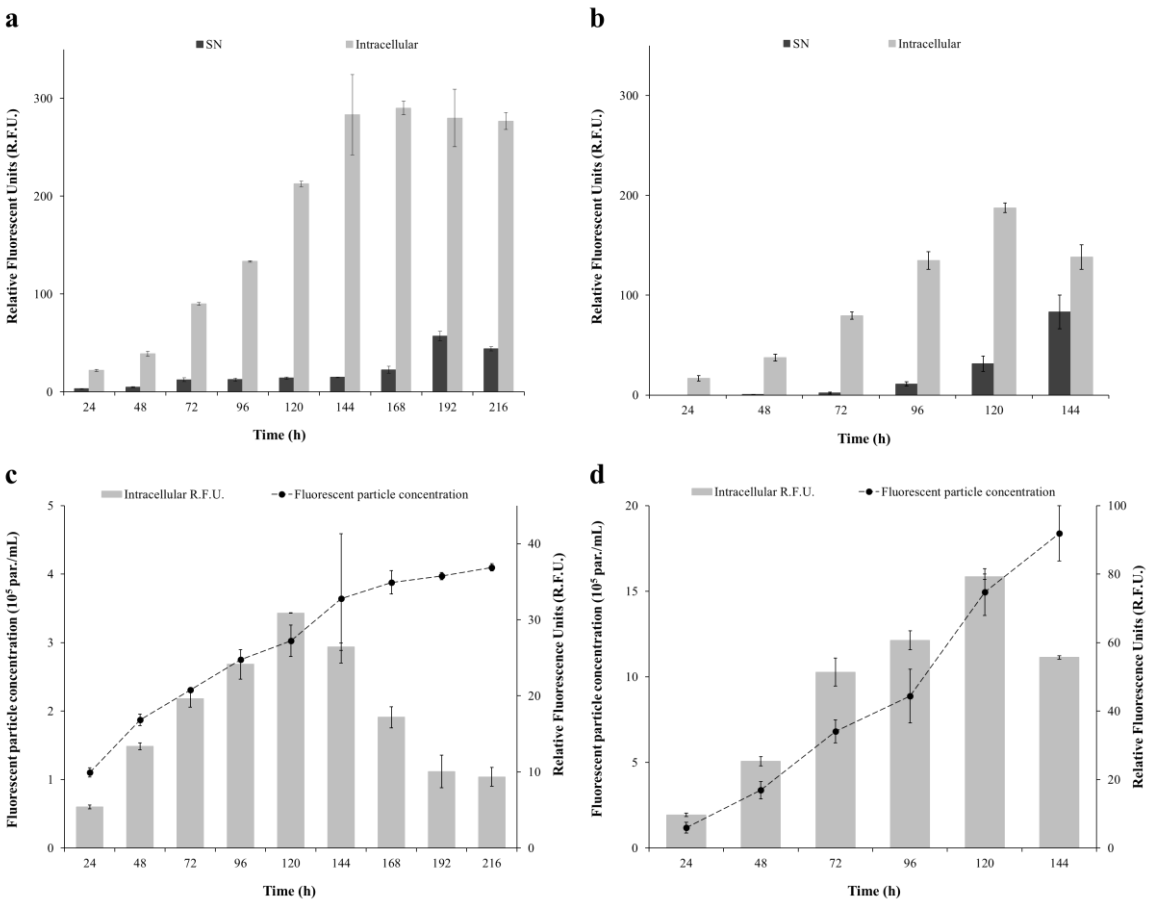

Figure 6. mCherry and GageGFP production kinetics in stable cell pools. (a – b) mCherry production and (c – d) GageGFP and VLP production profile in Sf9 and High Five cells, respectively. Intracellular fluorescence levels of mCherry and GageGFP were measured by spectrofluorometry whereas VLP concentration (fluorescent particles) were assessed by flow virometry. The average and standard deviation from triplicate experiments is represented.

Stable Gag VLP production has also been explored in Sf9 pools developed using the Piggy-Bac™ transposon system. In this case, Gag production ranged in between 0.1 – 1 ng/10^6 cell [32], which is similar to GageGFP production reported here for Sf9 stable pools (1 ng/10^6 cell) and lower to the 2.4 ng/10^6 cell shown for High Five cells. Also, comparison to Sf9 stable clonal cell lines expressing Gag-Cherry resulted in similar specific production levels (2.6 ng/10^6 cell) [21]. Several works have also evaluated the expression of Gag VLPs in stable High Five and S2 cell lines, with production titers comprised in the 1 – 3 mg/L [33] and 4 – 9 mg/L [34], respectively. The titers showed here for both GageGFP stable pools resulted in lower levels to those reported for the BEVS in chapter 2 and TGE in chapter 3. However, the possibility of having a continuous platform to produce Gag VLPs devoid of baculoviruses and baculovirus-derived proteins

highlights the use of this production system, especially in combination to production methodologies that enable the increase in maximum cell concentration and subsequently the final VLP titers [35]. Furthermore, more research is required to integrate genetic elements such as the homologous region *hr*5 [36] or stronger promoters that also allow for titer improvement.

Stability assessment of GageGFP stable pools

The performance of Sf9 and High Five GageGFP stable pools was evaluated during the course of a month (Figure 7). In both cases, the specific GageGFP fluorescence levels were maintained, indicating that GageGFP production was stable and was not subjected to variations in production due to a prolonged time in culture.

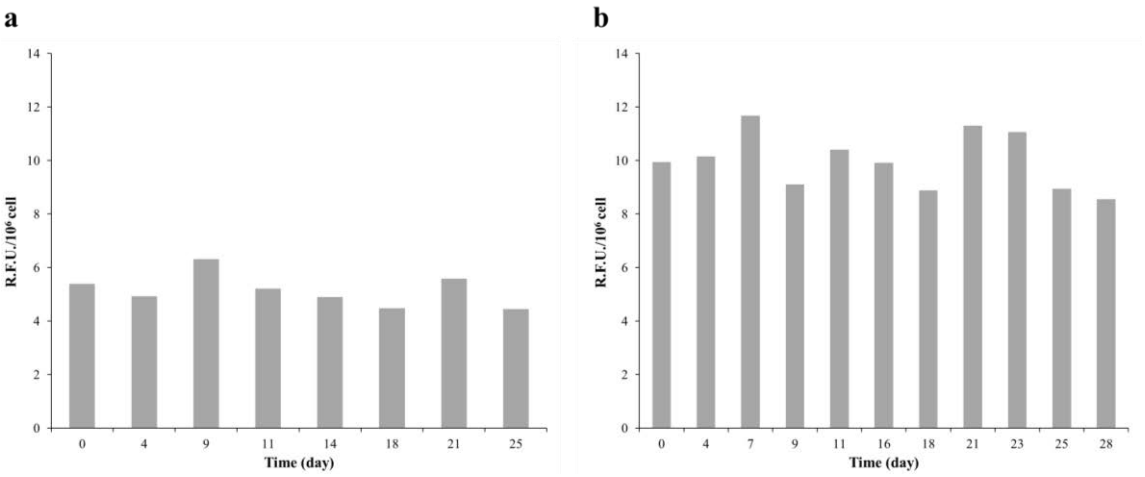

Figure 7. Analysis of the production levels of GageGFP stable pools. (a – b) Intracellular GageGFP fluorescence in Sf9 (a) and High Five stable pools (b) measure by spectrofluorometry. Cells were maintained in the exponential phase during the course of the stability experiment.

Overall, the development of stable cell pools represents a robust strategy to produce VLPs. The demonstration of production stability over time opens the possibility of using perfusion to substantially increase the final VLPs, particularly with alternating tangential flow filtration, which has recently been proven successful to produce influenza VLPs [37]. High Five stable pools showed higher specific VLP production yields than Sf9 cells, but this difference could be improved if further optimization of cell culture media for High Five cells is achieved since current media do not allow to achieve cell concentrations as high as those achieved in Sf9 cell cultures.

On the other hand, Sf9 GageGFP stable pools could also be an interesting option considering the 3.4-fold reduction in the production of EVs in comparison to High Five cells, which would facilitate the separation of these nanoparticles in the downstream processing.

The method selected to develop the stable pools was random integration and the production levels were similar to those offered by other non-targeted gene integration strategies such as the Piggy-Bac™ transposon [32], which theoretically seeks for highly active transcription regions, or directed integration by recombinase-mediated cassette exchange [21,29]. These methodologies have a higher advantage in finding high producer clones, but random integration also offers an attractive means to develop stable cell pools.

Cell heterogeneity has been one of the major arguments against protein production in stable pools. However, recent works have reported that heterogeneity is also present to a large extent in cells derived from an individual clone [38,39]. Other studies are starting to change their rationale and give more emphasis to the productivity of the system and the quality of the product produced, instead of whether the producing cells are mono- or polyclonal [40]. Then, the development of stable cell pools is shown as an attractive approach for the stable production of simple and more complex recombinant products. The time and efforts required to generate a stable cell line originated from an individual clone might not be worth if a substantial difference with stable pools is not achieved. In this work, similar production levels to those from stable insect cell lines [21,29] are reported.

Conclusions

The generation of Sf9 and High Five stable pools producing mCherry and GageGFP VLPs has been achieved in this work. The methodology employed was based on random gene of interest integration and pool enrichment using FACS.

This approach proved to be a fast and reliable strategy to produce recombinant proteins since stable pools were developed in a reduced window of time of 7 weeks for High Five cells and 10 weeks for Sf9 cells. The development times were higher than that required for TGE but shorter in comparison to the generation of clonal cell lines with a clonal origin. Furthermore, production levels of mCherry and GageGFP VLPs were in the range of other stable production systems but, in this case, requiring a shorter development time line. mCherry production levels were comparable to titers offered the BEVS and TGE, but VLP production was not competitive in comparison to TGE but specially with the BEVS. More rounds of sorting should allow for the selection of an even more reduced percentage of a high producer population in order to achieve larger VLP yields.

The main advantages of the stable production system reported here is that a continuous expression of the recombinant product is possible, and that the final titer depends on the maximum viable cell concentration attained. Therefore, process intensification by means of culture perfusion is an interesting approach to increase cell density and recombinant protein titers. This type of strategy is especially suited for stably producing systems since inoculation of the seed culture and medium perfusion are the only step required. Conversely, the use of perfusion in baculovirus or TGE-based production platforms requires the addition/s of baculovirus or DNA, which entail a higher degree of complexity and can economically and technically limit its application.

Acknowledgements

The authors would like to thank Dr. Paula Alves (Instituto de Biologia Experimental e Tecnológica, Oeiras, Portugal) for providing the BTI-TN-5B1-4 cell line and the pIZTV5-his plasmid, and Dr. Nick Berrow (Institute for Research in Biomedicine, Barcelona, Spain) for providing the Sf9 cell line. Ángel Calvache (Beckman Coulter) facilitated the access to CytoFlex LX flow cytometer. The support of Núria Barba (Servei de Microscòpia, UAB) and Manuela Costa (Servei de Cultius Cel·lulars, Producció d'Anticossos i Citometria, UAB) with confocal

microscopy and flow cytometry is appreciated. Irene González-Domínguez (Departament d'Enginyeria Química, Biològica i Ambiental, UAB) developed the mCherry standard curve and Sahar Masoumeh (University of Natural Resources and Life Sciences, Vienna, Austria) provided support in the ELISA quantification. Eduard Puente-Massaguer is a recipient of an FPU grant from Ministerio de Educación, Cultura y Deporte of Spain (FPU15/03577). The research group is recognized as 2017 SGR 898 by Generalitat de Catalunya.

Compliance with Ethical Standards

Conflict of interest

The authors declare that they have no competing interests.

Ethical approval

This article does not contain any studies with human participants performed by any of the authors.

References

[1] S. Gutierrez-Granados, L. Cervera, A.A. Kamen, F. Godia, Advancements in mammalian cell transient gene expression (TGE) technology for accelerated production of biologics., Crit. Rev. Biotechnol. 0 (2018) 1–23.

[2] J. Fuenmayor, L. Cervera, F. Gòdia, A. Kamen, Extended gene expression for Gag VLP production achieved at bioreactor scale, J. Chem. Technol. Biotechnol. 94 (2019) 302–308.

[3] S. Gutierrez-Granados, L. Cervera, M. de las M.M. de L.M.M. de las M. Segura, J. Wolfel, F. Godia, S. Gutiérrez-Granados, L. Cervera, M. de las M.M. de L.M.M. de las M. Segura, J. Wölfel, F. Gòdia, S. Gutierrez-Granados, L. Cervera, M. de las M.M. de L.M.M. de las M. Segura, J. Wolfel, F. Godia, S. Gutiérrez-Granados, L. Cervera, M. de las M.M. de L.M.M. de las M. Segura, J. Wölfel, F. Gòdia, Optimized production of HIV-1 virus-like particles by transient transfection in CAP-T cells, Appl. Microbiol. Biotechnol. 100 (2016) 3935–3947.

[4] S. Ansorge, S. Lanthier, J. Transfiguracion, Y. Durocher, O. Henry, A. Kamen, Development of a scalable process for high-yield lentiviral vector production by transient transfection of HEK293 suspension cultures, J. Gene Med. 11 (2009) 868–876.

[5] T. Gaj, C.A. Gersbach, C.F. Barbas, ZFN, TALEN, and CRISPR/Cas-based methods for genome engineering, Trends Biotechnol. 31 (2013) 397–405.

[6] Q.V. Phan, J. Contzen, P. Seemann, M. Gossen, Site-specific chromosomal gene insertion: Flp recombinase versus Cas9 nuclease, Sci. Rep. 7 (2017) 17771.

[7] J. Davies, M. Reff, Chromosome localization and gene-copy-number quantification of three random integrations in Chinese-hamster ovary cells and their amplified cell lines using fluorescence in situ hybridization, Biotechnol. Appl. Biochem. 33 (2001) 99.

[8] C. Lattenmayer, M. Loeschel, W. Steinfellner, E. Trummer, D. Mueller, K. Schriebl, K.

Vorauer-Uhl, H. Katinger, R. Kunert, Identification of transgene integration loci of different highly expressing recombinant CHO cell lines by FISH, Cytotechnology. 51 (2006) 171–182.

[9] J.J. Priola, N. Calzadilla, M. Baumann, N. Borth, C.G. Tate, M.J. Betenbaugh, High-throughput screening and selection of mammalian cells for enhanced protein production, Biotechnol. J. 11 (2016) 853–865.

[10] W. Pilbrough, T.P. Munro, P. Gray, Intraclonal protein expression heterogeneity in recombinant CHO cells, PLoS One. 4 (2009) e8432.

[11] T. Tharmalingam, H. Barkhordarian, N. Tejeda, K. Daris, S. Yaghmour, P. Yam, F. Lu, C. Goudar, T. Munro, J. Stevens, Characterization of phenotypic and genotypic diversity in subclones derived from a clonal cell line, Biotechnol. Prog. 34 (2018) 613–623.

[12] J. Ye, K. Alvin, H. Latif, A. Hsu, V. Parikh, T. Whitmer, M. Tellers, M.C. de la Cruz Edmonds, J. Ly, P. Salmon, J.F. Markusen, Rapid protein production using CHO stable transfection pools, Biotechnol. Prog. 26 (2010) 1431–1437.

[13] Y. Rajendra, S. Balasubramanian, N.A. McCracken, D.L. Norris, Z. Lian, M.G. Schmitt, C.C. Frye, G.C. Barnard, Evaluation of piggyBac-mediated CHO pools to enable material generation to support GLP toxicology studies, Biotechnol. Prog. 33 (2017) 1436–1448.

[14] A. Poulain, S. Perret, F. Malenfant, A. Mullick, B. Massie, Y. Durocher, Rapid protein production from stable CHO cell pools using plasmid vector and the cumate gene-switch, J. Biotechnol. 255 (2017) 16–27.

[15] J.A. Mena, A.A. Kamen, Insect cell technology is a versatile and robust vaccine manufacturing platform, Expert Rev. Vaccines. 10 (2011) 1063–1081.

[16] J.L. Hye, K.K. Yeon, S.H. Dong, J.C. Hyung, Expression of functional human transferrin in stably transfected Drosophila S2 cells, Biotechnol. Prog. 20 (2004) 1192–1197.

[17] F. Fernandes, M.M. Dias, J. Vidigal, M.F.Q. Sousa, M. Patrone, A.P. Teixeira, P.M. Alves, Production of rotavirus core-like particles in Sf9 cells using recombinase-mediated cassette exchange, J. Biotechnol. 171 (2014) 34–38.

[18] Z. Shoja, M. Tagliamonte, S. Jalilvand, T. Mokhtari-Azad, R. Hamkar, S. Shahmahmoodi, F. Rezaei, M. Tornesello, F.M. Buonaguro, L. Buonaguro, R. Nategh, Development of a stable insect cell line constitutively expressing rotavirus VP2, Virus Res. 172 (2013) 66–74.

[19] L. Hermida-Matsumoto, M.D. Resh, Localization of human immunodeficiency virus type 1 Gag and Env at the plasma membrane by confocal imaging., J. Virol. 74 (2000) 8670–8679.

[20] N.S. Berrow, D. Alderton, S. Sainsbury, J. Nettleship, R. Assenberg, N. Rahman, D.I. Stuart, R.J. Owens, A versatile ligation-independent cloning method suitable for high-throughput expression screening applications, Nucleic Acids Res. 35 (2007) e45.

[21] J. Vidigal, B. Fernandes, M.M. Dias, M. Patrone, A. Roldão, M.J.T. Carrondo, P.M. Alves, A.P. Teixeira, RMCE-based insect cell platform to produce membrane proteins captured on HIV-1 Gag virus-like particles, Appl. Microbiol. Biotechnol. 102 (2018) 655–666.

[22] G.M. Ehrenfeld, D.C. Heimbrook, S.M. Hecht, J.B. Shipley, H. Sugiyama, E.C. Long, J.H. van Boom, G.A. van der Marel, N.J. Oppenheimer, Copper-Dependent Cleavage of DNA by Bleomycin, Biochemistry. 26 (1987) 931–942.

[23] S.G. Chankova, E. Dimova, M. Dimitrova, P.E. Bryant, Induction of DNA double-strand breaks by zeocin in Chlamydomonas reinhardtii and the role of increased DNA double-strand breaks rejoining in the formation of an adaptive response, Radiat. Environ. Biophys. 46 (2007) 409–416.

[24] T.A. Pfeifer, D.D. Hegedus, T.A. Grigliatti, D.A. Theilmann, Baculovirus immediate-early promoter-mediated expression of the Zeocin resistance gene for use as a dominant

selectable marker in Dipteran and Lepidopteran insect cell lines, Gene. 188 (1997) 183–190.

[25] T. Okumura, K. Masuda, K. Watanabe, K. Miyadai, K. Nonaka, M. Yabuta, T. Omasa, Efficient enrichment of high-producing recombinant Chinese hamster ovary cells for monoclonal antibody by flow cytometry, J. Biosci. Bioeng. 120 (2015) 340–346.

[26] J. Pichler, S. Galosy, J. Mott, N. Borth, Selection of CHO host cell subclones with increased specific antibody production rates by repeated cycles of transient transfection and cell sorting, Biotechnol. Bioeng. 108 (2011) 386–394.

[27] J. Vidigal, M.M. Dias, F. Fernandes, M. Patrone, C. Bispo, C. Andrade, R. Gardner, M.J.T. Carrondo, P.M. Alves, A.P. Teixeira, A cell sorting protocol for selecting high-producing sub-populations of Sf9 and High Five™ cells, J. Biotechnol. 168 (2013) 436–439.

[28] L. Cherbas, J. Hackney, L. Gong, C. Salzer, E. Mauser, D. Zhang, P. Cherbas, Tools for targeted genome engineering of established drosophila cell lines, Genetics. 201 (2015) 1307–1318.

[29] F. Fernandes, J. Vidigal, M.M. Dias, K.L.J. Prather, A.S. Coroadinha, A.P. Teixeira, P.M. Alves, Flipase-mediated cassette exchange in Sf9 insect cells for stable gene expression, Biotechnol. Bioeng. 109 (2012) 2836–2844.

[30] Y. Durocher, S. Perret, A. Kamen, High-level and high-throughput recombinant protein production by transient transfection of suspension-growing human 293-EBNA1 cells., Nucleic Acids Res. 30 (2002) E9.

[31] F. Monteiro, V. Bernal, X. Saelens, A.B. Lozano, C. Bernal, A. Sevilla, M.J.T. Carrondo, P.M. Alves, Metabolic profiling of insect cell lines: Unveiling cell line determinants behind system's productivity, Biotechnol. Bioeng. 111 (2014) 816–828.

[32] A.G. Lynch, F. Tanzer, M.J. Fraser, E.G. Shephard, A.L. Williamson, E.P. Rybicki, Use of the piggyBac transposon to create HIV-1 gag transgenic insect cell lines for continuous

VLP production, BMC Biotechnol. 10 (2010) 30.

[33] M. Tagliamonte, M.L. Visciano, M.L. Tornesello, A. De Stradis, F.M. Buonaguro, L. Buonaguro, Constitutive expression of HIV-VLPs in stably transfected insect cell line for efficient delivery system, Vaccine. 28 (2010) 6417–6424.

[34] L. Yang, Y. Song, X. Li, X. Huang, J. Liu, H. Ding, P. Zhu, P. Zhou, HIV-1 virus-like particles produced by stably transfected Drosophila S2 cells: a desirable vaccine component., J. Virol. 86 (2012) 7662–76.

[35] S.M. Deutschmann, V. Jäger, Optimization of the growth conditions of Sf21 insect cells for high-density perfusion culture in stirred-tank bioreactors., Enzyme Microb. Technol. 16 (1994) 506–12.

[36] M. Bleckmann, M. Schürig, F.F. Chen, Z.Z. Yen, N. Lindemann, S. Meyer, J. Spehr, J. Van Den Heuvel, Identification of essential genetic baculoviral elements for recombinant protein expression by transactivation in Sf21 insect cells, PLoS One. 11 (2016) 1–19.

[37] J. Hong, J. Demirji, D. Blackstock, J. Lee, T. Dinh, A. Goh, F. Arnold, J. Horwitz, Development of an alternating tangential flow (ATF) perfusion-based transient gene expression (TGE) bioprocess for universal influenza vaccine, Biotechnol. Prog. (2019) e2831.

[38] S. Vcelar, M. Melcher, N. Auer, A. Hrdina, A. Puklowski, F. Leisch, V. Jadhav, T. Wenger, M. Baumann, N. Borth, Changes in Chromosome Counts and Patterns in CHO Cell Lines upon Generation of Recombinant Cell Lines and Subcloning, Biotechnol. J. 13 (2018) 1700495.

[39] S. Vcelar, V. Jadhav, M. Melcher, N. Auer, A. Hrdina, R. Sagmeister, K. Heffner, A. Puklowski, M. Betenbaugh, T. Wenger, F. Leisch, M. Baumann, N. Borth, Karyotype variation of CHO host cell lines over time in culture characterized by chromosome counting and chromosome painting, Biotechnol. Bioeng. 115 (2018) 165–173.

[40] C. Frye, R. Deshpande, S. Estes, K. Francissen, J. Joly, A. Lubiniecki, T. Munro, R. Russell, T. Wang, K. Anderson, Industry view on the relative importance of "clonality" of biopharmaceutical-producing cell lines, Biologicals. 44 (2016) 117–122.

Overall discussion and future directions

In this thesis, different approaches for production of HIV-1 GageGFP VLPs in Sf9 and High Five insect cell lines have been evaluated. These strategies include the baculovirus expression vector system (BEVS), transient gene expression (TGE) and stable gene expression (SGE). The production of Gag VLPs has been reported in insect cells, mainly with the *Autographa californica* multiple nucleopolyhedrovirus (*Ac*MNPV) BEVS. However, most of the process and product characterization performed thus far have been conducted by means of indirect methods. The analysis of VLPs in their native conditions, as well as, the presence of other nanoparticle population has been addressed in detail here. In addition, a better comprehension of the different systems has been achieved by Design of Experiments (DoE) in which several objective responses have been considered and combined. TGE and SGE have also been studied as alternatives to produce Gag VLPs overcoming the co-production of baculoviruses. In all cases, GageGFP VLPs were correctly formed but differences in the final VLP titers and contaminating nanoparticles were measured. In this section, a comparison of the two cell lines for each of the production systems is initially conducted and followed by a global comparison between the different platforms. All the discussion is centered in the production of GageGFP VLPs.

Overall, this thesis focuses on the optimization of the upstream part of each production system introducing as well an initial characterization of the obtained crude VLP preparations. The relevance of the downstream processing part in these bioprocesses is also recognized although it could not be evaluated in this thesis. However, current studies of the research group are specifically working on this topic to achieve a complete process that integrates both the upstream and downstream sections.

A key aspect in any given bioprocess, especially when developing a biopharmaceutical product, is the selection of a cell culture medium that enables standardization and reproducibility and avoids the use of animal-derived methods for safety consideration, being of particular interest to use chemically defined media. A limitation of insect cell culture media most extensively used in the past is the addition of serum, and when serum is avoided, the presence of protein hydrolysates [1]. Among the commercial media available at the beginning of this thesis, the Sf900III medium was selected since it is an animal origin-free low-hydrolysate formulation. This medium is

designed for Sf9 cells, but High Five cells were successfully adapted to it by progressive addition of Sf900III medium and cell culture passaging.

In the first chapter, Sf9 and High Five cells are evaluated as platforms to produce GageGFP VLPs with the BEVS under identical conditions of multiplicity of infection (MOI), viable cell concentration at infection (CCI) and time of harvest (TOH). The aim of this work is to set up the characterization techniques for both platforms and perform an initial comparison based on standard production conditions. Fluorescence quantification results in superior fluorescence yields for High Five cells, but direct quantification of VLPs using nanoparticle tracking analysis (NTA) yields higher VLP titers for Sf9 cells. This indicates that the correlation of the fluorescence measurements with the amount of GageGFP assembled as VLPs is not accurate [2]. Even though this could be expected at low viabilities due to intracellular GageGFP release to the culture medium, it is already observed at relatively high viabilities (>80 %). Then, although spectrofluorometry is a fast and affordable technique for indirect GageGFP VLP quantification, this technique should be carefully taken into consideration for absolute quantification if used alone since one could be incurring in titer overestimation. This methodology, which has been applied for GageGFP VLP quantification in a variety of cell lines including HEK 293 [3] and CAP cells [4], would benefit from GageGFP monomer separation techniques such as sucrose cushion ultracentrifugation, as shown in chapter 1.

Analysis of both insect cell lines by flow cytometry detects remarkable differences in terms of cell complexity upon baculovirus infection. First analyses point in the direction of vesicle-like structures in High Five cells that could explain the increasing cell complexity, but confocal microscopy shows that this phenotype is not widespread in all cells. A significant difference is detected when characterizing the cell supernatant with cryogenic transmission electron microscopy. A higher proportion of occlusion-derived baculovirus (ODV) is present in High Five-derived supernatants which could explain this increase in cell complexity. The ODVs are formed in the nuclear membrane of the infected cell which indicates that these specimens can only be released to the supernatant when cells lyse [5]. However, viabilities are similar at harvest, probably indicating a higher tendency of High Five cells to produce ODVs. Additionally, small

nanoparticles are encountered in High Five cell supernatants which could be related to exosomes, but some of these particles exhibit an icosahedral-like structure that could be associated to *Alphanodaviruses*. The presence of enveloped virus-like structures with multiple spikes in the lipid membrane is also detected but more research is required for a better comprehension of these specimens since their origin has not been identified. It has been recently reported that some insect cell lines are persistently infected by various adventitious viruses [6]. Regarding High Five cells, *Alphanodaviruses* were first described by Li and co-workers in 2007 [7] and have been detected as the principal contaminating virus of this cell line. For Sf9 cells, the Sf-rhabdovirus was discovered at the Center for Biologicals Evaluation and Research in 2014 [8]. In both cases, none of these contaminating viruses has shown to be pathogenic for humans thus far [6] and proof of that is the fact that some marketed biopharmaceuticals are being produced in these cell lines [9]. Virus-free insect cell lines are also being developed, such as the *Spodoptera frugiperda* rhabdovirus-free [10] and the *Trichoplusia ni*-derived QBTn9-4s [11], TnT4 [12], Tnao38 [13] and Tnms42 cells [14].

The comparison study conducted in chapter 1 results in Sf9 cells as the best platform to produce GageGFP VLPs. However, this study is performed in non-optimal conditions for both systems. In chapter 2, an optimization process is carried out integrating DoE with different objective responses and multiple criteria decision analysis. A DoE-based approach is selected after observing that previous studies targeting Gag VLP production maximization with the BEVS have been performed in a one-factor-at-a-time experimental approach [15,16], which hinders the determination of factor synergies in the achievement of optimal production conditions. Furthermore, the studies conducted so far have been made in serum-containing [15] or high-protein hydrolysate media [16]. The application of direct evaluation techniques to monitor the GageGFP VLP production process and for VLP quantification is also included to avoid VLP titer overestimation and the calculation of VLP concentration only based on correlations [17,18]. The optimal conditions for Sf9 cells are found at lower multiplicities of infection (MOI) and longer times of harvest (TOH) compared to High Five cells. The fact that low MOI are associated to longer TOH is to be expected since more than one round of baculovirus infection is required to

complete the infection process, which extends the time required to achieve the maximal VLP production. However, the reasons leading to the differences in MOI could be related to a combined effect of the cell growth kinetics of High Five cells and the cell culture media employed. A revision of different research studies conducted with High Five cells for VLP production using the BEVS indicates that moderate to high MOI (> 0.5 – 1) are best suited for VLP production in this cell line [19–21]. Interestingly, the cell growth kinetics of High Five cells is faster (~16 – 19 h duplication time) than that of Sf9 cells but the *Ac*MNPV infection do not progress as rapid as in Sf9 cells considering their accelerated cell growth, as shown in chapter 1. Then, it is possible that nutrients in the medium cannot sustain VLP production at lower MOI since these conditions require from larger TOH. On the contrary, a broader spectrum of commercial media is available for Sf9 cells and some of them can maintain cell growth to higher viable cell concentrations than media for High Five cells, the duplication time is slower (~23 – 25 h) and *Ac*MNPV baculovirus infection progresses more rapidly. These features introduce the possibility of finding the best production with lower MOI as shown in chapter 2. However, research studies conducted with this cell line for VLP production include the possibility of low [22,23] and high MOI [24,25], possibly due to differences in cell performance depending on the nutrient composition of the selected culture medium. Further analyses are currently being performed to better understand these differences in the optimal production conditions.

Maximization of VLP production in both cell lines using the BEVS result in similar VLP titers for the optimal conditions maximizing total VLP production (quantity optimum) (Table 1). However, comparison of specific VLP production yield a 3.2-fold increase for High Five cells. The optimized conditions for Sf9 cells are a useful option to achieve a high VLP concentration in batch culture with a lower proportion of contaminating nanoparticles and a better GageGFP assembling as VLPs. However, if a lower level of baculoviruses is required to decrease their interference with the target function of VLPs, the High Five optimum is of interest since a 3.2-fold reduction in baculovirus titers is achieved (Table 1). Furthermore, the development of commercial media that sustain higher viable cell concentration for this cell line could probably increase the final VLP titer. An alternative to reduce the number of baculovirus species and

increase the GageGFP assembly efficiency at expenses of reducing the VLP titer is to use the optimal conditions identified when optimization is performed to maximize the degree of assembled VLPs (referred as quality optimum). Taking into account the amount of GageGFP that remains inside the infected cells, especially in High Five cells, the co-expression of chaperons could improve their secretion in the form of VLPs [26]. Both optimal conditions are proposed as a useful strategy to achieve a high level of GageGFP VLPs but also for other VLP types, fusion proteins between the matrix and envelope and biochemical conjugation. Nevertheless, if protein complexes require the expression of more than one gene, an adjustment of the infection conditions and the production strategy (co-infection or co-expression) should be carefully evaluated [27,28]. VLP production by transient gene expression is explored in chapter 3. Initially, the conditions for polyethylenimine (PEI)-TGE in both insect cell lines are determined. This method is assessed as a strategy for fast VLP production eliminating the presence of baculovirus. Insect cell TGE is an emerging field in the production of recombinant products and few information is available in the literature. To date, a reduced number of immediate early promoters are known for insect cells, and among them the OpIE2 promoter from *Orgya pseudotsugata* multicapsid nucleopolyhedrovirus [29], which has been used in this thesis, has proven to be the strongest in both cell lines [30]. Nonetheless, more research is required to discover new promoters that boost TGE protein production in this system since VLP titers were significantly lower than those reported with the BEVS.

Medium replacement proves to be beneficial to achieve the highest transfection yields in both insect cell lines. For High Five cells, medium exchange is required to bear the toxic effect of PEI without a dramatic decrease in cell viability, whereas for Sf9 cells this step is needed to concentrate cells at a high viable cell density. However, the development of chemically-defined media enabling efficient transfection without medium replacement is desirable in the future. Approximately the double of PEI is required for each High Five cell to achieve the best TGE yields while DNA concentrations are similar for both cell lines. These optimal transfection conditions are in the range of DNA:PEI ratios used for TGE in other animal cell lines [31,32]. In terms of GageGFP VLP production, Sf9 cells achieve an 8.4-fold larger amount of these

nanoparticles and also a 2.7-fold considering specific VLP production (Table 1). However, a decrease in the titer is observed for Sf9-derived VLPs from 48 hpt onwards while VLPs produced in High Five cells do not decrease during the 72-h production phase. Although Sf9 cells prove to be more efficient for PEI-mediated GageGFP VLP production, the development of better chemically-defined cell culture for High Five cells could enhance VLP production. Additionally, the DNA plasmid used for TGE could be improved by the inclusion of the enhancer homologous region *hr*5, which has been recently reported to increase the production levels in combination to the OpIE2 promoter [33,34].

VLP production by means of stable expressing cell pools is also tested as a system for baculovirus-free GageGFP VLP production. A general criticism of stable cell pools is the fact that heterogeneity is higher compared to clonal cell lines. Nevertheless, heterogeneity has also been demonstrated to occur for clonal cell lines during cell growth along a culture process, with the presence of higher, medium and lower producer cells within the same clonal cell line culture after a number of generations [35]. Then, it is not clear if the efforts required to develop a stable cell line are providing a substantial advantage and clonal versus pool production is more on the discussion nowadays [36]. In this thesis, stable pools are generated as a system for rapid protein production in a stable manner. The selection of the high producer GageGFP expressing cells is performed taking advantage of the eGFP fluorescent reporter by fluorescence-activated cell sorting (FACS). This strategy is not only used in the development of stable cell pools but also in the selection of the high producer cells during the individual cell screening process of generating a stable cell line with a clonal origin [37]. This approach has proven interesting since it is then possible to replace the fluorescent gene of the cells within pools or in individual clone with another gene of interest (GOI) [38]. The application of fluorescence-based techniques has widened to targeting non-fluorescent top producers based on fluorescent antibody staining. However, this approach was limited to membrane or secreted recombinant products since it is difficult to select for high producer cells whether the product of interest is being produced intracellularly. In this case, a permeabilization of the cell membrane was required which compromised cell integrity. Recently, a fluorescence technique based on the measurement of the

mitochondrial membrane potential that correlates with the intracellular protein production levels has been developed [39]. This methodology holds a great potential of application for instance in the detection of high producing cells for scaffold proteins such as the HIV-1 Gag or influenza M1, thus avoiding the fusion of a fluorescent reporter to the GOI.

GageGFP VLP production titers in stable pools are 3.7-fold higher in the High Five compared to the enriched Sf9 cell pool and 8-fold considering specific cell production. In this case, High Five cells prove to be a better alternative for stable VLP production despite higher levels of contaminating particles are detected (Table 1). Differences in specific production for both cells might be explained by a higher tendency of High Five cells to integrate multiple copies of foreign DNA or integration in genome "hot-spots". More research is required to elucidate this and the recently published *Trichoplusia ni* genome should provide insights in this respect [40,41]. The stability of both stable cell pools for VLP production is successfully validated, which supports the potential use of this stable production strategy. Random integration is the most common method for stable gene expression, and it is the strategy adopted to create the stable cell pools in this thesis. Transposons are another methodology of random integration with the difference that they specifically target genomic loci of high expression. The Piggy-Bac™ transposon has been used to develop Gag stable Sf9 cell pools achieving comparable levels to the ones here reported [42]. Similar results are also observed for Gag VLP production in stable Sf9 cell lines developed using recombinase-mediated cassette exchange [38]. On the other hand, significantly lower Gag titers are observed in comparison to Drosophila S2 cells [43] and stable High Five cell lines [44]. From a molecular biology perspective, the use of stronger promoters and the inclusion of enhancer regions should facilitate an increase in the VLP titer in the same way as for TGE.

Table 1. Comparison of nanoparticle production levels of the different expression systems by flow virometry.

	High Five			Sf9		
	VLP concentration (10^6 par./mL)	**Total nanoparticle concentration (10^6 par. /mL)**	**Baculovirus titer (10^7 par. /mL)**	**VLP concentration (10^6 par./mL)**	**Total nanoparticle concentration (10^6 par. /mL)**	**Baculovirus titer (10^7 par. /mL)**
BEVS Quantity	2973.5 ± 50.4	10995.8 ± 837.3	13.2 ± 5.1	3297.9 ± 251.3	8180.2 ± 871.2	42.5 ± 19.1
TGE	2.9 ± 0.7	394.9 ± 56.9	-	24.7 ± 3.5	237.4 ± 32.2	-
SGE (pool)	1.5 ± 0.1	745.4 ± 88.1	-	0.4 ± 0.1	437.3 ± 55.7	-

Overall, different strategies are tested to produce GageGFP VLPs in Sf9 and High Five cells. The BEVS yield the highest VLP titers in comparison to TGE and SGE. The Sf9/BEVS is shown as the best strategy to produce GageGFP VLPs and it is proposed as a reference system to produce these nanoparticles. VLP yields and productivity in the BEVS are higher in comparison to the reference system of mammalian-based TGE [3,4], even combined with tailored additive supplementation [45] or gene inhibition strategies [18]. However, if the presence of baculovirus or baculovirus-derived proteins such as GP64 pose a risk for the final VLP application, other alternatives should be evaluated. Although some progress has been made in the separation of Gag VLPs from baculovirus with anion exchange chromatography [46], a complete separation of both specimens has not yet been achieved. Other studies have focused on the elimination of the GP64 envelope protein, which is a major responsible of spreading *Ac*MNPV infection, but the elimination of this protein has come at expenses of reducing the Gag VLP yields and infection also requires from significantly higher MOI to be fully completed [47]. Transient and stable production provide an advantageous platform to produce VLPs and other complex nanoparticles devoid of baculovirus and baculovirus-derived proteins. TGE GageGFP VLP yields achieved in this thesis in both insect cells are lower to that obtained in TGE with mammalian cells such as the HEK 293 cell line [3]. In this sense, TGE in insect cells could also benefit from production enhancement strategies developed for these cell lines to increase the VLP titers [18,45]. Still, efforts should be maintained in further optimizing TGE to take advantage of the unique properties offered by insect cells, including their high biosafety level due to lack of known human pathogens

and higher tolerance to by-products. Regarding SGE, lower VLP titers are achieved in comparison to TGE probably because higher levels of transitory DNA incorporation into the cells are achieved in the latter. Nevertheless, the continuou production of GageGFP VLPs is worth considering and especially if it is possible to increase the viable cell concentration since production is proportional to the number of viable cells [48]. Strategies based on fed-batch or cell culture perfusion would be an interesting approximation. Perfusion of Sf9 cells has been achieved using hollow fiber membranes [49] and acoustic filters [50] but advancements in the retention device technology such as the alternating tangential flow filtration (ATF) could result in higher yields. Proof of that is the successful application of the ATF system for stable protein production in Drosophila S2 cells [51]. This system has also proven useful for baculovirus-based protein production [52] and, in this case, a re-definition of the optimal conditions here developed would be required since they were determined to obtain the maximum VLP yield in batch mode. The use of perfusion in TGE is hitherto unknown though it should provide the conditions to increase transient VLP titers given that it has been recently demonstrated to work for influenza VLP production in HEK 293 cells [53].

The combination of several of these approaches has also been applied for recombinant protein production but was not explored in this thesis. For instance, TGE has been coupled to the BEVS as a strategy to avoid the time required to develop the working stock of the baculovirus and rapidly screen a variety of GOI [54]. This methodology termed as “transactivation” has proven to achieve protein production levels in between the TGE and BEVS [34] and their potential applications include multiple gene expression and the use in conjunction with stable producing cells. A similar strategy combining SGE with the BEVS has been recently reported for the production of influenza VLPs as a way to control multigenic expression and avoid genetic instability [55].

The results shown in this thesis by the application of direct nanoparticle quantification and characterization techniques make clear that the problem of contaminating particles goes beyond the presence of baculoviruses. Extracellular vesicles are present along with VLPs and are revealed as highly heterogeneous. A step forward has been achieved in this thesis by identifying which of these nanoparticles correspond to VLPs but there is still a requirement to properly isolate the

different extracellular vesicle populations. Some reports have been recently published in this respect based on chromatographic techniques but difficulties are still encountered to achieve a complete separation [56–58]. In addition, more research is needed to understand the relevance of extracellular vesicles in insect cell lines and their impact in biotechnological production processes. In this sense, future research should go in the line of integrating technologies with an improved nanoparticle resolution capacity and incorporate the possibility to stain specific markers to untangle each particular population.

The present work combines the use of rational development and advanced quantification and characterization techniques to produce and characterize GageGFP VLPs. The conditions here developed enable the production of GageGFP VLP and potentially other complex nanoparticles in a variety of systems. The BEVS is proposed as the reference platform since the highest VLP yields are achieved but TGE and SGE emerge as an interesting alternative if the final application of the VLPs is not compatible with baculovirus or derived proteins. Current work is focused on studying the nutritional requirements of each specific platform with the final goal to transfer these optimal conditions to bioreactor scale. The systems developed in this thesis will serve as the basis for future studies aiming to combine the expression of Gag VLPs with other recombinant products for targeted delivery or to increase their immunogenicity as vaccines.

References

[1] L. Ikonomou, Y.-J. Schneider, S.N. Agathos, Insect cell culture for industrial production of recombinant proteins, Appl. Microbiol. Biotechnol. 62 (2003) 1–20.

[2] S. Gutiérrez-Granados, L. Cervera, F. Gòdia, J. Carrillo, M.M. Segura, Development and validation of a quantitation assay for fluorescently tagged HIV-1 virus-like particles, J. Virol. Methods. 193 (2013) 85–95.

[3] L. Cervera, S. Gutiérrez-Granados, M. Martínez, J. Blanco, F. Gòdia, M.M. Segura, Generation of HIV-1 Gag VLPs by transient transfection of HEK 293 suspension cell cultures using an optimized animal-derived component free medium, J. Biotechnol. 166 (2013) 152–165.

[4] S. Gutierrez-Granados, L. Cervera, M. de las M.M. de L.M.M. de las M. Segura, J. Wolfel, F. Godia, S. Gutiérrez-Granados, L. Cervera, M. de las M.M. de L.M.M. de las M. Segura, J. Wölfel, F. Gòdia, S. Gutierrez-Granados, L. Cervera, M. de las M.M. de L.M.M. de las M. Segura, J. Wolfel, F. Godia, S. Gutiérrez-Granados, L. Cervera, M. de las M.M. de L.M.M. de las M. Segura, J. Wölfel, F. Gòdia, Optimized production of HIV-1 virus-like particles by transient transfection in CAP-T cells, Appl. Microbiol. Biotechnol. 100 (2016) 3935–3947.

[5] G.W. Blissard, D.A. Theilmann, Baculovirus Entry and Egress from Insect Cells, Annu. Rev. Virol. 5 (2018) 113–139.

[6] C. Geisler, D.L. Jarvis, Adventitious viruses in insect cell lines used for recombinant protein expression, Protein Expr. Purif. 144 (2018) 25–32.

[7] T.-C. Li, P.D. Scotti, T. Miyamura, N. Takeda, Latent Infection of a New Alphanodavirus in an Insect Cell Line, J. Virol. 81 (2007) 10890–10896.

[8] H. Ma, T.A. Galvin, D.R. Glasner, S. Shaheduzzaman, A.S. Khan, Identification of a novel rhabdovirus in Spodoptera frugiperda cell lines., J. Virol. 88 (2014) 6576–85.

[9] L.A. Palomares, M. Realpe, O.T. Ramírez, An Overview of Cell Culture Engineering for the Insect Cell-Baculovirus Expression Vector System (BEVS), in: Anim. Cell Cult.,

Springer, Cham, 2015: pp. 501–519.

[10] A.B. Maghodia, C. Geisler, D.L. Jarvis, Characterization of an Sf-rhabdovirus-negative Spodoptera frugiperda cell line as an alternative host for recombinant protein production in the baculovirus-insect cell system, Protein Expr. Purif. 122 (2016) 45–55.

[11] M.-J. Meng, T.-L. Li, C.-Y. Li, G.-X. Li, A suspended cell line from *Trichoplusia ni* (Lepidoptera): Characterization and expression of recombinant proteins, Insect Sci. 15 (2008) 423–428.

[12] F. Zhang, M.A. Manzan, H.M. Peplinski, S.M. Thiem, A new Trichoplusia ni cell line for membrane protein expression using a baculovirus expression vector system, Vitr. Cell. Dev. Biol. - Anim. 44 (2008) 214–223.

[13] Y. Hashimoto, S. Zhang, G.W. Blissard, Ao38, a new cell line from eggs of the black witch moth, Ascalapha odorata (Lepidoptera: Noctuidae), is permissive for AcMNPV infection and produces high levels of recombinant proteins, BMC Biotechnol. 10 (2010) 50.

[14] Y.-R. Chen, S. Zhong, Z. Fei, S. Gao, S. Zhang, Z. Li, P. Wang, G.W. Blissard, Transcriptome Responses of the Host Trichoplusia ni to Infection by the Baculovirus Autographa californica Multiple Nucleopolyhedrovirus, J. Virol. 88 (2014) 13781.

[15] S. Pillay, A. Meyers, A.L. Williamson, E.P. Rybicki, Optimization of chimeric HIV-1 virus-like particle production in a baculovirus-insect cell expression system, Biotechnol. Prog. 25 (2009) 1153–1160.

[16] P.E. Cruz, a Cunha, C.C. Peixoto, J. Clemente, J.L. Moreira, M.J. Carrondo, Optimization of the production of virus-like particles in insect cells., Biotechnol. Bioeng. 60 (1998) 408–18.

[17] L. Cervera, S. Gutiérrez-Granados, N.S. Berrow, M.M. Segura, F. Gòdia, Extended gene expression by medium exchange and repeated transient transfection for recombinant protein production enhancement, Biotechnol. Bioeng. 112 (2015) 934–946.

[18] J. Fuenmayor, L. Cervera, C. Rigau, F. Gòdia, Enhancement of HIV-1 VLP production using gene inhibition strategies, Appl. Microbiol. Biotechnol. 102 (2018) 4477–4487.

[19] T. Senger, L. Schädlich, L. Gissmann, M. Müller, Enhanced papillomavirus-like particle production in insect cells, Virology. 388 (2009) 344–353.

[20] F. Krammer, T. Schinko, D. Palmberger, C. Tauer, P. Messner, R. Grabherr, Trichoplusia ni cells (High Five™) are highly efficient for the production of influenza A virus-like particles: A comparison of two insect cell lines as production platforms for influenza vaccines, Mol. Biotechnol. 45 (2010) 226–234.

[21] G.R.-L.L. Chang, S.-Y.Y. Lai, P.-C.C. Chang, M.-Y.Y. Wang, Production of immunogenic one-component avian H7-subtype influenza virus-like particles, Process Biochem. 46 (2011) 1292–1298.

[22] L. Maranga, T.F. Brazao, M.J.T. Carrondo, Virus-like particle production at low multiplicities of infection with the baculovirus insect cell system, Biotechnol. Bioeng. 84 (2003) 245–253.

[23] J. López-Vidal, S. Gómez-Sebastián, J. Bárcena, M. Del Carmen Nuñez, D. Martínez-Alonso, B. Dudognon, E. Guijarro, J.M. Escribano, Improved production efficiency of virus-like particles by the baculovirus expression vector system, PLoS One. 10 (2015) 1–13.

[24] J.M. Wagner, J.D. Pajerowski, C.L. Daniels, P.M. McHugh, J.A. Flynn, J.W. Balliet, D.R. Casimiro, S. Subramanian, Enhanced production of Chikungunya virus-like particles using a high-pH adapted Spodoptera frugiperda insect cell line, PLoS One. 9 (2014) 1–14.

[25] E. Mortola, P. Roy, Efficient assembly and release of SARS coronavirus-like particles by a heterologous expression system, FEBS Lett. 576 (2004) 174–178.

[26] M. Martinez-Alonso, V. Toledo-Rubio, R. Noad, U. Unzueta, N. Ferrer-Miralles, P. Roy, A. Villaverde, Rehosting of Bacterial Chaperones for High-Quality Protein Production, Appl. Environ. Microbiol. 75 (2009) 7850–7854.

[27] S. Sokolenko, S. George, A. Wagner, A. Tuladhar, J.M.S. Andrich, M.G. Aucoin, Co-expression vs . co-infection using baculovirus expression vectors in insect cell culture : Bene fi ts and drawbacks, Biotechnol. Adv. 30 (2012) 766–781.

[28] A. Roldão, H.L.A. Vieira, A. Charpilienne, D. Poncet, P. Roy, M.J.T. Carrondo, P.M.

Alves, R. Oliveira, Modeling rotavirus-like particles production in a baculovirus expression vector system: Infection kinetics, baculovirus DNA replication, mRNA synthesis and protein production, J. Biotechnol. 128 (2007) 875–894.

[29] D.A. Theilmann, S. Stewart, Molecular analysis of the trans-activating IE-2 gene of Orgyia pseudotsugata multicapsid nuclear polyhedrosis virus, Virology. 187 (1992) 84–96.

[30] M. Bleckmann, M.H.-Y. Fritz, S. Bhuju, M. Jarek, M. Schürig, R. Geffers, V. Benes, H. Besir, J. van den Heuvel, Genomic Analysis and Isolation of RNA Polymerase II Dependent Promoters from Spodoptera frugiperda, PLoS One. 10 (2015) e0132898.

[31] J. Fuenmayor, L. Cervera, S. Gutiérrez-Granados, F. Gòdia, Transient gene expression optimization and expression vector comparison to improve HIV-1 VLP production in HEK293 cell lines, Appl. Microbiol. Biotechnol. 102 (2018) 165–174.

[32] M. Derouazi, P. Girard, F.F. Van Tilborgh, K. Iglesias, N. Muller, M. Bertschinger, F.M. Wurm, Serum-free large-scale transient transfection of CHO cells, Biotechnol. Bioeng. 87 (2004) 537–545.

[33] X. Shen, A.K. Pitol, V. Bachmann, D.L. Hacker, L. Baldi, F.M. Wurm, A simple plasmid-based transient gene expression method using High Five cells, J. Biotechnol. 216 (2015) 67–75.

[34] M. Bleckmann, M. Schürig, F.F. Chen, Z.Z. Yen, N. Lindemann, S. Meyer, J. Spehr, J. Van Den Heuvel, Identification of essential genetic baculoviral elements for recombinant protein expression by transactivation in Sf21 insect cells, PLoS One. 11 (2016) 1–19.

[35] J.J. Priola, N. Calzadilla, M. Baumann, N. Borth, C.G. Tate, M.J. Betenbaugh, High-throughput screening and selection of mammalian cells for enhanced protein production, Biotechnol. J. 11 (2016) 853–865.

[36] S. Vcelar, M. Melcher, N. Auer, A. Hrdina, A. Puklowski, F. Leisch, V. Jadhav, T. Wenger, M. Baumann, N. Borth, Changes in Chromosome Counts and Patterns in CHO Cell Lines upon Generation of Recombinant Cell Lines and Subcloning, Biotechnol. J. 13 (2018) 1700495.

[37] F. Fernandes, J. Vidigal, M.M. Dias, K.L.J. Prather, A.S. Coroadinha, A.P. Teixeira, P.M. Alves, Flipase-mediated cassette exchange in Sf9 insect cells for stable gene expression, Biotechnol. Bioeng. 109 (2012) 2836–2844.

[38] J. Vidigal, B. Fernandes, M.M. Dias, M. Patrone, A. Roldão, M.J.T. Carrondo, P.M. Alves, A.P. Teixeira, RMCE-based insect cell platform to produce membrane proteins captured on HIV-1 Gag virus-like particles, Appl. Microbiol. Biotechnol. 102 (2018) 655–666.

[39] L. Chakrabarti, A. Mathew, L. Li, S. Han, J. Klover, T. Albanetti, P. Hawley-Nelson, Mitochondrial membrane potential identifies cells with high recombinant protein productivity, J. Immunol. Methods. 464 (2019) 31–39.

[40] K. Talsania, M. Mehta, C. Raley, Y. Kriga, S. Gowda, C. Grose, M. Drew, V. Roberts, K.T. Cheng, S. Burkett, S. Oeser, R. Stephens, D. Soppet, X. Chen, P. Kumar, O. German, T. Smirnova, C. Hautman, J. Shetty, B. Tran, Y. Zhao, D. Esposito, Genome Assembly and Annotation of the Trichoplusia ni Tni-FNL Insect Cell Line Enabled by Long-Read Technologies, Genes (Basel). 10 (2019) 79.

[41] W. Chen, X. Yang, G. Tetreau, X. Song, C. Coutu, D. Hegedus, G. Blissard, Z. Fei, P. Wang, A high-quality chromosome-level genome assembly of a generalist herbivore, *Trichoplusia ni*, Mol. Ecol. Resour. 19 (2019) 485–496.

[42] A.G. Lynch, F. Tanzer, M.J. Fraser, E.G. Shephard, A.L. Williamson, E.P. Rybicki, Use of the piggyBac transposon to create HIV-1 gag transgenic insect cell lines for continuous VLP production, BMC Biotechnol. 10 (2010) 30.

[43] L. Yang, Y. Song, X. Li, X. Huang, J. Liu, H. Ding, P. Zhu, P. Zhou, HIV-1 virus-like particles produced by stably transfected Drosophila S2 cells: a desirable vaccine component., J. Virol. 86 (2012) 7662–76.

[44] M. Tagliamonte, M.L. Visciano, M.L. Tornesello, A. De Stradis, F.M. Buonaguro, L. Buonaguro, Constitutive expression of HIV-VLPs in stably transfected insect cell line for efficient delivery system, Vaccine. 28 (2010) 6417–6424.

[45] L. Cervera, J. Fuenmayor, I. Gonzalez-Dominguez, S. Gutierrez-Granados, M.M. Segura, F. Godia, I. González-Domínguez, S. Gutiérrez-Granados, M.M. Segura, F. Gòdia, I.

González-Domínguez, S. Gutiérrez-Granados, M.M. Segura, F. Gòdia, I. González-Domínguez, S. Gutiérrez-Granados, M.M. Segura, F. Gòdia, I. Gonzalez-Dominguez, S. Gutierrez-Granados, M.M. Segura, F. Godia, Selection and optimization of transfection enhancer additives for increased virus-like particle production in HEK293 suspension cell cultures, Appl. Microbiol. Biotechnol. 99 (2015) 9935–9949.

[46] P. Gerster, E. Kopecky, N. Hammerschmidt, M. Klausberger, F. Krammer, R. Grabherr, C. Mersich, L. Urbas, P. Kramberger, T. Paril, M. Schreiner, K. Nöbauer, E. Razzazi-fazeli, A. Jungbauer, Purification of infective baculoviruses by monoliths, J. Chromatogr. A. 1290 (2013) 36–45.

[47] L.C.S. Chaves, B.M. Ribeiro, G.W. Blissard, Production of GP64-free virus-like particles from baculovirus-infected insect cells, J. Gen. Virol. 99 (2018) 265–274.

[48] F. Tapia, D. Vázquez-Ramírez, Y. Genzel, U. Reichl, Bioreactors for high cell density and continuous multi-stage cultivations: options for process intensification in cell culture-based viral vaccine production., Appl. Microbiol. Biotechnol. 100 (2016) 2121–32.

[49] S.M. Deutschmann, V. Jäger, Optimization of the growth conditions of Sf21 insect cells for high-density perfusion culture in stirred-tank bioreactors., Enzyme Microb. Technol. 16 (1994) 506–12.

[50] V.M. Gorenflo, T.A. Pfeifer, G. Lesnicki, E.M. Kwan, T.A. Grigliatti, D.G. Kilburn, J.M. Piret, Production of a self-activating CBM-factor X fusion protein in a stable transformed Sf9 insect cell line using high cell density perfusion culture, Cytotechnology. 44 (2004) 93–102.

[51] L. Poulsen, W.A. de Jongh, Advances in the Application of Perfusion Technologies to *Drosophila* S2 Insects Cell Culture, in: Contin. Process. Pharm. Manuf., Wiley-VCH Verlag GmbH & Co. KGaA, Weinheim, Germany, 2014: pp. 165–182.

[52] E. Chico, V. Jäger, Perfusion culture of baculovirus-infected BTI-Tn-5B1-4 insect cells: a method to restore cell-specific beta-trace glycoprotein productivity at high cell density., Biotechnol. Bioeng. 70 (2000) 574–86.

[53] J. Hong, J. Demirji, D. Blackstock, J. Lee, T. Dinh, A. Goh, F. Arnold, J. Horwitz,

Development of an alternating tangential flow (ATF) perfusion-based transient gene expression (TGE) bioprocess for universal influenza vaccine, Biotechnol. Prog. (2019) e2831.

[54] S. Radner, P.H.N. Celie, K. Fuchs, W. Sieghart, T.K. Sixma, M. Stornaiuolo, Transient transfection coupled to baculovirus infection for rapid protein expression screening in insect cells, J. Struct. Biol. 179 (2012) 46–55.

[55] D.P. Sequeira, R. Correia, M.J.T. Carrondo, A. Roldão, A.P. Teixeira, P.M. Alves, Combining stable insect cell lines with baculovirus-mediated expression for multi-HA influenza VLP production, Vaccine. (2017).

[56] K. Reiter, P.P. Aguilar, V. Wetter, P. Steppert, A. Tover, A. Jungbauer, Separation of virus-like particles and extracellular vesicles by flow-through and heparin affinity chromatography, J. Chromatogr. A. 1588 (2019) 77–84.

[57] P. Pereira Aguilar, T.A. Schneider, V. Wetter, D. Maresch, W.L. Ling, A. Tover, P. Steppert, A. Jungbauer, Polymer-grafted chromatography media for the purification of enveloped virus-like particles, exemplified with HIV-1 gag VLP, Vaccine. (2019).

[58] P. Steppert, D. Burgstaller, M. Klausberger, P. Kramberger, A. Tover, E. Berger, K. Nöbauer, E. Razzazi-Fazeli, A. Jungbauer, Separation of HIV-1 gag virus-like particles from vesicular particles impurities by hydroxyl-functionalized monoliths, J. Sep. Sci. 40 (2017) 979–990.

Conclusions

From the results obtained in this thesis, the following conclusions can be highlighted from each section:

Chapter 1 – Comparison of High Five and Sf9 cells with the BEVS

1. *Ac*MNPV baculovirus infection progress more rapidly in Sf9 than in High Five cells at equivalent infection conditions.
2. Sf9 cells are more efficient than High Five cells in assembling GageGFP in the form of VLPs.
3. A larger sedimentation coefficient is observed for High Five-derived VLPs produced with the BEVS probably due to the higher number of cellular compounds released that can associate with VLPs.
4. The amount of budded baculoviruses (infectious particles) is higher in Sf9 than in High Five cells. On the contrary, High Five cells produce a higher proportion of occlusion-derived baculoviruses.
5. Extracellular vesicles and adventitious viruses are detected as an additional source of contamination in the culture of both insect cells.

Chapter 2 – Optimization of the BEVS

1. The optimal conditions maximizing VLP production (Quantity) in High Five cells with the BEVS consist in a CCI of 2 x 10^6 cell/mL, a MOI of 2.5 and a TOH of 69.3 hpi whereas for Sf9 cells they are a CCI of 3.7 x 10^6 cell/mL, a MOI of 0.01 and a TOH of 80 hpi. On the other hand, the optimal conditions finding a balance between VLP production and VLP assembly (Quality) result in a CCI of 1.1 x 10^6 cell/mL, a MOI of 1 and a TOH of 33.6 hpi for High Five cells and a CCI of 3.7 x 10^6 cell/mL, a MOI of 0.01 and a TOH of 60 hpi for Sf9 cells.
2. A higher degree of VLP assembly is achieved in Sf9 over High Five cells for both the quantity and quality optima.

3. A 10 and 2-fold increase in VLP production are achieved for the quantity over the quality optimum in High Five and Sf9 cells, respectively. Similar VLP titers are achieved for the quantity optimum in both cells while the VLP yield is increased by 4.5-fold in the quality optimum of Sf9 over High Five cells.
4. A 4.9 and 1.6-fold increase in VLP assembly are obtained in the quality over the quantity optimum in High Five and Sf9 cells, respectively. In all cases, a higher VLP assembly ratio is achieved in Sf9 over High Five cells for the quantity (3.8-fold) and quality optima (1.3-fold).
5. VLP quantification by nanoparticle tracking analysis and confocal microscopy result in the detection of higher VLP titers while flow virometry is the most accurate technique.

Chapter 3 – Transient gene expression

1. Medium replacement before transfection and the shortest incubation time between DNA and PEI is the best strategy to achieve the highest transfection efficiencies in both cell lines.
2. Smaller DNA:PEI complexes are the most efficient for High Five cell transfection while they are more heterogeneous in size for Sf9 cells.
3. The optimal conditions for TGE in High Five cells consist in a viable cell concentration of 1.5 x 10^6 cell/mL, a DNA concentration of 2.1 µg/mL, a PEI concentration of 9.3 µg/mL and harvest at 48 hpt. For Sf9 cells, the optimal conditions involve a cell concentration of 17.6 x 10^6 cell/mL, a DNA concentration of 17.1 µg/mL, a PEI concentration of 35.9 µg/mL and harvest at 72 hpt.
4. In the optimal conditions, an 8.4-fold improvement in VLP production is obtained in Sf9 over High Five cells.

Chapter 4 – Stable cell pools

1. An 8.1 and 3.4-fold improvement in GageGFP fluorescence intensity is obtained after three rounds of cell sorting for Sf9 and High Five stable GageGFP producing pools, respectively.

2. A 3.7-fold higher VLP production is attained in the enriched High Five cell pool in comparison to Sf9 cells.
3. The optimal harvest time considering the amount of VLPs produced and the productivity is determined as 144 h for Sf9 cells and 120 h for High Five cells
4. The stability of both GageGFP producing cell pools is demonstrated during one month in culture.